Large Scale Solar Heating

Evaluation, Modelling and Designing

Heller, Alfred

Link to article, DOI:
10.4122/184893

Publication date:
2001

Document Version
Publisher's PDF, also known as Version of record

LARGE SCALE SOLAR DISTRICT HEATING

EVALUATION, MODELLING AND DESIGNING

ALFRED HELLER

Ph.D. Thesis

REPORT
R-046
2000

ISSN 1396-4011
ISBN 87-7877-050-5

DEPARTMENT OF BUILDINGS AND ENERGY

TECHNICAL UNIVERSITY OF DENMARK

IBE

PREFACE

The Thesis represents the ending of my Ph.D.-project at the Department of Buildings and Energy, Technical University of Denmark. It was carried out between 1997 and 2000 under the supervision of Prof. Svend Svendsen and in the first years, Assoc. Prof. Simon Furbo.

The Thesis consists of the current main report and an Appendix-report: "Large Scale Solar Heating – Evaluation, Modelling and Designing – Appendices", R-047, Department of Buildings and Energy, Technical University of Denmark, 2000, ISBN 87-7877-051-3.

The most relevant thanks go to my wife Anette and my children Isabel and Philip, who had to bear a large share of the burden for the work behind this thesis. It would not have been possible to carry out the work without the great support from my loved ones.

Right after my family, I am indebted to the people from the **Marstal Fjernvarme A/S** who have shown the world a possibility for future sustainable energy systems, the innovative plant designer of the Marstal central solar heating plant, **Rambøll**, the consultants for the plant owners **Planenergi,** and last but not least, the solar collector producer **Arcon Solvarme A/S**. The thesis would not have had its relevancy without the impressive and futuristic contributions from these people. Thanks, especially to all of you and to all the people making an effort in constructing the sustainable future, the only way capable of being sustainable for a relevant number of generations.

Thanks also to my supervisors. Thanks to my colleagues and the staff at the Department, especially to Louise Jivan Shah for her supervision, and also Anne Rasmussen and Kirsten Gammelgaard who have done a great job in proofreading.

Thanks to my colleagues from the Department of Energy Engineering and the Dept. for Mathematical Modelling at DTU for their help. Also thanks to the colleagues from the Chalmers University of Technology, Gothenburg, Sweden, and the people from the European Large-Scale Solar Heating Network for their support.

A special thank to Hannah Arlaud, WriteNow Communications for her enormous work in proofreading this thesis.

Acknowledgements

The project was mainly financed by a scholarship by the **Technical University of Denmark** under the Ph.D.-programme "Society, Planning and Technology".

The monitoring and some travelling to conferences were financially supported by the **Danish Energy Agency** under the Ministry of Environment and Energy.

Thanks to these organisations for their support of this rather futuristic work.

SUMMARY

The main objective of the research was to evaluate large-scale solar heating connected to district heating (CSDHP), to build up a simulation tool and to demonstrate the application of the tool for design studies and on a local energy planning case.

The evaluation of the central solar heating technology is based on measurements on the case plant in Marstal, Denmark, and on published and unpublished data for other, mainly Danish, CSDHP plants. Evaluations on the thermal, economical and environmental performances are reported, based on the experiences from the last decade.

The measurements from the Marstal case are analysed, experiences extracted and minor improvements to the plant design proposed.

For the detailed designing and energy planning of CSDHPs, a computer simulation model is developed and validated on the measurements from the Marstal case. The final model is then generalised to a "generic" model for CSDHPs in general. The meteorological reference data, Danish Reference Year, is applied to find the mean performance for the plant designs. To find the expectable variety of the thermal performance of such plants, a method is proposed where data from a year with poor solar irradiation and a year with strong solar irradiation are applied.

Equipped with a simulation tool design studies are carried out spreading from parameter analysis over energy planning for a new settlement to a proposal for the combination of plane solar collectors with high performance solar collectors, exemplified by a trough solar collector.

The methodology of utilising computer simulation proved to be a cheap and relevant tool in the design of future solar heating plants. The thesis also exposed the demand for developing computer models for the more advanced solar collector designs and especially for the control operation of CSHPs.

In the final chapter the CSHP technology is put into perspective with respect to other possible technologies to find the relevance of the application of large-scale solar heating. A discussion on possible barriers for the breakthrough of the technology results in the findings that the technology is mature for wide application, but that the economical key-values must be improved to achieve a breakthrough of the technology.

The thesis is then finalised by a summary and discussion and by an outlook.

Keywords:

Large-Scale Solar Heating, Central, Computational Modelling and Simulation, District Heating, Energy Planning.

RESUMÉ PÅ DANSK

De vigtigste formål med det foreliggende forskningsstudie var at evaluere store solvarmeanlæg koblet til fjernvarmesystemer, såkaldte solvarmecentraler, at opbygge et simuleringsværktøj til bestemmelse af sådanne anlægsydelser og at demonstrere anvendelsen af simuleringsværktøjet til designstudier og til energiplanlægning af et lokalområde.

Evalueringen af solvarmecentraler bygger på målinger på en Case, Marstal-anlægget på Ærø, og på erfaringer fra andre, hovedsagelig danske solvarmecentraler. Evalueringer af den termiske, økonomiske og miljømæssige ydelse for anlægstypen er præsenteret, baseret på de sidste 15-års driftserfaringer.

Målinger, gennemført på Marstal-anlægget, er analyseret, erfaringer er høstet, og mindre forbedringer er foreslået.

For at kunne gennemføre detaljerede designstudier og energiplanlægningsopgaver er der opbygget et simuleringsværktøj for solvarmecentraler. Dette værktøj er valideret med måledata fra Marstal-anlægget. Med det validerede værktøj er der til sidst udviklet en mere generelt anvendelig model. Ved at anvende vejrdatasættet, the Danish Reference Year, kan den gennemsnitlige ydelse af solvarmecentraler blive bestemt. For at finde frem til den variation i ydelsen, der kan forventes pga. varierende solindfald, er der fremlagt en metode til estimering af denne variation. Ved at anvende målinger fra et meget solfattigt og et solrigt år i simuleringerne kan man finde denne variation.

Udstyret med det nævnte simuleringsværktøj er der gennemført en række analyser , der spreder sig fra simple parametervariationer, over energiplanlægningsopgaver til designforslag til en fremtidig solvarmecentral.

Metoden at anvende simuleringsværktøjer har vist sig at være en meget anvendelig, relevant og billig metode til design og analyse af solvarmecentraler. Man kommer dog frem til et behov for yderligere udvikling af modeller, specielt for de styringsstrategier der anvendes på store solvarmeanlæg.

I de afsluttende afsnit diskuteres relevansen af solvarmecentraler i et større perspektiv og af at sammenligne pris-ydelsesforholdene for sådanne anlæg med andre solvarmeteknikker. En diskussion om begrundelsen for en manglende anvendelse af teknikken er præsenteret, og afhandlingen afrundes med en opsamlingsdiskussion og et kig ud i fremtiden.

Nøgleord:

Solvarmecentraler, store solvarmeanlæg, computersimulering, modellering og simulering, fjernvarme, energiplanlægning.

CHAPTERS

CONTENTS – SURVEY

CONTENTS – DETAILED

1. INTRODUCTION

1.1 BACKGROUND

1.1.1 The Environmental Issue

There is no longer any doubt about the tragic impact of human activities on the global ecosystem. The concept of "Sustainable development" was introduced in the so-called "Brundtland Report", and is recognised as the path to solve this global problem, (World Commission on Environment and Development, 1987) and in Danish (FN, 1988). A number of international conferences have led to the signing of conventions, treaties and agreements by the European countries, among many others. Consequently, the nations have an obligation to meet the objectives of these agreements. Most relevant for the current study is the obligation of stabilising and reducing the outlet of greenhouse gases, where the EU agreed to a reduction target of 8% and Denmark to a target of 21%.

There are a number of strategies for the stabilisation and reduction of green-house gas emissions, among others more efficient utilisation of primary energy, substitution of sources with high green-house emission with less polluting sources, extraction and deposition of the green-house gases at the sources, the oil- and gas well. These strategies still rely on future exploitation of natural resources for "simple" applications (e.g. heating) that demand investments to be replaced again in the long run. More sustainable strategies are energy conservation and the application of renewable energy sources. The current study deals with a single piece of the large puzzle of developing a sustainable energy system and hereby a sustainable society.

1.1.2 The Resource Infinity Issue

Resources are not infinite. This also applies to energy sources, such as oil, gas and coal. Although new resources are found and the technology developed rapidly, an end is foreseeable. The question is when, in 20, 50 or 100 years? Seen in a long-term perspective, a new question arises – If we exploit these resources, do we worsen the global climatic conditions? A final question posed here is: Is it wise to take a resource with a long-term (mill. of years) storage capacity and an uncountable potential for application and use it for primitive applications as heating and transport with minimal energy efficiency?

1.1.3 The Population Issue

As shown above, the world already is facing the most dramatic challenge with the size of today's population. By simple extrapolation of the current world population, experts foresee an increase of the world population to 10 billion people, before we get a chance to control the growth, if at all. Accepting the vision that all human beings have the right to live a descent life, encompassing all the necessary requirements for living, we can foresee the dramatic impact on the global ecosystem. This will impose a dramatic growth in demands for food, shelter, energy and other resources. Facts on the subject can be found e.g. in (Sørensen, B., Kuemmel, B., and Maibom, P., 1999).

In light of all the problems the world is facing in forms of poverty, war and catastrophes, it is clear that the developed world must bear the larger share of this burden. A future energy system must meet these demands and research must address the issue.

1.1.4 Is there any hope?

Years back, when the above-mentioned issues were unveiled, by e.g. the "Club of Rome", (EC, 1991) and before possible solutions were investigated, there was shock and hope was scarce. Since then, hope has been established and documented, e.g. by (Illum, K., 1996) and (von Weizäcker, E., Lovins, A. B., and Lovins, H. L., 1998).

Most important for the current work is the fact that the solar energy reaching the globe is estimated to thousands of times the total yearly demand for energy.

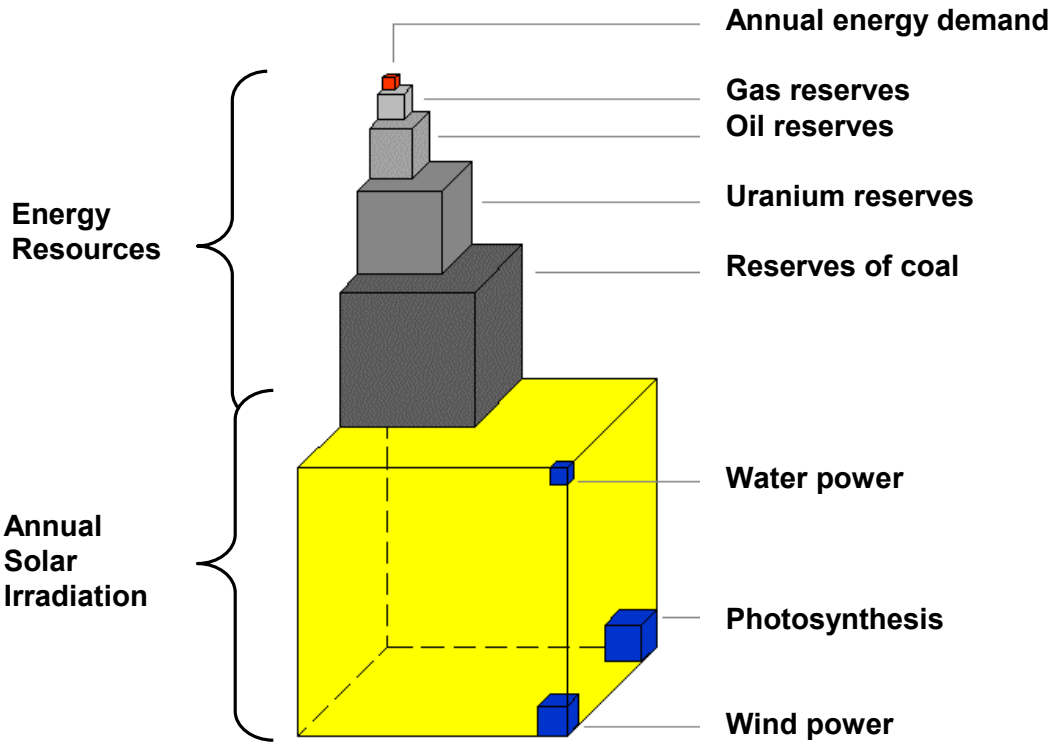

Figure 1. World energy resources. Source: Nye fornybare energikilder, Norway.

Source: Politiken (Danish Newspaper)

The potential is enormous and inexhaustible. Therefore, the answer to the question of whether there is hope, is clearly: "Yes"! – A very short answer with far-reaching consequences. It is worthwhile taking the path of sustainability. One mission is to do so. The other is to define how. The challenge is to develop and employ methods for harnessing this huge potential with minimal consumption of other resources, such as metals, chemicals etc. Hereby, these resources are free to meet all the other demands for living, shelter, food etc.

One of the most distinguished challenges for the engineer profession is "to give birth" to a reality. Hereby facts are created and can (hopefully) not be pushed aside. The current work is one step in the effort to show the world the facts of large-scale solar heating

technology, to provide evidence of methods and technologies that are realistic, reliable and capable of surviving the "Sustainability (R)evolution" to come. The objective of this enterprise is to take a few steps in the direction of a sustainable world, but not to be blind in the process; reflecting reality, possibilities and barriers on the chosen path. The tool to do so is chosen under the scientific paradigm of objectivity (See sketch). It is left up to others to argue by other values.

Note: A wider catalogue of ideas for other efforts on the path to sustainability can be found in "Factor Four" by (von Weizäcker, E., Lovins, A. B., and Lovins, H. L., 1998).

1.1.5 The Danish Perspective

Unfortunately, Denmark is one of the most CO_2-polluting countries in Western Europe, and hereby the world (Miljø- og Energiministeriet, 1995). The cause is the large consumption of fossil fuel, especially fuel oil and coal. Already in the seventies, the environmental problems were addressed and, together with the oil crisis, the first energy master plan was implemented by the Danish Ministry of Trade (Handelsministeriet, 1976). Due to the focussing on nuclear power and the acceptance of growing energy consumption, a number of independent researchers came up with an alternative energy plan shortly afterwards. The debate of the following years led, in 1990, to the first “green” energy master plan, Energy 2000, set up by the Danish Ministry of Energy (Energiministeriet, 1990). Some important points in this plan were: the renunciation of nuclear energy production, the application of co-generation involving large-scale district heating (DH) and R&D in renewable energy sources. Due to these choices, there was a rapid application of district heating in large-scale. These rather large, long-term investments in a rather static infrastructure are placed and must be addressed by plans for future energy systems. This is one of the reasons for the efforts regarding large-scale solar heating in Denmark which is also partly true for other Nordic countries. If solar heating is meant to play a major role in a future energy system, the displacement between the solar production in summer and the demand in winter must be taken into account. This was the reason behind activities in large-scale, long-term thermal storage activities in Denmark, also called seasonal storage (SS). Therefore, seasonal thermal storage activities are closely related to the development of large-scale solar heating, but this does not have to be the case.

The above-mentioned path to sustainability must start at the stage of today. Energy systems are different for every country and region, due to climatic, historical and political reasons. Hence, it is wise to find solutions for the future energy systems in coherence with the existing energy system and it's "surroundings". Due to the fact that district heating is widely applied in Denmark, the study of large-scale solar heating focussed on the district-heating variation from the beginning. This is, as an example, not the case in Germany, where the main effort in large-scale solar heating is focused on "small district heating systems", called "Nahwärme". Having an infrastructure with a lifetime of a number of decades with an extensive investment bound to that it is relevant to ask, what this technology will look like in the future, where the natural resources are limited or even emptied. Should the infrastructure be applied by other means, or should it be replaced? From this point of view, the question of the relevancy of large-scale solar heating seems answered and hereby the relevancy of the current study.

It is not normally the custom to cite references not available for the readers through common sources. This is, however, necessary in the current work, due to the fact that most national documentation in the field is published in technical reports, not widely spread. Even scientific publications are rare, mostly dominated by conference contributions and workshops. It is one of the objectives of this study to bring part of this knowledge to the attention of a wider public. Especially the Danish experiences are relevant here. Hereby, the underlying objective is to increase the understanding of the technology and it's potential.

1.1.6 Plans and Reality

Signing treaties is one thing, but the ratification subsequently necessary for it to come into force and eventually hopefully leading to implementation, is another. Unfortunately, both the US and certain countries within the EU still have not completed this procedure. Things seem even less clear regarding the actual implementation and concrete activities in reducing greenhouse gases. This is not a subject of the current study and will be left to more competent people to expose.

The fact that Danish energy policy shows difficulties in reaching the objectives form their own energy master plans, Energy 21, (Wittrup, S., 2000) is even worse. Hence, new and even stronger efforts must be made to meet the goals. As we will see, central solar heating is one of the most powerful solutions in this respect.

1.2 DEFINITIONS

There is no consistent vocabulary in the field of large-scale solar heating, or in general in solar energy technologies. This is demonstrated by citing the definition of the "European Large-Scale Solar Heating Network" (ELSSH), the main body for the development of the technology.

> *Large-scale solar heating systems or Central Solar Heating Plants (CSHP) are here defined as solar heating systems designed to provide heat to large and small building areas, i.e. residential buildings areas or large buildings including more than 20-30 residential units, as well as industries, via central block and district heating plants.*

This "fuzzy" definition is proposed redefined to a more consistent one below.

The terms in the different countries involved cover different technologies.

Solar Heating: A term for the assembly of all solar energy technologies producing heat that is independent of the purpose.

Large-Scale: A fuzzy term that is dependent on the technology.

Large-Scale Solar Heating (LSSH): A term for the assembly of all solar heating technologies implemented in large-scale, proposed applicable for solar collector areas larger than 500 m^2.

Central Solar Heating [Plants] (CSHP): Large-scale solar heating technologies servicing small and large district heating systems.

The technology services two types of heating networks: 1) "**District** heating" over large distances and "**Block** heating" for a group of buildings by a common network. Inspired by this classification, CSHPs are here proposed classified by: **Central Solar District Heating Plants (CSDHP)** and **Central Solar Block Heating Plants (CSBHP)**. Note: Using different languages makes things even worse: The Danish tradition in solar heating splits the solar heating technologies in small, medium, large and central. The large solar heating systems would be comparable to the central solar heating by the European Large-Scale Solar Heating Network (ELSSH) to be found on the Internet.

District Heating System (DH): A system that consists of one or more heat production plants, distributing the heat to "customers" through a pipe network. Here the term District is a term, to assembly all sizes, from a few buildings to a complex city structure. Note: The German terms **Fernwärme** and **Nahwärme** would be more precise to be applied. By free translation, the proposal could be **District Heating** for the former and **Close Heating** or **Near Heating,** not a perfectly matching set of terms. An alternative is

published in (Dahm, J., 1999) proposing the term **Small District Heating**. As we have seen above, the term **Block** is applied for "Nahwärme".

Seasonal Storage: A thermal storage that is capable of storing heat from summer to winter, consequently, long-term storage would in many ways, be a more appropriate term.

Net Solar Gain: Alt. Net Solar Energy Gain: The part of the solar energy production that is made accessible to the consumers, here the district heating network.

Solar Fraction: The ratio of net solar energy gain to total heat demand in the system.

Solar Efficiency: The ratio of net solar energy gain to total incident irradiation on the solar collector area.

Furthermore, some terms are widely used in the current thesis. They must be specified due to the possibly strange usage in the current context, but must not be defined as such:

In the following, the readers will find terms such as production and consumption of heat and energy, implying the model of having a product to be consumed by somebody. Bearing the basic doctrines of thermodynamics in mind - that energy cannot be "used", but only transformed, lost to somewhere etc. - this must certainly be understood symbolically.

By similar assumptions, the two interchangeable terms, **load** and **heat demands**, are used to describe the heat to be delivered to the customers of a given district heating system – the demand. This demand is defined by all the particular “sinks” together making up the total demand/load.

A number of technical terms are defined on a continuous basis during the text. It is not up to this work to explain all these terms to the reader.

1.3 ABBREVIATIONS

Specific solar abbreviations:

CSHP	Central Solar Heating Plant	
CSDHP	Central Solar District Heating Plant	
CSBHP	Central Solar Block Heating Plant	
CSHPSS	Central Solar Heating Plant with Seasonal Storage	
CSHPDS	Central Solar Heating Plant with Diurnal Storage	
CSHPxS	Central Solar Heating Plant without Storage	
LSSH	Large-Scale Solar Heating	
ELSSH	European Large-Scale Solar Heating Network	
SF	Solar Fraction	
SE	Solar Efficiency	
HP	High Performance	
DH	District Heating	
DHW	Domestic Hot Water (Systems)	
HWP	Hot Water Preparation	
SH	Space Heating	
TES	Thermal Energy Storage	
		Examples
UTES	Underground Thermal Energy Storage	bore hole storage, geothermal storage
OTES	On the ground Thermal Energy Storage	steel tank storage
ITES	Proposal: In the ground Thermal Energy Storage Alternative: Sub-Terminal (STES)	pit storage, artificial aquifer

General abbreviations:

R&D	Research and Development
IEA	International Energy Agency
EU	European Union
DEA	Danish Energy Agency, Danish Ministry of Environment and Energy
IST	Industrial Solar Technology, US firm producing solar collectors.
HT	High Temperature Solar Collector Type.

1.4 THE HISTORY OF CENTRAL SOLAR HEATING PLANTS

Note: The terms "large-scale" and "central" solar heating systems will be applied interchangeably in this section.

Sweden has played and still plays a major role in the development of large-scale solar heating. According to Dalenbäck, (Dalenbäck, J-O., 1993), the first steps were taken in the early seventies in e.g. Linköbing. Based on the experiences gained from these plants, a revision took place in the following years. And an improved design was introduced in 1983 in Lyckebo. In the mean time, other countries had opened their eyes for the technology, Finland (Kerava) and Netherlands (Groningen). The plants are documented in the final report of an international project under the International Energy Agency, (Dalenbäck, J-O., 1990). It is worth mentioning that already at this time there is a close connection between the development of large-scale solar heating and seasonal storage.

First designs involved site-built solar collector arrays (Torvalla, 1982, 2000 m^2, SE and Malung, 640 m^2, SE). Prefabricated large collector modules where introduced in (Nykvarn, 4000 m^2 in the first phase, 1985, SE). Other plants were placed in Studsvik (1979), Lambohov (1980), Lyckebo (1983) and Ingelstad (1979-1987). Important here is the fact that a strong international co-operation was established, already at the time of the first plants e.g. under the International Energy Agency (Dalenbäck, J-O., 1990) and the European Communities, (Dalenbäck, J-O., 1995), followed up later by the European Large-Scale Solar Heating Network, located at: http://www.hvac.chalmers.se/cshp/. This international co-operation was central for the transfer of knowledge to Denmark, today a major player in the field. Other projects are carried out during the time of the presented development. However, it is not the intention of this work to summarise the history of CSHP in total, but rather to provide an overview and a background for the developments in Denmark. Readers searching for further information on other plants, projects and countries involved are referred to the above listed Internet-site.

Note: Not all plants are presented in the above summery, e.g. the plant in Slovenia, (Arkar, C., Medved, S., Novak, P., Frankovic, B., and Lenic, K., 1998), and all the plants outside Europe.

The development of CSHPs in Denmark was, and still is, organised by an expert group under the Danish Energy Agency, involving partners from universities, institutes, industry and enterprises, dominated by non-scientific partners. The solutions and techniques, applied to Danish CSHPs, are closely related to the knowledge of this group. In the first years, scientific partners were in majority leading to research projects and among others to the first experiment in Vester Nebel, presented shortly below. After this first attempt, connection was made to the international forum, led by the Swedish partners. During these years, the emphasis shifted from being scientific to being practitioner oriented with focus on demonstration projects. A main feature for the Danish activities in the field of large-scale solar heating, is the focus on cheap and simple solutions, especially for the seasonal storage development summarised later.

The development of the current designs, are strongly determined by rather cheap ground prices, enabling use of large areas for ground-mounted collector fields and for large storage. This is a decisive fact that makes the design in other countries as Germany and Switzerland, rather different from the Danish solutions. This will be discussed later in this study, when describing the different techniques for large-scale solar heating.

Another topic is the existence of a high groundwater level in many places in Denmark. This is an impediment to the application of underground thermal energy storage, and solutions for storage on the ground must therefore be found. Contrary to Sweden where under ground storage is domineeringly developed.

In the following, the term "generation" will be used, a non-unique term that helps to differentiate large-scale solar heating plants in chronological order.

In Figure 2 the locations of the solar plants, mentioned in this thesis, are shown by "Suns".

Figure 2. A map of Denmark, 1:2 mill. Source: Kort & Matrikelstyrelsen, from Internet URL: http://www.kms.dk/landetrundt/danmarkskort/dk1.gif, with location of CSHPs.

It can be mentioned that, according to a survey to be found at the above Internet-site, 6 out of 55 European large-scale solar heating plants are situated in Denmark. The plants comprise 19.600 m^2 (21% of EU-total) solar collector area from the total 90,000 m^2, installed in large-scale solar heating plants in Europe. Another relevant fact is the very intense utilisation of central solar heating on the island of Ærø, where the two newest plants are placed in Marstal and Ærøskøbing, comprising 13.940 m^2, accounting for 15% of the EU-total. Thanks to these icebreakers of the "Southern Seas", another plant is under way in Store Rise, and the Marstal plant is expected to expand dramatically in the next year/s.

1.4.1 Vester Nebel (Esbjerg) – A first and premature attempt

After the oil crisis in the seventies, the development of solar collectors was pushed forward, from a starting point with recycled, black painted radiators to the highly efficient production of

collectors using aluminium sheet with selective surface coatings. At first, single-family installations were dominant. In the late eighties, large-scale solar heating was introduced. The first solar heating installation in Denmark which could be called a CSHP, was built in 1983-85 in Vester Nebel near Esbjerg. The hybrid-plant involved, among other elements, a windmill, a heat pump, energy collectors and a few solar collectors, contributing with a solar fraction of 2%. Conclusions about solar heating systems connected to district heating were not favourable (Ørsted, H. and Majland, O., 1987). The costs were too high, thermal requirements to the DH-system too demanding and experiences too few. However, this first attempt inspired an alternative approach.

1.4.2 The Saltum and Ry-Plants – The First Generation

Based on the expertise in Sweden, presented above, two plants were erected in 1988 near Saltum and in 1989 near Ry. In the same technology transfer package, the fabrication of collector modules was transferred from the Swedish manufacturer, Teknoterm to the Danish company ARCON and the technology further developed to the SCAN-CON-HT solar collectors, applied today. The main feature of these first generation plants is simplicity. The solar collector loop is run by constant flow, directly connected through a flat-plate heat exchanger to the district-heating network. No thermal storage is involved, and the solar production is hereby limited to the production being delivered at a given time. Post-heating of the solar heat is often necessary, also in summer.

1.4.3 The Marstal Plant – A Second Generation

After Saltum and Ry, a number of CSHPs were erected by similar designs. Mainly in Sweden, a diurnal storage was introduced in such plant designs, bringing the solar share further up.

A major step in the development of CSHP, was taken in the design of the Marstal plant – at this time Europe's largest, in fact one of the world's largest. A number of novelties are introduced in the plant which is the reason for the differentiation to the first generation. The main features for the plant is the applicability of variable flow control which adjusts the return temperature from the collector field to a given set point temperature. In this way, the solar production can be directly led through the supply pipe to the district heating with constant temperature. A diurnal steel tank enables the storage of a few days production. During long periods in summer, no post-heating is necessary. The plant is the main topic of this thesis. It forms the "Model Object" and will therefore be presented in detail in the sections below.

1.4.4 The Connection To Long-Term Thermal Storage

As mentioned above, the development of CSHPs was, in the later years, directly related to the development of long-term storage with the goal of achieving economical and reliable seasonal storage and thereby a rise in solar fraction for central solar heating systems. Hence, the same group of experts involved in the R&D for CSHPs, worked on long-term storage technologies. A survey on the development and advances of seasonal storage in Denmark can be found in (Heller, A., 2000a) and in general from the international thermal conferences, e.g. Megastock 97 in Sapporo, Japan and in Terrastock 2000 in Stuttgart, Germany.

After initial investigations, some technologies, such as chemical storage, geothermal storage and others, were considered irrelevant for Danish applications due to geological and environmental reasons.

Preliminary investigations and one single research application of a bore hole storage in Ballerup resulted in the conclusion that this type of storage could not be competitive with pit water storage (Duer et. al., 1995). No further work has been done on these technologies.

Here the Danish activities clearly diverge from the activities in other countries such as Sweden, Germany and the Netherlands, where activities are related to "Underground Thermal Energy

Storage" (UTES). The Danish activities are mainly concentrated on "In/On the Ground or Sub Terrain Thermal Energy Storage" (ITES/OTES or STES) such as pit water, artificial aquifer and steel tank storage.

A map of the location of the seasonal storage mentioned in this text is shown on the map in Figure 3.

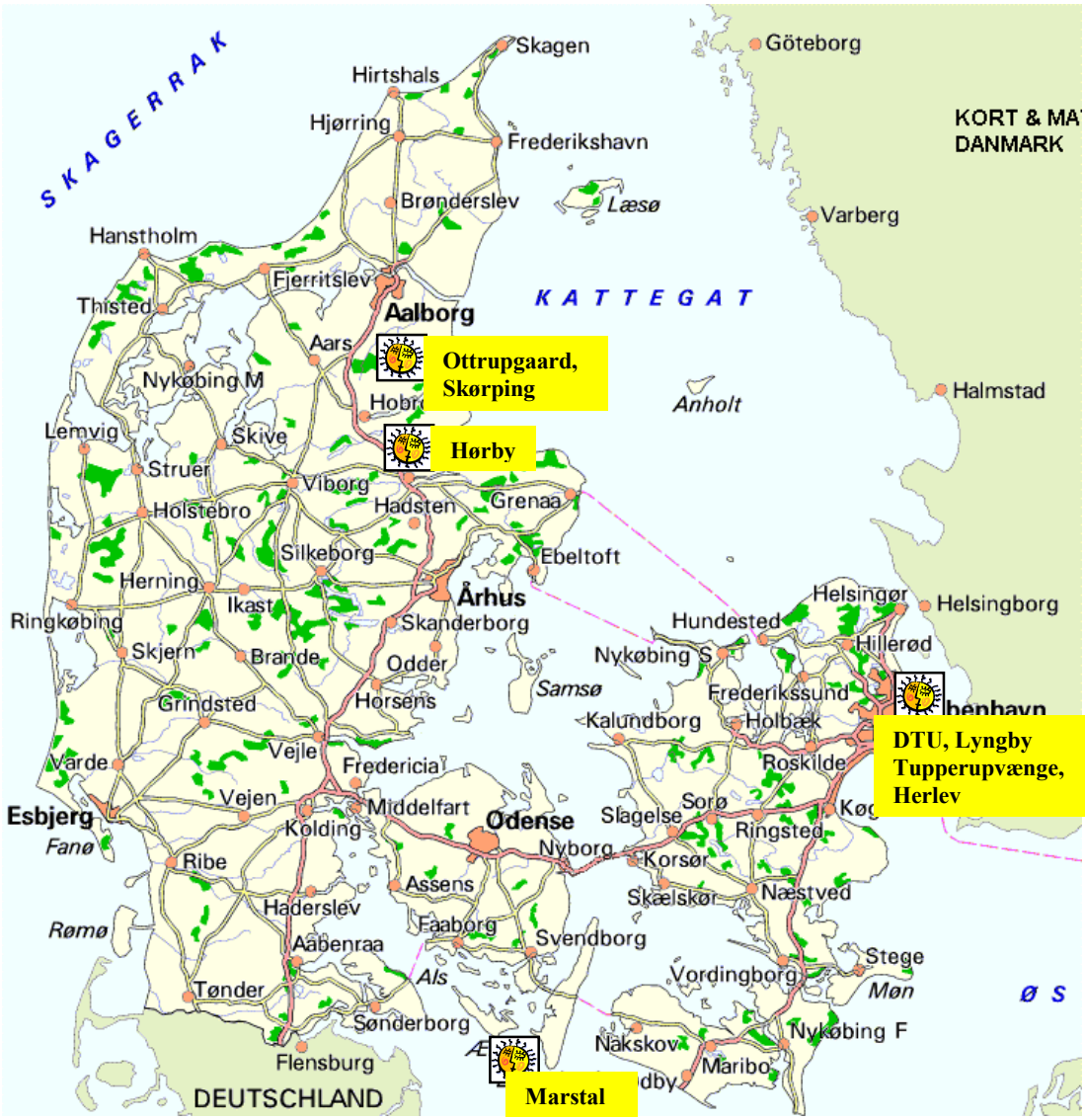

Figure 3. A map of seasonal storage in Denmark, 1:2 mill. Source: Kort & Matrikelstyrelsen, from Internet URL: http://www.kms.dk/landetrundt/danmarkskort/dk1.gif.

1.4.4.1 Tank Storage Systems

The most obvious thermal storage, the insulated, unpressurised steel tank, is widely applied in co-generation and district heating systems. Hence, this technology seems to be obvious for the application of long-term storage, although there are no experiences regarding heat losses over long periods. A first investigation of the application of steel-tanks is presented in (Lawaetz, H., 1993). The conclusion was that the technology is applicable, can be improved and the price[1] in 1993-terms can decrease to 285 DKK/m^3 for a tank of 100,000 m^3 in volume. Own investigations on the subject show severe fluctuations in price level, mainly due to fluctuating

[1] The exchange rate between Danish Crones and Euro is approximately 7.4 DKK per Euro.

state of the market and consequently fluctuating labour-costs, with a difference of up to 100% between a few years. Own estimations, based on price-examples from the same sources, as applied by Lawaetz, show a corresponding minimal price of 550 DKK/m^3 and some technical question marks arise as to the possibility and the rationality of building such huge single tanks. From this point of view it seems that the steel-tank technology is the favourite technology, due to it's wide application and established reliability, but it is not economically competitive with other technologies described below for volumes above 20,000 m^3 storage, (Wesenberg, C., 1996).

Other investigations are carried out on the utilisation of existing technologies. In Hoerby, prefabricated concrete elements, normally applied for liquid manure from farming, was tested for thermal storage. The tank had a volume of 500 m^3, and it was sealed by a dense bentonite-concrete coating on the inside, (Wesenberg, C., 1990). Examination of the concept showed rather severe water losses due to damage of joints between elements and cracks on the concrete surface (Pedersen, V. P., 1992). Due to rationalisation of production, the cost is very low for small volumes. Regarding medium or large size volumes, profit actually disappears. The picture is rather different if the boundaries for the study are changed. Hence, other conclusions can be found in a German study by (Kübler et. al., 1997, Fisch et.al. 1997), where ground cost is a dominating factor.

In 1991, a seasonal tank-pit water storage (a big, tightened and insulated hole or cavity in the ground) was integrated in a CSHP at Tupperupvænge, in Herlev. The project included a number of technical novelties, such as a central collector field mounted on the top of the seasonal storage together with collectors distributed on the buildings. The 3.000 m^3 storage is constructed by steel sheet piles which are normally used for temporary sealing of construction sites. The storage is insulated inside and tightened by a plastic liner. Polyurethane foam plates sealed by an EPDM rubber membrane insulated the concrete lid (Pedersen, V. P., 1992). The installation was rather complex, and many problems occurred during the operation of the plant. Already in the first year of operation, the tank leaked. A first rescue effort was started in 1992. The seasonal storage, together with a connected heat pump, was then out of operation for a number of years. In 1997, based on the experiences from Rottweil, Germany, a 600 m^3 on-site cast concrete tank with steel-lining inside, (Kübler, R., Fisch, N., and Hahne, E. W. P., 1997), a solution using thin stainless steel sheets was developed (Wesenberg, C., 1998) and reported successful in 2000 (unpublished).

1.4.4.2 Pit Water Storage with Floating Lid

The first attempt at developing a pit water storage with a floating lid was made in 1983 at the Technical University of Denmark, Lyngby (Kielsgaard, H. K., Nordgaard, H. P., and Ussing, V., 1983). The storage of 500 m^3 (designed for research purposes only) was sealed with a 2.5 mm HDPE liner and covered by a floating lid built up of an HDPE-liner, expanded Polystyrene insulation and a Butyl top liner. The storage worked well, but long-term monitoring was not possible, due to changes at the pit.

After laboratory investigations on clay layer liners for the sealing of the pits, the Ottrupgaard CSHP was built in 1995, involving a 1.500 m^3 pit water storage with a floating lid of prefabricated sandwich elements of polyurethane foam. The design is presented in (Wesenberg, C., 1994a) and (Wesenberg, C., 1994b).

The concept of a floating lid is studied in (Heller, A., 1997) and conclusions on the Ottrupgaard design investigated in (Heller, A., 1997). A floating lid construction was calculated to be cheaper than static lid designs (Wesenberg, C., 1991). The project showed clearly that a floating lid could be a reliable solution, but that the construction details must be reconsidered. Either the applied material must meet the rather demanding thermal and hydrodynamic conditions, or economical encapsulation must be found. Work on floating lids is ongoing, testing is to be made in 2000, and conclusions cannot be made at the time of writing.

The hybrid clay layer concept is published by (Duer, K. and Svendsen, S., 1993). Severe leakage was found already from the beginning, increasing in water losses during the years, (Andersen, P., 1998). A final solution by applying bentonite, clay mixtures are proposed in (Porsvig, M., 1999), hereby a solution is found. Latest facts and details are published in (Heller, A., 2000b). It is worthwhile mentioning that clay liners are not waterproof. Due to the fact that the clay must be wet (not to crack), the pit looses quite a large amount of water. This must be taken into consideration, when choosing this solution. A final report on the tightening is expected soon.

In defiance of the problems, pit water storage is estimated to be built for approximately 40 USD per cubic metre storage. This is the cheapest solution for large-scale thermal storage.

1.4.4.3 Artificial Aquifer Storage

The Lyngby pit water storage was reconstructed in 1990 to form an artificial aquifer storage by filling the pit with gravel, and by adding direct and indirect (plastic pipes) heat exchangers (Ussing, V., 1991). Unfortunately, no clear conclusions can be drawn from this experiment.

A second gravel pit storage is constructed at the Marstal CSHP based on experiences made in Germany, where similar designs are placed in e.g. Stuttgart and Chemnitz, (Urbaneck, T., 2000).

A polypropylene liner, welded on-site tightens the pit. Layers of sand and clay are placed alternately. The heat exchange of the solar heat is indirect though plastic-pipes of PEX-material, covered by the sand layers. The pit is filled with water to improve the heat exchange. Alternatively, as shown in the German pits, the heat exchange is direct by letting the fluid enter the pit. No definitive conclusions can be made yet, but we can already determine that the heat exchange is very slow. First economical indications are that the technology cannot compete with pit storage. On the other hand, the static qualities of the solution make it preferable for areas requiring that the ground area be used for other purposes. The observation of low temperatures explains the fact that most UTES are equipped with a heat pump for increasing the temperature to a utilisable level for domestic needs.

1.5 GENESIS AND OBJECTIVES FOR THE RESEARCH PROJECT

When defining the objectives of this study in 1996-97, large-scale solar heating was a reality, due to the newly established Marstal plant. The design was mainly based on experience, but also on a "rule of thumb" and not least on some courageous experiments. Design tools were available, but the fact was that the tools were not widely used by the designers. Scientific servicing and follow-up was limited to a few affiliated projects.

Objective 1:

Being placed in this position one of the main objectives for the study was to collect all the relevant data, experiences etc. for the Marstal Central Solar Heating plant. In this thesis and the otherwise published work by the author this objective is met.

Objective 2:

A second objective is defined by the "study-plan" (the research plan) by the following terms:

> *A known barrier for the wider exploitation of the technique is lack of confidence and knowledge. To strengthen the confidence, demonstration plants are needed. To do so, methods and tools for dimensioning, optimisation etc. are needed, but so far absent or too difficult to use.*

Therefore the first objective of the study was:

> *to develop theoretical methods for the analysis and design of CSHPs.*

Having collected experiences with a number of design- and simulation tools, including SEASONSOL that is developed at the Department, the dominating simulation tool in the field, TRNSYS (Klein, S. A. and many others, 1996) was chosen due to:

- The high level of development.
- The ability of using already documented and validated component models.
- The modular build up.
- The extendibility with own components.

However, this made it superfluous to develop own components. Hereby the task was reduced to the purpose of enhancing the reliability in using this tool for large-scale solar heating. This subject will play a major part in this thesis.

Objective 3:

The application of the final simulation model for large-scale solar heating is developed and demonstrated by a number of examples. Hereby the third objective of the thesis can be defined as executing energy planning on local district heating systems involving central solar heating.

Some simulation examples are documented to answer open questions in the field of central solar heating. Other examples are chosen to bring the development one step further from the current stage. Here a widely spread dogma is confronted, namely, the claim that solar heating is only feasible for low temperature applications, e.g. below 80^{o}C. By introducing high performance solar collectors, the next generation large-scale solar heating technology is proposed, leading to high efficiencies even at high temperatures and hereby to better total performance. The solution will hopefully be demonstrated in the coming years in Marstal. Through these means, the current study has gone even further than the objectives defined during the research.

Objective 4:

What is the reason for the lack of penetration of large-scale solar heating? (Barriers)

Increasing own knowledge on the technology by analysing the large-scale solar heating plant in Marstal, the question of missing dissemination became even more pronounced. Here we have a successful, full-scale demonstration of a 100% sustainable technology, with good economical key-figures, the best possible ambassador for a technology. So – why is this technology not applied in a wider range? In this work, a technological point of view is chosen, pointing in the same direction as the demonstration in Marstal – to increase the confidence in the technology. Now this barrier is not "real" anymore, and we must turn our attention to structural, political and economical reasons. Some minor topics on these subjects will be discussed below, but due to a lack of theoretical background, it was not possible to present a final answer. Hence, the main thesis still remains for further work. A thesis on this work could be formulated as follows:

> *Which structural and man-made phenomenon can be identified as central as obstacles for the penetration of large-scale solar heating [and other renewable energy technologies].*

General Remarks:

It is my belief that the work undertaken in this thesis has enhanced the knowledge of the technology, although the result, from an international perspective is not unique. However, the effort led to the fact that the main objective can be addressed and the development of the technology thus be brought one step forward, especially for Denmark, giving us the chance to build up the sustainable society of tomorrow.

1.6 METHODOLOGY

From a strict "science of science" or "science theoretical" point of view, the current thesis is non-scientific. The classic procedure of science is not obeyed. No hypothesis is formulated, to be tested, "proven" or "falsified".

As given by the thesis title, the research project is, **Large-Scale Solar Heating**, a wide range of technologies, spreading from simple low temperature heat production, to highly concentrated energy for solar electricity and chemistry. In this work the wide range of large-scale solar heating technologies is reduced to **Large-Scale Solar Heating connected to District Heating Systems**, even more precisely, **..with a focus on low-temperature and low-pressure systems**.

The first limitation is necessary to exclude solar heating systems that serve block-heating systems. The latter is to avoid the transfer of the findings to district heating systems with much higher temperatures and pressure than applied in Denmark, characterised by the fact that the temperatures are "low", typically below 90^{o}C in the supply, and that the distribution medium from the pipelines enter the buildings, demanding low-pressure solutions. This must be kept in mind when applying the results of this study in other parts of the world. By this limitation, we exclude a number of solar heating plants, but include all central solar heating plants in Denmark and Sweden, as the research object with special focus on the Marstal case.

The often very complex research object has in three steps been simplified to a so-called model object by: 1) Isolation of the model from its surroundings 2) Abstraction by applying mainly thermodynamic theories for the description of the plant performance 3) Idealisation by assuming the findings from the Marstal plant and especially the simulation model to be valid for a wider range of central solar heating plants.

When isolating the object from its surroundings, a system approach is chosen, where the solar plant is defined as the system, and the meteorological conditions and heat load by an “external” district heating as the boundary condition for this system. This is certainly a simplification due to the fact that the system and the boundaries influence each other. Assumptions made in the step of abstraction are defined in the relevant sections below, but have also been discussed in detail in (Heller, A., 2000c).

The method for generalisation of the findings from the Marstal case is to apply computerised, mathematical modelling and simulation. Here the real-world model is reformulated into an abstract model by quantitative formulation in mathematical construction, based on physical laws and theories, so-called analogous model, (Julio, De S. and Ruberti, A., 1984).

The drawback for the applied method is the fact that a reproduction is hardly possible. Collecting data from another CSHP and implementing the model by other regressions in another tool would more than likely lead to other results. Some examples will be found in the analysis chapter of the thesis. From this point of view, the work here is not strictly scientific, but still qualifies as reasonable engineering work.

Having built an abstract model, input-output, also called stimuli-response, can be applied as experiments, interpreted to be true for the real world system of the given class, too. Hereby the method makes it possible to examine the different designs with a minimal economical impact. It is also worth mentioning that the model can be applied for prediction, as demonstrated later in this thesis, but furthermore for control, where the inputs are used and parameters adjusted to obtain a desired output, response.

This method of building and applying models can, in the current case, be explained by the following steps, where step 1-5 relate to the task of building up a model, the (modelling) part and step 6 relates to the application (simulation)[2] part:

1. Collecting data by monitoring and analysing the Marstal plant.
2. Abstraction: Mathematical-physical modelling of the thermal and, if necessary, the hydro-dynamical characteristics of the plant.
3. Implementation in a simulation environment. (Computer program)
4. Calibration of model parameters and validation by collected data from the real plant.
5. Generalisation of the validated model by "average input conditions".
6. Extrapolation for prediction of experimental objectives.

[2] Note: The terms modelling and simulation are unambiguous. To be able to adjust the parameters in the process of modelling, simulations are carried out.

1.7 OUTLINE OF THIS STUDY

Chapter 1: The research object, central solar heating in connection with district heating, is described in detail. Hereby the similarities and differences for the plant designs are extracted. This survey leads up to a discussion of the fact that this research field lacks a consistent terminology.

Chapter 2: The research object, the Marstal central solar heating plant, is monitored from its first days of operation. The data from this permanent monitoring is hampered by detailed data logging. In 1999, a supplementary monitoring program is carried out to find the missing data. This is performed as a part of this Ph.D.-study. From these two monitoring systems, the data is collected for the analysis in the following chapter.

Chapter 3: The data collected at the Marstal plant is examined and analysed leading to the first findings for the monitoring in general. Among others, the solar irradiation measurements and measurements from temperatures along a collector row are discussed. First experiences on the performance of the Marstal plant are extracted from the measurements. A more comprehensive collection of experiences is gathered in Chapter 7.

Chapter 4: A simulation model is built in the computer and simulation program TRNSYS® and the results from the model are compared with the measurements from the monitoring programmes. Hereby the confidence in the results from the program is examined.

Chapter 5: The simulation model is then examined in detail by applying parameter variations on the most important parameters. Hereby, an insight into the model and the model object is gained simultaneously as work progresses. A sensitivity analysis is employed to make the parameters comparable. The sensitivity analysis is here seen as one of the most powerful methods for users of models who are not familiar with the detailed structure of the program or the models behind.

Chapter 6: From the analyses of the previous chapters, we are now able to collect the findings for central solar district heating plants, based on a literature study, measurements by others and the author, on the first simulations and analysis of the results. This chapter is relevant to readers interested in collecting experiences regarding large-scale solar heating in general. A number of findings are not summarised in the final sections again, because this would confuse the overall conclusions and the discussion of the thesis.

Chapter 7: Equipped with a simulation tool, we are able to investigate designs of future plant generations. This is even more relevant and indeed a challenge since one to three plants is being designed at the time of writing. Two main studies are documented here: 1) Evaluation of variable versus constant flow control in CSHPs. 2) A study on the utilisation of high performance solar collectors in CSHPs.

Chapter 8: The thesis then moves on to a perspectivation, a summary and an outlook.

In the perspectivation section, the technology of CSHP is set in relation to other possible technologies with the same targets. The potentials for the technologies and the barriers for the penetration of the technology is discussed etc. Hereby, we are able to estimate the relevancy of the technology and the results of this work.

The summary section gathers the main findings of this work, leading to discussions and conclusions of the method applied here and the hereof-resulting findings.

An outlook into a very challenging future then finally concludes the thesis.

2. CENTRAL SOLAR DISTRICT HEATING SYSTEMS

A central solar district heating system consists of a Central Solar Heating Plant (CSHP) and a district heating network. In this chapter, the system is described with focus on the solar plant. The basics of the plant design are presented in section 2.1. CSHP can be classified by different means, as discussed in the final section of this chapter. The designs presented here are 1) a plant with no thermal storage, 2) a plant with diurnal storage and a simple control strategy and 3) the Marstal plant type, with diurnal storage and a more advanced control strategy. The focus is on the plants built in Denmark for the reason that the data is available from the source and that others have already published the experiences from other plants.

The Danish CSHPs are of type 1 and 3, while type 2 is employed in Sweden. The plant designs are presented in the above order in section 2.3 to 2.5, following a description of common aspects for the Danish plants in section 2.2. The chapter is finalised in section 2.6, by a discussion of common criterions for a definition of an unambiguous terminology in the field of central solar district heating plants. It is left to a standardisation to make a final choice for a terminology.

2.1 BASICS

2.1.1 The central solar heating plant

The basic configuration for a central solar heating plant is sketched in Figure 4.

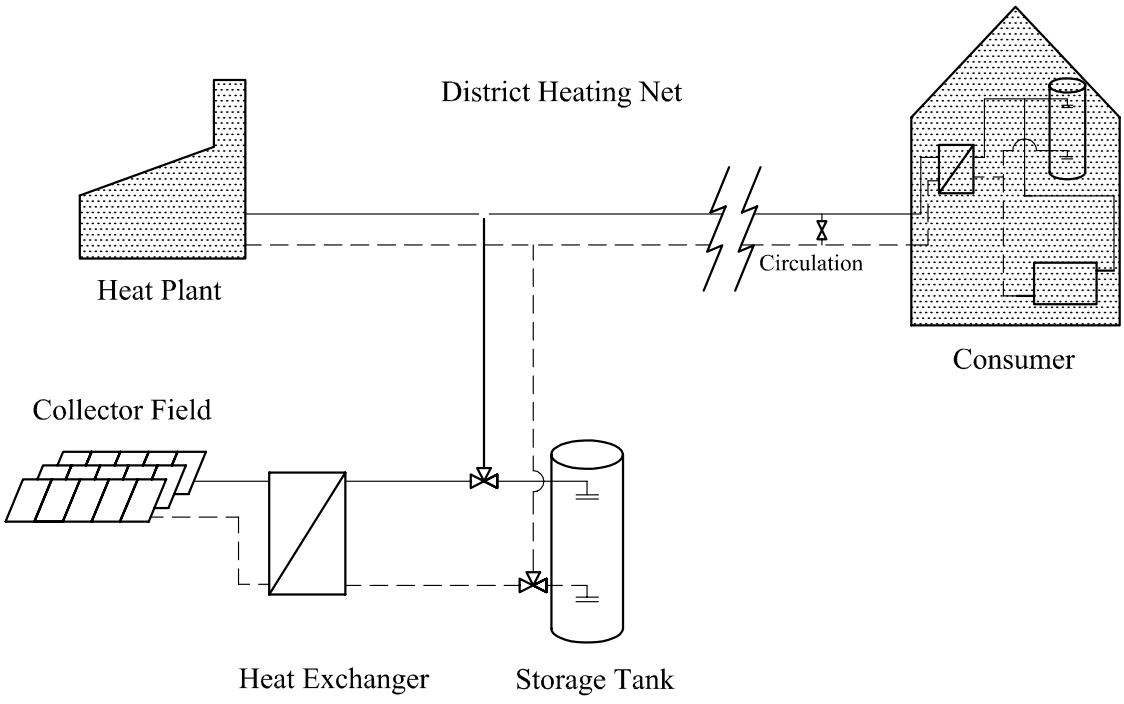

Figure 4. The basic configuration of a central solar heating plant.

Fundamentally, the CSHP consists of a solar collector field and a collective distribution pipe network for the supply of the heat to the consumers. In most cases the solar share, also called solar fraction (SF) is rather small compared to the total demand in the given system. Hence, another heat production unit, here called heating plant, must be involved in the overall system, e.g. a heat plant or co-generation plant. In some cases, at least one storage unit is employed to increase the solar share.

2.1.2 The consumer

The consumer is defined as the buyer of heat for e.g. space heating and domestic hot water. There are always many consumers with many different demand patterns involved when dealing with distribution networks.

The term consumer covers complex structures, such as buildings, space heating installations, hot water installations and much more.

2.1.3 The distribution pipe network

The distribution pipe network is a web of pipes, connecting the heat production units with the consumers. The net configurations can involve from 2 up to 4 pipes, depending on the design. In the current work, if not defined differently, a two-pipe system is assumed. Such a two-pipe system consists of a supply pipe (the warm pipe, supplying the heat to the customer) and a return pipe (cold return from the consumer to the heating plant).

Distribution networks can supply large areas, called district heating, or a group of buildings only, called small district heating.

2.1.4 The solar collector field / collector array

The solar collector field or simply collector field / array is the main part of a solar heating system, collecting the incident solar energy and transferring it into a heated medium for usage. The collector field can be placed on the ground (ground-mounted) or on rooftops of buildings (roof-mounted).

Field configurations can be very different, especially for the roof-mounted collector fields. For ground-mounted collectors, the configuration is dominated by placing the collectors in rows (serial connections) and the rows placed in blocks by parallel connection.

A fluid medium is pumped through all modules to receive the collected heat and transport it back to a heat exchanger. The involved medium is in most cases a mixture of water and an anti-freezing additive (normally propylene glycol).

2.1.5 Possible field connections

The following configurations for the connection of a solar collector field on a distribution network can be found in Figure 5:

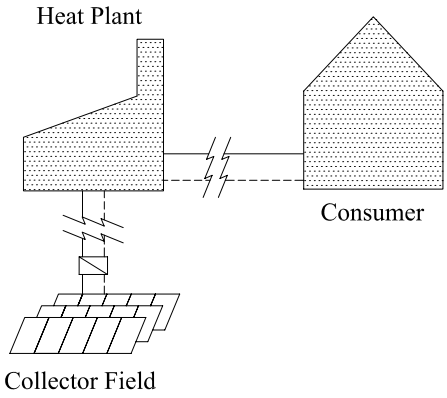

(a)

(a) The CSHP is placed at a distance from the heating plant with no connection to the distribution network directly.

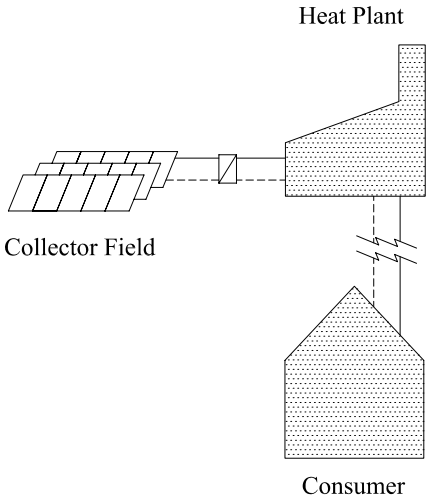

(b)

(b) The CSHP is placed at a heating plant which is the case in e.g. Ærøskøbing.

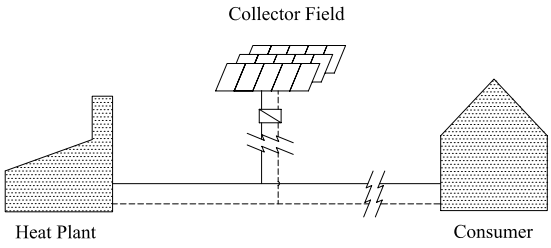

(c)

(c) The CSHP is placed at a distance from the heating plant with a direct connection to the distribution network as in Marstal. A variant hereof, is the connection of the CSHP to a branch of the pipe network. This is a good idea if the DH-system consists of areas far apart, connected by a transmission pipe couple. Here closing down the branch, supplying heat locally from the CSHP saves the heat loss in the transmission pipe.

Figure 5. Configuration for connection of central solar heating to a distribution network.

2.1.6 The fluid loops

As found in the drawing above, the heat transfer medium from the collector loop is circulated in the collector loop and to a heat exchanger. This collector loop is also called primary loop. The configuration of the primary loop can be very different. Nine basic configurations and control strategies are presented in (Mikkelsen, S. E., 1988) for large solar heating systems placed in buildings.

For ground-mounted systems, we find the following configurations for existing systems and in new systems:

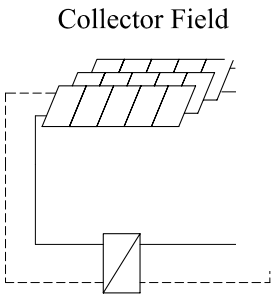

(a)

(a) Single array field (Saltum and Ry).

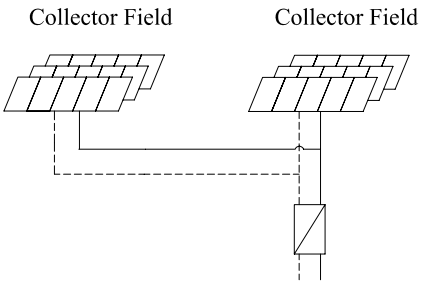

(b)

(b) Multi array field (Marstal and Falkenberg with 2 arrays).

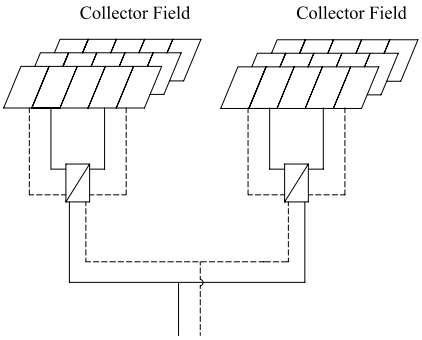

(c)

(c) Multi field configuration (Kungälv, possibly Marstal extension).

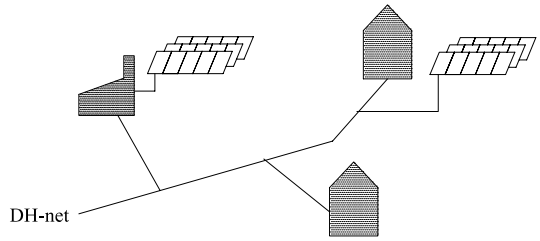

(d)

(d) Multi plant configuration (future).

Figure 6. Solar collector field configurations for ground-mounted modules.

There are other characteristics than those above which are not mentioned here. A single domestic hot water DH-system exists with tap water coming into the CSHP, tapped at the consumers, (Vajen, K., Krämer, M., Orths, R., Boronbaev, E. K., Paizuldaeva, A., and Vasilyeva, E. A., 2000). Certainly such systems can be made very simple and lead to impressive efficiencies. The application of water instead of the application of anti-freezing fluid in the collector row leads to higher efficiency due to higher thermal capacity. The Dutch producer ZEN designs such systems.

From the primary loop, the collected heat is extracted through a heat exchanger to the secondary loop which in all cases applies water as a transport medium. In some cases the water is prepared for district heating use. The secondary loop is in some cases very simple, involving the return pipe of the district heating only, in other cases it is connected to a storage and the district heating network simultaneously. This design characteristic will be discussed later in detail together with control strategies for the two loops involved.

2.1.7 The solar collectors

Basically, there are a number of different solar collector designs on the market. The most applied design is the plane collector.

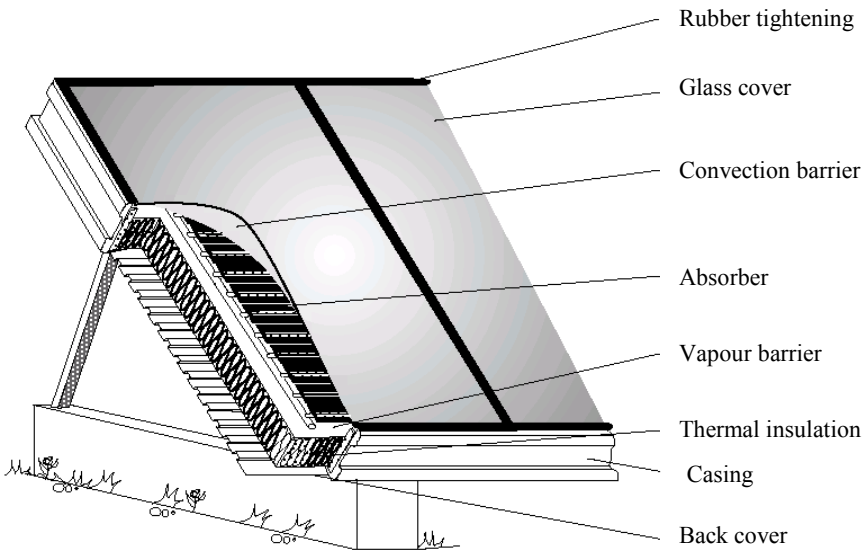

Figure 7. A flat plate solar collector design, typically applied for central solar heating plants. Drawing by ARCON Solvarme A/S, Skørping, Denmark.

Fundamentally, the flat plate solar collectors consist of a well-insulated box, holding the other parts together, mainly the absorber and the cover.

The absorber is the main part of the solar collector, "catching" the solar radiation and transforming it to thermal energy. Hence, absorbers are highly developed to efficiently absorb radiative energy.

The cover must be transparent for short-wave solar radiation and is designed to avoid long-wave heat losses through the top of the collector. It can be designed as a single or multi-layer cover.

For large-scale solar heating, especially large designs are produced, so-called collector modules. Such modules typically apply a kind of strip-absorber, a thin metal foil with

integrated flow channel and high efficient absorber surface, a cover of Teflon-foil inside and iron-free glass cover outside. To the back and side, the construction is insulated to avoid heat losses. A thin aluminium sheet then covers the insulation.

The flat plate solar collectors are characterised by a very high efficiency for low absorber temperatures, decreasing with increasing temperatures in the collector. This can be visualised in a number of ways, among others by the dependency of the efficiency of the temperature difference between mean absorber temperature, T_m, and ambient temperature, T_a, divided by the solar irradiance, G in W/m^2. This is illustrated by the graph in Figure 8.

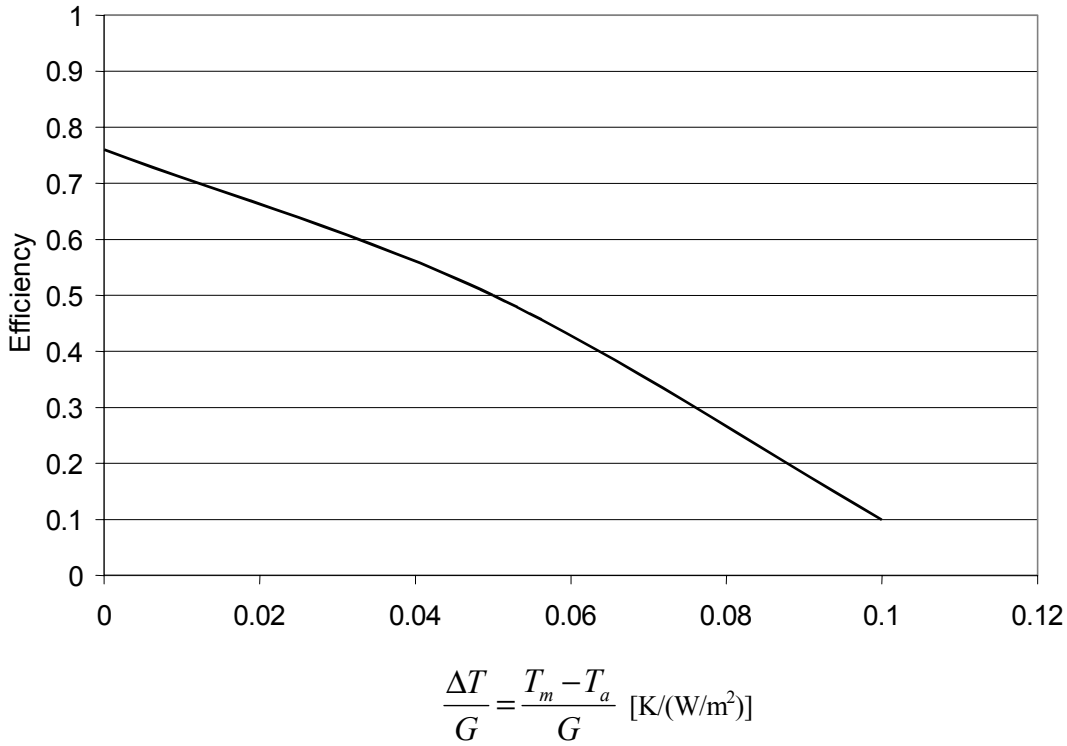

Figure 8. The typical efficiency curve for a plane solar collector.

From the efficiency curve of Figure 8 we can deduce that the efficiency is described by $\frac{\Delta T}{G}$ and that the efficiency decreases with increased ΔT or decreased solar irradiance. At the start efficiency, at the ordinate axes, the temperature of the absorber is similar to the ambient temperature, and no loss will occur. As the temperature in the absorber rises, heat loss is increased. We find from the figure that this heat loss is not linear. A second order polynomial is generally applied for the heat loss description in efficiency terms.

A goal of collector design is to achieve high "optical" efficiency, high start efficiency and low heat loss with increasing collector temperatures.

One way of doing this is to apply advanced insulation technologies for covering (the Teflon example is one of them). Theoretically, vacuum is the most efficient insulation method. Therefore, attempts are made to apply vacuum in plane constructions. This has shown to be very difficult due to 1) the large (negative) pressure and 2) the problem of sealing the construction with no heat barriers. Therefore, a more applied approach is to utilise the tubular form, due to its natural stability and strength. Such solar collectors are called evacuated tubular collectors, involving a number of different absorber designs.

Figure 9. A tubular vacuum solar collector design. Source: Internet URL: http://www.ifdesign.de/awards/1996/product/topten/bigpicture/solar-tubosol_01_e.html.

Theoretically, another approach is to focus or concentrate the solar irradiation into an absorber, by different means. The designs are numerous, ranging from simple concentration foils to highly advanced mirroring and focal systems. A simple example of a concentrating collector type (CPC) is a newly developed concentrating collector, called MaReCo. A sketch of the principal mode of operation for the design is shown in Figure 10.

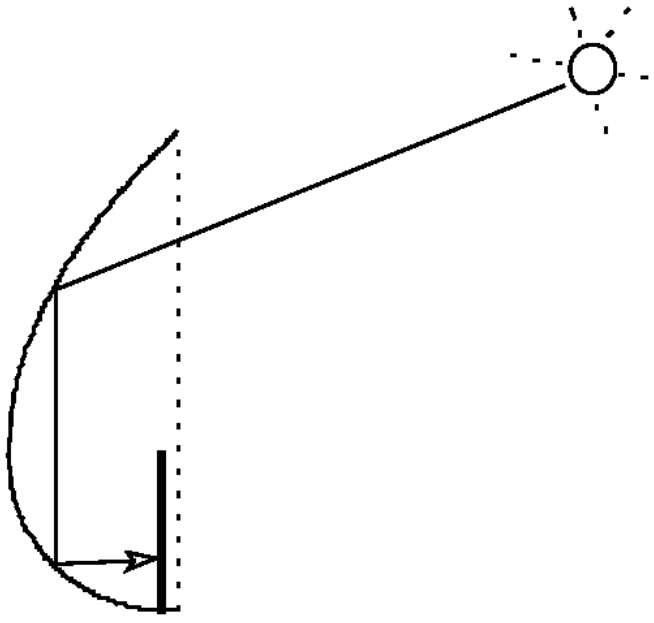

Figure 10. MaReCo, a concentrating foil solar collector with simple strip absorber. Source: (Karlsson, B. and Wilson, G., 2000).

Another example is the so-called trough collector, mainly applied in the US for electricity production by thermal solar energy.

Figure 11. Trough collector with concentrating foil and tubular absorber. Source: Test Facility at DLR Cologne (Germany) with parabolic trough systems of Industrial Solar Technologies. Source: (Krüger, D., Heller, A., Hennecke, K., and Duer, K., 2000).

Combinations of solar collectors can be found. As an example, the CPC2000 collector by SOLEL® is a flat-plate collector with small concentrators inside.

Comparing the efficiency of the different designs leads to a "typical" result as exemplified in Figure 12.

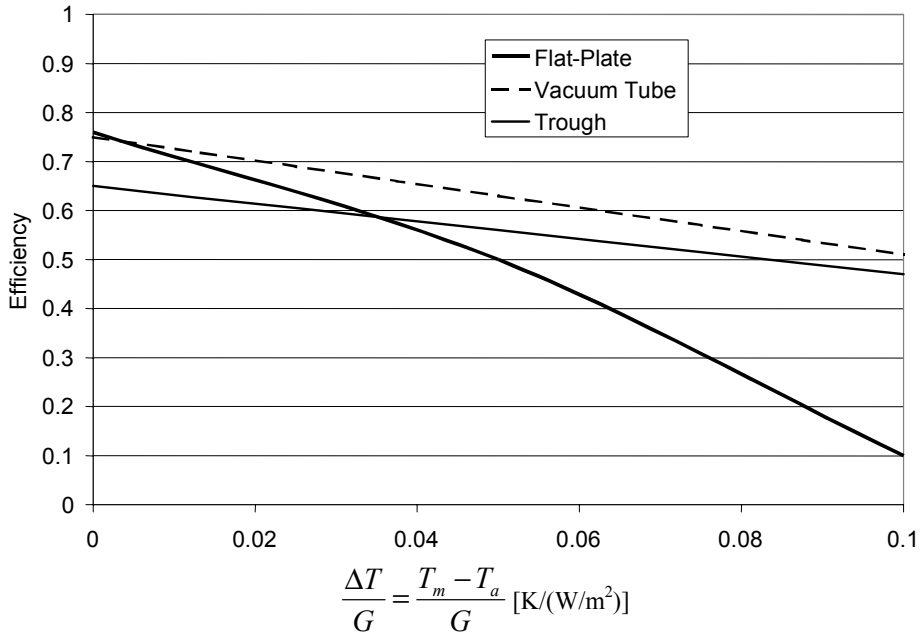

Figure 12. Comparison of fictive efficiency curves for a flat-plate, an evacuated tubular and a trough solar collector versus evacuated tubular collector designs.

The evacuated and the trough collector designs clearly maintain the efficiency over a wider range of temperatures. This partly explains the fact that these technologies break through the above-mentioned temperature-barrier of approximately 80°C where solar heating is traditionally recommended. Facing the facts of collector developments, the temperature barrier for the application of solar energy is evaded! This is true for an outlet temperature from the collectors up to far above 100°C. In the following, this subject will be discussed further.

2.1.8 The storage

In some CSHPs no storage is involved. However, if storage is applied, the volume can vary greatly, from capacity to store a few days solar production in summer to a seasonal storage, able to store heat from summer to winter.

The technologies involved are presented above in the section describing the history of large-scale solar heating and will not be repeated here. A more comprehensive survey on the developments in large-scale thermal storage is presented by the author in (Heller, A., 2000) followed up in (Heller, A., 2000a) and some detailed work on the pit storage technology in (Heller, A., 2000b).

2.2 COMMON CHARACTERISTICS FOR THE DANISH CSDHP

All CSHP of a certain size apply ground-mounted solar collector modules. The SCANCON-HT collector design by ARCON Solvarme A/S is the most applied in CSHPs. The HT-module, shown in Figure 7, has a 12.6 m^2 aperture area with a length of 6 m and a height of 2.3 m. The module is composed of a low-iron glass cover, Teflon film convection barrier, a selective surface absorber and mineral wool insulation is placed in an aluminium frame with aluminium back plate. The absorber consists of 16 strips connected in parallel, and is made using SunStrips (new strips in a new design!) of aluminium with black nickel coating.

The collectors are placed in rows of 10 modules and the rows are connected parallel to blocks. An anti-freeze fluid is applied in the primary loop. The heat is withdrawn through a heat exchanger to the district heating net.

2.3 THE FIRST DK-GENERATION PLANT (SIMPLE 5%-CSDHPXS)

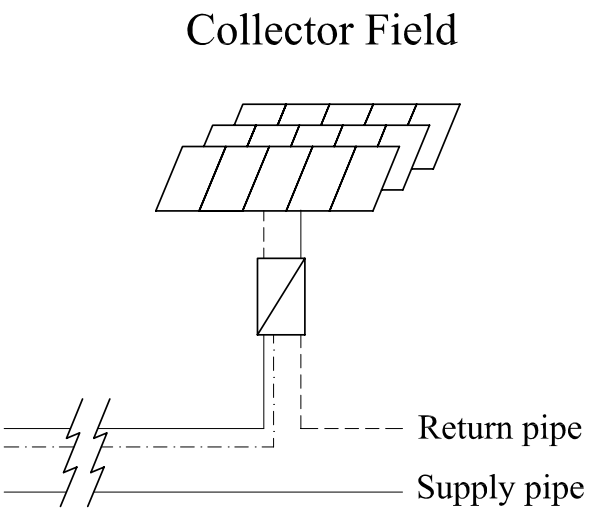

All the plants built from 1988 to 1996 can be classified as first generation plants. The main feature of the plants is simplicity.

Figure 13. Simple drawing of the first generation CSHP, built since 1988. Examples are the Saltum and Ry plants.

The pumps of the collector loop are started for solar irradiation above a certain threshold, typically 100 W/m^2, by an on-off control strategy for the pump. The solar heat is fed to the return,

cold pipe of the DH system, preheating the fluid in the DH-system. A post-heating backup is necessary, also in most periods in the summertime. No storage is included. Hence, the plant type can be classified as the CSHPxS.

Both of the larger examples in Denmark, the Saltum and the Ry plants, consist of a single collector array. The collector field in Saltum is placed on a tilt ground, leading to less shading from the row in front to the one behind.

2.4 THE SWEDISH INTERMEZZO (SIMPLE 10%-CSDHPDS)

The next step in the development of CSHP is the application of thermal diurnal storage with a capacity of a few days. This is among other demonstrated in Nykvarn and Falkenberg, Sweden. The plant is described in detail by (Isakson, P. and Schroeder, K., 1996). The plant is, above the tank, fundamentally very similar to the first generation plant. The simplified layout scheme is shown in Figure 14.

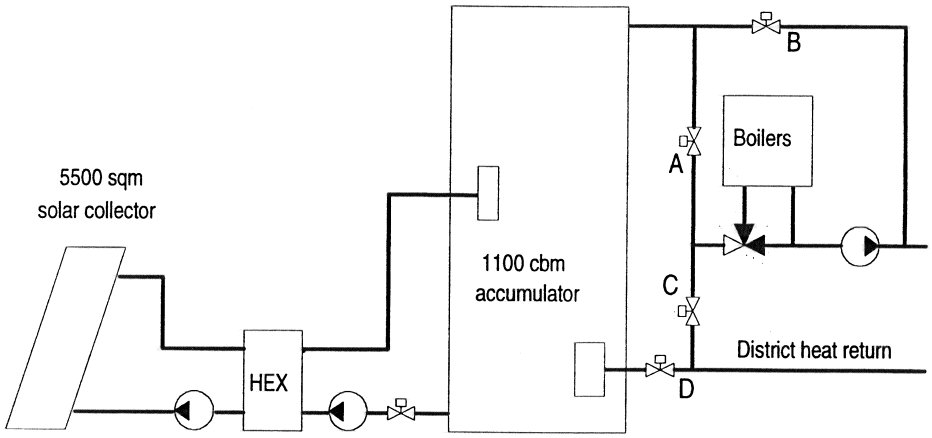

Figure 14. Layout scheme for the Falkenberg CSHP. Source: (Isakson, P. and Schroeder, K., 1996).

Filling the tank in the middle and drawing off the heat at the top runs the storage. The return flow from the DH enters the tank above the outlet to the solar collector loop. Hereby the coldest temperature is not/less disturbed by the DH-system.

2.5 THE SECOND DK-GENERATION PLANT (COMPLEX 15%-CSDHPDS)

The Marstal plant, built in 1996, introduced a number of innovative characteristics qualifying the design as a new generation CSHP. Due to the fact that the plant is the model object of the author's research activities, many publications in the recent years deal with the explanation of the plant design and first experiences in (Heller, A. and Furbo, S., 1997) and the evaluation of the operation in (Sørensen, P. A., Tambjerg, L., Holm, L., and Ulbjerg, F., 2000) and (Heller, A. and Dahm, J., 1999). A general survey of CSHP is published in (Heller, A., 2000) and a follow up in (Heller, A., 2000), with the Marstal plant centrally placed as the new design. In the following, a detailed description of the Marstal plant is repeated to give the readers the necessary understanding of the technology. The section ends with a generalisation to a more generic[3], second-generation plant.

[3] The term "generic" is here used for the collection of all plant designs with the common characteristics that define the second generation CSHPs.

2.5.1 Introduction to the Marstal plant

Motivated by law and the shortage of other renewable resources on the island, the DH-plant for the village of Marstal on the island of Ærø, initiated a preliminary investigation for the adoption of solar heating in 1993. First tests on the final concept were carried out on a small (75 m^2) solar heating installation at an indoor swimming pool. Prior to the introduction of a new solar heating plant, the existing district heating net and the consumers' installations were modernised and adjusted to low-temperature operation.

The 1996-version of the district heating, with installed boiler capacity of 10 MW and an annual output of approximately 100 TJ, services a large share of the total heat demand of the 1,200 houses in the village, mostly single-family and row houses. Similar to other Danish systems, the consumers are directly connected to the DH networks, thus the transport medium of the district heating net enters the building installation. This approach entails low-pressure ($6*10^5$Pa = 6 bar) and low-temperature (< 90°C) operation for the distribution network which is an advantage, or rather a requirement, for the successful application of solar heating. The DH-net in Marstal is operated with a delivery temperature of 72°C and a return temperature of 44°C in summer, and 32°C in winter.

The designer of the plant (Flemming Ulbjerg, RAMBØLL Consultants), trained in the DH-business, used a number of tools and guidelines from DH-design. The design was settled in co-operation with the collector producer ARCON Solvarme A/S, the Marstal District Heating A/S and their consultants, Planenergi. Basically, the demarcation of the enterprises was that ARCON designed the collector field (above ground) and the district heating consultant, RAMBØLL, carried out the connection (under ground). The contracts involved a solar guarantee for the performance of the collector loop, settled to 3250 MWh per year, and other functional claims to the performance, such as e.g. the heat exchangers involved, a subject to be taken up later in this work.

2.5.2 The solar collector loop and design procedure

The collector area of 8064 m^2 is arranged in 2 equal blocks with 32 parallel-coupled rows of 10 collector elements in series. They face south with a tilt angle of 40°. The modules are mounted on a steel construction on top of concrete blocks, placed on the ground. Pressure valves ensure equal flow through all rows. The return streams are mixed to a single main loop. The system comprises two parallel heat exchangers, three pumps on the collector side and two on the storage side, pressure tanks etc. The collector circuit medium is a 50% mixture of water and propylene glycol mixture to avoid freezing in the wintertime.

The design procedure applied in Marstal is very simple. The collector area is estimated based on the assumption of an annual collector production of 400 kWh/m^2. For the specified solar fraction of 12%, ca. 12 TJ, the collector area requires about 8300 m^2. Assuming an optimal output with a row of 10 collectors (based on Swedish and Danish experiences), the collector area was then calculated exactly. The pump volume capacities were determined by simple steady-state considerations, based on the requirement of a temperature rise over the DH-loop of 30 K under relatively extreme conditions. These considerations led to a variable flow in the range of 20 m^3h^{-1} – 160 m^3h^{-1}, or 0.042 – 0.33 l $min^{-1}m^{-2}$. By defining the required number of days for the storage capacity, the Danish computer program, SOLPAKKEN, calculated the tank volume. The heat exchangers are to meet the peak power with a logarithmic temperature drop of maximum 5 K.

2.5.3 The steel tank storage

The 2,100 m^3 steel tank storage with a height of 16 metres is designed for a capacity of approximately 3 days' heat demand under summer conditions. The tank is insulated with 300 mm mineral wool and has a vapour barrier of nitrogen at the top of the water volume to avoid

corrosion. Three identical inlet/outlet arrangements with plate diffusers are placed at the bottom, at a height of 3 m and at the top. Dependent on the situation, different combinations of inlet/outlet can be used.

2.5.4 Overall connection scheme

In the following CAD-drawing, the overall scheme for the design of the Marstal plant is visualised.

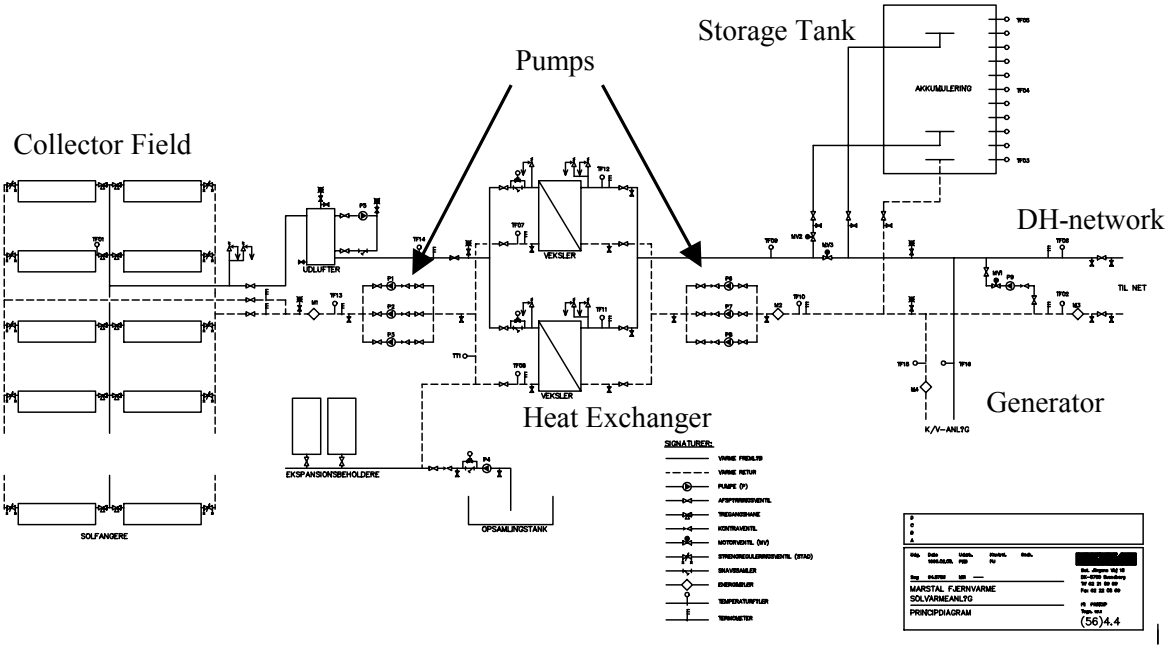

Figure 15. CAD-drawing of the overall connection scheme for the Marstal CSHP. Source: RAMBØLL. Note a larger version can be found in the Appendices-report.

The solar collector field is placed to the left, connected by heat exchangers in the centre of the drawing. The secondary loop is drawn on the right side of the figure with the tank on the top right and the district heating system pointing out to the right. The Diesel-generator (backup) is pointed to by the two connections on the lower right side.

We find, as mentioned above that redundant components are applied, such as the heat exchangers, the pumps and so on. We find the two tank inlet arrangements on different heights. Finally, we find that the district heating loop is directly connected to the secondary loop. Contra-valves serve to ensure proper flow directions.

2.5.5 Control and underlying design strategy

As one is able to read out of the above CAD-drawing, the many valves involved in the system enable a variety of possible control strategies. Even more so, remembering that there are control possibilities also at the heating plant. Hence, the current presentation is a compromise between simplifying to make things understandable and giving a complete description.

The main difference from the first generation plant is the employment of variable flow in the solar loop by adjusting the pumps. The main goal of this operation is to obtain constant temperatures back from the collector field. Another reason is the reduction of parasitic energy which here means electricity for pumping.

The Marstal plant is operated in two different modes: A “winter-mode” and a “summer-mode”.

In the winter-mode, the solar plant supplements the main waste-oil fired plant. The pipe network branch between solar plant and heating plant is run, only if there is relevant solar

energy, or if there is a need for storing heat from the heating plant. The solar plant is connected to the heating plant in a manner to preheat the return flow of the DH. Regardless of the fact that a desired return temperature is set, the low solar irradiation will result in a control strategy, very similar to that of the first generation plants.

In the summer-mode, the waste oil fired plant is out of operation. The solar heating plant is run to supply 100% of the DH demand, backed up by a small fuel-oil burner. In this mode, the CSHP is connected to the forward pipe of the DH, and the operation is designed to supply the necessary delivery temperature to the DH-net.

For both modes, the primary loop is started before the secondary loop, understandably done to bring the collector fluid up in temperature. The secondary loop is started, when the possibility of extracting relevant energy is present. This is simply the case, when the return temperature at the collector loop is a certain number of degrees higher, typically 2 K, than the temperature to be exchanged to. This again is either the district heating cold side temperature, or the tank bottom temperature. The secondary side is turned off, when the conditions, based on the mentioned temperatures, are not obtained. Note: This control is similar for all large solar heating plants, not only CSHPs.

In order to explain the start-up conditions for the primary side, some introductory background is necessary.

In the summer-mode, the requirement of a constant delivery temperature demands a control strategy that appropriately handles the distinction of the time constants for, on the one hand the relatively rapid fluctuations in solar irradiation, and on the other hand, the very slow response of the return temperature from the collector loop. Due to the large collector arrays involved, one must be aware of the fact that the passage time for the fluid is very different depending on the collector row to be passed. The flow is pumped to the field in a single pipe and comes back in a single pipe with a mixed temperature. This temperature is the "average" of all the flows meeting each other in the hot pipe and returning to the heat exchanger. Some flow has only travelled through the nearest row, other flow parts had to travel a long way up to the far-most row, traversing the row and travelling all the way back to the collection pipe. A drawing of the situation is shown in Chapter 5, Section 5.1.3. Hence, adjustments on the flow operation will influence the average over this period.

Instead of applying a control-theoretical approach, the Marstal strategy employs the theories of solar heating for this purpose. Fundamentally, it is assumed that the above introduced efficiency curve description for a collector can also be applied for the whole collector field. This is certainly a simplification and will be discussed in the Section 8.1.6, but leads, as we will see later, to rather impressive results. The transformation from an efficiency expression to a flow control is described below.

The general expression for the collector efficiency is given in (1).

$$\eta = \eta_0 - k_1 \frac{\Delta T}{G} - k_2 \frac{\Delta T^2}{G} \qquad (1)$$

where
- G global irradiance, W m^{-2}
- ΔT relevant temperature difference discussed in the text, K
- k_1 heat loss coefficient, linear part of efficiency expression, W m^{-2} K
- k_2 heat loss coefficient, quadratic part of efficiency expression, W m^{-2} K^2
- η efficiency for solar collector field.

In the following explanations of the control strategy, the efficiency expression will be found in two variations, as η_e, the estimated efficiency for solar collector field when running, and η_0 the start efficiency.

The involved parameters are found by standardised testing to be found on data sheets. For a given computation, the momentary solar irradiance is used. During the control algorithm, the efficiency expression is repeatedly applied with different temperature differences involved. This will be described clearly below.

The start criteria for the first pump on the collector side are:

#1 Note: There are temperature measurements at all outlets of the rows. Most measurements are taken outer surface of the pipes. Six measurements are taken in the flow medium. The highest of these six measured temperatures must be a few degrees, pre-set to 8-10 K, higher than the temperature at the bottom of the storage tank. The #1-condition is commonly used in CSHP-control. The temperature in the absorbers is higher than the temperature at the row outlet. Hence, the collector loop could be started earlier which is achieved with #2.

#2 The efficiency expression (1) must lead to a positive estimated efficiency and thereby an expected production or at least preheating of the collector loop mass. Due to the fact that the average temperature of the medium, expected in (1), is not known, the coldest possible fluid temperature at the bottom of the storage tank is applied instead. To avoid oscillation, the expression $\Delta T = T_{t,b} - (T_a + T_{set1})$ involves a set temperature, T_{set1}, of a few degrees, pre-set to 2 K.

If the two conditions #1 and #2 are met, the pump is started at a minimum flow of 0.05 l/min/m^2. The mass flow is increased up to the maximal flow capacity, based on the following set of expressions. Firstly the estimated efficiency of the collector loop is calculated from (1) applying a temperature difference $\Delta T = \frac{T_{set} + T_{coll,in}}{2} - T_a$ involving the demanded set point temperature, T_{set}, set by the operators, the measured return temperature, $T_{coll,in}$, from the collector field, and the ambient temperature, T_a. The resulting estimated efficiency, η_e, is then inserted into the expression for the estimation of the flow rate in m^3/h.

$$\dot{M}_p = \frac{\eta_e \cdot G \cdot A}{\rho \cdot c_p \cdot \Delta T} \qquad (2)$$

where ΔT is the same temperature difference as inserted into the expression for the estimated efficiency, ρ the density and c_p the specific heat of the medium.

It is worthwhile mentioning that the control condition results in a minimal collectable power of approximately 45 kW.

2.5.6 Generalisation to a third generation plant design

Other plants of the third generation are placed in Ærøskøbing, on the same island of Ærø as Marstal. Here all solar collectors are close to the heating plant, partly placed on the roof of the plant and partly ground-mounted. The collector field is increased in a number of steps up to 4900 m^2. A 1200 m^3 storage steel tank has recently been installed bringing the three tanks up to a total storage volume of 1400 m^3, a very similar volume-area ratio as found for the Marstal plant.

The newest CSHP plant in Sweden (the Kungälv plant) is built this year 2000, presented by (Dalenbäck, J-O., 2000), in a first phase, consisting of 5000 m^2 SCAN-CON HT collectors by ARCON. The novelty here, is the anti-reflective coating (NIOX) of the cover glass by SunArc A/S, Denmark. The control strategy is similar to the Marstal plant, except from the control of the secondary side which for the Kungälv plant is based on pressure control from the heating plant, by adjusting a temperature controlled valve.

2.6 CLASSIFICATION OF CSHPS

As already demonstrated in the section with definitions, the terminology in large-scale solar heating is very poorly developed. This is certainly the case for the classification of the involved technologies. However, for discussions of large-scale solar heating and central solar heating a unique classification would be very helpful. In this section, an attempt is made to give some ideas for a common terminology which might be used in standardisation of the terminology in this field.

Common for all central solar heating is the application of a large solar collector field (> 500 m^2) and a collective (central) heat distribution network, supplying a small or large building with heat. A definition could therefore require the presence of the defined size for a solar collector field and a distribution pipe network.

The first classification to be found in literature, is the differentiation in district heating and block-heating systems, (Dalenbäck, J-O., 1995). As we found above, this classification is adopted above for the demarcation of the research activities. The characteristics of the two system types are not unambiguous. It seems that the district heating type preferably applies ground-mounted collector fields with a central storage unit, while the block-type preferably applies roof-mounted solar collectors and a number of local storage placed in the building, possibly supplemented by a central large storage unit. So a criterion for the unambiguous definition of the above terms could be that an application of central solar collector fields versus distributed collector fields is applied instead. Hereby the terms Central Solar Heating and Distributed Solar Heating would be a possibility.

The capacity of the storage is already applied in the first IEA work, (Dalenbäck, J-O., 1995), distinguishing between CSHP with no storage (xS), with diurnal storage (DS) and seasonal storage (SS). This seems a rather premature and inconsistent classification, due to the fact that the boundary between diurnal and seasonal storage is not definable.

In the same publication, classifications based on the collector type, the method of placing the solar collectors on a building (Integrated, where the solar collector replaces the roof material (partly), versus Mounted, where the collector is placed on the roof cover) are used.

Another classification applied in this work, is the temperature range for the collector; e.g. HT for high temperature and LT for low-temperature. This is a widely applied terminology, but it is very confusing and related to the technology and application. As an example, high temperature in solar chemistry is many thousand degrees Kelvin, while it is only above 80 degrees Celsius for the district heating business.

An alternative and more applicable classification would be based on the solar share to the total demand by applying percentage. A CSHP with a solar fraction (to be defined uniquely) of 10% is a 10%-CSHP. This on the other hand describes nothing about the design.

Other identification items could certainly be used as a basis for the terminology, application of reflectors between collector rows, drain-back instead of the application of anti-freezing fluid in the collector row and on-site built contra prefabricated collector fields.

The term generation is used above and has simultaneously been applied by (Sørensen, P. A., 2000) and the author, (Heller, A., 2000). The term differentiates between numbers of characteristics simultaneously, as we will see in the detailed descriptions of the two generation plants developed in Denmark, and other steps in the genesis of CSHP. In general, this classification only fits the Danish survey of plants and cannot be applied on an international level.

3. MARSTAL CASE MONITORING

The Marstal plant is successfully monitored since 1996. The monitoring programme is published in (Sørensen, P. A., Tambjerg, L., Holm, L., and Ulbjerg, F., 2000), (Holm, L., 2000) and in detail (Danish) in (Holm, L., Ulbjerg, F., Nielsen, J. E., Sørensen, P. A., and Tambjerg, L., 2000).

After first validation work published in (Heller, A. and Dahm, J., 1999), it became clear that the data from the stationary monitoring system in Marstal was not precise enough for validation of the current models. The objective of carrying out supplementary measurements at the central solar heating plant in Marstal was therefore to collect data for model calibration and validation. Supported by the Danish Energy Agency, a supplementary monitoring program was carried out between July and September 1999. In the current section this monitoring program is described and the first data analysis for control of the monitoring and the solar heating system is carried out.

In section 3.1 the plant is described shortly followed by a description of the stationary and the supplementary monitoring systems in section 3.2. The data is then analysed for errors and first results for e.g. operation in section 4.

3.1 THE MARSTAL PLANT FROM 1999

The Marstal plant has been extended during its existence. In 1997, the plant consisted of 8064 m^2 plane solar collectors and a storage tank with a capacity of 2100 m^3. In the first years of operation the plant supplied between 12 and 15% of the total demand (solar fraction), servicing 1250 households. In 1999, the year the current monitoring is carried out, the number of households connected was increased to 1350, the solar collector field extended with four rows to 9070 m^2 and a seasonal gravel storage taken into operation. The current work does not include the seasonal storage in the analysis due to the fact that the data is not available at the time of writing.

3.2 THE DATA ACQUISITION SYSTEM

Since 1996, the Marstal plant has been monitored by a permanent and rather advanced control system described in section 3.2.1. The data from this permanent acquisition system, for 1997, is used for first analysis of the plant performance and operation conditions, reported in (Heller, A. and Furbo, S., 1997). The rather novel control strategy at the plant is investigated and results presented in (Heller, A., 1998). First modelling and validation of the plant performance is reported by (Heller, A. and Dahm, J., 1999) supporting the need for further detailed data collection. These studies made it clear that the data from the permanent monitoring system was not sufficient for an exhaustive analysis.

In the summer of 1999, from May to September, a supplementary, temporary data monitoring is carried out. The data acquisition was based on a permanent and a temporary monitoring system. The schedule for the acquisition is as follows:

The whole supplementary monitoring project was carried out between May and October 1999 where measurements with 5-minutes intervals are applied, except for the periods 27/6-4/7-1999, 4/8-10/8-1999 and 22/9-24/9-1999, where 1-minute intervals are logged. On 7 August, the reference pyranometer was taken down since it was needed in another project. Some data

acquisition by an extended permanent system went on until November 1999 collecting with 1-minute-sample intervals.

The permanent system is described in section 3.2.1 and the supplementary data collection system in section 3.2.2. The latter consists of an extension of the permanent monitoring system, described in section 3.2.2.1 and a temporary system described in section 3.2.2.2.

3.2.1 The permanent monitoring system

The permanent monitoring and control system at the Marstal central solar heating plant consists of 4 control computers (PLC) connected to personal computers by a computer network. The computers squirrel the PLC's trough InTouch® terminal software. The monitoring system collects a large number of data controlled by events. This means that, if a data channel changes between a given scan interval, the channel data will be logged. In other types of acquisition systems, all channels are logged for every log interval. The force of the event-driven logging systems is the reduction of the data to be stored. The drawback is the rather complex task of deriving data from the database.

Each day the following data sets, files, are stored on the operator's computer:

- Detailed measurements of all measurement points in the system, by the InTouch® terminal software. It turned out that almost any kind of data is logged, but the plant operators do not exactly know what is logged. It is up to the consultants for the data acquisition system to make the data available to the operators. (Approximately 1.1 MB of data per day)
- Text file of selected, detailed measured data, generated by a report tool of the InTouch® terminal software. See Appendix C for an example. (Approximately 1.13 MB of data per day)
- Key-values for the plant performance and operation determined by a spreadsheet macro from the text files, mentioned above, and filed as spreadsheet file. See Appendix C for an example. (Approximately 92 KB of data per day)

As we see, the amount of data is overwhelming, and systematic approaches are needed to analyse the measurements which is partly accomplished in spreadsheet reports gathering the key values for the heat production and the system operation. →More work could be done on this subject to enhance operation safety and understanding of the complex system to improve it or the next generation systems.←

Unfortunately, the format of the InTouch® database is of a unique binary format, rather useless if the InTouch® terminal software is not available and extensive experience with the software is not available. →It is advisable to adopt systems that can be controlled fully by the operator and have no need for consultants.← Hence the current work is based on data collected in the text files generated by the InTouch® report tool. An overview of the data acquired is presented in the Appendices.

3.2.2 The supplementary, provisional acquisition system

The provisional acquisition system is partly an extension of the permanent acquisition system, described in section 3.2.2.1 and a transportable squirrel system, described in section 3.2.2.2.

3.2.2.1 The extension to the permanent monitoring system

To extend the ongoing acquisition at the Marstal plant with the missing measurements and an adjusted daily report with an acquisition interval of 1 minute instead of the default 5 minutes, a new database is defined in the InTouch acquisition system. In the extension data set, all the energy and mass flows in the system, and all the control values of the operation system are stored.

Due to the very large number of measuring points in the system, the description in this text is kept to the most relevant measurements for the current work.

It is worthwhile mentioning that the permanent monitoring is storing energy and mass flow data as accumulated values, while the extension data are stored as momentary values →A better alternative would be to apply integrated values over scan-interval time.←.

A definition of the data points can be found in the Appendices.

The accuracy of the equipment used in the monitoring system in Marstal is separately documented for every instrument in the system. →We found that there were missing or incomplete documentation for some of the equipment. This should be avoided and operators should require detailed documentation for all acquisition equipment.←

To get an overall insight of the accuracy of the applied sensors and measurement equipment, Table 1 gives a summary, drawn out of calibration data sheets and equipment documentation, where the ΔT is defined by the calibration test procedures.

Table 1. Specification for permanent monitoring equipment at the Marstal plant.

Measuring point	Equipment		Uncertainty
M501	Flow, Danfoss, DN125		±0.3 %
M502	Flow, Danfoss, DN100		±0.1 %
M503	Flow, Danfoss, DN100		±0.1 %
M103	Energy, Kamstrup, Maxical	ΔT=50	±0.3 %
M105	Energy, Kamstrup, Maxical	ΔT=50	±0.2 %
M102	Energy, Kamstrup, Maxical	ΔT=50	±0.3 %
M501	Energy, Kamstrup, Maxical	ΔT=50	±0.7 %
M502	Energy, Kamstrup, Maxical	ΔT=50	±0.9 %

Four pyranometers are applied in Marstal. These sensors are partly specified in Table 2. For all pyranometers of type "Soldata", the accuracy is defined by International Standard, (ISO, 1999) for "Class 1" type instruments with a demanded accuracy below 3 %. See section 3.2.2.3, for details about pyranometer accuracy.

Table 2. Equipment specification for permanent pyranometer measurements.

Identification no.	Calibration constant	Position
442	127 mV/(W m^{-2})	Row 8, close to reference pyranometer (north).
444	127 mV/(W m^{-2})	In centre of field.
105SP	155 mV/(W m^{-2})	Front of field (south).

Note: The pyranometer on the storage tank was defect under the supplementary measuring programme.

3.2.2.2 The GRANT® acquisition system

The temporary GRANT® acquisition system collects solar radiation measurements for the supplementary measurement equipment and the temperatures along one collector row. All data points are scanned every 5 seconds, and stored for every minute or with 5- or 1-minute intervals, depending on the date. The data point definition and channel allocations can be found in the Appendices.

For the current supplementary monitoring program, two sets of equipment were built up: 1) Solar radiation control and measuring. 2) Temperature measurements along a collector row. The position for the instruments is outlined in Figure 16.

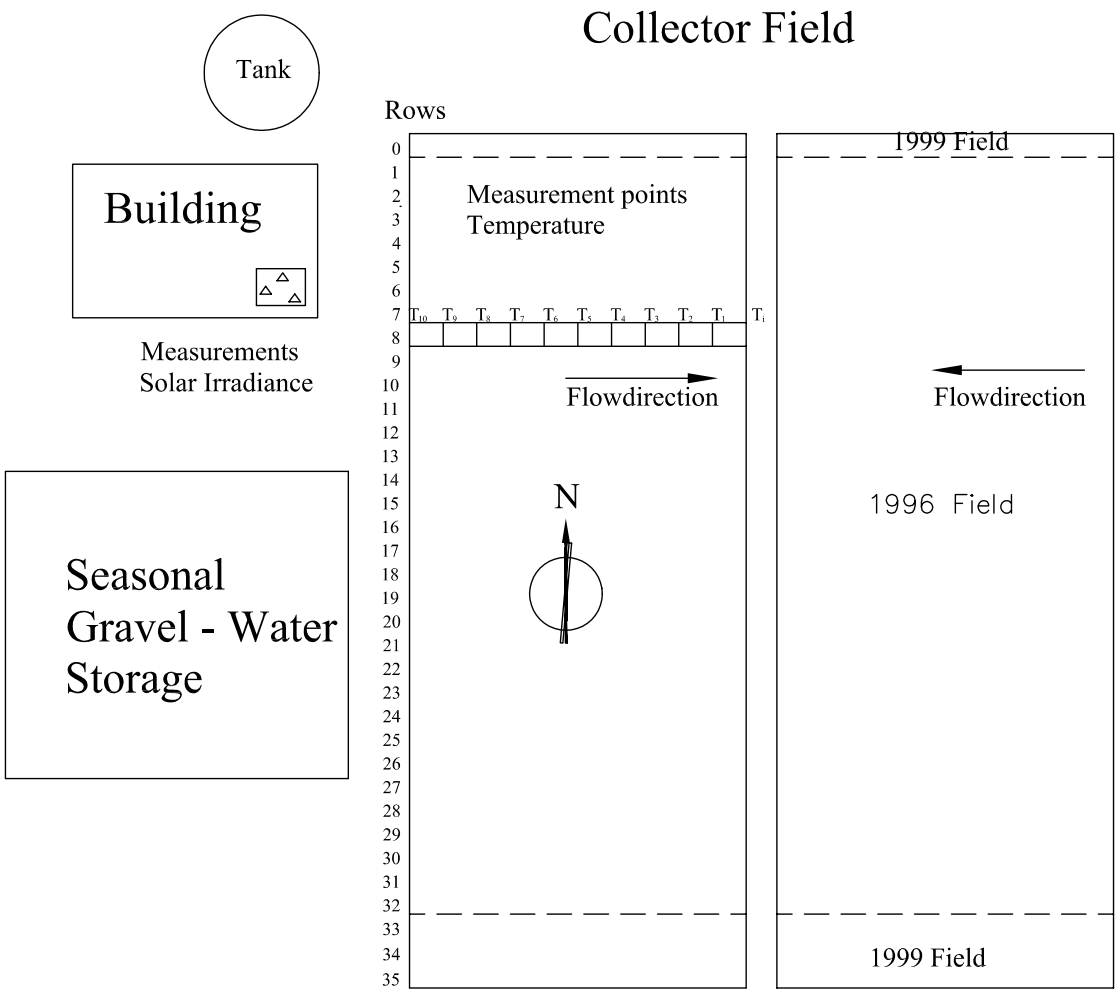

Figure 16. Supplementary monitoring equipment at the central solar heating plant in Marstal. Pyranometers are placed on the building roof (upper left corner of figure). Temperature measurements are carried out in row 8. The cold-water inlet to the row is placed at temperature point $T_{10,}$ and the hot outlet from the row in the centre of the field at temperature point T_i that is not measured explicitly.

Figure 16 outlines the layout of the Marstal solar plant. A steel tank storage (circle) is placed behind the operators building and a seasonal storage in front. On the building roof, pyranometers are placed and connected to the datalogger positioned in the building. To the right of the building, the collector field is ordered in two blocks of 36 rows, where row 0, 33, 34 and 35 are added in 1999. Temperature measurements are executed along row 8 which is

located in extension of the building. The flow direction is from the flank into the centre, where the hot water is collected from all rows and returned to the control building.

3.2.2.3 Solar radiation measurements

A photo of the pyranometers, placed on the building roof as shown in Figure 16, is presented in Figure 17.

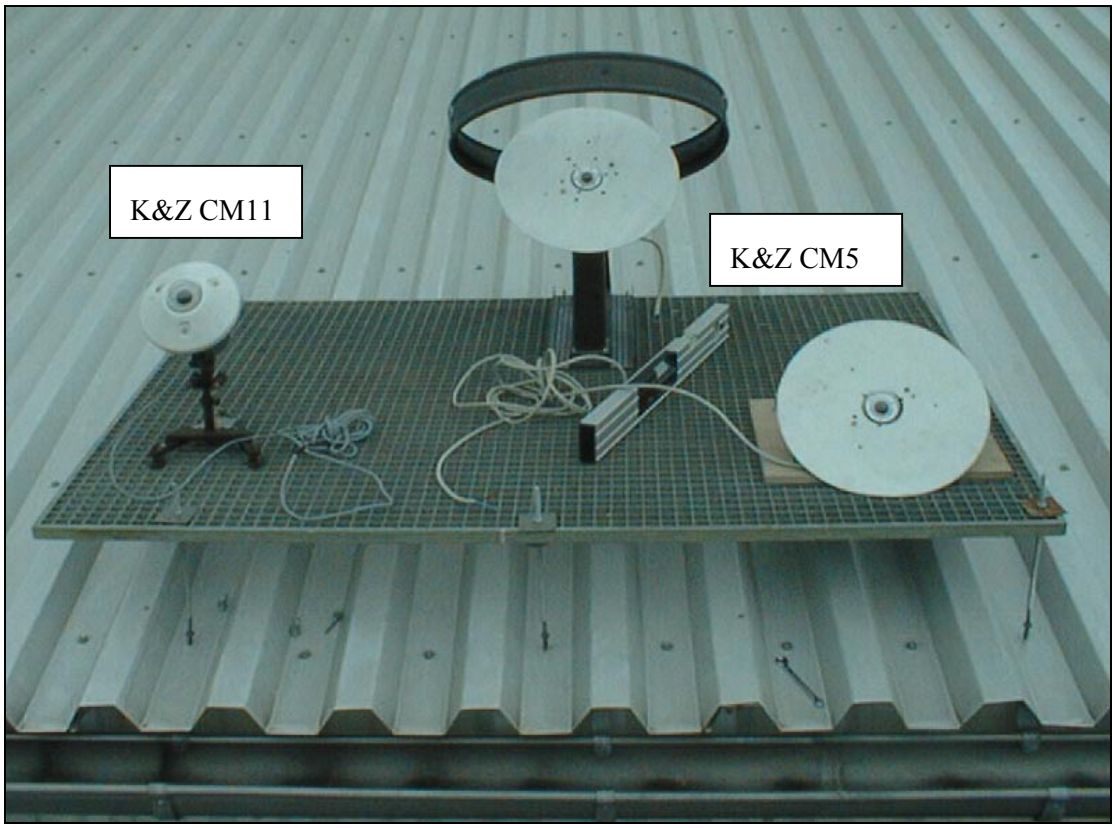

Figure 17. Set-up of pyranometers at the roof of the operation and control building for the Marstal plant. Reference pyranometer (left), diffuse radiation measurement at the back and direct radiation measurements (right, front).

Three pyranometers, as shown in Figure 17, are installed for supplementary monitoring;

1) A reference pyranometer of type Kipp & Zonen (K&Z) CM-5 pyranometer. This instrument is used for precision measurement to compare with all the other instruments.
2) A pyranometer of type Kipp & Zonen CM-11, for measuring of the global irradiation on tilt surface: (front right).
3) A pyranometer of type Kipp & Zonen CM-11, to measure the diffuse part of the solar irradiation on tilt surfaces: (at the back). The instrument is equipped with a shadow ring with a diameter of 46 cm and a width of 7 cm.

Measurement of solar irradiation is a rather complex task. Each type of instrument and each individual instrument have their own characteristics and uncertainties. To standardise these characteristics, the "World Meteorological Organization" (WMO) classified the pyranometer types into standards and classes, (WMO, 1983), as reproduced in the Appendices.

The instruments applied in the temporary monitoring system can according to this classification, be categorised as shown in Table 3. In this table, references to the accuracy of the instruments are cited. We find a rather large variety of accuracy estimations for the instruments.

Table 3. Equipment specification for provisory solar irradiation measurements at the Marstal plant.

Description		**References**
Type	Kipp & Zonen CM-11	
Identification no.	892540	
Calibration constant	4.51 μV/(W m^{-2})	
Total accuracy	± 2.5-3 %	(Ambrosetti, P., Andersson, H. E. B., Liedquist, L., Fröhlich, C., Wehrli, Ch., and Talarek, H. D., 1984)
	± 1.5 % (max. ±5 W/m^2)	(Hilmer, F., 1996)
	± 2.2 %	(Overgaard, L. L., 1998)
Total irradiation		
Type	Kipp & Zonen CM-5	
Identification no.	773550	
Calibration constant	12.5 μV/(W m^{-2})	
Total accuracy	± 3 %	See Table 1, K&Z CM-6.
	± 3 %	(Dalenbäck, J-O., 1993)
	± 2-3 %	(Ellehauge, K., 1993)
Diffuse irradiation		
Type	Kipp & Zonen CM-5	
Identification no.	742216	
Calibration constant	10.8 μV/(W m^{-2})	
Total accuracy	See above, shadow ring must be adjusted properly.	
Shadow ring	Diameter of 46 cm. Width of 7 cm.	

Based on the accuracy classifications by the WMO, the estimations cited in Table 3 and last but not least on the help by the colleague Hans Lund from the Dept. of Buildings and Energy, the K&Z CM11 pyranometer was applied as reference for the testing of the other pyranometers. For the K&Z CM5 pyranometer, applied for global and diffuse irradiation measurements, the overall accuracy is in this work assumed to lie 0-2% above the precision of the CM-11 instrument, hence 3-5% uncertainty.

3.2.2.4 Temperature monitoring along a collector row

The temperature profile along a collector row is measured for validation purposes but also to get a documented insight in the temperature evolution along the row. The temperature sensors are placed in row 8 as shown in Figure 18 (se also Figure 16).

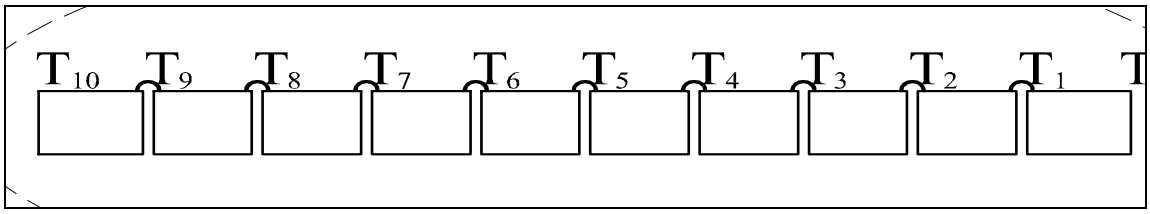

Figure 18. Close-up on row 8 with temperature measurements. Note: Flow direction in row 8 is from T_{10} to T_1.

Note: Temperature measurement plots can be found in the figures of Section 4.3.

All temperatures in row 8 are measured by copper/constantan thermocouples (Type TT) that are placed in the connection pipe between the collector modules as shown in Figure 19.

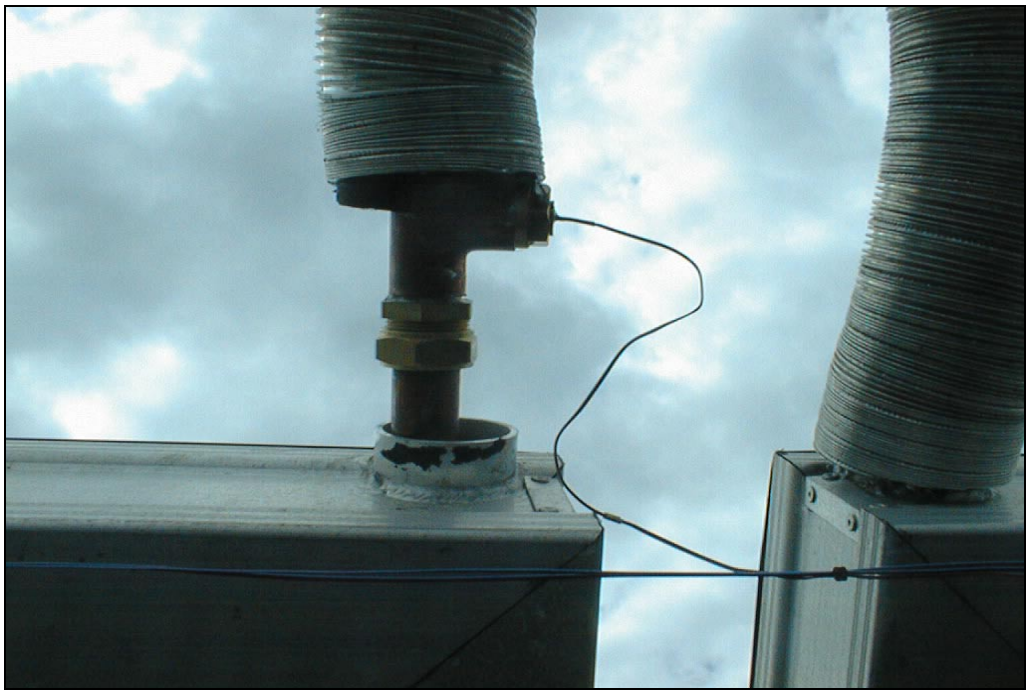

Figure 19. Photo of temperature sensors placed in the connection pipe between two collector modules.

Figure 19 illustrates the connection between two collector modules. We see that flexible piping insulates the flow pipe. On the left side of the connection, the measuring point is visible as a T-piece where the wire exits. Note that the connection is insulated after installation of the sensor. A close-up is sketched in Figure 20.

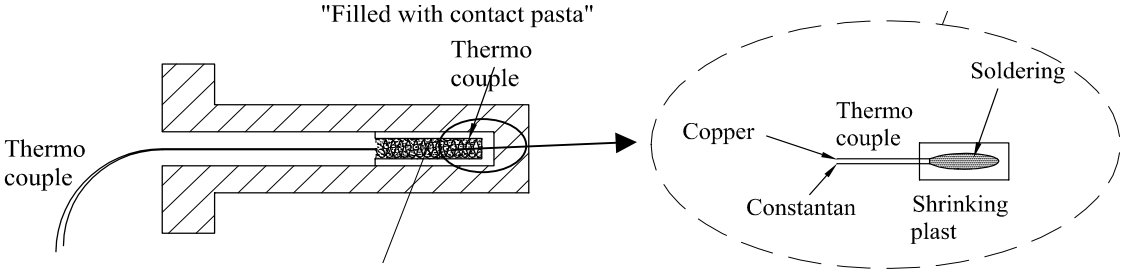

Figure 20. Temperature sensor design for provisory measurements in collector rows. The TT-type wire is formed into a spiral to enlarge the contact length for the sensor and hereby to ensure constant thermal influence and accurate measurement results. The contact between cartridge case and sensor wire is ensured by thermal pasta. To the right is a close-up of the end of the thermocouple where the two wires are soldered.

The thermocouple produces an electric potential logged as digital values by the Grant datalogger, where the thermocouples are mounted into special input sockets that again are mounted in an isothermal block, so that their temperature can be measured by a thermistor. Hence, this method involves a datalogger internal reference. This is the case for channel 1-8 in the given data set-up. For the remaining channels 9-13, the datalogger is not able to convert. Hence, an external cold junction reference has to be used, and explicit conversion between voltage and temperatures is to be applied. For this conversion, the correlation of the voltage and the temperatures are presented in standard tables, given for typically a reference temperature of 0^oC. Using an ice-bath for the reference, the table values can be applied directly for the conversion.

In the current measurement set-up, the reference temperature is found for a massive lead block, placed close to the datalogger. Hence, the reference is not at zero degrees, and this must be taken into consideration. Physically, this is done by placing the cold junction in the lead block and measuring the temperature of the lead block by one of eight channels with internal references described above. By these means, we know the temperature of the lead block and the corresponding voltage value for this temperature. Knowing these reference values, we are able to find the temperatures for the voltage channels 9-13 by the above-mentioned tables, and also by recommended power polynomials given in general by the expression:

$$T = a_0 + a_1 x + a_2 x^2 + ... + a_n x^n \tag{3}$$

Inserting the coefficients, a_i, given in literature, we find the corresponding temperatures from the voltage value, x.

At the Department of Buildings and Energy, a 3rd order power polynomium is developed by Thomas Lund Madsen for such conversion (unpublished), leading to the following algorithm:

$$\begin{aligned} T_m &= T_{ref} + 12.95 \cdot S \\ T_d &= S \cdot \left(25.9 - 0.06 \cdot T_m + 0.00027 \cdot {T_m}^2 - 0.000001 \cdot {T_m}^3\right) \\ T &= T_{ref} + T_d \end{aligned} \tag{4}$$

where T_{ref} is the measured reference temperature in ^oC,
S measured potential in mV.

We find that a reference temperature, T_{ref}, is involved in the algorithm by Lund Madsen. Assuming this reference to lie at zero degrees, we can compare the values with the standard tables, e.g. the "Handbook of Chemistry and Physics", 55th Edition, or "Thermocouple Reference Tables, Based on the IPTS-68", NBS Monograph 125.

To compare the accuracy of the Lund Madsen algorithm the results from the method is compared with table values for the temperature ranges and reference temperatures relevant for

the current work, which are conversions in the temperature range of 0-100°C with reference temperatures at 0, 10, 20 and 30°C. Due to the fact that the tables are given for zero degrees reference temperature only, voltage difference between actual reference temperature and zero degrees are computed for comparison. This is in the following done by subtracting the voltage value for the reference temperature (table value) from the voltage value for the actual measured value. This difference is then inserted into the Lund Madsen algorithm to find the corresponding temperature. In the following table, the table values are shown together with the absolute deviation for the Lund Madsen algorithm for the relevant reference temperatures:

Table 4. Accuracy for the Lund Madsen algorithm for voltage to temperature conversion of measurements with thermocouples, using different reference temperatures. Source: "Thermocouple Reference Tables, Based on the IPTS-68", NBS Monograph 125.

Voltage	Temperature	Absolute Temperature Deviations			
[mV]	[°C]	Tref=0	Tref=10	Tref=20	Tref=30
0.400	10.23	-0.01	0.23	0.26	0.08
0.800	20.26	0.01	0.24	0.26	0.08
1.200	30.09	0.06	0.26	0.27	0.09
1.600	39.73	0.11	0.30	0.29	0.10
2.000	49.18	0.16	0.33	0.30	0.10
2.500	60.74	0.22	0.36	0.31	0.09
3.000	72.06	0.31	0.41	0.33	0.09
3.400	80.95	0.38	0.46	0.36	0.10
3.800	89.71	0.48	0.53	0.41	0.13
4.300	100.48	0.62	0.64	0.49	0.19

From Table 4 we find that the deviation between table values and the Lund Madsen algorithm is below 0.64K. In the current case, the reference temperature placed in the lead block had a temperature in the range of 20-30°C. We find from the table that the deviation in this range lies below 0.5 K.

The overall accuracy for measurement of temperature in flows by applying thermocouple covered in cartridge cases is estimated in Table 5.

Table 5. Accuracy estimates for temperature measurements.

Temperature		
Type	copper-constantan thermocouple Type TT	
Accuracy	±1 K	(Hilmer, F., 1996)
	±0.5 K	(Ellehauge, K., 1993)
		(Furbo, S., 1983)

We find from Table 5 that the accuracy is estimated differently in literature. →Based on different calibration of instruments at the institute, an accuracy of 0.5K is seen as most probable for the direct measurements resulting in an accuracy of 0.7-1K for the temperature measurements involving voltage-to-temperature conversion.

4. DATA CONTROL AND ANALYSIS

The monitoring of the Marstal solar plant is a rather unique opportunity with an enormous potential for collecting experiences with such plants. One objective of this report is to share these experiences.

In this section the most relevant findings are summarised partly from publications by the author and others in (Heller, A. and Furbo, S., 1997), (Heller, A. and Dahm, J., 1999) and (Heller, A., 1998).

After introducing pre-processing of the collected data, the accuracy of the permanent pyranometers at the Marstal plant and the influence on the control strategy applied, is investigated and discussed in section 4.2. Note: The control strategy is discussed in Chapter 8. The temperature development along the monitored collector row is then presented in section 4.3 followed by some concluding remarks on monitoring in section 4.4.

4.1 PRE-PROCESSING OF DATA

Before using the measurements from the two acquisition systems, the data had to be pre-processed in a number of ways.

The Grant® data channels, measuring potentials, had to be converted into the proper temperature units by the procedure described in section 3.2.2.4 and the corresponding channel data to solar irradiance units by the relevant calibration constants for the individual instruments shown in Table 3 section 3.2.2.3.

Due to the fact that the timer in the two acquisition systems was not synchronised, the data of the Grant datalogger was adjusted to the InTouch® system by simply 'moving' the data in time.

4.2 SOLAR IRRADIATION MEASUREMENTS

To ensure accurate data monitoring with the provisory solar radiation instruments, a reference pyranometer of type Kipp & Zonen (K&Z), Type CM-11 is installed for the first acquisition period, from June to the 5th of August 1999. Hereafter the instrument is taken down, to be applied in another site. After the 5th of August, the two K&Z CM-5 instruments for direct and diffuse irradiation measurements are the most accurate instruments in the set up.

4.2.1 Accuracy for temporary installed pyranometers

In the supplementary measurements, two K&Z CM-5 instruments measure the total and the diffuse part of the solar radiation. For controlling the instrument measuring the total irradiance, a reference instrument of type K&Z CM-11 is installed in addition in the period from June to the 5th of August 1999. All instruments are adjusted in the same orientation (south) and tilt angle (40^{o}, as the solar collectors).

In Figure 21 the radiation data from two half-days, measured in 1-minute intervals are presented. This data is chosen to give a good insight into the deviation between the CM-11 and CM-5 values.

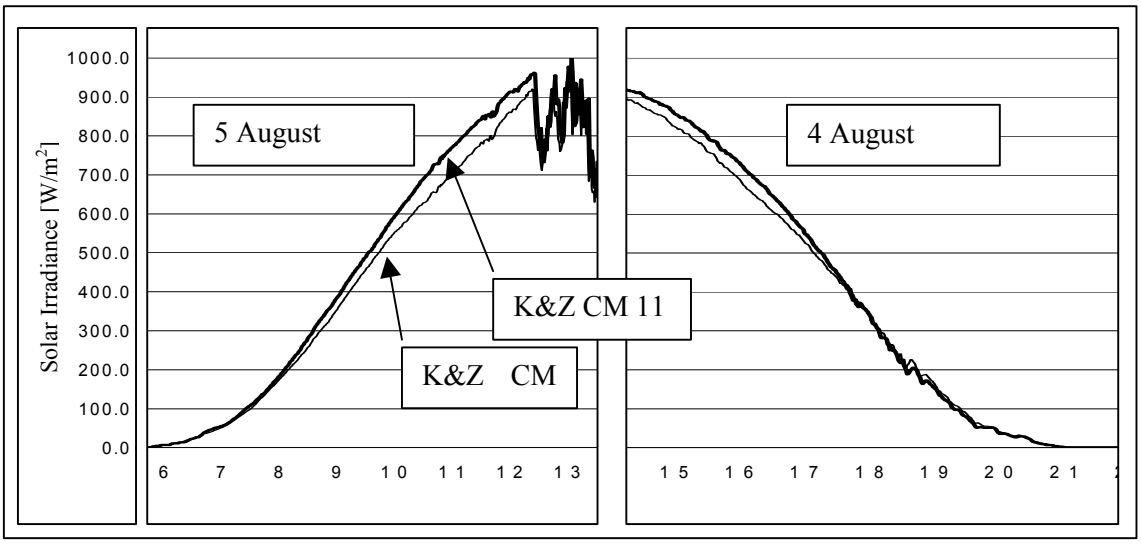

Figure 21. Measured solar irradiation at CSHP of Marstal: Reference pyranometer, K&Z CM-11 contra CM-5 (Total).

From Figure 21 it can be seen that there are rather large deviations between the two sets of measurements and that the deviation is larger before noon than after noon. This indicated that the two instruments were not orientated perfectly, in spite of great efforts to get the installation right. →It turns out that the placing and orientation of pyranometers is a rather demanding task. A procedure for this task is necessary to avoid errors.←

For further comparison of the measurements data from two days are chosen as cases.

Date	Description
30 June 1999	High and non-steady solar irradiance.
22 September 1999	High and steady solar irradiance.

The total solar irradiance for the two chosen cases is shown in Figure 22.

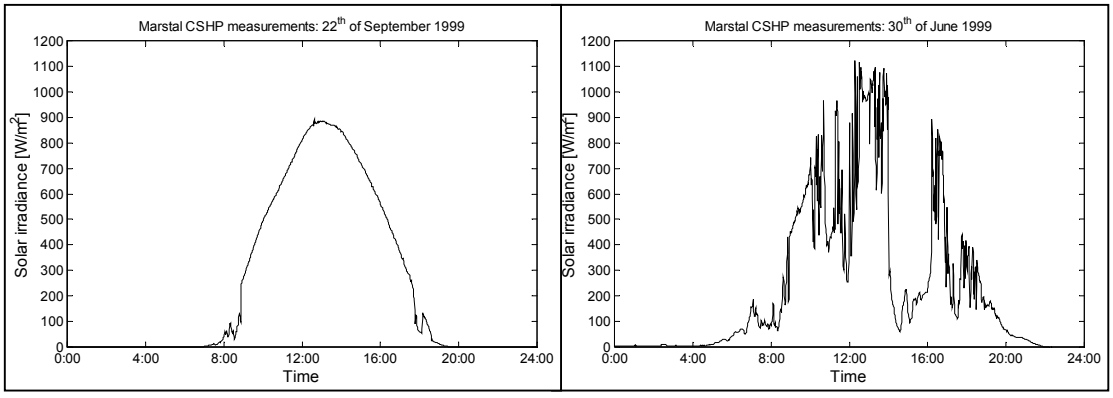

Figure 22. Measured total solar irradiance at a 40 degrees tilt surface for 2 days:

1) A day with high and steady solar irradiance (left).

2) A day with high but fluctuating solar irradiance. (right)

Due to its simplicity, the first case will be used to get a better understanding of the matter. The second case is applied when checking the observation from case 1 for non-steady conditions.

Among many others (Ambrosetti, P., Andersson, H. E. B., Liedquist, L., Fröhlich, C., Wehrli, Ch., and Talarek, H. D., 1984) estimates the long term error for total irradiation measurements to be below 3%. Plotting this maximum error estimate together with the absolute deviation measured we find the following plot.

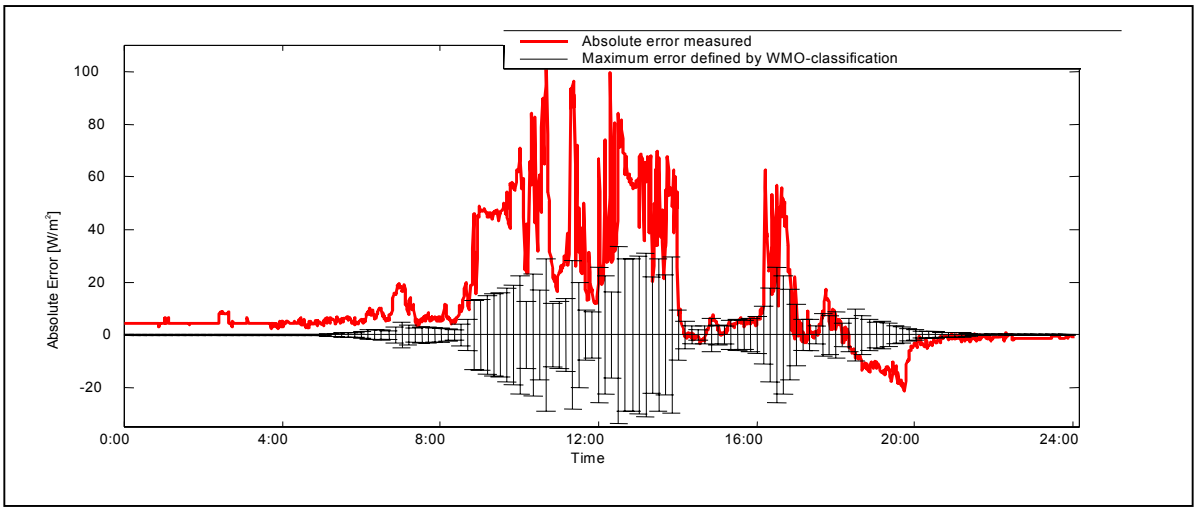

Figure 23. Measured solar irradiation at CSHP of Marstal: Maximum error by First Class instruments, based on WMO-classification (WMO, 1983) contra absolute deviation between CM-11 K&Z CM-11 and CM-5 values for the 30th of June 1999.

We find from Figure 23 that the deviation between the applied instruments is larger than estimated by Ambrosetti and by Andersen.

The absolute deviation for the 22 September 1999 is plotted in Figure 24.

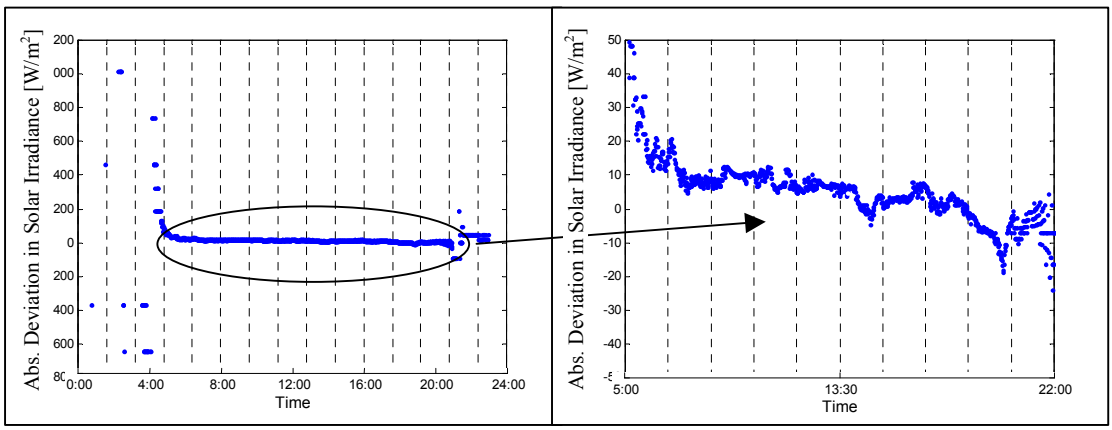

Figure 24. Measured solar irradiance at CSHP of Marstal: Absolute deviation between K&Z CM-11 and CM-5 values of total irradiance on 30 June 1999.

It becomes clear that there is a systematic decreasing error from the left to the right which supports the above-mentioned hypothesis that the two instruments are orientated differently. This error can be eliminated by correcting the values from the K&Z CM-5 instrument by a regression approximation based on a linear approximation of the shown deviation of the data from 22 September 1999 and controlled by other data sets. We find corresponding error estimation after correcting with the linear regression approximation as shown in Figure 25.

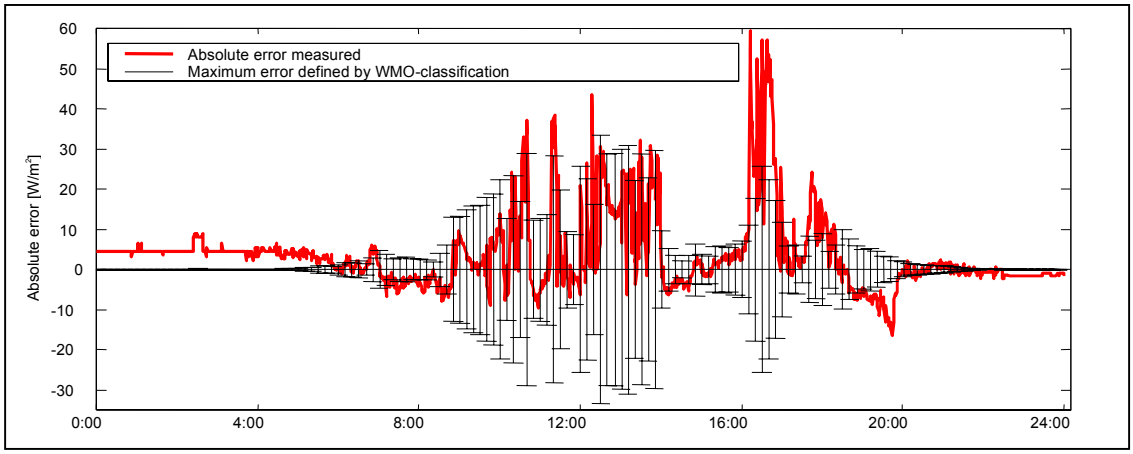

Figure 25. Absolute error between K&Z CM-11 and CM-5 measurements contra maximal absolute error estimated in literature for First Class instruments.

We see clearly that the absolute deviation is now closer to the estimated accuracy for such measurements. However, a number of peaks are still outside the necessary precision. The most realistic explanation for these peaks is the different dynamics for the two instruments, which gives a response time deviation of almost the same length as the data sample intervals.

4.2.1.1 Conclusions for the accuracy of the temporary pyranometers

The current analysis showed orientation errors for the instruments applied in the set up. This proves that the positioning of pyranometers can be very tricky and a procedure to ensure the exact set up must be developed.

The error due to orientation can be corrected by simple means. Hereby the error is reduced to some dynamic errors caused by the instruments themselves.

Based on the presented analysis we will in the following, apply the measurements from the K&Z CM-5 instrument with correction for the control of the other permanently installed instruments applied at the CSHP in Marstal. The overall uncertainty for the resulting findings is approximately 3% for steady solar periods, and up to 5% for fluctuating solar conditions.

Note: The rather large errors found in the morning and evening hours will not affect an overall plant evaluation in any significant way, due to the fact that the solar irradiation is very small for these periods and hereby the error minimal.

4.2.2 Accuracy of permanent pyranometers applied in Marstal

At the Marstal solar plant, 4 pyranometers are installed as shown below.

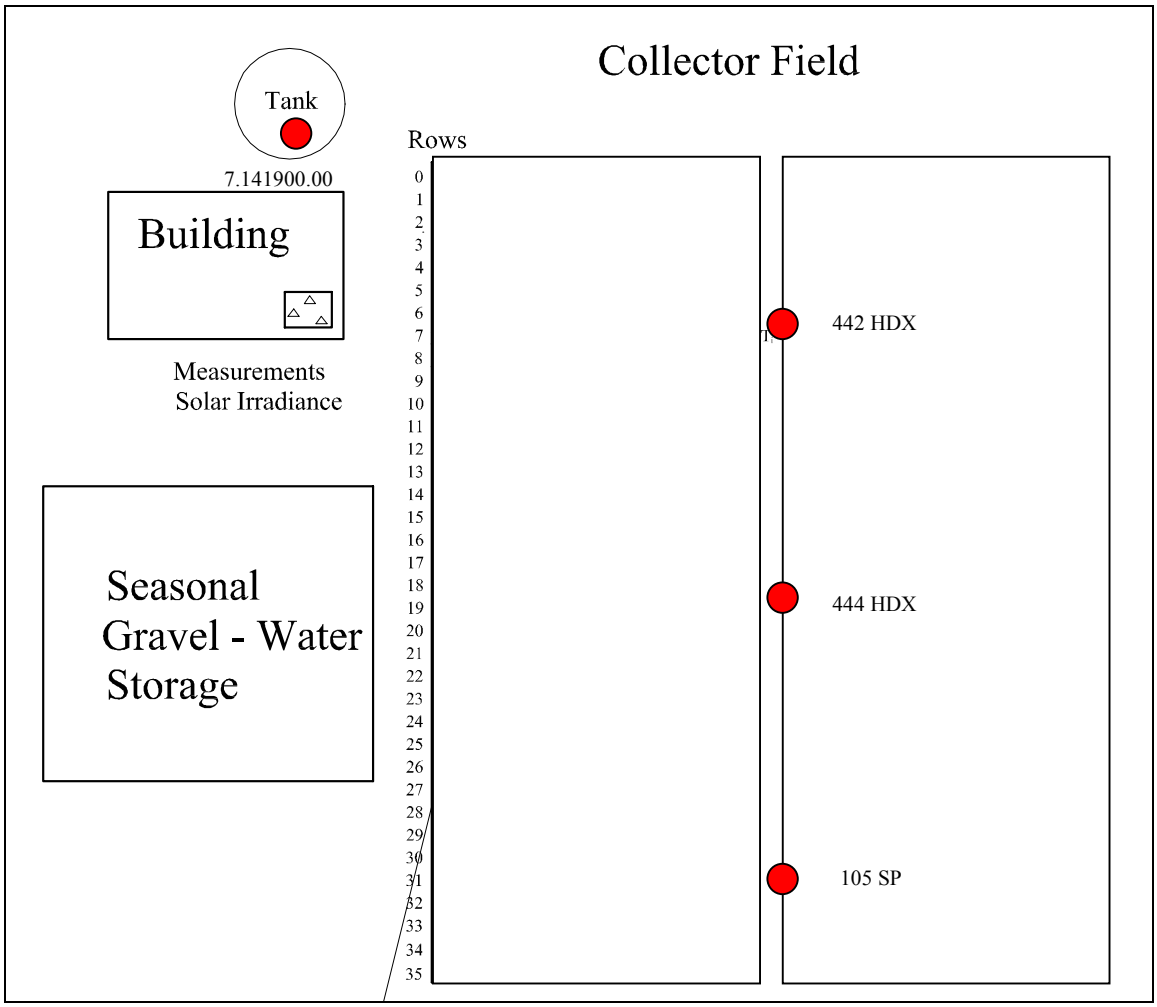

Figure 26. Pyranometers (Circles) placed at the central solar heating plant in Marstal.

The positions of the instruments are shown in Figure 26, one placed on the top of the storage tank, and three spread in the collector field.

The first instrument, a Silizium-fotoelement, type 7.141900.00, was damaged during the current project. This is surprising due to the fact that the instrument is approximately 4 times more expensive than the other instruments applied in the set-up. More relevant for the current project is to extract that the instrument lost its accuracy already in the first year of operation becoming useless after approximately 2 years of operation. The current project is not in a position to judge the quality and applicability of the instrument type in general. →However, it is the place to conclude that unstable instruments with such a performance cannot be applied on any kind of solar systems.←

The remaining three instruments of the brand SOLDATA are also Silizium-fotoelements. They are installed along the centre line collector field. Two types of instruments are applied: 1) A photocell with glass-couple (Label: 105SP) 2) Two instruments with flat cover glass cover (Label: 442HDX and 444HDX). In the following, we will compare the accuracy of these instruments with the measurements with the K&Z CM-5 instrument.

The values of the different instruments cannot be visualised in a reasonable manner in one single plot. However, in Figure 27, an attempt is made to show the accuracy of the instruments on 22 September.

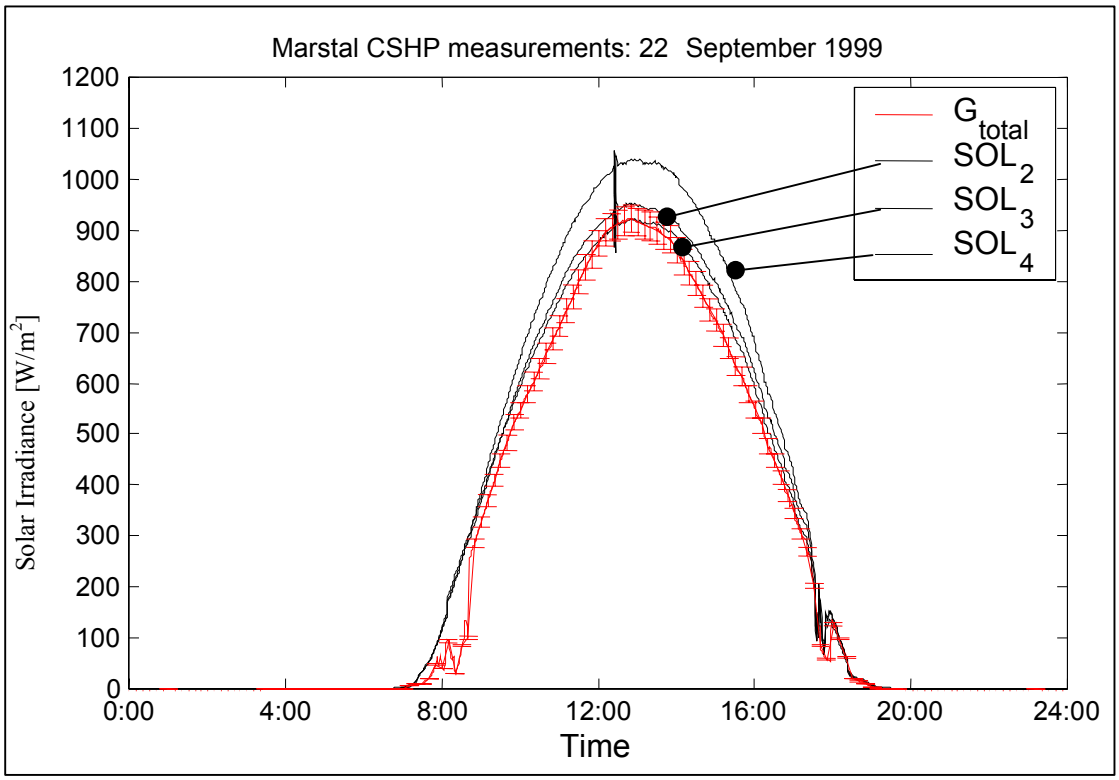

Figure 27. Measured solar irradiance at CSHP of Marstal: Total solar irradiance measured with a K&Z CM-5 instrument, G_{total}, is plotted with the error band of 3% found above for a stable sunny day. Measured solar irradiance with the permanently installed instruments of type SOLDATA.

From Figure 27, we can conclude:

- The SOLDATA-instruments give values that, during the whole of the solar period, lie outside the 3%-tolerance of the CM-5 instrument represented in the figure by the error-bars.
- The two instruments SOL_2(442HDX) and SOL_3 (444HDX) produce similar values for the total irradiance with an approximate deviation of 3%.
- The third instrument SOL_4 (105SP) produces very different values for the total irradiance than the other instruments.

From these observations, we can conclude:

1. The precision for SOLDATA-instruments of the type HDX can be expected to reproduce total solar irradiance with accuracy acceptable for 'Second Class' instruments of the WMO-classification, (WMO, 1983).
2. The precision for SOLDATA-instruments of the type '105SP' cannot be expected to reproduce total solar irradiance with accuracy acceptable for 'Second Class' instruments of the WMO-classification, (WMO, 1983).
3. All SOLDATA-instruments show rather poor performance for low solar irradiance.
4. The applied fourth instrument of brand THIES Clima, type 7.141900.00, is the most expensive instrument in the set-up. Measurements show a severe deterioration already after a period of one-year rendering the instrument useless after 2 years of operation. The current

project is not in a position to judge the instrument type in general, but the currently applied instrument is unacceptably poor in performance, and it cannot be recommended as an instrument for solar application before it has proved stable.

5. The SOLDATA-instruments are not accurate enough to be applied for validation of mathematical models of solar systems. Hence, supplementary measurements are necessary if one applies such classified instruments at solar applications. This furthermore means that the validation published by (Heller, A. and Dahm, J., 1999) is based on weak irradiation data that may be less accurate.

4.2.3 Influence of pyranometers on control strategy

The operation of a solar heating plant is in all large systems based on the solar irradiance in some way. This irradiance is measured by sensors as discussed above and therefore the operation and control strategies for such solar systems depend on the performance of these sensors.

In most solar heating plants, the flow in the collector loop is controlled by on off of the pump/s involved. In this case, the solar irradiance is used to determine the start-up of and the shut down for the pumps in the collector loop. If the solar irradiance is above a certain threshold (e.g. 100 W/m^2) the pump is on, otherwise it is off. For such plants the uncertainties of the pyranometers are as follows:

1) In the mornings and evenings, the Soldata-pyranometers showed rather large uncertainties. This will lead to rather large control-difficulties in the on-off control strategy. In earlier work the author showed that this phase is not critical for the overall performance of a central solar heating plant, the consequences of the discussed measuring uncertainties are very limited.

2) During the periods with solar irradiance above the threshold, the pump is running (on) and the control strategy is not affected by the uncertainties of the solar sensors.

The solar plant in Marstal is operated differently. Here the operation for sunny periods (summer) is controlled to obtain constant and high temperatures back from the collector field. Adjusting the flow rate in the solar loop does this. Two influences are to be considered while controlling the return temperature: 1) The solar irradiance. 2) The time-delay in the solar loop: This is the time from the entering of the medium into the collector loop until the time where the same medium is back at the starting point. In the Marstal case, the circulation time is up to one hour. If the flow rate is controlled on the return temperature at the outlet, the reaction on the given conditions would be up to one hour late. Hence, the control strategy must take this delay into account.

The strategy applied at the Marstal plant is designed for this purpose with no references to lean on. The algorithm is as follows: From the four possible measurements, the highest and lowest values are excluded to eliminate possible extreme measurements (e.g. due to shading). The average of the remaining two instruments is chosen to represent the current total solar irradiance value representative for the collector field. This final value is then applied in the algorithm described in 2.5.5. We find that the solar irradiance measured too low will lead to delayed start-ups and to overestimated flow rates. The opposite is the case for measurements with too high solar values. We can summarise some conclusions:

As determined above, one of the four installed pyranometers was damaged and one pyranometer measured unrealistic high values. Hence, the algorithm described has only the three SOLDATA instruments for controlling. As shown in Figure 27, the different type of instruments leads to systematically different values. This leads consequently to the exclusion of the instrument most different from the others which was not desired by the designers.

Based on this experience it is recommendable:

→If the control strategy of a solar plant is similar to the strategy in Marstal, the involved pyranometers must be of similar brand and type.←

→If one of the instruments is installed for validation purpose of the other instruments, this reference instrument should not be included in the control algorithm, or the algorithm must be adjusted.←

→The case proves the necessity of a quality assurance and maintenance procedure for large solar plants, to be discussed in other publication by the author.←

4.3 TEMPERATURE DISTRIBUTION IN A COLLECTOR ROW

In the current monitoring programme, the temperature along a solar collector row is measured. Here some plots are presented and discussed. In the following two graphs, the solar irradiance and temperatures along row 8 are plotted for a day with very nice stable solar conditions (22 Sept. 1999).

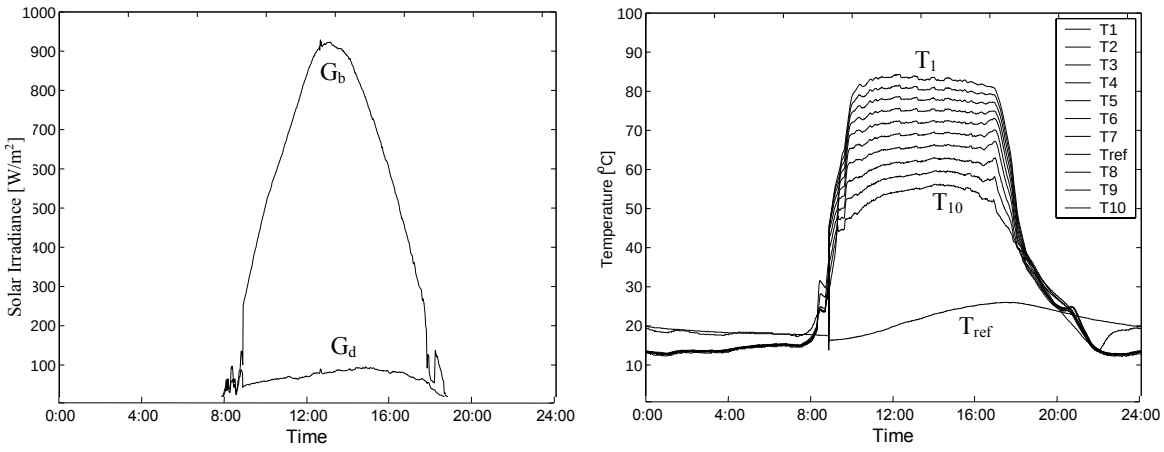

Figure 28. Solar irradiance (direct, G_b and diffuse G_d) and temperature distribution in a solar collector row for a nice sunny day (22 Sept. 1999). Flow direction from T_{10} to T_1. Note: Scan Interval is one minute.

As we expect for a stable, sunny day as shown in Figure 28, the temperature rises in the morning to an almost constant, high temperature and then drops in the evening. From the figure we can also extract the ability of the algorithm to keep the constant outlet temperature from the solar field. By zooming in to the top temperature of Figure 28, we find the upper most temperatures at the outlet of the row and between the collector modules from Figure 29.

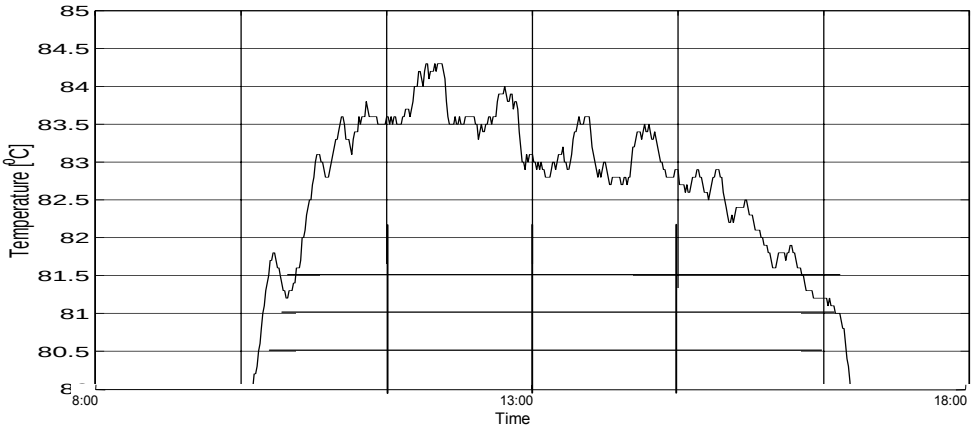

Figure 29. Return temperature from the collector field. The control should keep the temperature to 82 degrees Celsius. Note: Scan Interval is one minute.

The control strategy is to keep the temperature return from the collector field close to 82°C. We find that the temperature is kept around one degree too high which compensates for the heat losses in the piping back to the plant. We find that the strategy keeps the temperature stable with approximately 1.5°C tolerance. This is a reasonable result.

For an unstable, sunny day, the temperatures along the row are as shown in Figure 30.

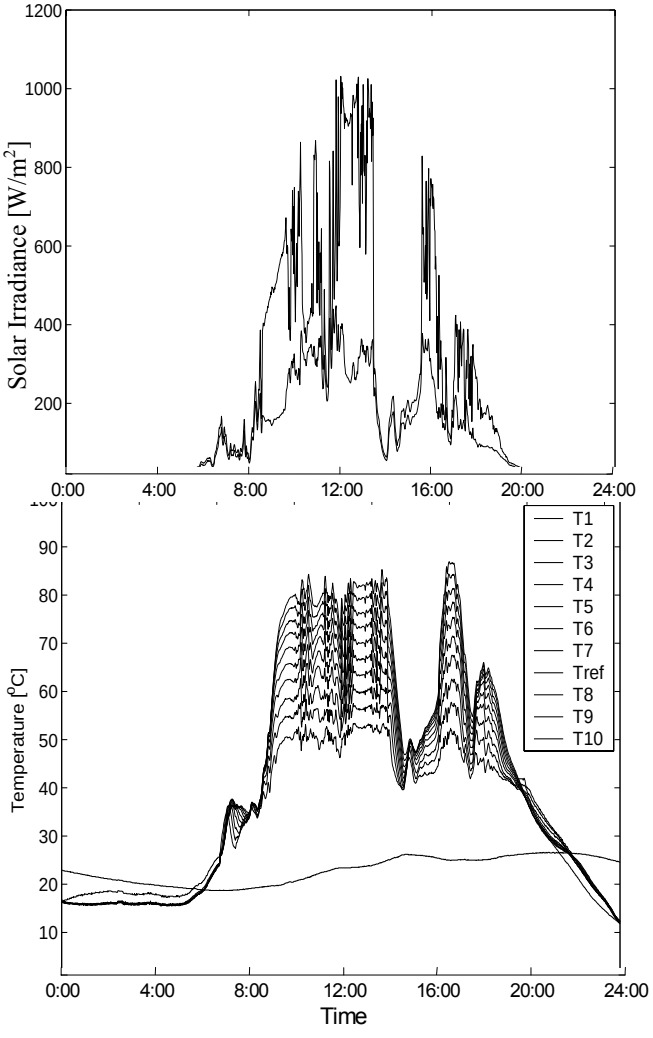

Figure 30. Solar irradiance (direct, G_b and diffuse G_d) and temperature distribution in a solar collector row for an unstable, sunny day (30 June 1999). Flow direction from T_{10} to T_1.

From the rather confusing plots in Figure 30, we are able to extract a number of things:

In the very early morning, the solar irradiance is increasing, resulting in a temperature rise in all temperature sensors. The solar power is too small to keep the temperature up at the outlet which causes the stop of the pumps again at a little before 8:00. We see that the temperature at the inlet decreases due to cold water supply to the row. This temperature drop spreads in the row as time goes. At the end of this process, approximately after one hour, the temperature in the whole row is increased from 25 to 30 degrees Celsius.

For the first half-day, the control strategy is trying to keep the temperature back from the collector field close to a constant value. This is the case only at the end of this period due to the strong fluctuation in the solar irradiance. However, the strategy stabilises the temperature in comparison with a strategy that is only able to turn the pumps on or off.

For a very strong fluctuating irradiance, around 14:00 the strategy is not able to keep the temperature stable.

In the evening, we find that the temperature decreases rapidly, keeping down. This is a perfect close down of the collector loop with cold supply temperature in the whole row, not leaving any energy unutilised.

The plot above indicates that the temperature differences between the modules are higher in the cold end of the row, decreasing along the row. This is to be expected due to the decreasing efficiency of the collector for high temperatures. Looking closely at these temperature differences, we find the values arranged in Figure 31 for the observation in a stable period.

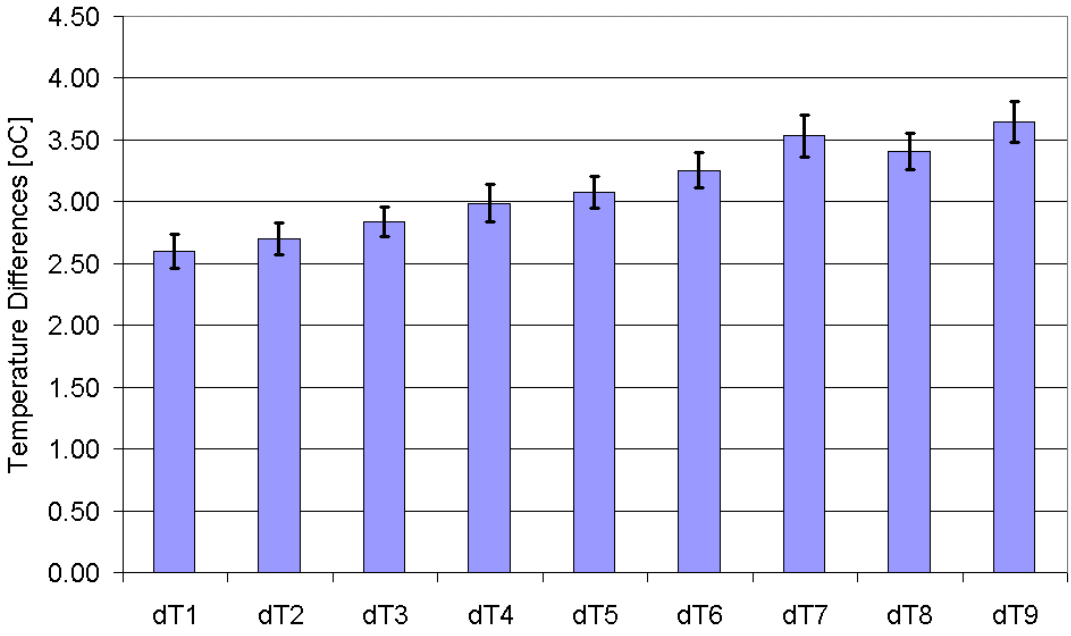

Figure 31. Mean values for temperature rise over solar collector modules for the sunny hours of the day 22 June 1999.

We find from Figure 31 that the mean temperature raise over the collector is largest at the inlet (dT9) decreasing to the outlet (dT1). We note also that there are some outliners for this conclusion for dT7 and dT8. The involved temperatures T8 up to T10 are measured in voltage to be converted into temperature values. Hereby a systematic uncertainty is introduced. The corresponding accuracy for the measurement and conversion is estimated to be at a level of 0.5 K. The above plot shows that this estimate may be rather high, and an uncertainty near 0.2 K would be more realistic. However, we find that the temperature rise at the inlet of the row is

approximately 1 K higher than at the outlet. This can be explained by the decreasing efficiency for the collector with high temperatures. For low collector temperatures at the inlet, the temperature difference to the ambient is low and the heat loss therefore low. Assuming an ambient temperature of 20 °C, a solar irradiance of 900 W/m^2 and a mean absorber temperature of 30 °C for the inlet module, we find an apses-value of 0.033. From Figure 8 we read the efficiency for this apses-value to approx. 0.6. At the outlet, the high temperature in the collector leads to high heat losses. Hence, the temperature rise will be lower than for modules at the inlet of the row. We estimate from Figure 31 that the temperature rise in the first module (right side of plot, due to flow direction) is 3.6 K with the found efficiency of 0.6. For the last module and an efficiency of 0.4, we find a temperature rise of $\Delta T_{10} = 3.6K \frac{0.4}{0.6} = 2.4K$ which is 1.2 K lower. This corresponds to the 1K value found above under the actual circumstances. For the maximum increase of temperature over the row in early summer of 50K, the difference in temperature rise over a module can be estimated to 1.7K by the same assumptions.

The above temperature plots are well suited to find the time for the fluid to pass the whole row. We see that the time when the first temperature sensor increases to the time where the outlet sensor follows is from 8 to 15 minutes dependent on the flow rate. In the start-up stage in the mornings, this time is even up to 30 minutes. With maximum flow rate this reaction time is 8 minutes, and for low flow rates above 15 minutes. Adding the time for the medium to move from the plant to the collector field and back, the traverse-time for the medium can be up to 1 hour. Considering this, the control strategy is doing a reasonably good job.

From the same data we see that large peaks of solar irradiance is influencing the whole collector row at once, but that the peak-shape response in temperature is flattened considerably at the high temperature end of the row. Here the efficiency of the collector is much lower due to the high medium temperature. Hence, a strong fluctuating solar irradiance will not affect this part of the row as much as at the cold end part. This is a general finding for a collector row: The longer the row, the more stable the solar production. On the other hand the more mass involved, the more power used for pumping.

A final relevant observation is the fact that the temperature at the inlet of the row increases after the collector loop is closed down. This behaviour is due to the placement of this sensor in the building which is supported by the fact that the reference temperature is at the similar temperature.

4.4 CONCLUSIONS

The findings and conclusions found concerning the monitoring programme are summarised here. Some of the findings and recommendations support the recommendations by (Ambrosetti, P., Andersson, H. E. B., Liedquist, L., Fröhlich, C., Wehrli, Ch., and Talarek, H. D., 1984):

- It is recommendable to apply 'Secondary Standard' instruments for testing with an estimated accuracy close to 1% [4].
- It is recommended to apply 'First Class' instruments for model validation procedures and quality assurance assessments.

[4] Note: (Ambrosetti, P., Andersson, H. E. B., Liedquist, L., Fröhlich, C., Wehrli, Ch., and Talarek, H. D., 1984) estimates an uncertainty due to "the calibration procedure and the day-long variability we can expect an overall accuracy of ± 2.5 to 3% for the measurement of global irradiance in solar energy applications." This very high estimate differs from the estimates of colleagues at our Institute and the Danish Solar Research Institute where an accuracy of 1-1.5% for 'Secondary Class' and 2.5-3% for 'First Class' instruments is used.

- All solar instruments require rather strict maintenance procedures to avoid moisture problems among other things.
- When buying pyranometers, the purchaser should obtain data sheets about the dependency of the instrument accuracy on e.g. orientation, tilt effects, linearity, response time and so on.

Moreover, it is relevant to summarise the following findings and recommendations:

- For on-line control strategies, 'Second Class' instruments can be acceptable in accuracy and a cheap solution.
- To ensure accuracy for measurements, some kind of quality checks must be scheduled in the quality assurance procedures for plants.
- To ensure usability of the often-overwhelming amount of data collected by a monitoring system, some form of automated data handling must be applied.
- Data acquisition systems should be chosen to give the operator full access to the specifications and data with no need for monitoring or computer experts.

In relation to the measurement we found:

- Measurement of solar irradiance is rather difficult if high accuracy is needed. The orientation of the instruments is a very demanding task and procedures to ensure the proper orientation are needed. In this work, corrections of measured values were necessary to rectify improperly positioned instruments. The resulting uncertainty for solar irradiance measurements was close to the uncertainty specified for the given instruments.
- Temperature measurements with thermocouple of type TT lead to uncertainties below 0.5 K for typical measurements in the range from –20 to 100^{o}C.
- The Lund Madsen algorithm leads to very accurate results in the range of –20 to 100^{o}C that lies below 0.5 K in comparison with the algorithm recommended by HP.
- The accuracy of a temperature measurement by thermocouples of type TT, and the involved conversion from voltage to temperature, is in the same range as if no conversion were to be applied.

The temperature along a solar collector row was monitored and some results discussed above. We find:

- As expected, the temperature rise in the modules at the cold end of a collector row is approximately 1-2 K higher than at the outlet. This is explained by the decreasing efficiency of the collectors for high temperatures and is one of the main arguments for applying high-performance solar collectors for the upper ends of the row. This will be discussed in Chapter 8.

5. MODEL DEVELOPMENT

The objective of this chapter is to document the development of the simulation mode that will be applied in the research work. The development consists here of two steps, the validation and the generalisation. The validation in Section 5.1 is focussed on the collector field and the main boundary condition that is different from other solar heating technologies, the district heating. The generalisation in Section 5.2 involves a large jump from the validated collector field and heat demand models to a final CSDHP-model including control strategies, heat exchangers, a storage tank and much more. An exclusion of a validation of these enhancements is justified by the argument that the validation is published in (Heller, A. and Dahm, J., 1999) and (Heller, A., 1998). Some less central subjects for the model development, e.g. choice of meteorological data and simplified models for air and ground temperatures are mentioned in (Heller, A., 2000c).

5.1 VALIDATION

In the current validation, the solar collector field is carried out by two steps, the validation of the temperature development along a single collector row in Section 5.1.2 and the validation of the collector row and the whole solar collector field in Section 5.1.3. After having introduced heat demand modelling in Section 5.1.4.2 a final model is developed and examined in Section 5.1.5. Conclusions are presented in Section 5.1.6.

5.1.1 Method for validation

The theory of validation is very extensive and rather advanced. No attempt is made to meet the requirements presented in literature. However, for readers interested in the subject, reference is made to the work of (Ljung, L., 1987), a schoolbook used in the field of "system identification", among others validation. Unfortunately, no publication is found by the author, in which the subject is presented in a more accessible way.

The task of validation is to compare a given model with the real world phenomenon, process or object. However, a perfect model is a fiction. Both the model and the real world phenomenon are reductions of the reality. Validation in this context means to examine whether the model is "good enough" - a very subjective characteristic. Theories in the field are dealing with the definition and demarcation of the "good enough". The procedure is similar for all definitions to generate and carry out tests. They involve various ways to assess: How the model relates 1) to observed data, 2) to prior knowledge 3) to its intended use. The current validation procedure reflects these basic objectives.

In this work, no own models are developed. Hence, validation of component models is not presented, assuming that the modellers of the applied system components (hopefully) applied advanced theoretical frameworks to define, build and validate the component models, e.g. chose the proper implementations and parameter sets.

Here, the objective of validation is to increase the confidence in applying existing models in a combined manner for the modelling of large-scale solar heating, especially for the application with variable flow control in the solar loop. Basically, "good enough" is here defined as the ability to reproduce measured data from the real solar heating system, given well-defined input data, within the uncertainties of the measurements. If a model computes results in the range of uncertainties of the measurements, the model is assumed valid for the application in central solar heating systems, else the model must fundamentally be rejected. Due to a lack of alternatives, this is in some cases not practicable. If no alternative is available, some reservations are made on the generality and limitations of the model and the findings.

In the validation procedure, parameters are classified, according to the following criterion:

Parameter values measured in real systems are classified highest and are not changed during modelling and simulations. Examples of such parameters are the solar collector area, the storage volume etc.

Parameter values found by well-defined test sequences are given second priority. These parameters are adjustable, if the free parameters do not lead to valid results. Examples of such parameters are the solar collector coefficients determined by test sequences. The number of test sequences does not represent all possible cases, especially the case of variable flow control in the collector loop. Therefore, the parameters are classified as "semi-empirical", meaning adjustable to a certain degree, if the free parameters cannot lead to any reasonable result.

The "weakest" classified parameters are the "unknown". This can be due to lack of physically detectable quantities, lack of knowledge, due to unrealistic test sequencing and due to statistically interpreted model adjustment. The correlation between heat load and ambient temperature for a degree-hour method is an example of such a parameter. Free parameters can be adjusted to give the best agreement between measured and computed outputs (best "match", best "fit").

In literature on solar heating, it is often seen that the validation is split into two steps: 1) The calibration and 2) the validation. In the first step, the boundary conditions for the model are defined by measured input values. The objective of this step is to tune parameters to give the best agreement between measured and computed outputs. In the second step, the parameters of step one are kept, and input data from a second period is applied to check whether the parameter settings lead to a similar good agreement between computed and measured outputs.

In the current work, the two steps are employed backwards and forwards, involving two time series of measurements. This means that some parameters are adjusted by one data set and validated by the other, and other parameters are adjusted and validated by the opposite employment of the measurement data sets.

In the following section, details on the applied criterion for the validation are presented in more detail for the given validation task.

5.1.2 Temperature development along a solar collector row

In the current section, a model for the solar collector rows, conceptually sketched in Figure 32, is evaluated.

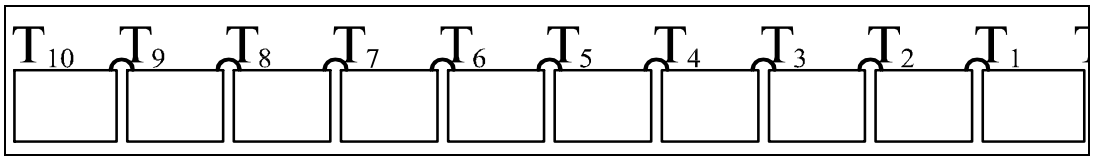

Figure 32. Sketch of a solar collector row. The row consists of 10 modules. Temperatures are measured at all connections between modules (T_9 to T_1), including inlet temperature at T_{10}.

For the modelling of solar collectors in TRNSYS, there are three possible components (TYPEs):

1) The standard component model, TYPE 1 (Klein, S. A. and many others, 1996).

2) The non-standard component model by Per Isakson, TYPE 101 (Isakson, P., 1995) and (Isakson, P. and Eriksson, L. O., 1993).

3) The so-called Perez-model, TYPE 132, (Perers, B., 1995).

TYPE 1 implements the theoretical models described in (Duffie, J. A. and Beckman, W. A., 1991). None of the models implements the dynamic aspects of the involved mass in collector

and flow media. This is acceptable for small-scale, high-flow solar collectors, but leads to erroneous estimations for low-flow systems and large-scale solar systems. TYPE 132 is designed to include the dynamic response of the thermal mass in the collector, keeping the basic assumptions similar to the TYPE 1- model. An alternative approach is introduced by TYPE 101. Here another numerical scheme, the plug-flow model scheme, is applied, and the thermal capacities introduced. Detailed discussion on the numerical schemes is presented in (Heller, A., 2000c).

Most collector validation is based on constant mass flow conditions. In the current case, the mass flow is controlled to ensure constant outlet temperature from the collector field back to the district heating plant. Hence, the specific objective for the current validation procedure is to focus on the applicability of the collector model for variable controlled flow conditions.

5.1.2.1 The row validation model

Validation of collector models includes some necessary other TRNSYS components as represented in the following flow chart. Note that the bullet texts are examples and not a complete list of actions.

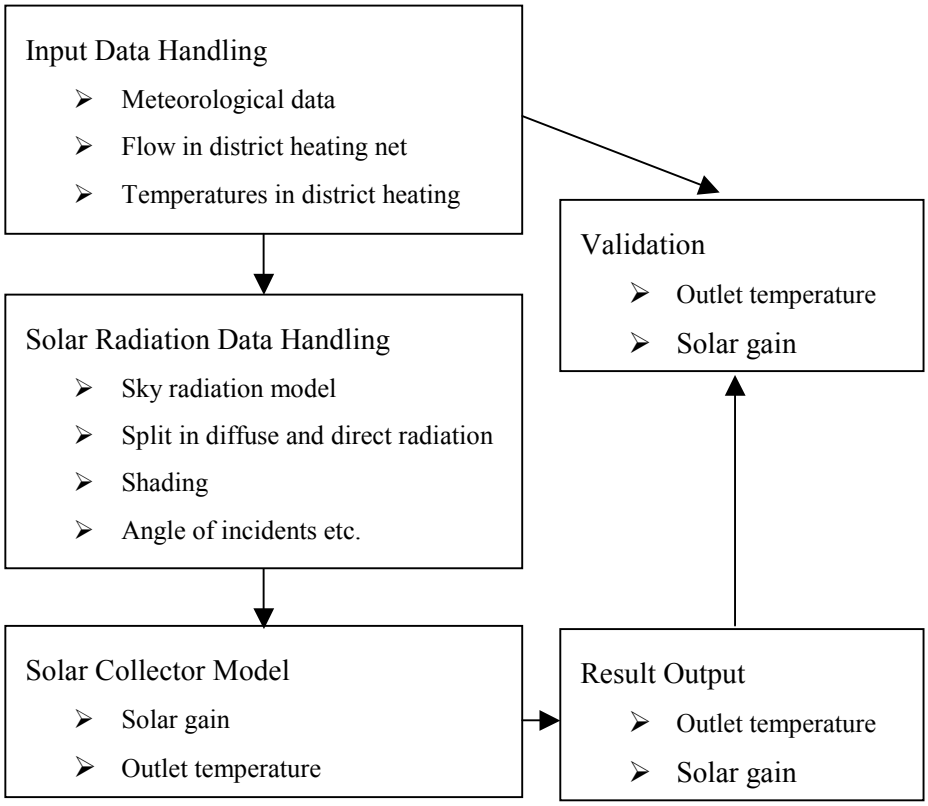

Figure 33. Flow chart for the most relevant model components for the row temperature validation.

The flow chart in Figure 33 shows the idea behind the TRNSYS-model that involves the following components.

Service components: All TRNSYS models must include a "Simulation Controller" component to e.g. start, stop the simulation, chose a proper numerical method and simulation conditions. Moreover, the TRNSYS-model consists for the validation of some equations and constants, a solar radiation processor and external data reading by an "Input Data Reader". External data, such as ambient temperature, measured flow data and radiation data are read from data files

into the model and connected to the relevant components. In the following, the data handling will be described in more detail, due to the rather special handling of measured data for validation.

Solar radiation data is normally measured in horizontal plane and subsequently converted to a given tilt angle of the solar collector and the given conditions by a "Solar Radiation Processor". The pyranometers involved in the current validation are oriented similarly to the collector's orientation. Hence, conversion to the tilt angle and orientation is not necessary for the validation of the collector row and collector field. The measured data is directly applied to the solar collector model. The Solar Radiation Processor is also necessary for splitting the total solar irradiation into a direct and a diffuse part. This is not necessary for the validations due to the fact that total and diffuse irradiation are measured independently. However, a Solar Radiation Processor is necessary to compute the solar incident angle at a given time step, necessary for the collector model to compute the solar gain.

Shading of the collector area onto rows behind must be computed by a "Shading"-component.

Boundary Conditions: For the validation of the collector row, temperatures along the row and solar irradiation data are measured together with the flow through the whole collector field. For validation, the following input data define the boundary condition for the computations:

- The total and diffuse solar irradiance in the collector plane with accuracy of 3% for 1-minute measurements and 5% for 5-minute measurements.
- The inlet temperature to the row with accuracy of 0.5-1K.
- The flow into the row which involves a very large uncertainty. The flow is measured for the whole collector field only. To find the flow through the individual rows, the total flow is divided by the number of rows. We know from measurements for the applied periods that the flow differs between the rows by 5K *at the outlets* which is for a temperature increase of 30K over the collector row, an uncertainty of approx. 5K/30K=17%. From this point of view, the mass flow rate through the collector row is seen as a free parameter that can be adjusted to give best fits. This weakness will be overcome in the next step of validating the collector field as a whole.

Parameter estimation procedure: All model parameters are chosen to represent the values documented in the test-sheets for the given components. E.g. start efficiency coefficient and heat loss coefficients for a solar collector, or by physical means e.g. the area of a row, distance, tilt angle of the modules etc. The capacity in the collector row is found by adding the capacity of the module found on the data-sheet to the mass from the connection piping. By this procedure, one parameter, the mass flow, is free, as discussed above.

Time-Series adjustments: Unfortunately the timers for the two data acquisition systems for the permanent and the supplementary monitoring were not synchronised. This led to serious problems with regard to matching the data in time. This is even worse with simulating solar systems, where time is important for the solar position and hereby the solar incidence computations. To avoid conflicts, data from only one data acquisition system is applied, if possible, and simulation time is adjusted to match the measured time.

The conditions for the period from 20 July to 4 August applied in the validation are plotted in Figure 34.

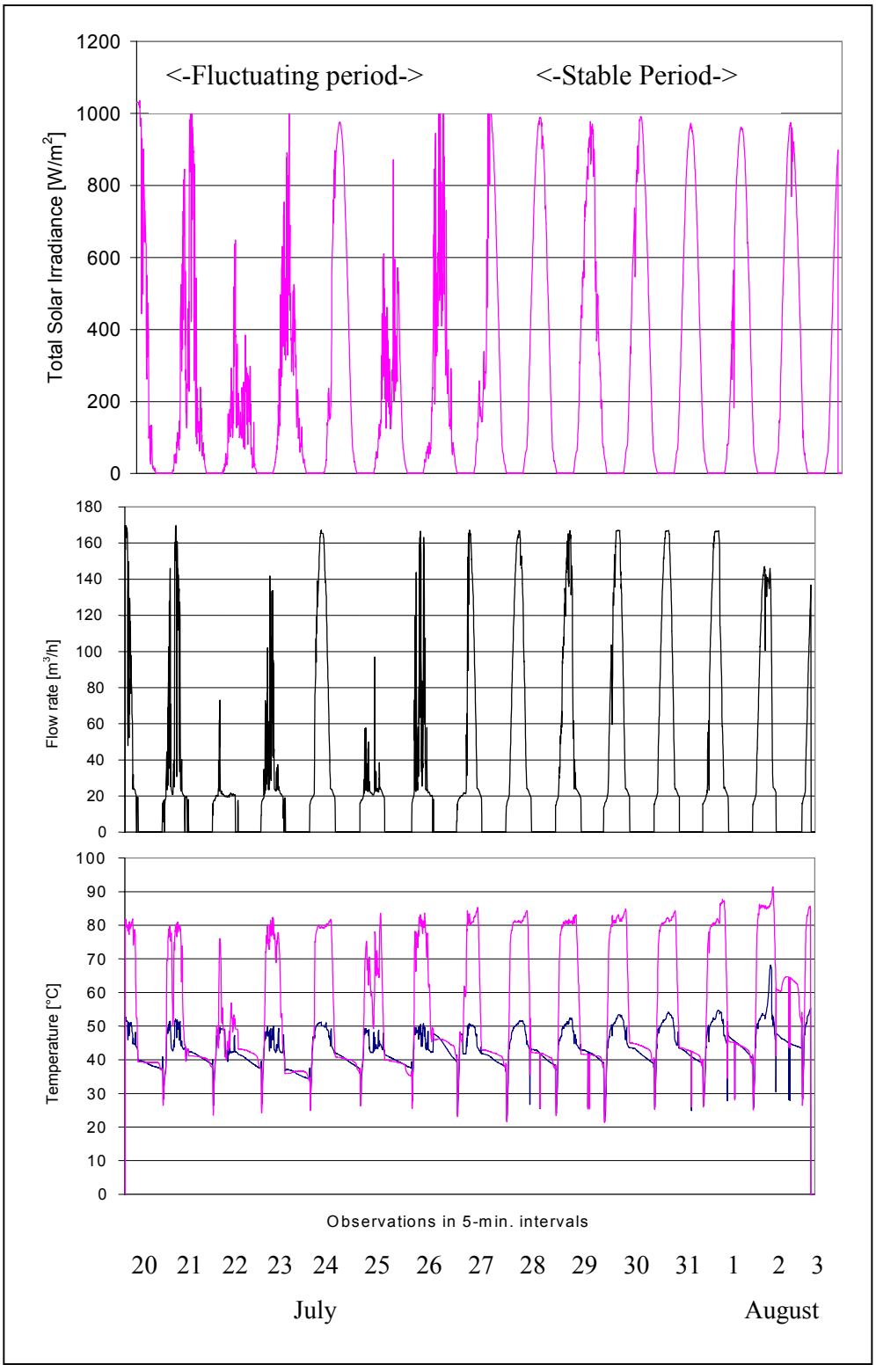

Figure 34. Boundary conditions and results for the validation period 20 July to 4 August:

Top: Total solar irradiance in W/m^2.

Middle: Mass flow rate through the collector field in m^3/h.

Bottom: Cold inlet and hot outlet fluid temperatures for the row in ^{o}C.

The observation period is split into two sub-periods for two reasons: 1) to enable crosschecking of results, 2) to investigate a simple case and a more complex case. In the following the simple case with strong and "constant" solar irradiation, also called the "smooth case", is investigated, followed by the second case with strongly fluctuating solar irradiation, called the "dynamic case". The overall results from the computations are presented in Figure 35.

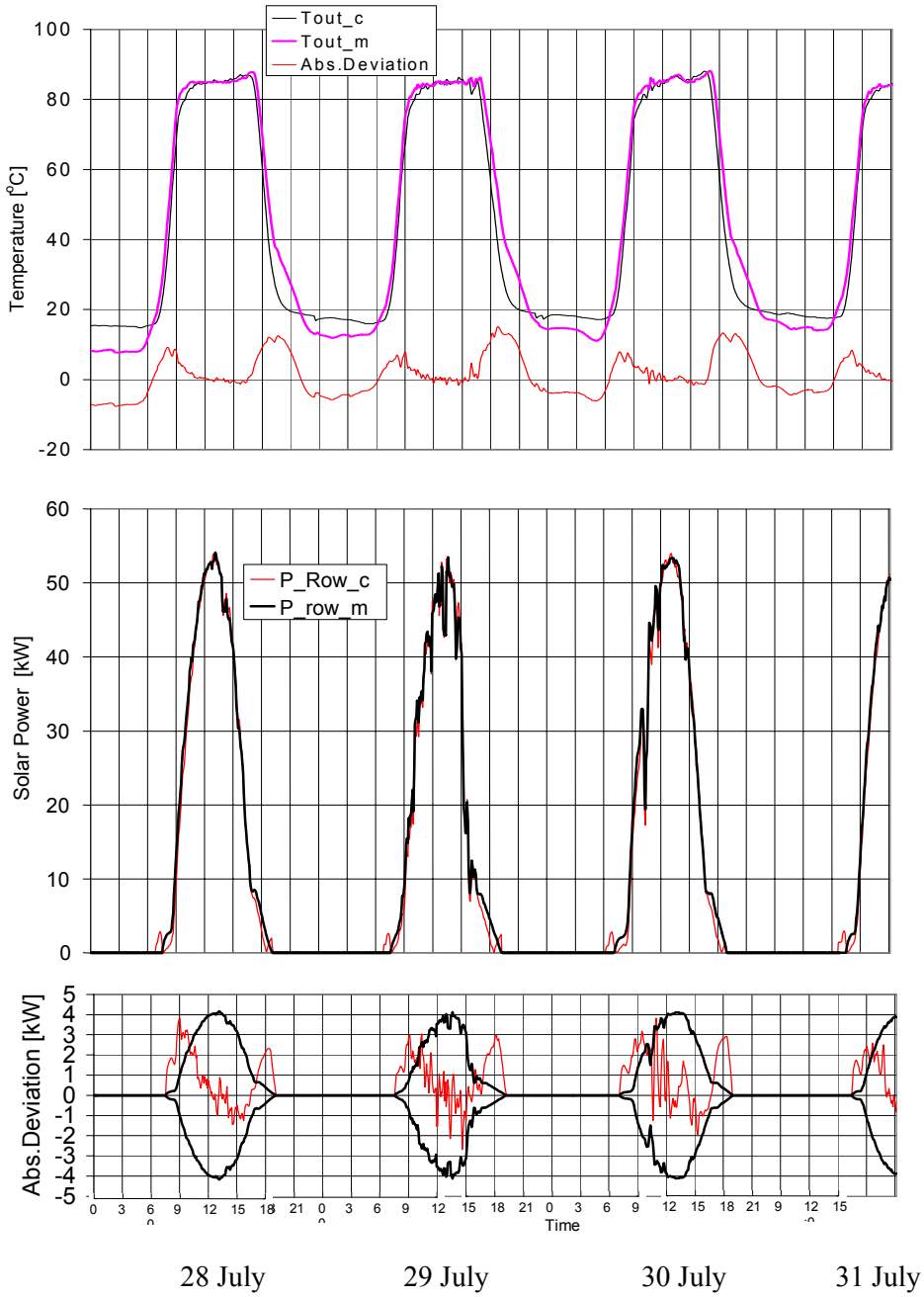

Figure 35. Results for validation for a period with "stable" solar irradiation.
Top: Comparison of computed (Tout_c) and measured (Tout_m) temperatures at the row outlet and the corresponding absolute deviation, lowest in the top, plot in °C.
Middle: Comparison of computed (P_Row_c) and measured (P_Row_m) solar power out of collector row in kW. Deviations are not visual by this plotting method. Hence the bottom plot shows the deviation in more detail.
Bottom: Absolute deviation between measured and computed solar power in kW of the measured, plotted between uncertainty boundaries computed by theoretical means (thick lines).

In Figure 35 first results for a 4-day period with stable, strong solar irradiation is presented in three plots. The figure at the top shows the measured and computed temperature out of the collector row and the absolute deviation between the measured and computed temperatures. In the centre plot, the corresponding solar power produced by the collector row is plotted, resulting in the absolute deviation plotted in the bottom graph. In the bottom plot, we find also the uncertainty for the measurements which is estimated for each measurement and calculated by theoretical means for the whole day and the period shown in Figure 34. Due to the fact that the measurements are within the boundary, defined by the uncertainties for the current measurements - except for the start-up and closedown period - the solar power computations for the collector row in the given period is accepted to be within the uncertainty of the measurements. Hereby, the row model is accepted to be representative for the actual case.

From the plots, we clearly find a systematic disagreement between the measured and computed values. In the following plots, this is examined in more detail by focusing on a single day, the first in the above series. For this day, we find the conditions and results in Figure 36.

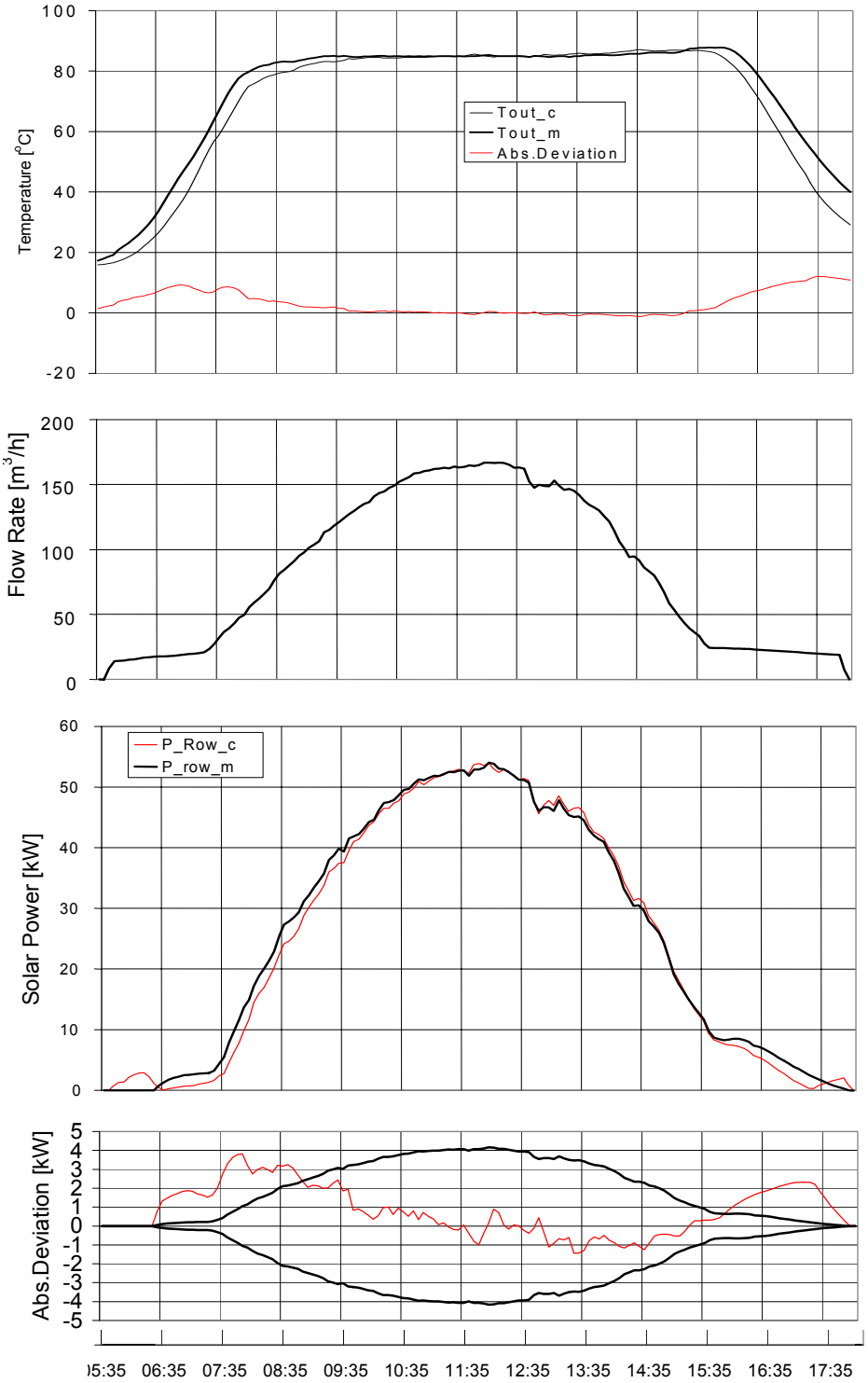

Figure 36. Zoom in on a single day with "stable" solar irradiation (first day of period in Figure 34).

Top: Comparison of computed (Tout_c) and measured (Tout_m) temperatures at the row outlet and the corresponding absolute deviation in ^{o}C at the lower part of the top plot.

Plot 2: Flow rate in m^3/h through the whole collector field to visualise flow pattern.

Plot 3: Comparison of computed (P_Row_c) and measured (P_Row_m) solar power out of collector row in kW.

Bottom: Absolute deviation between measured and computed solar power in kW of the measured values, plotted between uncertainty boundaries computed as above (thick lines).

From the top plot, we find that the computed temperature is lower for both the start-up and closedown period.

The analysis can be based on the flow control strategy which is reflected by the volume flow rate plot. Basically, the strategy is as follows: 1) the solar loop starts up when the solar irradiance leads to positive estimated solar power. The pump is then started to a minimum flow rate. In this case, we find the flow rate at very low level, suddenly increasing in the next phase, 2) where the flow is increased due to high temperature out of the collector row. In this phase, the control aims to keep the outlet temperature constant at a set point temperature. 3) When the sun sets in the evening, the flow control decreases rapidly, but is not able to keep the temperature out of the collector at constant level. 4) After a short while, the minimal flow rate is reached and kept until no heat can be extracted. Then the pump is turned off.

Based on this flow control description, we can extract the following finding from the plots above:

- Under start-up and closedown conditions, here called shoulder periods where the flow control is kept at a minimum, the deviation between computed temperatures and solar power is the largest. This is partly due to the temperatures applied in the validation which are measured in the building of the plant. Hence, temperatures in the start-up period are dominated by indoor temperature and not by ground temperatures from the buried piping to the building. Therefore, the deviation in solar power is large, but cannot be interpreted as a characteristic of the model and should be disregarded by the reader.
- In phases 1 and 3, a systematic displacement in time between measured and computed solar power is observed. This is certainly a characteristic of the model and shows some imperfection.
- During the production phase 2, the model computes very realistic results for the validation case where the flow rate is an input parameter.

From these observations we can conclude, that:

- The solar power over a day with strong and steady solar radiation is computed in good agreement with measured solar power, except from the shoulder hours, where disagreement in measurements lead to significant differences between measured and computed solar power.
- The deviation in the shoulder hours (morning, evening) does not dominate the results due to the very insignificant solar power in these periods. This can be seen from the accumulated solar gain for the whole “stable” period of 4 days plot in Figure 37.

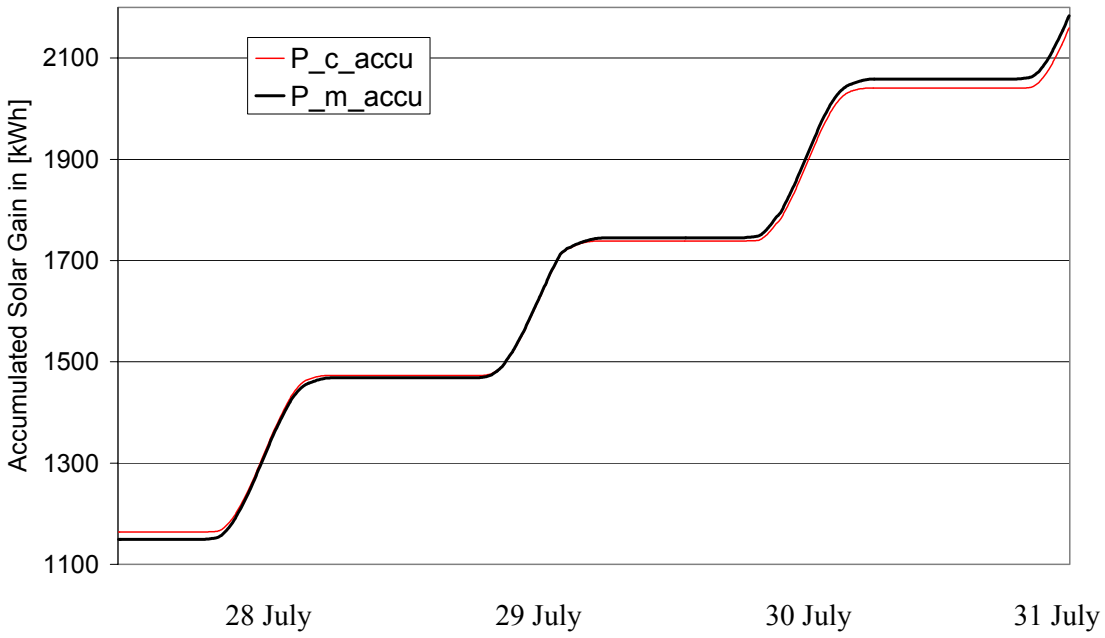

Figure 37. Computed and measured accumulated solar gain for the row case for the similar data as plotted in Figure 35.

From the accumulated solar gain plot in Figure 37, we find that the computed value is a small offset from the measured. However, the difference between measured and computed values is not explained in detail, and one can wonder if the error is due to any modelling mistake. Some of the possible modelling errors are discussed in the following:

Orientation of the collector in the model: We find small systematic errors in the bottom plot of Figure 36. This can be corrected by the orientation parameter of the model. Due to missing accuracy of the orientation of the solar collectors in Marstal, this makes no sense. The error is minimal compared to the total deviation found.

Number of components: The collector model is implemented as a plug flow model. The model is in detail discussed in (Heller, A., 2000c). One characteristic for such models is the fact that an increase in number of "plugs" representing the flow medium and piping leads to better results. In the TYPE 101-implementation, the collector component consists of up to 25 plug-elements. By inserting the maximum number of component models which is four, we expect to get better results from the computations. Comparing computations with a single collector component, with the maximum number of components, we find very small differences in output results. Hence, this does not explain the discussed deviations.

Component model: As mentioned above one could try to apply alternative collector models for computations. We find that the standard-component, TYPE 1, leads to even larger deviations. It makes no difference if one applied a single or 10 component for the collector row. Due to fact that the TYPE 132 was not available for the author at the time of writing, this component was not investigated.

So far, the focus has been put on the reproduction of a solar collector row for rather stable and smooth solar conditions. The corresponding computations with the second set of data shows the following picture. Note that in this time-series, the solar irradiance is very smooth and stable.

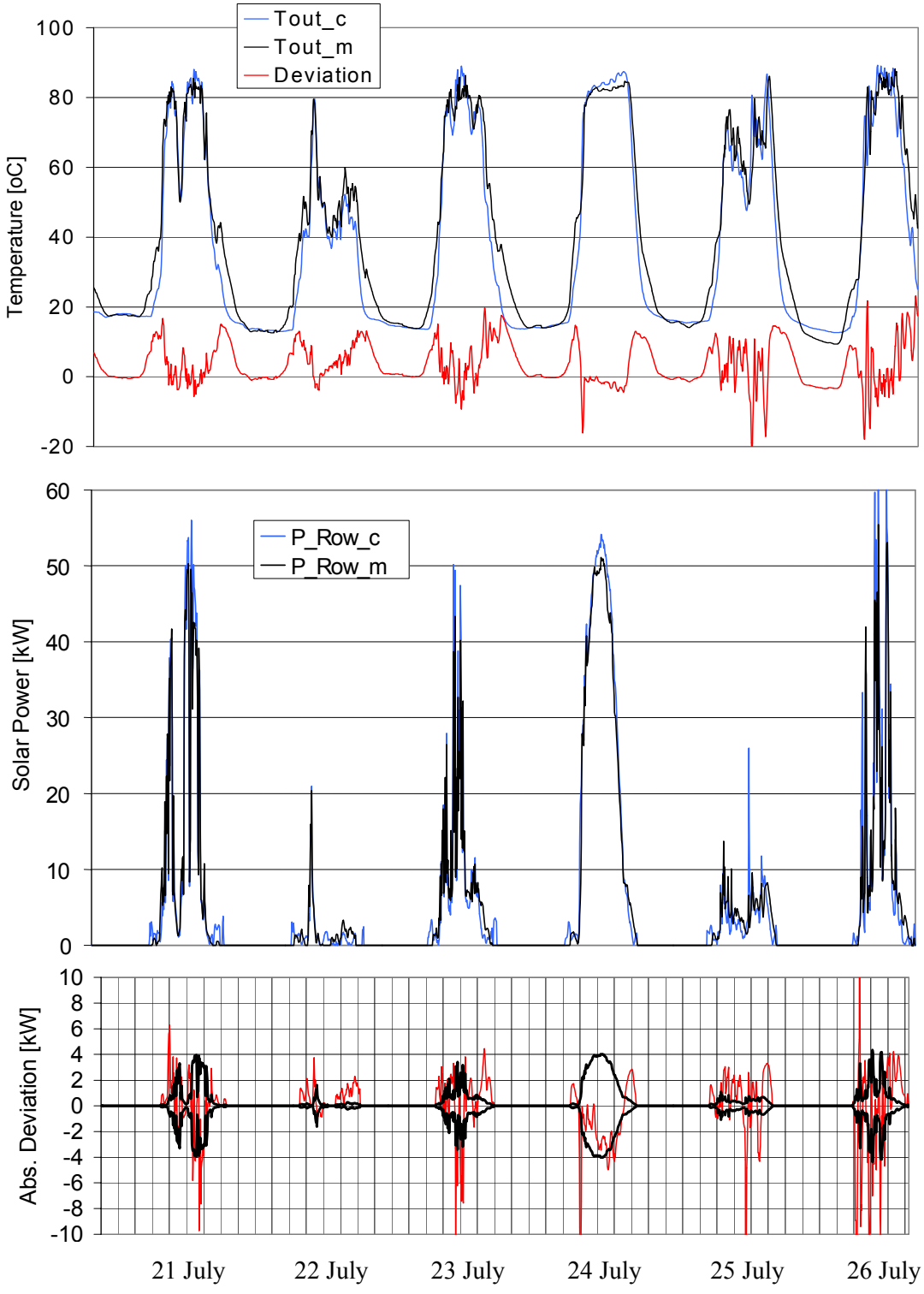

Figure 38. Results for validation period with fluctuating solar irradiation. (3Hours between guide lines.)
Top: Comparison of measured (Tout_m) and computed (Tout_c) temperatures and the corresponding absolute deviation in ^{o}C.
Middle: Comparison of measured (P_Row_m) and computed (P_Row_c) solar power out of collector row in kW.
Bottom: Absolute deviation between measured and computed solar power in kW of the measured values, plotted between uncertainty boundaries computed as above (thick lines).

From Figure 38, we find that:

- For tendencies in temperature and solar power computations, results are similar to the case with stable solar irradiation.
- The deviation in temperatures is in the same magnitude as for the "smooth" case computations presented above.
- The deviation in solar power is much larger than in the "smooth" case. This is not surprising, due to the fact that the strongly changing solar irradiation must be countered by the control of the fluid flow rate. The deviation cannot be explained by measurement uncertainties and must be explained by the model or numerical reasons.
- The deviation in total solar power between measured and simulated is in general within 4kW, with some peaks above this value for conditions changing very fast, similar to the start-up and close down conditions of the previous “smooth” case.

The accumulated solar gain is plotted in Figure 39 for the fluctuation case.

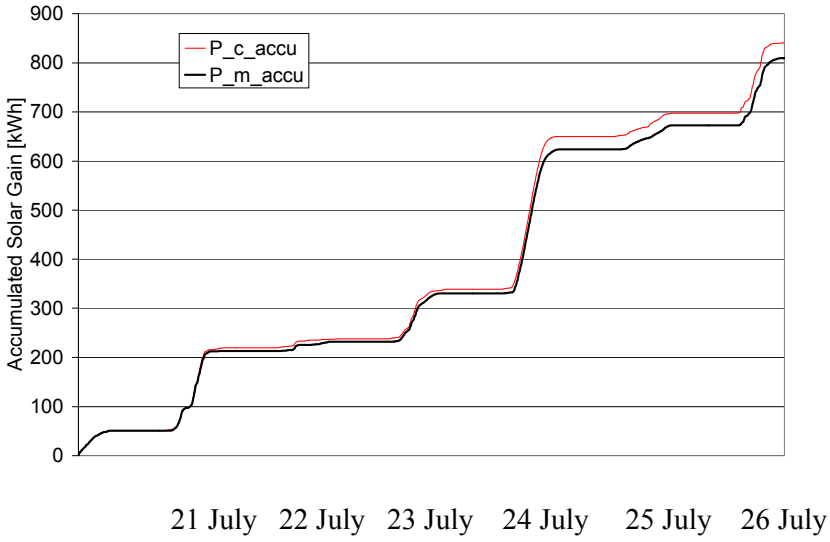

Figure 39. Computed and measured accumulated solar gain for the row case for the similar data as plotted in Figure 38.

From the accumulated solar gain plot in Figure 39, we observe similar characteristics as for the "smooth" case. The total error is the difference between the two curves, which, for the 6 day period, is 3.7% of the total accumulated, measured value.

Summing up the uncertainties observed, for the two parts of the total validation period, we find a value of 4.2+3.7=7.9%.

The uncertainty for the power measurement is defined by the uncertainties for the individual sensors and the number of measurements. By applying theoretical models for the estimation of the resulting uncertainty for the whole period, we estimated a value of 7.7%. Moreover, the uncertainty due to the solar irradiation inputs to the model and the very large uncertainty in relation to the flow distribution between rows must be added. Hence, the total uncertainty for the above validation is much above the 7.9% found for the computations.

We find from this point of view that the model shows results that are close to the uncertainty due to the validation measurements. Hence, it makes no sense to adjust the model further, even so the errors for individual measurements can be very large. Based on these considerations we are able to accept the model for the realistic representation of a solar collector row.

5.1.2.2 Conclusion on row validation

The validation of a single row is difficult due to poor measurements. The mass flow rate for the row is computed from the total flow through the collector field and is therefore not known exactly. There were also difficulties with involved timers not synchronised, and this had to be addressed by the current computations. These difficulties let to inexpedient uncertainties for the validations. However, the criterion for the acceptability of computations is kept to the uncertainties for the measurements, disregarding these difficulties.

The solar gain computations are in reasonable agreement with measured values, except for very strongly fluctuating solar irradiation and the start-up and closedown conditions. These large deviations are due to the way the measurements are collected, and do not show any characteristics for the simulation model.

Deviations are large for the periods with strong fluctuation in solar irradiation. This makes computations very demanding, especially for the control strategy in Marstal, where variable flow controls is applied. Totally, we can conclude that the absolute deviation in solar gain is very high, but that the impact on the total computed solar gain for a period is below the uncertainty for the measurements. Hence, no better correlation can be justified by the current measurements.

Based on the fact that the current investigation involves rather large uncertainties, it is not possible to conclude on the question of whether the deviation is due to the solar collector model formulation or to other reasons. However, one can conclude from the current investigation that the MFC -model by Isakson is able to reproduce reality by reasonable means. This is especially relevant in this case, because variable fluid flow is applied in the validation.

Some computations were carried out. They are not documented in this report, but they produce relevant insight in the modelling of solar collector systems – here a few of them:

The findings from above are also true regardless of whether the row represents a single component or a number of components. The results are very similar for the two methods. Due to simplicity, the application of a single component is recommended.

Different collector modules are available. It is strongly recommended to apply the MFC-module, TYPE 101 for computations of large-scale solar heating. TYPE 1 would lead to unrealistic results for dynamic conditions.

5.1.3 The collector loop and collector field

The collector loop consists of piping between the operator building and the collector field. In the collector field, the collectors are arranged in two symmetrical blocks, consisting of 36 rows of 10 collector modules. In the current section, the whole collector loop model is examined by comparing simulation results by values from the permanent monitoring system.

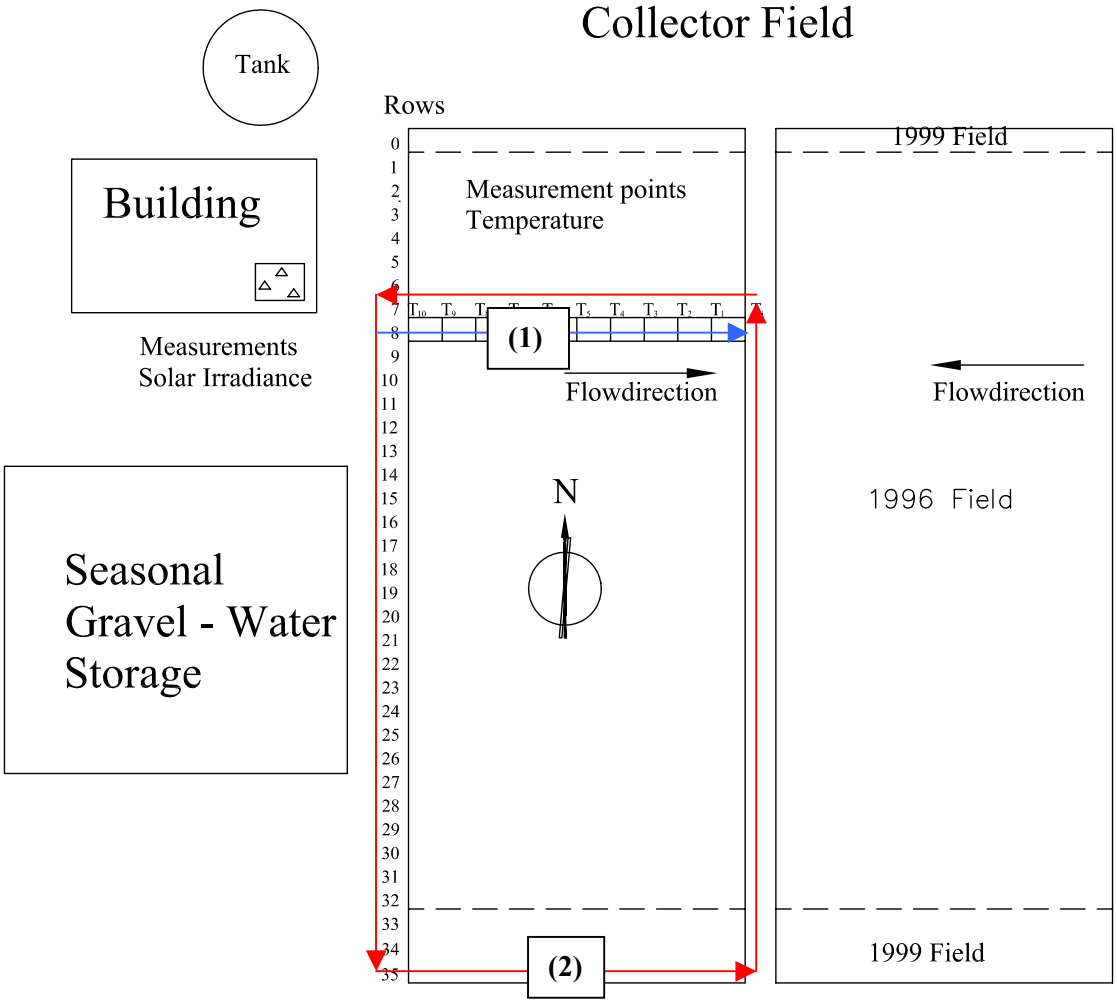

Figure 40. Central Solar Heating plant in Marstal. Measurement points (dot) for collector loop validation.

Measurement points and boundary conditions: Measurements for temperature to and from the field and flow through the collector loop are measured in the building, labelled "Building" in the figure. For the validation of the solar collector field, the inlet temperature and mass flow to the field, measured in the operator's building is applied. Note: Measurements at night time show indoor temperatures and not ambient temperatures. Due to this condition, no comparison can be made in periods with any flow in the collector loop. This circumstance is also one of the reasons for substantial deviations in cases of start-up and close down of the collector loop, as mentioned in the row validation case above.

Mixing of temperatures: Due to the size of a collector field, flows are diverged into each of the rows and collected afterwards again. Some flow streams must travel a longer distance than the others – See Figure 40 arrows: Arrow (1) shows the short passage and arrow (2) the long passage through the collector loop. Hence, the resulting temperature back to the monitoring point, is a mixture of the outlet temperatures over the period from the shortest flow interval to the longest. By maximum pumping power, this interval is approximately 10 minutes and for minimum flow approximately 2 hours. When applying constant flow operation, this must be considered. Applying a control strategy as in Marstal, controlling the outlet temperature to 80°C, this temperature-mixing is not a subject, expect for periods with low solar irradiation.

The simulation model: Similar to the row validation case, we apply a model as sketched in Figure 33. The main difference lies in the inclusion of the piping between solar collector field and operator's building. The thermal behaviour for the piping is adjusted by averaging physical values e.g. length, diameter and insulation thickness.

It is worthwhile emphasising that the piping model is strongly dependent on the case to be modelled. Hence, results from the Marstal case cannot be generalised.

5.1.3.1 Validation case 11-days period

Main differences to the row validation case for the period shown in Figure 34:

1. The mass flow rate is known for the collector field with an uncertainty of 0.3%.
2. The connection pipes are added, introducing an extra uncertainty for the simulation model, or in other words a free parameter.

Applying the same time period for validation of the solar field as used before, we get similar results for the complete solar collector field as found for the row case. The results are of such similarity that the plots from the row case are also applicable for the field case. The average deviation for the individual observations is found to be 2%. The accumulated solar gain is found as shown in Figure 41.

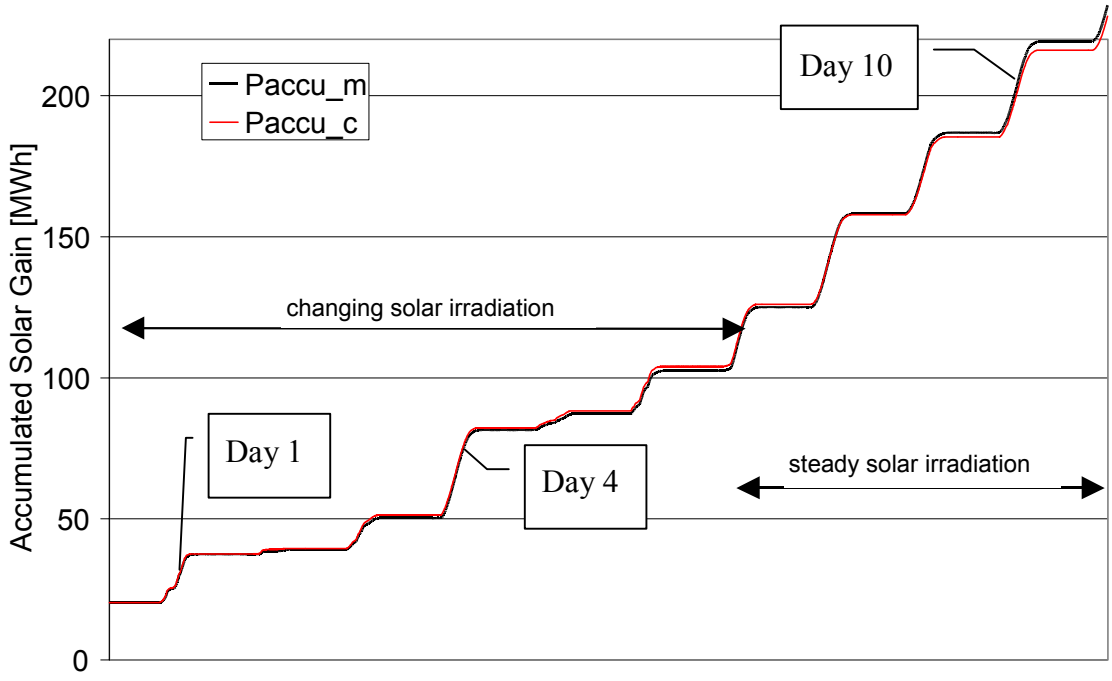

Figure 41. Computed and measured accumulated solar gain for the field case for the conditions presented in Figure 34.

From Figure 41, we find that the model represents the solar gain from the collector field by reasonable means. The production is computed to 197 MWh which is 4.1% below the measured production. This is a very good agreement, taking into consideration the involved uncertainties, e.g. from solar irradiation as an input to the model, from the power estimation that is approx. 7.7% for the 11 days period.

Comparing "Day 4" and "Day 10" with a comparable solar production of 31 and 32 MWh respectively, we find that the former leads to a better agreement with the measured production. This is due to the time shifting between the involved monitoring systems and the simulation system which is not characteristic of the model, but an artefact of the poor measurements. This

means that the simulations are much better than shown in the accumulated plot above, eliminating this artefact.

Comparing a fluctuating day ("Day 1" with 17 MWh solar gain) with a "steady" day ("Day 4" with 31 MWh solar gain), we find that the uncertainty for the "smooth" day is, in absolute values the double, but in relative values, smaller, compared to the dynamic day. This shows that the simulation of the periods with fluctuating solar gain introduces larger relative deviations to the computation results than simulation of periods with steady solar conditions. In other words, while the relative deviation in computed values is rather large, the impact on the total deviation is limited.

Plotting the result by a correlation matrix, we find the following picture.

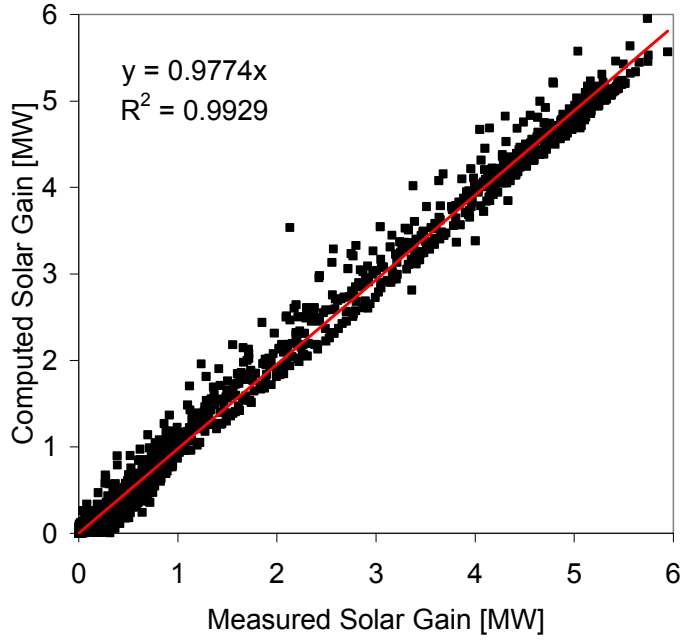

Figure 42. Correlation plot of the measured and computed data for the period 20/7-3/8-1999 and a linear trend line for the observations.

We find from the correlation plot in Figure 42 that there is a very good agreement between computed and measured solar gain. This is deduced from the facts 1) that not many dots are spread out from the central diagonal line, the perfect match, and 2) that the coefficient for the trend line is very close to one. However we find a weak tendency of overestimating the solar power for a large number of observations.

To give the reader a better insight in the response of the model, we concentrate our analysis in the following on a single day's results.

5.1.3.2 Validation case: Single days period

To control the model in more detail, the data from a day with strong, smooth solar irradiation (22 September 1999) and a day with strong fluctuating solar irradiation (30 June 1999) are investigated in the following. Note: In the previous computations, 5-minute intervals were applied here one-minute intervals are applied.

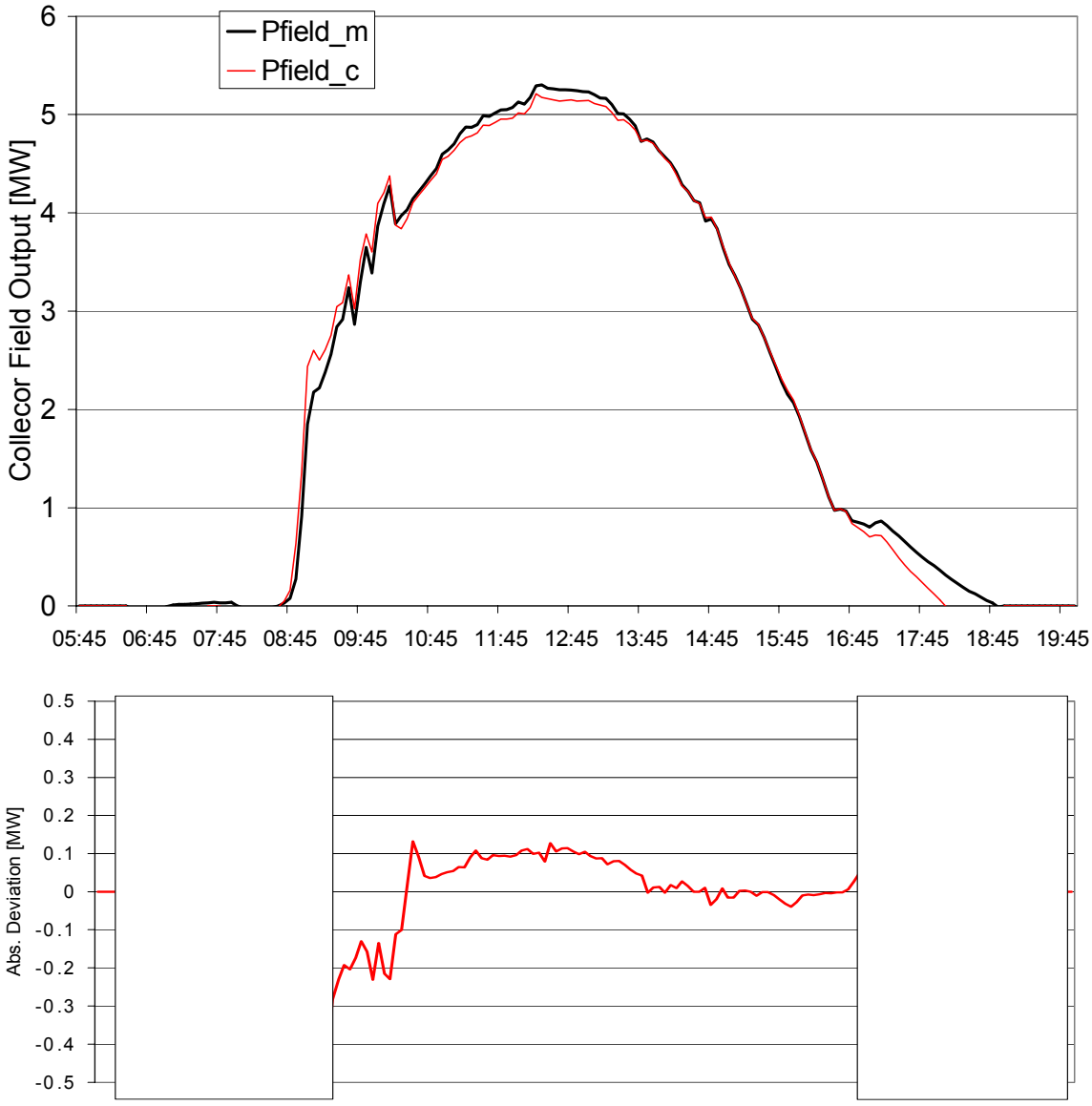

Figure 43. Results for validation for a day with strong and smooth solar irradiation.

Top: Comparison between measured (PField_m) and computed (PField_c) solar power out of collector field in MW.

Bottom: Absolute deviation between measured and computed solar power in MW.

We find from the top figure of Figure 43 that the solar power is estimated very well during the daytime with variable flow control. Main differences in production can be observed in the morning hours which again is due to monitoring artefacts and not characteristic of the model.

Hence, the results are hidden in the lower plot. Focusing on the main production period during the daytime, we find from the bottom plot that the deviation between measured and computed solar power is below 0.1 and –0.2 MW and for the whole day below 1%. This result is well below the uncertainties due to measurements show that the model is capable of computing variable flow in a realistic manner for steady and strong solar irradiance conditions.

The results for a corresponding day with stronger fluctuating solar irradiance Figure 44:

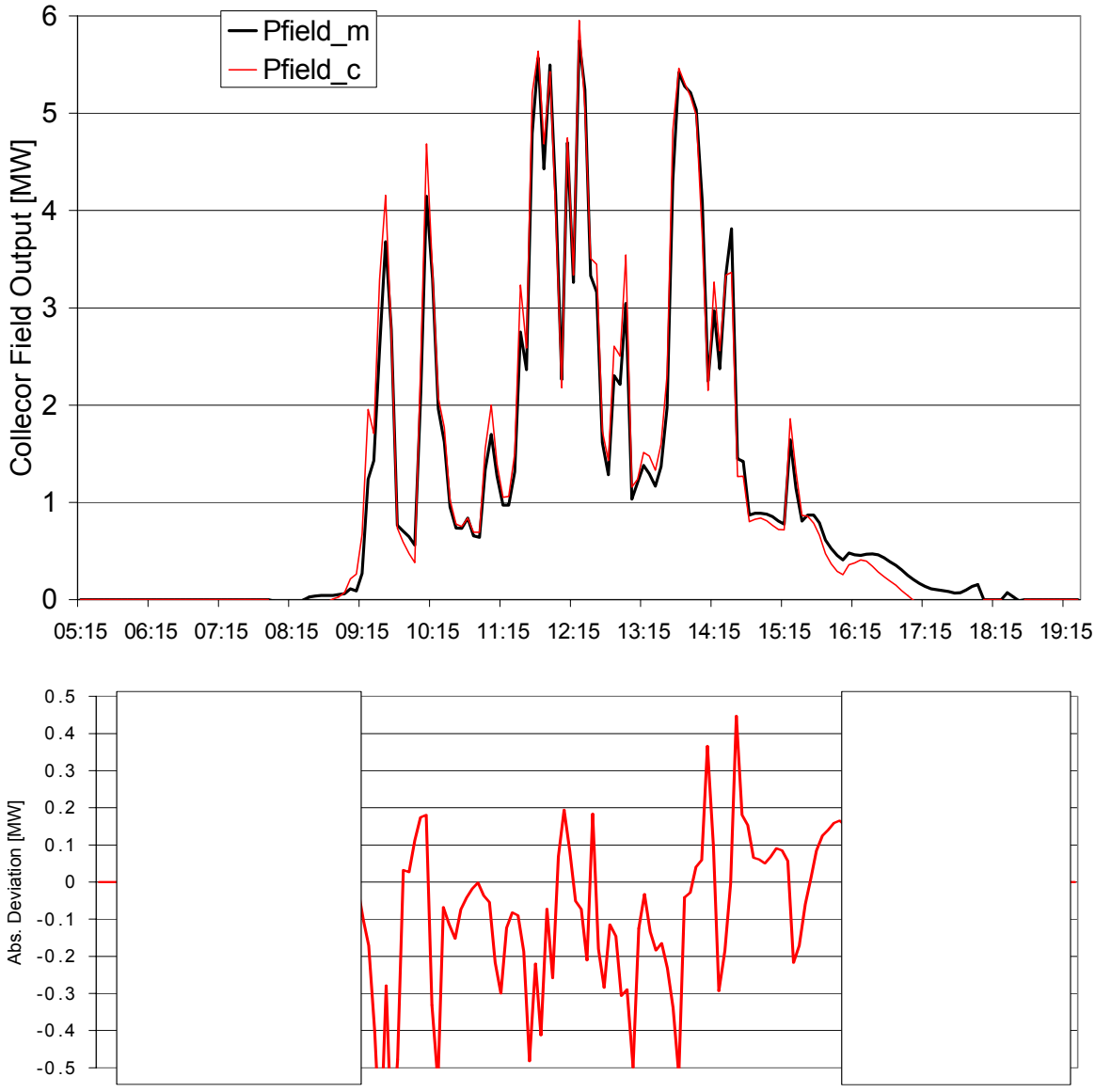

Figure 44. Results for validation for a day with strong and fluctuating solar irradiance.

Top: Comparison between measured (PField_m) and computed (PField_c) solar power out of collector field in MW.

Bottom: Absolute deviation between measured and computed solar power in MW.

Figure 44 shows the computed and measured solar power for the solar collector field, including the connection pipes. It becomes obvious from the plots that the deviation in the dynamic case

is much stronger than for the smooth case. We find deviations up to 0.5MW. The total deviation between measured and simulated solar power is 2.5% for the dynamic day, excluding the start-up and closedown periods visualised in the plot with frames above.

5.1.3.3 Conclusions on collector field validation

The validation procedure was hampered by poor monitoring, especially the lack of synchronising the involved timers for the different monitoring systems. From this observation. it is recommended that: If more than one monitoring system is applied, make sure that the involved timers are synchronised.

For simulation the real time must be recomputed to simulation time, e.g. summer time must be recomputed to real solar time. This must be taken into account and adjusted for the timers involved, so that computations are not hampered by lack of precision in time. This is especially relevant when applying solar thermal computation involving incident angle modifier methods etc.

Orientation of pyranometers is a rather demanding task. In this validation we find minor deviations in orientation which could be corrected in the simulation. Due to the minor impact, this was not necessary for the current validation. However, it is advisable to check orientation and tilt angles for sensors and collector fields very precisely.

An element of the poor monitoring - and hereby the validation - is the fact that some of the temperature sensors were placed indoors, instead of outdoors. This led to confusion of the validation, misleading the analysis to focus on the wrong findings, not part of the model.

Having taken these elements into account, we can conclude that the simulation model reproduces the solar gain and temperatures for the collector rows and the collector field within the uncertainties of measurements. Therefore, the model is accepted as "good enough" for application for large-scale solar heating with variable flow.

The collector performance can be modelled by a number of different TRNSYS-components and different number of components per model. The analysis shows that a single component of a plug-flow type as implemented in the MFC-model (TYPE 101) is giving sufficient accuracy. There are no evident improvements of accuracy from the application of a series of the component.

The application of the standard solar collector component, TYPE 1, is not recommended due to large overshooting of temperatures and solar gains for this component for solar collector rows and fields. The collector model can simply not reproduce the dynamics of collectors with large thermal capacities.

5.1.4 The heat demand model

Heat demands/loads are mostly very complex, especially for large-scale systems involving many heat consumers. There are models spreading from simple steady-state models to complex computer simulation methods. In this section, the heat demand is discussed as an introduction to readers not familiar with the subject, followed by a survey of models for "demand modelling". Readers especially interested in such "load modelling" are referred to e.g. (Werner, S. E., 1984), (Aronsson, S., 1996) and (Larsson, G., 1999), the basic sources for the current survey. A more detailed presentation can be found in (Heller, A., 2000c).

After the introduction on the basics of heat demand modelling, the individual causes for heat demands will be discussed. Having built up the necessary understanding, the different methods are compared on the load for the Marstal district heating. The section is finalised by the built-up of an overall load model and an analysing of first results.

5.1.4.1 The basic model

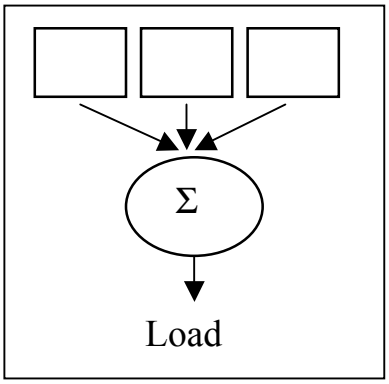

A general load model is introduced by (Werner, S. E., 1984), where the assumption is made that loads are a composition of additive elements that are based on physical theory. The composition elements are not correlated. This assumption introduces a certain error into the model that must be kept in mind.

The model can be generalised to the mathematical form

$$Y = \sum_{i=1}^{n} X_i \qquad (5)$$

where Y is the dependent model variable (the heat load),
X_i independent model variable element (e.g. wind speed),
i number of the actual element (1,2,..,n),
n total number of independent elements that shape the dependent variable.

Werner presents a survey of model descriptions of the general kind, followed by a specification of a more general applicable model involving model coefficients, β_i. These coefficients are used to adjust the independent model variable, X_i, in expression (5), resulting in the following adjusted model:

$$Y = \sum_{i=1}^{n} \beta_i X_i \qquad (6)$$

The puzzle is now to identify the relevant components and then somehow to determine the model coefficients for the individual load components. For the determination of the model coefficients, also called parameters, most authors adopt a statistical method, "multi-regression analysis". Alternatively, one could adopt time-series analysis or a neural network (Note: Neural network can be implemented very similar to multi-regression analysis methods). Based on such analysis on measured data, typically hourly data, the cited authors were able not only to estimate the parameter values but also the significance of the load components and hereby to decide the relevancy of the components.

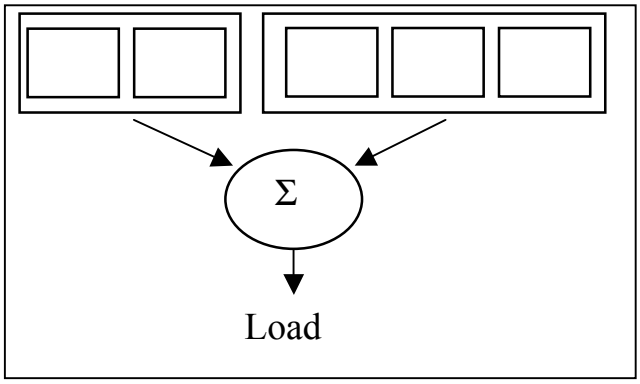

As mentioned, Werner represents a number of independent components and finds the corresponding coefficient based on measurements. Werner also proposes that similar elements could be collected to so-called load components.

(Aronsson, S., 1996) chooses this approach by combining components with similar influencing input parameters to abstract groups. For at typical district heating system we find the following four load components that together shape the total heat load:

- space heating (SH) for buildings
- domestic hot water preparation (HWP)
- distribution loss (DL)
- additional workday loads (WDL).

By additional workday loads, the author means the loads that are dependent on the day in the week.

The analytical work for this approach is similar to the above, namely to find the corresponding coefficients, but for fewer elements compared to the Werner-model.

The individual heat load elements or components have various impacts on the total heat load profile and they are discussed widely in literature. In short, the above mentioned authors came to the following conclusion.

Based on daily heat load observations covering between 5 and 11 years of six Swedish district heating systems, (Werner, S. E., 1984) estimates the significance of the individual load components. In short, the findings are that space heating (≈60%) and hot-water preparation including heat losses in the installations (≈30%) are the dominating factors for load modelling for residential areas. The district heating losses accounts for a minor contribution of approximately 6-8%. It is also analysed in Werner that the HWP varies dependent on weekday variations (user behaviour dependent on the weekday) and monthly variations (cold water temperature variation during the year). The hot-water preparation showed a significant seasonal dependency with higher hot-water consumption in winter than in summer. Significant parameters were identified to be the ambient temperature, the solar radiation and the wind speed. These parameters show influences on more than a single component model. Hence, component models are correlated and the claim of independence between additive components not justified.

According to Werner, load simulation is sufficiently accurate when including space-heating, hot-water preparation and heat loss from the DH-system.

(Aronsson, S., 1996) carried out a study, where 50 substations of the Gothenburg district heating were monitored with 15-minute measurement intervals over a period of 18 months. HWP accounts, according to this study, for 11-15% of the total load only, independently of building type, sizes and age. This is significantly lower than the estimation by Werner. Aronsson shows correlation between space-heating and hot-water preparation. Due to the model formulation by Werner that claims independence between elements, such correlation cannot be modelled.

Note: The discussed resulting error will especially be accentuated for low-energy housing and optimised systems. This must certainly be considered if modelling futuristic systems.

Table 6. Estimation values for heat load components found in literature.

Load Component	Significance estimations in %		
	Werner	Aronsson	Bøhm
Space heating (SH) for buildings	60		
Domestic hot water preparation (HWP)	30	11-15	
Distribution loss (DL)	6-8		>20
Additional workday loads (WDL)	Rest		

The summary in Table 6 shows very wide variety of estimation for the significance for the individual load components. This shows, among other things that different systems show very different significance. The Bøhm estimation will be commented below.

A study by (Larsson, G., 1999) was focusing on the district heating load as a boundary condition for his own modelling, similar to the current work. The main subject in Larsson was the fluid dynamic behaviour of DH systems and the modelling of this phenomenon. Unlike the prior authors, building on physical models, Larsson applies a black-box method. Applying a

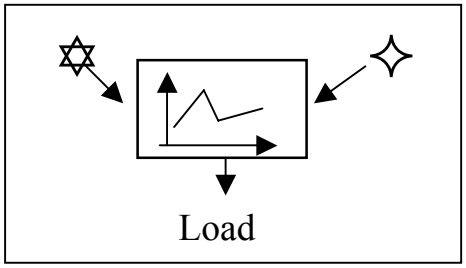

regression analysis on daily average values for the heat power load of the Gothenburg district heating, Larsson investigated the heat load pattern based on input parameters instead of components. Seen from this perspective the approach seems similar to an energy characteristic method presented later in the section.

Larsson found the significance as shown in Table 7:

Table 7. Estimation values for input parameters found in literature.

Input Parameter	Significance estimation in %
Ambient temperature	83
Cold-water temperature	8.8
Solar radiation	7.7
Wind	0.2
Humidity	< 0.1

The studies quoted above find the parameters defining the DH-system model for a given case, based on statistical regression analysis of measured daily data over a given period. There are two handicaps attached to this approach. 1) Normally, one does not have this kind of data in the required sampling frequency. 2) The presented source did not describe how they handled influences having impact on more than a single component and parameter. Moreover, the methods are rather demanding. A more applicable method is presented by (Bøhm, B., 1999). Here the author bases his estimation of heat losses for district heating on the measurements of at least two large systems in Copenhagen finding much higher heat losses in percentages for Danish systems than estimated by Werner. The high value can be explained by the very low "density" of user demand in relation to the length of the district heating net. In Denmark, also single-family areas are covered by DH, due to the very high heat overflow from the production of mainly electricity production (co-generation).

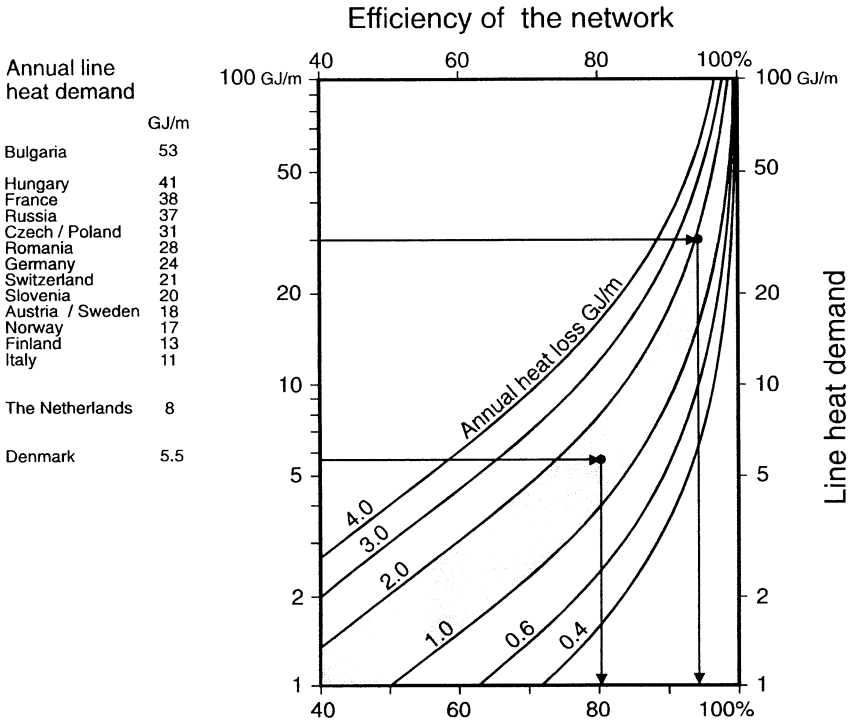

Figure 45. Annual efficiency of a district-heating network as a function of annual line heat demand. Inserted are annual line heat demands for European countries. Source: (Bøhm, B., 1999).

In Figure 45, the efficiency of a DH-network is plotted on the apses, spreading from 40 to 100% efficiency. On the ordinate axes, the line heat load is plotted on a logarithmic scale. The line heat load is the total annual heat load divided by the length of the pipe net, two values that are simple to find. Central heating systems with high-line heat loads tend to have lower heat losses than systems with low-line heat loss ("energy density"). This seems also reasonable from a logical point of view. The curves in Figure 45 can now be used for an estimation of the heat loss per metre of pipe in the DH-system, knowing the age, design etc. of the system - all information known to the system operators. Hence, the method is easy to apply and leads to realistic heat loss estimations.

Note: The annual line heat value for Denmark is very low. Knowing that the insulation level for the Danish DH-systems is reasonably high, this supports the finding of "low density" for the systems.

Concentrating on a single curve, we find that for increasing line heat load, the efficiency of the system is growing. More demand on a short DH-net leads to few heat losses and high efficiency. This seems reasonable. Comparing the plots for different annual losses per metre of pipe, we find the efficiency decreasing with increasing heat loss.

The above introduction to the heat load modelling and understanding, we are now able to go through the most relevant methods applied for load simulations.

5.1.4.2 Load model methods – A survey

In the current section, a number of methods for load estimations are surveyed and results compared to the findings for the Marstal district heating of the year 1997. The results are presented in two figures: 1) A load plot with hourly values from the measurements, compared to the load profile computed by the method. 2) The duration curve for the measured and the computed results. For many readers duration curves are not well known and must be explained

here in short. The individual loads, here in hourly values, are sorted in declining order. The highest values are then plotted on the left side of the plot, followed to the right by the lower values. The plot gives a fast insight into the distribution of loads, and it is often used for dimensioning of technical solutions, e.g. heating systems.

Due to the context of the current thesis, the outcome of the methods is examined for the application in solar heating simulations and recommendations will be stated.

The here presented methods spread from simple to complex. Simple methods need a few insights into the heating system to be modelled. Complex methods require large knowledge of the system to control the method. The choice whether to apply a simple or a complex method, depends on the objective of the application. However, simple models are unable to deal with accurate result generation, and complex method gives a large possibility of getting wrong results, if they are not controlled with care and insight.

The energy characteristic method is simple, but demands more knowledge of the given system than the previous method. However, in many cases a "general" characteristic valid for many cases is applied. This is recommendable only if no detailed knowledge is available.

5.1.4.2.1 Extreme simple load models

For very rough estimates, yearly values for the load and a percentage distribution of this total value over the twelve months, is a commonly used method. By applying this method for the Marstal case, by using the measured monthly value, the following duration curve in Figure 46 can be found.

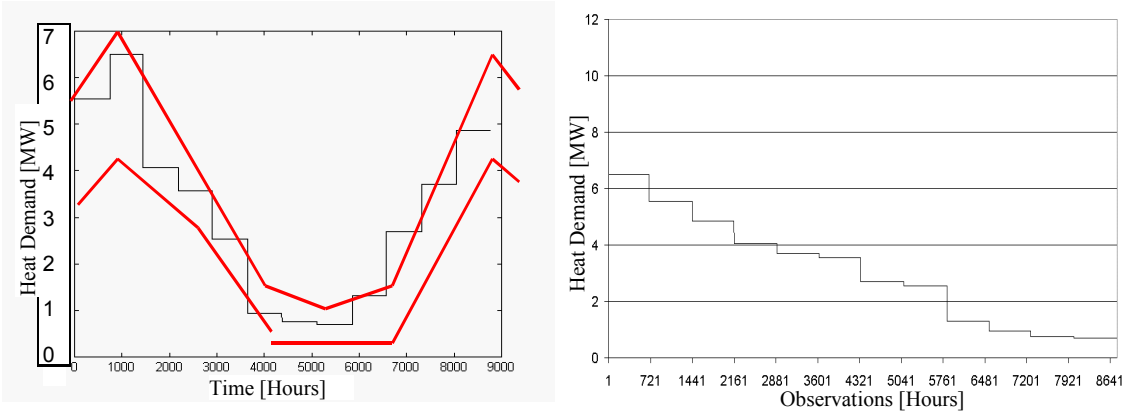

Figure 46. Hourly heat loads for a very simple monthly weighted load profile (left) and the resulting heat load duration curve (right).
Note: The thick line is found as a rough boundary for the measured load for the Marstal case over a three years period. See Figure 57.

We find for the very simple method that the results are also simple, not taking any response by the system into account except from the monthly-defined values. This is seen from the jumping results in both heat load (left) and duration curve (right).

5.1.4.2.2 Energy characteristics / Signature models

Another very simple method for the description of heat loads is called energy characteristics or energy signature. The method is described and applied by (Aronsson, S., 1996) for the correction of measured district heating loads.

Simple functions are applied for the description of any kind of relevant influence on the system, e.g. the dependency of the load on the ambient temperature. Such curves can be obtained by plotting measured data and finding a realistic approximation which is a very simple procedure.

In addition, black-box approaches can be applied to find such dependencies. Even so, non-linear functions could be applied, this is not seen in literature by the author.

For the Marstal case, the characteristic curve was found for the DRY data-set by the following procedure, by relying on the authors' observations cited in this section that the load consists of an ambient temperature dependent part and an independent part:

1. The maximum load of 8 MW is found at –5 degrees and below.
2. The ambient temperature dependent part stretches between 8 MW at –5°C down to 1 MW at the ambient temperature of 16°C.
3. The ambient temperature independent part is found for temperatures above 16°C with a minimum load of 1 MW.

These assumptions lead to the signature shown in Figure 47.

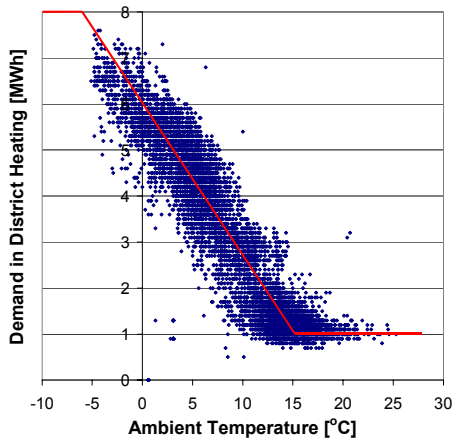

Figure 47. Assumed energy characteristics (thick line) for the Marstal case, for 1997 data.

Applying this pattern on the heat load estimation we find the duration curve of Figure 48

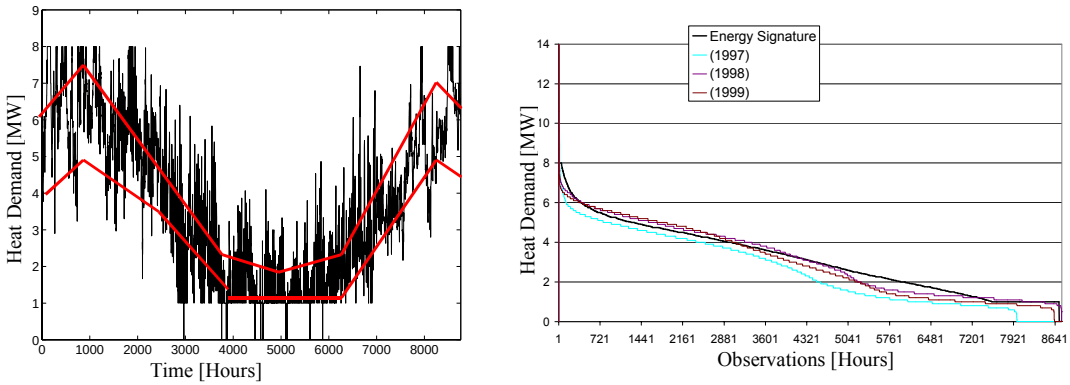

Figure 48. Hourly heat loads for the Marstal case during the year used for the energy signature method (left plot) and correspondent duration curve (right plot).
Note: The thick line is found as a rough boundary for the measured load for the Marstal case over a three years period. See Figure 57.

We find from Figure 48 that the annual changes are computed realistically, but that the values in general are too flucutating compared with the measured values (sketched lines).

The duration curve can be adjusted by working with the signature, if necessary. It is relevant to mention that applying similar characteristic curves to other input parameters, e.g. solar irradiation, can enhance the method.

5.1.4.2.3 Normalisation of measured data

The above methods assume measurements of load data from a given period. Each season has an individual pattern. To make data from different years comparable, two methods can be applied – the degree-day correction presented and applied in (Aronsson, S., 1996), (Lawaetz, H., 1987) and (DANVAK, 1999) and the energy signature correction, presented in (Aronsson, S., 1996).

The degree-day (alt. degree-hour) method is based on meteorological measurements. The degree-day value, GD_p, for the actual period is calculated as the number of observations where the average ambient temperature is below a given threshold, in the Danish case 17 degrees Celsius, times the temperature difference up to the threshold. This is the case, if the actual period is defined as heating season that again is defined on the ambient temperature. If the ambient temperature in autumn is below 12°C for three days the heating season is started. If the ambient temperature rises above 10 °C for three days, the heating season is stopped. In the current computations the heating season definition is not included. The time length of an observation is typically an hour or a day (hence the naming). By summing the values over the period, a degree-day value is determined for this period. This is done for a "normal" period, GD_n. Hereby, the heat load for an actual period, Q_p, is then normalised by the expression $Q_n = Q_{sh}\frac{GD_n}{GD_p}$, where Q_{sh} is part of the load directly affected by the ambient temperature, mostly the space-heating load only. Other load components, such as domestic hot-water preparation, are normally not degree-day normalised. This is often done by normalising 80% of the load.

The threshold value of 17°C is chosen to reflect the need of heating for residential buildings, heated to an indoor temperature of 20-21°C by accounting for the internal heat gain (heat from equipment, people ect.) and the dynamic influence of the building's thermal capacity. Therefore, the method will lead to uncertainties for building stocks with strongly different characteristics in the internal heat gain and the thermal capacity.

It is worthwhile mentioning that the current description is a simplified version of the degree-day methods applied in Denmark, where degree-values are set to zero for warm periods. The method is also defined to include corrections for solar irradiation and wind.

For the Marstal case, by applying the DRY data set, the yearly degree hours are 83710 degree hours with temperature below 17°C times the temperature difference up to this temperature. For this example, we assume 20% of the heat load to be independent of the ambient temperature and 80% dependent. The load is then combined by a corrected and a not corrected part. By this procedure, we find a load profile and duration curve as shown in Figure 49.

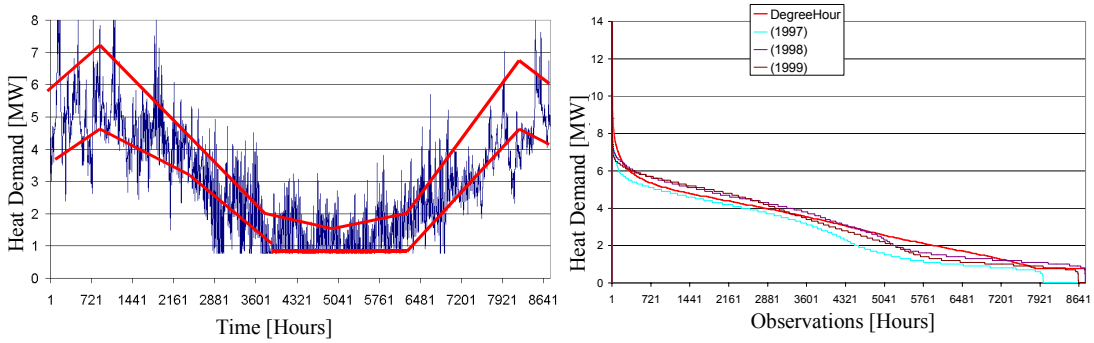

Figure 49. Hourly heat loads for the Marstal case during the year for the degree hour method (right plot) and correspondent duration curve (right plot).
Note: The thick line is found as a rough boundary for the measured load for the Marstal case over a three years period. See Figure 57.

The results in Figure 49 prove reasonable agreement of the computed values by the degree-day method. Similar to the dynamic method of the load generator tool the fluctuation of the results is larger than measured. However, this very simple method leads to surprisingly realistic results as we find from the right plots.

5.1.4.2.4 Steady-state models

The above methods can be classified as a kind of lookup-table. The following methods are fundamentally different. Here the system is simulated based on any kind of model/representation. The simplest simulation method is based on steady-state assumptions, where temperatures and flow rates are kept constant for short or long time periods. Assuming the constant conditions for a given period, the corresponding heat load is estimated by well-defined and standardised calculations.

5.1.4.2.5 Back-Box methods

If one is not able to find any theoretical description of a given phenomenon, the input-output (stimuli-responds) method is applied in many scientific fields. Here a so-called black box is coupling the input in a manner that the output is representing the results as expected. The theory for such black-box methods is rather advanced and readers are referred to e.g. (Ljung, L., 1987).

5.1.4.2.6 Dynamic modelling and simulation

Dynamic modelling is different from the above methods by the fact that the method can handle changing surroundings to a given system. In the steady-state method, the surrounding is simplified to constant values. This is actually also the case for most dynamic methods, but with the difference that the present interval where an ambient influence is assumed constant is very short.

There are two basic paradigms for building dynamic models - stochastic and deterministic. Deterministic models are often seen as more realistic and as giving more insight into the matter. On the other hand, deterministic models cannot always reproduce the real world by satisfactory accuracy. In such cases, the basically deterministic models are supplied with some stochastic parameter estimates of even stochastic parts of the models. This is a common approach to escape lack of knowledge for a given system.

5.1.4.2.6.1 Stochastic modelling

Almost all the models that are mentioned in this text could be classified as deterministic models, where the load components are well-behaved patterns that can be described by theories based on mathematics and physics. However, load patterns for heating systems show some more arbitrary load parts that cannot be handled by the deterministic models and must be described by stochastic (based on statistics) models. An example of such arbitrary behaviour, the simultaneousness of user loads, is for instance many people taking a shower at the same time. The idea is to base a given load model on some statistic probability of a given occurrence, combination of occurrence and so on. For further reading on such models, see for instance (Sejling, K., 1993), (Madsen, H., Pálsson, H., Sejling, K., and Søgaard, H. T., 1990) and (Pálsson, O. P., 1993).

5.1.4.2.6.2 Deterministic modelling

Deterministic models are implementations of physical theories often described in mathematical terms, e.g. natural laws and empirical models described as expressions and equations. In some cases, e.g. the heat losses in buildings, the model can include multi-dimensional heat transport phenomena described by partial differential equations. For long-term simulations, such approaches would need an enormous amount of computer power. To simplify the task, the

equations are reduced to ordinary differential equations by discretising the problem in space, leading to a set of equations dependent on one space dimension and the time only. Such system models are solved by dynamic simulation, where the load is found for very short periods, e.g. minutes or hours, assuming the boundaries for the system constant in these time intervals. The approach is central for the current work and will be discussed in detail below.

5.1.5 Heat demand model development and validation

In the current work, dynamic modelling and simulation are applied for the generation of annual heat load profiles with hourly values. In this section, the model development for the load model is presented. The load model consists of the most significant load components discussed above: 1) Space heating described in 5.1.5.1. 2) Hot-water preparation in section 5.1.5.2 and heat losses in district heating and hot water distribution networks in section 5.1.5.3. In the final heat load model, described in 5.1.5.4, the individual heat components are set together. In Section 5.1.5.5, the results are examined on the Marstal case, similar to the above examinations of other load models. Note that the current survey is a short version of the presentation in (Heller, A., 2000c).

5.1.5.1 Space heating

Space heating ensures a proper thermal comfort in buildings by maintaining the indoor temperature at a desired, uniform level and serving for proper admission of fresh air. In some regions, cooling must be included which is not a dominating factor for the typical central heating system in Denmark. A space-heating model is normally represented by computer models similar to the load or CSHP model of the current work. Such models must, in one way or another, deal with heat transport phenomena of many origins, e.g. convective heat losses through windows, cracks, ventilation and other paths, conductive heat transports through walls and radiative energy transport through windows. Space-heating models are numerous, spreading form very simple to dynamic and multi-dimensional models. A comprehensive survey is not possible here hence the reader is referred to the normative texts for building heat loss computation in the following publications:

Heat loss computations for Danish conditions can be based on work by the Danish Building Research Institute in (Aggerholm, S., Zachariassen, H., Christensen, G., Olufsen, P., Clausen, V., and Pedersen, P. E., 1995), or on norm texts as in (Dansk Standard, 1986) and related amendments, (Dansk Standard, 2000d), (Dansk Standard, 2000c), (Dansk Standard, 2000b) and (Dansk Standard, 2000a). See also European Norm (EN 832) for simple computations.

Building models include, in the current context of district heating, the system to supply heat to the building. Hence, heat supply system modelling must also be handled. This subject is among others discused in (Dahm, J., 1999). The load component for space heating consists therefore of the heat compensation plus the efficiency losses of a given installation. The latter is, among many others, described in (Qin, L., 1998) and (Eriksson, L., Zinko, H., and Dahm, J., 1998).

The space-heating model implementation presented here is the third of a series utilised by the author during the current ph.d. study. The first is published in (Berger, R., 1997), applied in a European research project and also applied in the generation of the findings in (Heller, A. and Dahm, J., 1999). Hence results from this model will later be discussed indirectly in this thesis.

A second attempt is made in connection with a Master Thesis by (Laustesen, J. B., 1999), and in connection with a co-publication on the application of CSHPs in new settlements with the current author in (Laustesen, J. B., Svendsen, S., and Heller, A., 2000). Fundamentally, the method is to apply a building model, representing a building according to the Danish Standards from 1995, implemented in the thermal building simulation program TSBI3, (Johnsen, K., Grau, K., and Christensen, J. E., 1993). Based on this reference, two futuristic low energy

buildings were modelled with 60 and 30% respectively of the heat demand of the reference building.

The final implementation, presented here, is based on current work done in a co-operation project under the International Energy Agency (IEA) under the Solar Heating and Cooling Programme (SHC), Task 26, "Solar Combisystems". Also here three heat demand levels are applied similary to the above attempts. The choice to base the current work on this co-operation is manly that the communication of the methods applied and the findings found is made easier and that the results are comparable with other work. I hope that the methods and models will base a common platform for similar work. Hereby wasting time on discussions on the assumptions for modelling is shortened or even avoided. This is one of the main reasons for the rather comprehensive effort in the load modelling by the author. The drawback of the procedure is unfortunately that the models may change during the ongoing IEA work and that the documentation of the model has not been published in a final version yet. The "Task 26" building model is in detail documented by (Streicher, W., 2000). The TRNSYS-tool PREBID is used for the definition of the building. PREBID prepares a set of output text files that are used by the overall TRNSYS-model. From this resulting building component model, the heat demand for heating the building is estimated in chosen time steps. The necessary heat demand is satisfied by a radiator system, implemented in the Task 26 work in the TRNSYS-IsiiBat tool, re-implemented in a TRNSYS-PRESIM tool for our own simulations by my colleague Louise Jivan Shah. The general models are then run with Danish climatic conditions to generate space-heating profiles for Danish buildings. Two building types are implemented, a single-family house and a multi-family house. The latter is not applied in this work. The resulting heat loads are shown as duration curves in Figure 50.

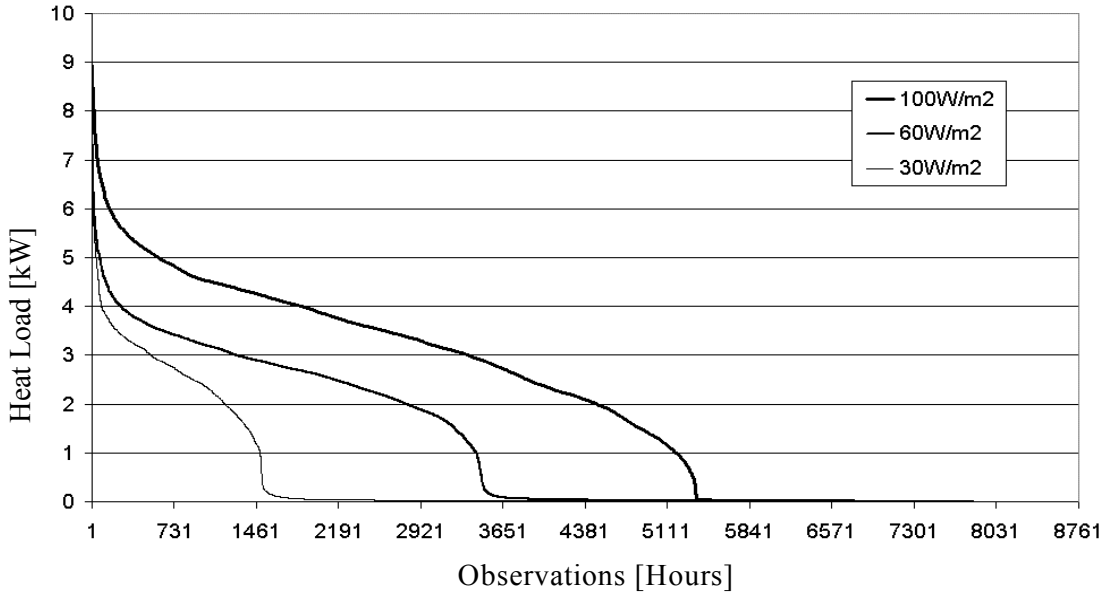

Figure 50 Duration curve for the heat demand in kW of the Task 26 building with three insulation levels under Danish DRY weather conditions.

On the left side of Figure 50, one finds the largest observations, decreasingly ordered to the right side of the plot. We find that all curves show a rapidly decreasing space-heating demand, flatting out in a close to linear shape and ending in a strongly decreasing manner (S-shape). We

find, as expected that the heat demands for the three insulation levels are decreasing – in magnitude but also in number of observations with given demands[5].

As mentioned above, the current space-heating model is the third in a row of three applied models. To enable comparison with findings from older work published by the author and others, the results from the three generations of load data are compared in Figure 51.

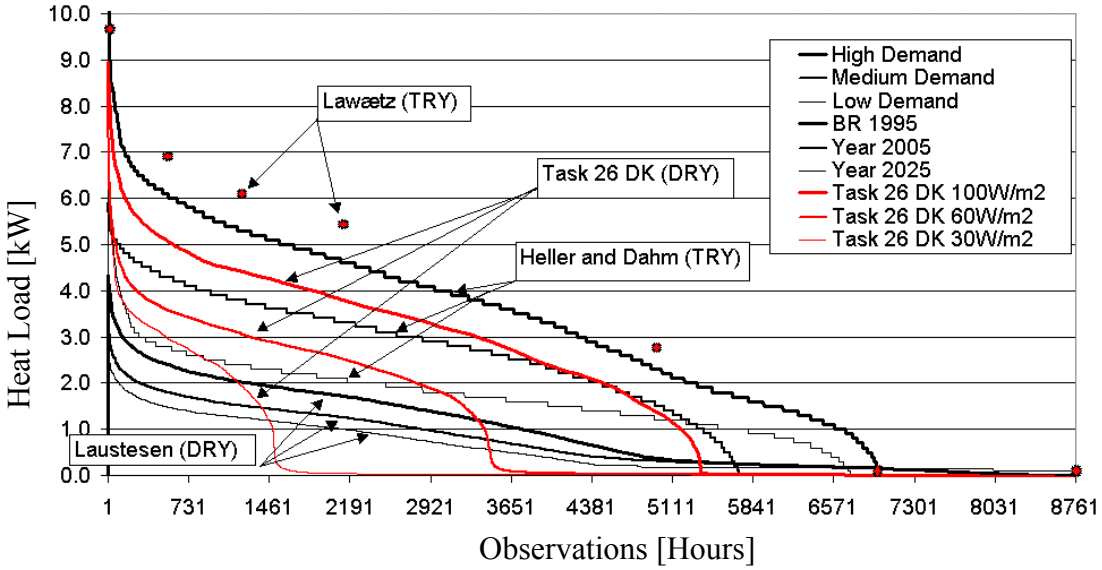

Figure 51. Duration curve for the load profiles in kW applied by the author and others.

The oldest observation (dots) is made by (Lawaetz, H., 1984) and shows the highest load demand.

Three curves are plotted for the heat loads applied by (Heller, A. and Dahm, J., 1999). Here we find the characteristic S-shape with strong decreasing heat demands at highest and lowest observations and a close to linear decreasing demand in between.

We find similar curves for the currently applied space-heating model, labelled "Task 26 DK", but on a lower level.

At the very lower part of the figure, three curves labelled "Laustesen" are representing the load patterns for the buildings applied by (Laustesen, J. B., 1999) and (Laustesen, J. B., Svendsen, S., and Heller, A., 2000).

From the many curves in Figure 51, we can extract the following findings:

- The magnitude of loads decreases from older studies to newer work. This can be explained by the fact that the regulations in building codes are imposing stronger claims for thermal insulation of buildings with a resulting decrease in demand.

- The S-shape load distribution is found by all authors, except Laustesen. Reasons for the deviation of the latter could be 1) that the very low demand for low energy buildings wipes out the S-shape, 2) that the implementation of the building model affects the shape and, 3)

[5] Some general reflections can be connected with this S-shape. Heating systems are designed on norms with implicit assumptions to the maximum load of buildings. From the curves above, we find that the "worst case" is only observed for a minimum number of hours during the year. As shown in (Aronsson, S., 1996) for Swedish conditions, it would be wise not to apply the worst-case scenario for the dimensioning of heating systems. Hence revision of the codes in at least Sweden, Denmark and Germany would be recommendable to avoid oversizing of heating systems.

that some characteristics of the applied TSBI3 simulation program affects the shape of the curve. More work would have to be done to uncover this systematic deviation.

- The Task 26 models spread over a rather large variety of space-heating demands. The S-shapes for the curves are more accentuated compared to the results of other implementations. This shows that the demands are still rather high, but on the other hand that the number of hours with demand is decreasing. Hence, savings can be expected in fuel, but not due to a downsizing of the heating system.

From the above findings we can assume that the results in (Heller, A. and Dahm, J., 1999) are comparable with the results in the current work. Due to the absence of very low heat loads for the Task 26 curves, compared to the "Heller-Dahm" implementation, one can expect a tendency of lower summer loads for the current implementation. The findings by Laustesen cannot be compared directly with the findings in Heller and Dahm and the current work, due to the rather dramatic deviation in total loads for low-energy buildings not focused on in this work.

Not so important for the current work, but, however, impressive, is the fact that the Lawaetz implementation of a simple two node mode shows a duration curve that can be compared with the findings by the TRNSYS-models. See dots in Figure 51.

Having generated specific loads for a set of single buildings, an overall load can be found by combination. This subject will be discussed in relation to an overall heat load model below.

5.1.5.2 Hot water preparation

Domestic Hot Water (DHW) loads depend on a large range of factors, e.g. number of residential units, heat losses in the installation itself, intersection of building components due to the installations, the number of inhabitants and their behaviour. In many cases, it has been tried to explain the behaviour by social parameters such as age, sex, social ranking and more. Measurements are carried out for a number of cases, spreading from a few residential units to large areas. The measurements show large fluctuations and variations between different objects, users etc. A load model based on all these varying influences would be unadoptable. Hence, mean-values and simple models are in general applied to reflect average daily, weekly, monthly and yearly variations in demand defining the resulting load pattern.

Heat load for domestic hot water for single family and multi-family buildings can be estimated based on the Danish Standard (Dansk Standard, 2000). Research work has been made to determine the demand of hot water, e.g. (Qin, L., 1998) and (Mazin, M. and Maleki, M., 1995) give some starting points for load estimation in Denmark. No final models are presented, except from the fact that, Danish (Mazin, M. and Maleki, M., 1995), German (Mack, M., Schenk, C., and Köhler, S., 1998) and Swedish (Aronsson, S., 1996) measurements show similar patterns and a distinct over-dimensioning of DHW-installations, based on standards. Hence, reconsideration of standards would be relevant.

For small systems, the term "domestic hot water" (DHW) is applied. In the studies on district heating systems, the term Hot Water Preparation (HWP) is preferred for the including of e.g. hot-water demands for industrial purposes. HWP demands show a seasonal pattern due to varying hot-water consumption with higher loads in winter than in summer periods. This results in a superposition of total loads for central heating systems. Similar seasonal pattern can be related to the supply temperature, the cold-water temperature. This water temperature varies according to (Aronsson, S., 1996), (Mack, M., Schenk, C., and Köhler, S., 1998) and (Yang, L., 1994) in a smooth sinus-formed curve. The user behaviour is certainly a very important factor for HWP-loads. The diurnal pattern shows two peak load periods; one in the morning and one larger peak in the evenings. The weekday has an impact on the load, due to the different behaviour in workdays and weekends. Most authors reported this pattern. According to (Aronsson, S., 1996) HWP consumption is correlated, in the case of district heating systems, to building age, size and building area to be serviced. This seems not to be the case for residential

buildings. The dependency between HWP demand and the age is also found by (Mazin, M. and Maleki, M., 1995) up to the 70ies, when the demand drops due to the oil crisis. A later drop is reported by Aronsson possibly based on the fact that sanitary installations in recent years tend to save resources. Hence, parameters reflecting this correlation should be included if the system includes non-residential areas.

Similar to the situation for the space-heating models above, the author applied a series of implementations of previous work. The first HWP-model was based on work by Dahm leading to the findings in (Heller, A. and Dahm, J., 1999). Here on the one hand, a complex, dynamic flow model for the piping, heat exchangers and on the other hand, a very simple daily and yearly profile correlation are lumped. The current implementation is an extension to this approach.

A second implementation was in relation to a Master Thesis, (Laustesen, J. B., 1999), basically a variant of the model by (Qin, L., 1998). Here daily, monthly and yearly fluctuation patterns are combined in a spreadsheet computer program to a final HWP-load profile outputted to a text file.

The third attempt is applied in the current work and is chosen to avoid a discussion on all these many factors on the load component for hot-water preparation. A model developed in a project under the International Energy Agency (IEA) programme for Solar Heating and Cooling (SHC), Task 26 "Solar Combisystems" is adopted here. The method involves a stochastic approach, covering the statistical distributions and probabilities of the hot-water demand from single families to a large number of involved persons. The model is reported by (Jordan, U. and Vajen, K., 2000).

Fundamentally, the method is as follows: For the generation of the heat load, four categories of loads are included: A) Small draw off (washing hands). B) Medium draw off (dish washing). C) Bath and D) Shower. Each category is presented by a Gauss-distributed curve describing the interrelation (the probability) between the flow rate and the number of draw off, building together the overall draw-off probability distribution. For the four categories the key-values presented in Table 8 are assumed for the Austrian, Swiss and German participants in the co-operation.

Table 8. Key-values for the Hot-Water consumption model by Jordan, applied in IEA SHC Task 26 work.
** Once a week.*

Type		**Unit**	**Single-Family Draw Off**			
Maximum energy draw off		Wh	5680			
Medium load volume per day		l	200			
Total water demand per year		l	70200			
Description	**Units**	**A**	**B**	**C**	**D**	**Total**
Flow rate	l/min					
Duration	min					
Incidents per day		28	12	0.143*	2	
Standard deviation		2	2	2	2	
Volume per load	l	1	6	140	40	
Volume per day	l	28	72	20	80	200

Portion of total		0.14	0.36	0.10	0.40	1.0

Moreover, the following influences on the HWP are applied:

- The probability that a given situation occurs is defined by $P(\tau) = P(year) * P(weekday) * P(day) * P(holiday)$. Hence, yearly, weekly, daily and weekday influences are taken into account by the following means.
- The probability of the demand during the year can be described by a sinus-function with amplitude of 10%.
- The probability in relation to the weekday is described for each category. In the current implementation, all categories, except the category "bath", are gathered under a single distribution. The bath category is handled by its own distribution, due to the high probability of taking bath in the weekends. Resulting distribution during the weekdays is, Medium load for all days: 100%. Monday-Thursday: 95%. Friday: 98%. Saturday: 109% and Sunday: 113%.
- For the daily distribution, profiles are defined for each category, defining together a profile with two peaks in mornings and evenings with constant demand during the day and no demand in the night.
- The holiday distribution is defined by dates. For defined holidays, the probability distribution for the hot water draw-off is reshaped for the given day.

As an example, the daily load due to hot-water consumption in a single-family house is sketched in Figure 52.

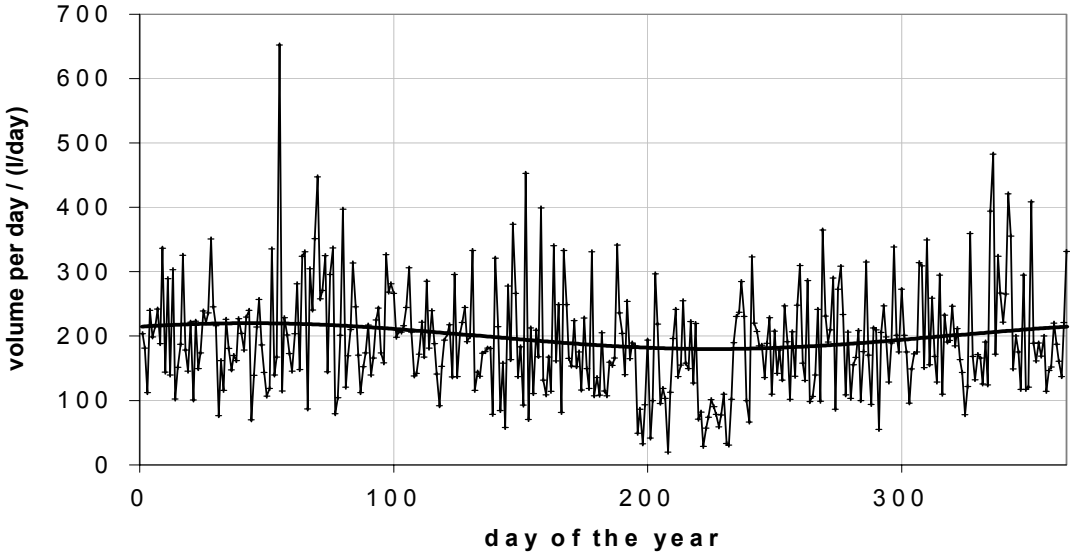

Figure 52. Hot-water draw off-for a single-family house based on the Jordan algorithm and the key-values described above. Source: (Jordan, U. and Vajen, K., 2000).

We find that the method generates a time-series for the hot-water draw-off for a single family, a building complex or combinations hereof. To examine the necessity of generating draw-off profiles for a very large number of individuals, we compute in the following two cases, where the results are presented in Figure 53.

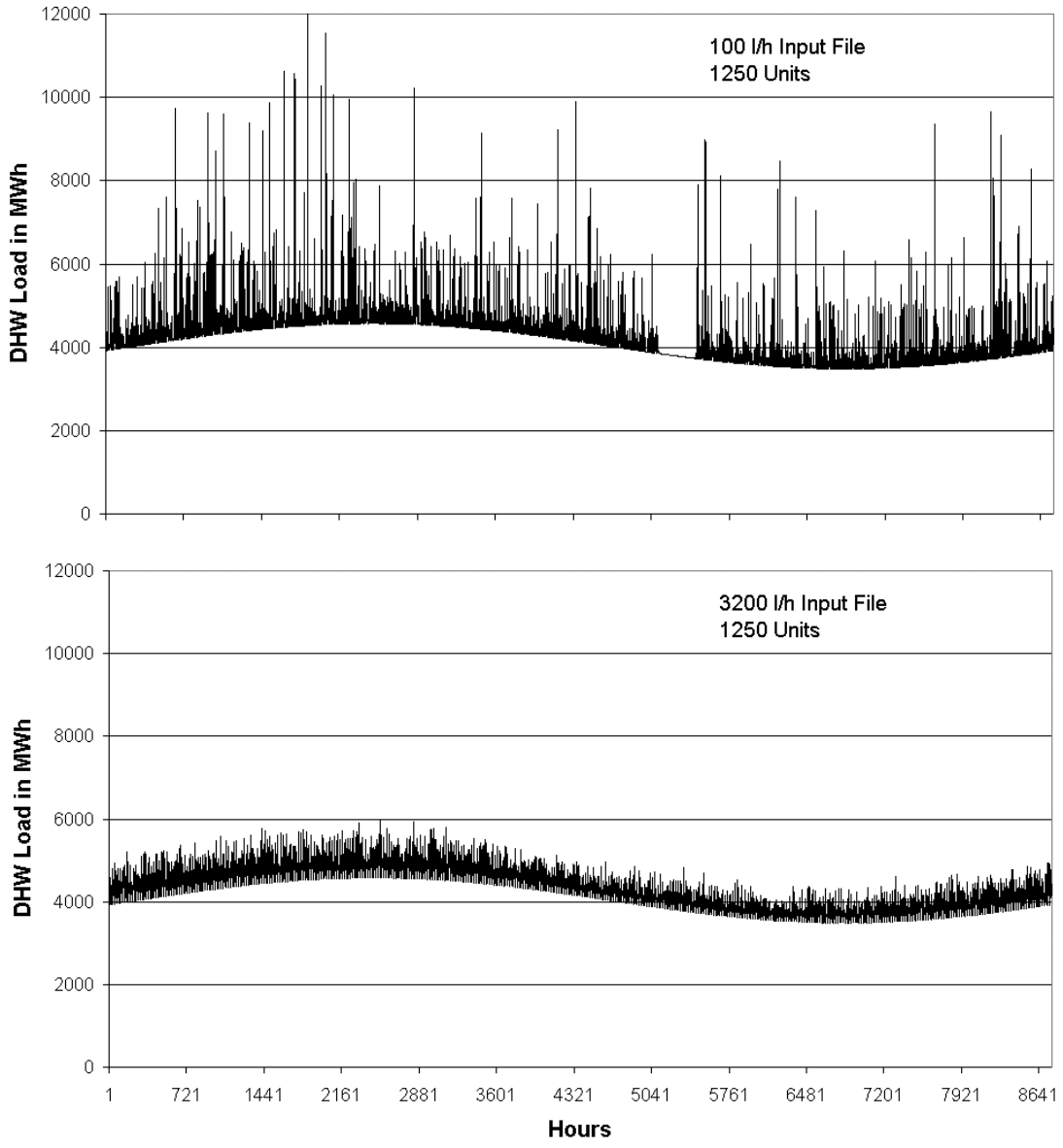

Figure 53. Total heat load for hot-water preparation for 1250 individuals, based on Jordan-algorithm with 100 l/h profile (left plot) and 3200 l/h profile (right plot).

In Figure 53 [6] the resulting load profile for two cases with the same number of involved individuals are plotted. In the top plot, the profile generated by the Jordan-algorithm for a single user (a whole family) multiplied with 1250, leads to very high peaks for the heat demand during the year. In the bottom plot, the result is presented when using a generated file prepared for 32 units and multiplied by approximately 40. We see that here the peak characteristic is flattened from maximum amplitude of 6000 down to near 2000 MWh. It is worthwhile pointing out that the bottom plot represents a more realistic model.

[6] Note: The applied hot-water load profiles are based on 1-minute values that are averaged to 5-minute values for this work. This procedure is certainly introducing some inaccuracies to the analysis. However, the main points and results are still valid.

From the figure, we find clearly that the Jordan-algorithm is avoiding peak effects due to stochastic computing of many users in a single hot-water system. From this comparison, we can conclude that it is necessary to include stochastic methods for the user behaviour distribution, in this case the hot-water consumption. Consequently, a load profile for a central heating system must be prepared by applying the Jordan or similar stochastic algorithms if the load profile ought to be realistic.

5.1.5.3 Pipe heat losses

Two main causes of heat loss are included in the current presentation; pipe heat losses in the buildings hot water supply net and heat losses in the district heating distribution net. Additional heat losses are due to the connection between the distribution and the supply network, see (Yang, L., 1994) and (Dahm, J., 1999). This subject is not discussed in the current work.

5.1.5.3.1 Heat losses in the HWP distribution and circulation net

The consumption of hot-water causes heat losses in the pipe network, due to 1) the loss due to transporting the medium to the consumers, and 2) loss due to circulation applying to ensure high temperature at any point of the network at any time.

Literature on measured heat loss in circulation is rare. Hence, uncertainties are very large. Reports by (Svendsen, B. and Carlsson, P. F., 1995), based on one-year measurement on a four-storied, multi-family block with 67 residential units, show that heat loss due to circulation can be up to 3 times the demand for hot water. Similar high results are reported based on measurements on an educational building by (Esbensen Consultans, 1991). (Boye-Hansen, L. and Furbo, S., 1995) report monthly values for circulation heat losses between 80 and 90% of the hot-water demand for a 44 residential unit, three-storey, row-housing area. A similar circulation loss, close to 100%, is found by (Kristensen, F., 1995). Even losses in the range of 200-400% are found in recent monitoring cases. Such systems are not representative and can be ignored here. In general, the assumption is made that heat losses due to circulation are between 50 and 100% depending on the age of the system, the insulation level and the length of the distribution pipes. German and Swedish results seem to be much lower, lying between 10 and 50% in Sweden, (Dalenbäck, J-O., 2000) and 15-25% in Germany, (Vajen, K., 2000).

Circulation heat losses in buildings are presented in (Qin, L., 1998) and by the standard for hot-water systems presented in the previous section. Heat loss in district heating pipes can be computed according to the Danish Norm (Dansk Standard, 1994) for buried pipe couples.

5.1.5.3.2 Heat losses in district heating net

Literature of modelling of District Heating Losses is very extensive. (Bøhm, B., 1999) is a good starting point together with the Danish Norm (Dansk Standard, 1994).

Values for heat loss in district heating systems are very uncertain. The estimated heat losses from the distribution net are by (Werner, S. E., 1984) estimated at 6-8% and by (Bøhm, B., 1999) at around ¼ of the total heat load. The Marstal case shows heat loss between 20 and 23% during the last four years. However, there is no doubt that realistic net heat losses are crucial for the current work as one of the main boundary conditions for the modelling of CSHP. Hence, the subject is described in more detail than the previous load components.

A district heating net consists of a large number of heating pipes which must be represented in a given model. It is certainly possible to describe a net with all its details which will demand a lot of information and resources. The complexity must therefore be reduced. Reduction procedures are proposed in (Bøhm, B., 1998), (Pálsson, H., Larsen, H. V., Bøhm, B., Ravn, H. F., and Zhou, J., 1999) and (Larsson, G., 1999). Any reduction or simplification will lead to loss of precision. It is the task of modellers to find a compromise which is not a trivial task.

Here a short introduction to possible simplification in models for the representation of complex net structures.

A very general approach for system reduction is known from electric analogy methods, where e.g. thermal systems are modelled by electrical circuits. Here a system of three nodes connected in a fourth central node can be reformulated by a triangle with three nodes only. Readers are referred to basic schoolbooks in electric and computational analogy theory, for further reading on the subject, e.g. (Mills, A. F., 1992).

(Pálsson, H., Larsen, H. V., Bøhm, B., Ravn, H. F., and Zhou, J., 1999) investigate so-called equivalent models where the net is successively reduced to less complex structures. The results of these models were then compared with the results of a very complex model. The authors report two alternative procedures for the reduction: 1) Ignoring parts of the net from the small pipes up to the larger ones. 2) Reducing the net based on logical considerations, such as e.g. the area around a large single user. By examining the response of a reduction in terms of deviation in return temperatures to a DH-plant, the researchers were able to estimate the precision of the equivalent models. The most relevant result of this investigation for the current work is that the complexity of a net can by applying a proper reduction procedure, be reduced from e.g. 50 branches to approximately 10 without severe loss of accuracy. The error in returntemperature to the plant is less than 2 K. Reducing the net to even fewer branches leads to decisive loss of accuracy. This must be kept in mind when we look at single branch net representations in the following. By representing a network by a single pipe couple, as applied in the final heat load model below, the uncertainty, according to the cited work, lies in the best case at approximately ±15%.

(Larsson, G., 1999) presents an alternative approach to the above simplification of DH-nets based on hydrodynamic considerations for the simplification. The approach has shown astonishing precision for three presented cases. The following reduction procedure is reported:

1) The branch of a DH-system is reduced to one single point at the ramification of the pipes. Hereby the hydrodynamic influence of the branch is still realistically modelled.
2) To compensate for the missing thermal influence of the removed branch, the thermal capacity is assigned to a single virtual "load-point".

For all simplification methods presented above, the procedure is either poorly documented or not easy to apply for others in the given stage. Hence, other procedures must be found until better documentation is presented. A very simple and applicable method for the net reduction is presented by (Bøhm, B., 1998) and (Bøhm, B., 1999):

1) The DH-network is reduced to two pipes.
2) The fluid volume in the DH-system must be the same for the real DH-system and the equivalent model.
3) The diameter for the pipe is found based on documentation material on, or knowledge about, the net as average.
4) Applying insulation thickness corresponding to the pipe diameter found by common dimension practice.

Other simplifications in the net modelling are numerous. A survey is presented in (Heller, A., 2000c). In this publication some analyses and discussions on the numerical artefact, numerical diffusion, are presented. Here we focus on the application of the pipe models available in the TRNSYS simulation program. Two alternative models are available at this moment. None is implementing the Danish or European norm computations for heat loss in district heating pipes. Both models are single pipe models, not considering the interaction between the supply and the return pipe. Both models are implementations of the plug-flow scheme with maximum 25 segments. The Standard-Type 31 is a pipe in air model, as the Non-Standard-Type 80 by

(Dahm, J., 1998) implements buried pipe model, considering the interaction with the ground, based on the simplification of undisturbed ground temperature.

The heat loss per metre of pipe, *UA/l*, can be found on basis of (Bøhm, B., 1999) by the following simplified expression

$$\frac{UA}{l} = \frac{2\pi}{R_s + R_i + R_c + R_g + R_{cp}} \tag{7}$$

where R_s is the thermal resistance for the steel pipe in m K/W,
R_i thermal resistance for the insulation material in m K/W,
R_c thermal resistance for polymer cover in m K/W,
R_g thermal resistance for ground in m K/W,
R_{cp} thermal resistance for the couple pipe in m K/W.

In the Dahm-model the corresponding expression[7] is

$$\frac{UA}{l} = \frac{2\pi}{R_i + R_g} = \frac{2\pi}{\frac{1}{\lambda_{iso}} \ln \frac{d_o}{d_i} + \frac{1}{\frac{d_o}{2}\lambda_g}} \tag{8}$$

where l is the length of the pipe in m,
λ_{iso} thermal conductivity of the insulation in (W/m K),
λ_g thermal conductivity of the ground in (W/m K),
d_o outer diameter of the insulation cover in m,
d_i inner diameter of the steel pipe in m.

It is easy to find that the Dahm-pipe model neglects the resistance of the steel pipe and the cover, which is acceptable.

The error applying the TRNSYS Standard-Type 31 can be estimated on the fact that this component model computes the heat loss either on a user-specified constant or varying temperature, e.g. ambient temperature. In the latter case, the heat loss will be overestimated by the difference for the ambient temperature changing between –7 and +21°C compared with the average temperature in the ground of 8°C.

Comparison of simulation results from the TRNSYS components with the results from accurate computational models by Bøhm shows that:

From steady-state computations of pipe couple with length of 1, 5 and 10 km, we find by applying the Bøhm and the Dahm models, that the temperature at the outlet is computed with a difference of 2, 3 and 4 respectively with a flow rate of 1 kg/s.

For dynamic conditions with changing boundary conditions, we find that the flow model for piping in TRNSYS leads to reasonably realistic results. See (Heller, A., 2000c). This is due to the application of a plug-flow mode implementing a numerical method called a wind-up differential method. Therefore, the uncertainties involved in heat loss computations are caused by simplifications to the net and less by the numerical artefact, called numerical diffusion.

5.1.5.4 The final heat load model

We have now described the details of the individual load components and possible model implementations. In this section, these components are gathered to an overall load model able

[7] Note: The units in the expression are erroneous. This can be explained by the preliminary state of the applied publication by Dahm. The error may be changed in a final version.

to generate heat load profiles with user-defined time steps. In the following, only hourly heat load profiles are applied. The heat load model is visualised in Figure 54.

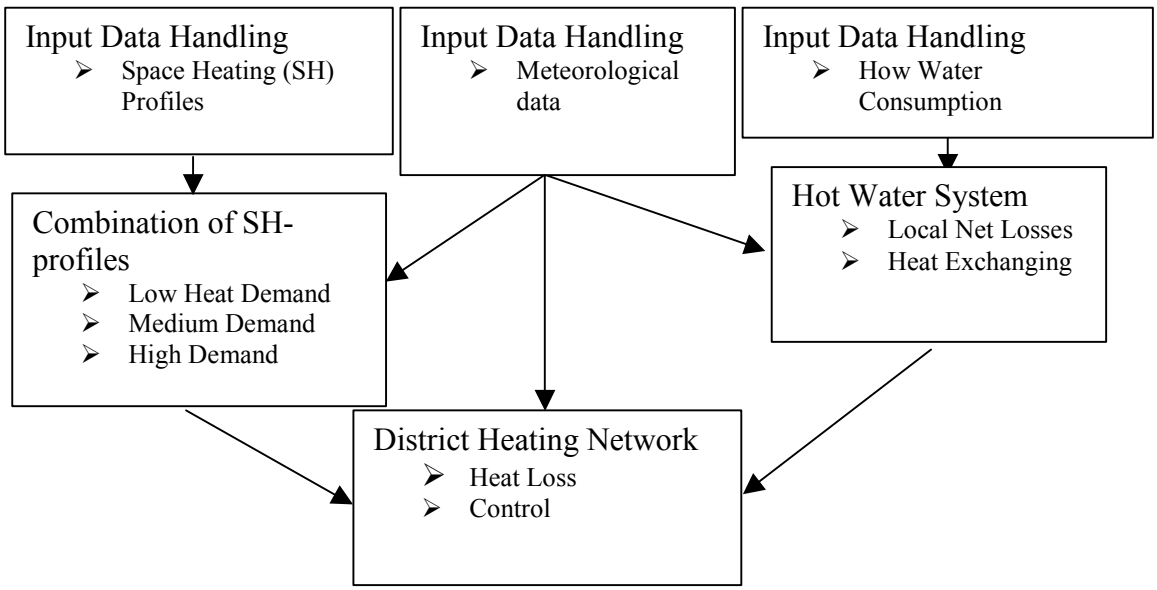

Figure 54. Flow chart for the main components in the final heat load model for district heating and other large-scale heating systems.

The overall layout of the heat load model implements the individual heat load components individually: 1) Space Heating (SH) 2) Hot Water Preparation (HWP) including heat losses in local network 3) District Heating Network Losses.

The space-heating model consists of up to three different types of buildings, each of them with different space heat characteristics. The buildings available from the overall model are in the given case defined by the IEA-SHC Task 26 work, discussed above. The total space-heating load is then computed for the given temperature and mass flow rates by simple means. The resulting mass flow necessary for the given district heating temperature conditions, $\dot{M}_{sh,ist}$, is then found by a simple ratio of the current supply temperature and the demanded supply temperature from the energy balance for the two conditons, as follows

$$\dot{M}_{sh,ist} = \dot{M}_{sh,soll} \cdot \frac{T_{h,soll} - T_{l,soll}}{T_{h,ist} - T_{l,soll}} \tag{9}$$

where
$T_{h,soll}$ demanded hot supply temperature in ^oC,
$T_{l,soll}$, demanded hot supply temperature in ^oC,
$T_{h,ist}$ actual hot supply temperature in ^oC,
$T_{l,ist}$, actual hot supply temperature in ^oC,
$\dot{M}_{sh,soll}$ demanded mass flow rate in *kg/h*.

with indices from German language "Soll" for the demanded values and "Ist" for the current, actual values – a very applicable concept. The necessary flow is "diverged" from the main flow and returned at the demanded return temperature for the space heating, mixed with the other part that has not entered the space-heating sub-model.

The hot-water preparation model is fed by a profile for a number of individuals from external source, e.g. the Jordan algorithm results. The heat load is used as an input to a pipe network

model, implemented in the TRNSYS load model. In this part of the model, a single pipe network is implemented including circulation flows. A heat exchanger model is applied for the heat exchange between district heating and local water distribution networks.

The district-heating network is implemented as a single pipe couple with necessary flow control. The district heating pipe network model consists of two heating pipes, represented by the standard TRNSYS component, TYPE 31, and an auxiliary heating equation, for the determination of the minimum heat load necessary to bring the flow medium up to the necessary supply temperature at the main heating plant. Alternatively, one could use other TRNSYS models for this purpose, but due to the goals of the current load generator, the current implementation causes minimum complexity. Heat loss for the buried pipes is estimated based on an average temperature of 8 degrees Celsius. The total flow is a sum of the individual load components, space heating, hot water preparation and, if wished, circulation in the district heating system.

The load model can be adjusted to a certain purpose by a number of parameters and input data sets. By these means, the model can be tuned to serve many objectives. The model is able to supply online information from the simulations, when running, and a set of output to files for later analysis, among others a final heat load profile for the given simulation with time, temperatures, flow and power.

5.1.5.5 The load model applied on the Marstal case

The developed load model for heat load generation of large heating systems is in this section applied on the Marstal district heating case. Model parameters known from measurements and other facts are set to values known from these sources:

- The number of buildings connected to the plant is 1320.
- The buildings are mainly old, single-family buildings. Hence, high demand space heating load files are preferable.
- The buildings are spread over a relatively large area with low-line heat demand leading to relatively high heat losses for the system. This heat loss is estimated at 23% by the plant based on measurements.
- The district heating network (approx. 32000 m) and the installations in the buildings are renovated in the recent years, leading to low heat losses and high efficiency for the system.
- The hot-water consumption in the summer rises to the double due to tourism.

By applying these factual values in the load generator model, we get the following picture of the load for the Marstal plant:

- The overall heat load for the plant is computed 800 MWh too high.
- The heat loss in the DH network is found very accurately to 23.5%.
- The heat load in winter is too high and in summer too low.

As we see from these rough estimates, the model must be adjusted to represent the measured load. Here lack of knowledge makes things difficult and enables many combinations of parameter set. A few main parameters must be adjusted to get a best fit. The space-heating component is adjusted to 465 buildings with high heat demands and the rest with medium heat demands. Hereby we find the following results.

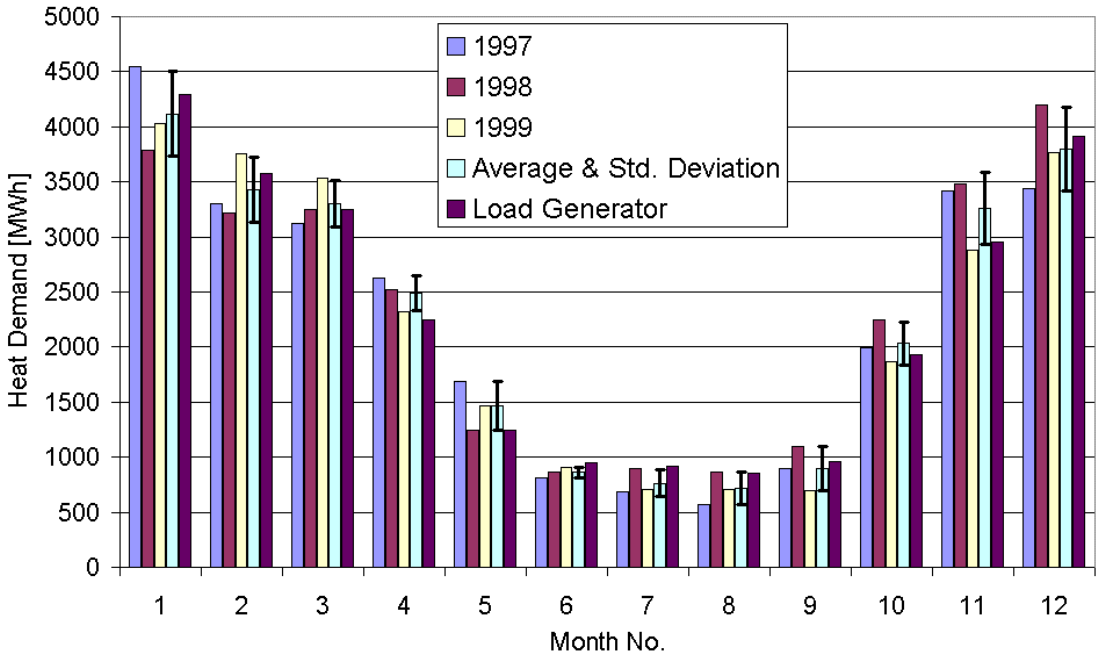

Figure 55 Monthly heat load values for the Marstal district-heating plant measured from 1997 to 1999 (left three bars). The measured average and standard deviation values for this period are plotted as the fourth bars from the left. The right-most bars show the computed values for the adjusted parameter set.

The comparison in Figure 55 shows that the heat load for the coldest winter month and the summer months are estimated rather high, as the values computed for April, May and November are too low. Such deviation can be adjusted by the model parameters. It turns out that the heat loss is of very great importance to the overall performance. Two experiments are carried out in this study: 1) A one-level approach, where the heat loss during the whole year is fixed. 2) A two-level heat loss model with different circulation loss in winter and summer. The latter certainly showed the best result. For the two experiments, we get a duration curve as presented in Figure 56.

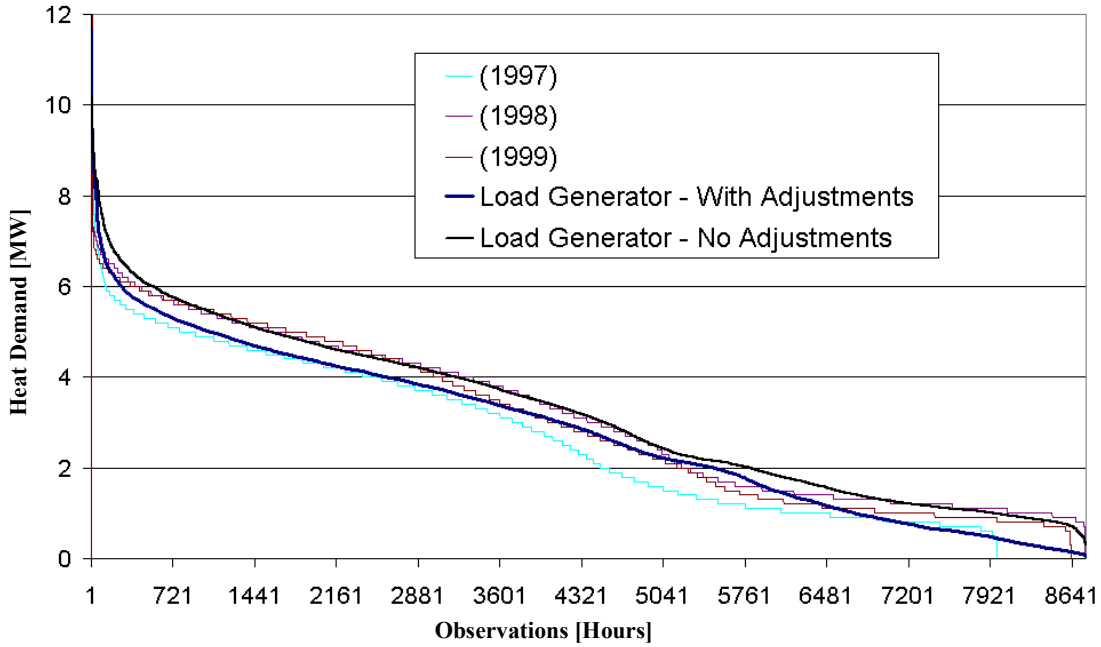

Figure 56 Duration curve for heat load measured for 1997 to 1999 and compared with two computation results: 1) "Load Generator – No Adjustments" for the computations with one yearly circulation value and hereby one single district heating heat loss parameter. 2) "Load Generator – With Adjustments" where there is circulation in non-summer periods as in 1) and a minimum heat loss in summer chosen to keep up the supply temperature at the consumers.

The duration curve for the simulations with summer and winter circulation parameters gives the best fit for the large demands but less accurate results for low heat loads. This could certainly be adjusted by choosing an even better circulation model and hereby a better heat loss simulation in the district heating.

From these results, we can conclude that the heat loss model for the district heating must be chosen carefully and based on the observations at the given district heating plant.

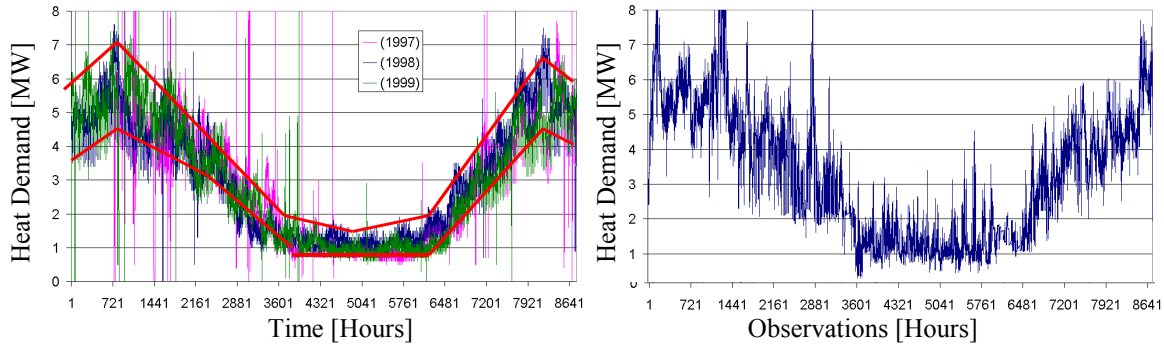

Figure 57 Measured contra simulated heat loads for the Marstal district heating plant. Note: The thick line is to show an overall picture of the measured data. Hereby the computed values are easier to be compared.

Figure 57 shows a reasonable overall agreement between measured and computed heat loads for the whole district heating system. However, the fluctuations in the simulated results are

larger than the measured resulting in too high and low values. The same is the case for the temperature fluctuations in the computations. This shows that the dynamic representation in the load generator, the heat load assumptions for space heating and possibly hot-water preparation, are not modelled well enough.

Another subject of interest is to choose the right set of load files. It turns out that the buildings in Marstal are too old and have too high heat load to be modelled by loads generated by the IEA, Task 26 work. Hence, the loads applied by (Heller, A. and Dahm, J., 1999) are used above to get a better agreement with measured data.

The last point to be mentioned here is that a procedure as the one applied is not simple to handle. Therefore, a more efficient procedure must be applied to make the approach a success. Here again, one can apply the approach applied in Heller and Dahm, where a stochastic method is applied to find the most appropriate parameters for the model by "dynamic data fitting".

From the comparison of the results from the different load estimation methods, we can summarise the following conclusions:

- The simple heat load model based on monthly assumptions is very simple and therefore easy to apply. The method shows a stepwise heat load and duration curve with rather poor agreement with measured data.
- The energy signature and degree-day methods show surprisingly similar results in terms of duration curves. However, the energy signature method seems to lead to higher loads than measured.
- It turns out that the profiles produced by the energy signature and the degree-day method show even better agreements with the measured data than the load generator applied in this work, even though, we apply the DRY data set! Astonishing! Therefore, the question comes up if it is necessary to make such a great effort to build up complex models for load generation. The answer is up to the reader and requires a long discussion presented in the final conclusion and discussion section below.
- The load generator did not represent the load data of the Marstal case perfectly when keeping the parameters to the physical case. This is due to lack of knowledge. Therefore, the number of parameters is too high and some of the parameters must be adjusted to non-physical basis. Here the dynamic data fitting approach demonstrated by Dahm in (Dahm, J., 1999) for small district heating systems can be utilized.
- The disagreement between the measured and the computed values for the Marstal case can be explained by the following reasons: 1) the heat load in the buildings is based on the mix of up to three load profiles. The overall load is a multiple of the single-building load profiles. This leads to very high load peaks. Hence, a stochastic distribution of the loads for the involved buildings must be adopted similar to the hot-water profile generation by (Jordan, U. and Vajen, K., 2000). 2) The hot-water load defined by Jordan, ibid., seems to give reasonable results. For large systems, involving many users, new load profiles must be prepared to avoid peak loads. 2) The heat loss in the district heating is not only dependent on the description of the distribution network but also on the flow. Investigations above indicate that the sub-model for this circulation is very important for the overall results by the load generator. Due to lack of information on this subject, this enhancement is not examined in detail in this work.

5.1.6 General conclusion on the validation

The validation presented in this chapter shows severe weaknesses in behaviour of validation data. This implies rather undesired uncertainties to the analysis and hereby the results found.

However, we can conclude with a high degree of certainty that the MFC solar collector model gives very realistic results, also for variable flow control conditions as applied in Marstal. We find agreement between temperatures and solar gain lying within the uncertainty of the involved measuring equipment. The investigation showed that there is no reason for the application of more than one single collector component, although one expects better results by this procedure. We can also conclude that the standard collector component in TRNSYS should not be applied for large-scale solar heating simulations due to the rather poor response on the thermal capacities involved.

The conclusion on the modelling of the overall central solar heating system is strongly influenced by uncertainties due to the two boundary conditions, the solar irradiation model and the heat demand model. The former is handled by the application of the Danish DRY reference data. The latter is examined above; showing difficulties in reproducing measured load profiles for existing plants. Hence, load models are too complex for general application on existing central heating systems, due to lack of knowledge of the system. The model is, however, obvious for designing new plants with well-known building designs and district heating network.

Focusing on the objective of the current validation, we can conclude that the confidence in applying TRNSYS components for simulation of large-scale solar heating is strengthened by this work. This is also the case for the application of variable flow in the range as applied in Marstal. The current validation showed that the simulation model for the solar plant meets two of the three requirements for a "good enough" model: 1) to reproduce observed data, 2) to reproduce prior knowledge. The third requirement – to meet the intended use – is more difficult to answer. Applying a whole set of procedures and methods for the modelling and simulation, the answer is yes. This demands a rather advanced knowledge of the user of the model which is not the case for most users, even for the author. Most users do simply not have the necessary methodology available, and certainly not the time necessary for handling this procedure. Therefore, we can conclude that complex models as the present involve far too many parameters to meet the "intended use", leading to erroneous choice of parameters and hereby to false confidence in the simulation results.

5.2 GENERALISATION

The generalisation involves the development of an overall CSHP simulation model by:

1. Extending the solar collector field model, applied in the validation, to a comprehensive CSDHP-model including storage tank, heat exchangers, control algorithms and so on. This subject is dealt with in Section 5.2.1.1.
2. Applying general heat load profiles for the district heating. This subject is dealt with in Section 5.2.2.
3. Utilising reference data for the meteorological boundary conditions for the simulations. This subject is dealt with in Section 5.2.3.

Note: Also control of the plant is a subject of the generalisation, however, chosen to be handled later in the Design Study chapter.

5.2.1 The whole CSDHP model

In the step of extending the validated solar collector field model from above to a comprehensive CSDHP model, a rather large step is taken. This procedure is chosen due to the fact that the main features of the final model already were defined in the work by (Heller, A. and Dahm, J., 1999). Hence, validation of this previous model is assumed to cover the current model. It is relevant to mention that the results in temperatures for single day analysis are very similar to the results found above. In this previous work, statistical methods were applied to adjust parameters. In this way, the load profile was correlated very well leading to a total difference of 1.2% for the heat load and 1.3% for the simulated solar gain. An analysis of these surprisingly good results reveals that some of the semi-empirical parameters are adjusted by rather unrealistic values. This is justified from a general modelling point of view. In the current work, the bonds to the method are strengthened in relation to the adjustment of parameters. This makes it difficult to match the good results of the previous study.

The TRNSYS-model for the central solar heating system is sketched in Figure 58.

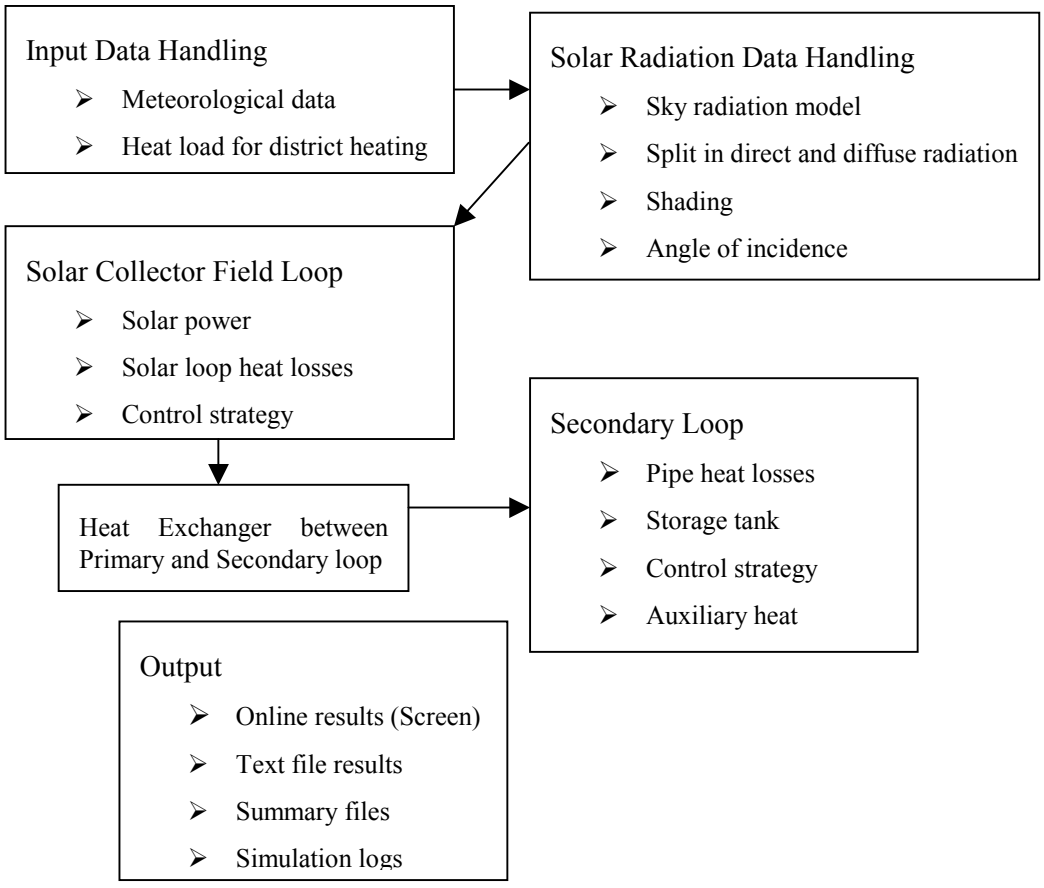

Figure 58. Flow chart of the CSDHP-model applied for validation by 1997-data with the Marstal solar plant.

The central solar heating model in Figure 58, consists of

- Input data handling components, preparing the boundary conditions for the current case.
- A "Solar Collector Field Loop", also called primary loop, the collector field and its connecting pipes.
- A "Secondary Loop", distributing the produced solar heating to either the district heating net or the storage tank including a component for the estimation of auxiliary heating by simple means.

- The "Output" components handling the presentation of the results, partly when running the simulations and partly by text files to be used for analysis.

For the handling of the solar irradiation, two methods are applied dependent on the computational case. If the reference data or the validation data from the supplementary monitoring system is used, no splitting between direct and diffuse irradiance was to be computed. Else, if the monitoring data from the permanent data set is applied, the split was done by the following simple method: If the total value is below 200 W/m^2, the whole value is considered diffuse, otherwise 20% is considered diffuse and the rest is direct solar irradiance.

The applied TRNSYS program is sensitive to the application of algebraic computation, involving values to be determined by the iterative process of solving the system. To avoid such problems, all equations for the control of the plant are excluded and substituted by components, such as controllers etc. Here the current implementation is systematically different from the previous work by (Heller, A. and Dahm, J., 1999), where equations were adopted. Hence, results from the current work are more accurate from this point of view.

The control strategy applied in the current evaluation is discussed later in the Design Study chapter. Relevant here is the fact that a variable flow strategy is applied. The hydraulic components for splitting and combining flows are rather complex and therefore not explained here. The tank includes three flow cycles, two to store solar heat at two different heights in the tank (as found in Marstal) and one to withdraw heat from the storage. The strategy of loading the tank is as follows: the heat is stored in the upper part, if the temperature is higher than in this upper part, otherwise the heat is stored in the centre inlet.

To make the model more robust for parameter variations, some of the values, explicitly defined for the Marstal case, are parameterised as follows:

By assuming a fixed value for the heat exchanger between primary and secondary loop, there is no need for determination of the value for the computations in the following.

The tank volume is specified in the TRNSYS model. Other dependent values, such as e.g. height, are computed. Hereby no errors are introduced due to missing adjustments of dependent parameters.

5.2.1.1 Simulation checking procedure

Before focusing on the results, attention is led to the procedure applied to ensure proper simulations.

By inserting an "Equation" component, a number of logical quantities are controlled for each computation step. In this way, the flow directions, control values and other quantities are checked.

TRNSYS produces a log-file with warnings. This file is studied in detail to avoid crucial mistakes in computations.

TRNSYS gives the opportunity of controlling the results as screen-plots while running the simulations. This procedure is used extensively to avoid problems with computations.

All these tools are applied to avoid unwanted mistakes and errors in the simulations.

5.2.2 Load profile for the Marstal case

In this evaluation of the load models for the district heating system and all the connected consumers, two implementations can be applied in the same computer model: 1) A degree-hour method. 2) Heat load profiles defined in a single input file as described above. In the current section, the two load generation methods are examined by comparing the resulting monthly values for the heat loads. The results are shown in Figure 59.

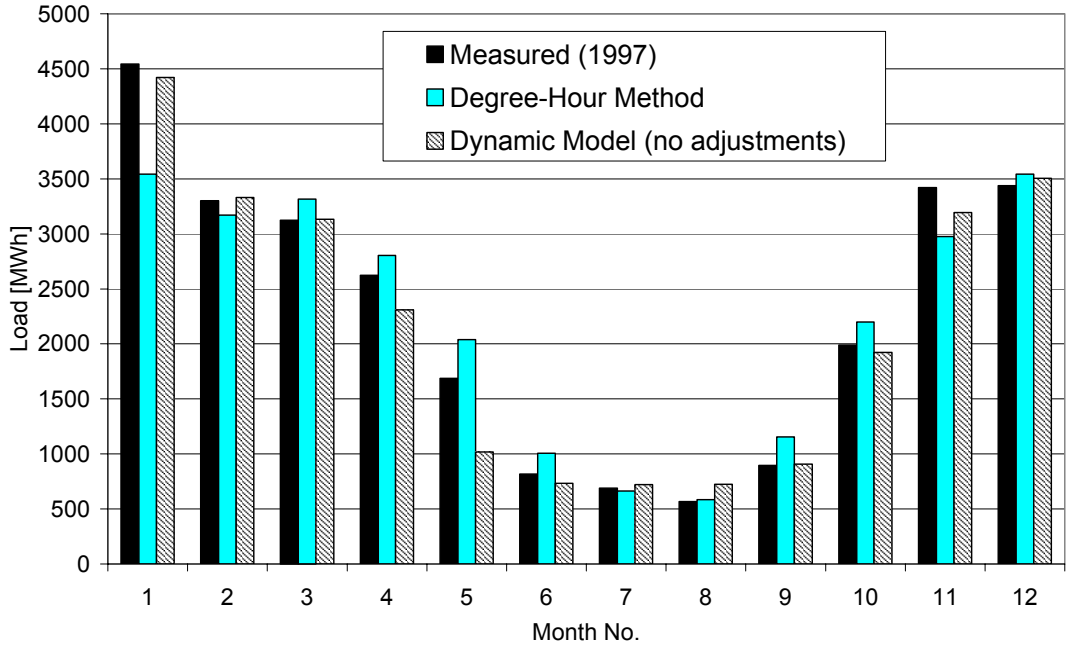

Figure 59. Comparison of monthly demands for the Marstal district heating for the year 1997.

We clearly find from Figure 59 that both the degree-hour method and the dynamic approach lead to large monthly deviations to the measured values. The dynamic approach gives better agreement in general, but underestimates the load especially for May (Label "5") and the summer month. Both methods could be adjusted to match better. Due to the simplicity of the "degree-hour" method, an adjustment is limited and many cases, it would in change the basics of the method. This is not the case for the dynamic model, where parameters can be chosen to adjust the results without changing the basics of the method.

The above load profile for the dynamic method is adjusted by a compromise of gaining a reasonable duration curve fit and in the same time a reasonable fit in monthly values. The monthly data for the final load profile is shown in Figure 60 and the correspondent duration curve in Figure 61.

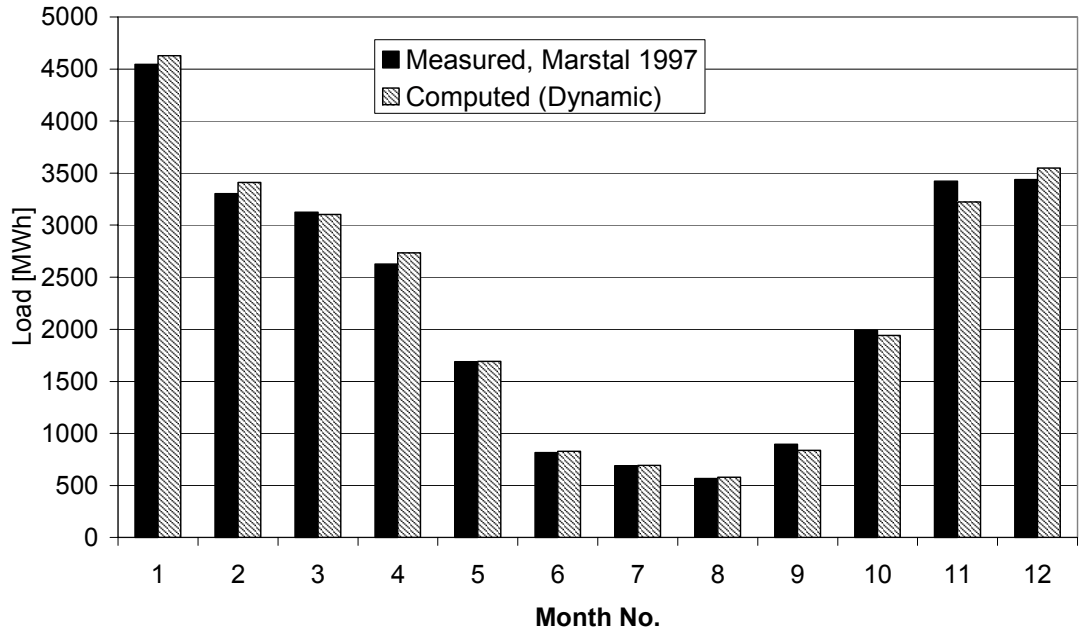

Figure 60. Monthly values for the final load profile for the Marstal plant, 1997.

From Figure 60 we find that there is a systematic deviation between the computed and the measured heat load. In spring the heat load is computed too high, in autumn the values are computed too low. No explanation can be offered to this finding.

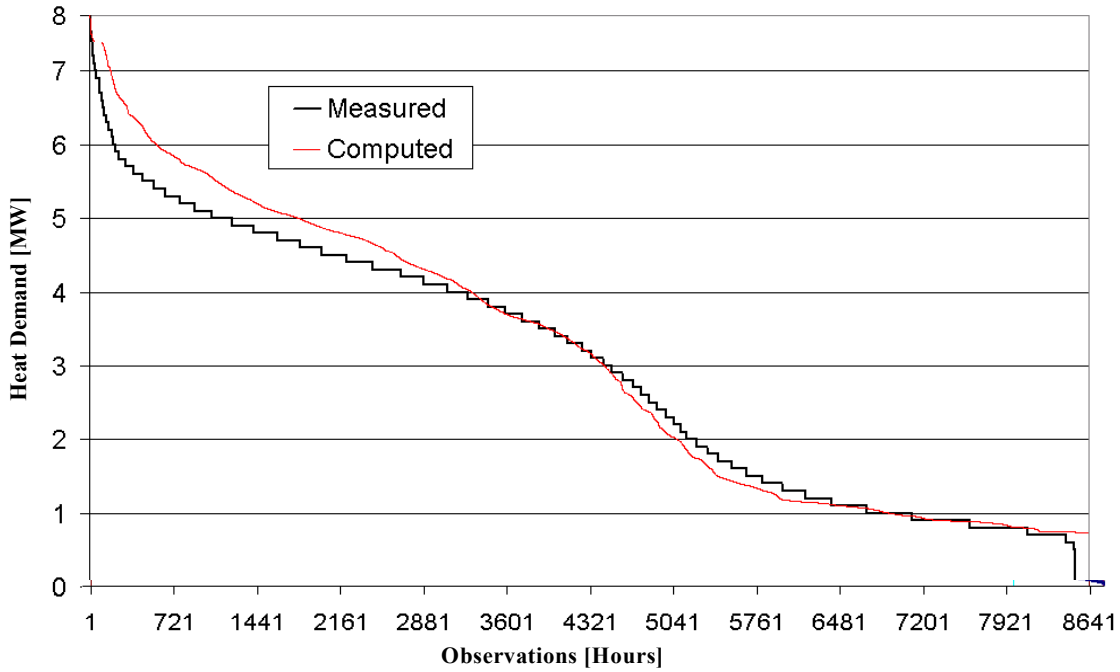

Figure 61. Duration curve for measured and final computed load profile for the Marstal plant, 1997.

From Figure 61, we find a relatively large deviation, especially for the high demands. However, high demands occur in wintertime, and since the solar gain is mainly produced in the summer months, the impact is rather small. Hence, the impact of the load on the results is less decisive

for central solar heating systems with short-term storage. For systems with seasonal storage, the lack of accuracy in load modelling is also decisive for the estimation of the solar production.

In the following, the described load profiles are applied. For the Analysis chapter, the dynamic load profile is applied. This is also the case for the design studies keeping reference to the Marstal case. For the more general design studies, the degree-hour method is applied to make the load profile easily adjustable.

5.2.3 Applying the Design Reference Year

Two general weather-data-sets are available for Denmark, the older Test Reference Year (TRY) and the Design Reference Year (DRY). The former is described in (SBI, 1982) and the design reference year in (Jensen, M. J. and Lund, H., 1995). The difference between the two data sets is mainly the methods by which the data is collected for a reference year. The TRY is a summary of real measured hourly data, where representative periods from the years 1959-1973 are stitched together. The method is very different in the DRY, where 5-minute data measured between 1975-1990 are applied. To design the reference year, the data is composed systematically from a collection of the data, a statistical approach.

Both reference sets can be found on the author's Internet site at:

http://www.ibe.dtu.dk/forsknin/cshp/meteo/meteo.htm.

Readers especially interested in the subject of general meteorological data sets and simple models to weather data parameters are referred to (Heller, A., 2000c). In the current work, the newer DRY data set is applied.

Applying the DRY data set in the heat load model from the section before we find the following load profile compared to the measured data from the Marstal case.

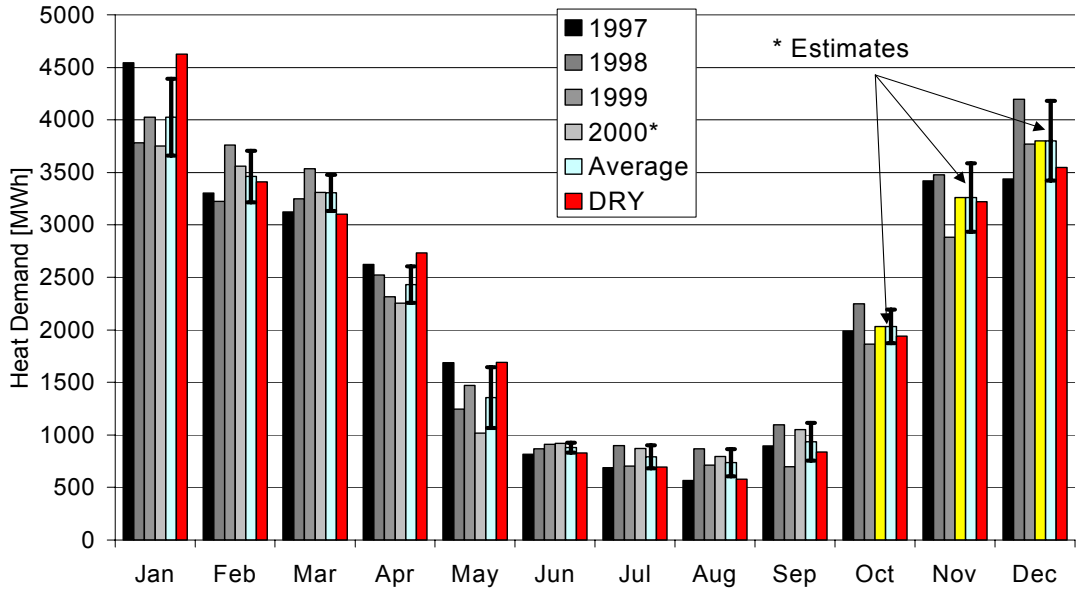

Figure 62 Monthly load values for the heat demand based on the DRY data set, compared with measured values from the Marstal plant, 1997-1999.

We find from Figure 62 that the dynamic method does not represent the average heat load for the Marstal system in a satisfactory way. Especially January, April and May are estimated much higher than measured and March, August and December lower than measured. Similar to

the load profile in Figure 60, there is a tendency of overestimating loads in the first half year and underestimating in the second half.

The annual heat demands measured in average to 27140 MWh and computed to 27210 MWh by the DRY representation.

The corresponding solar production is shown in Figure 63.

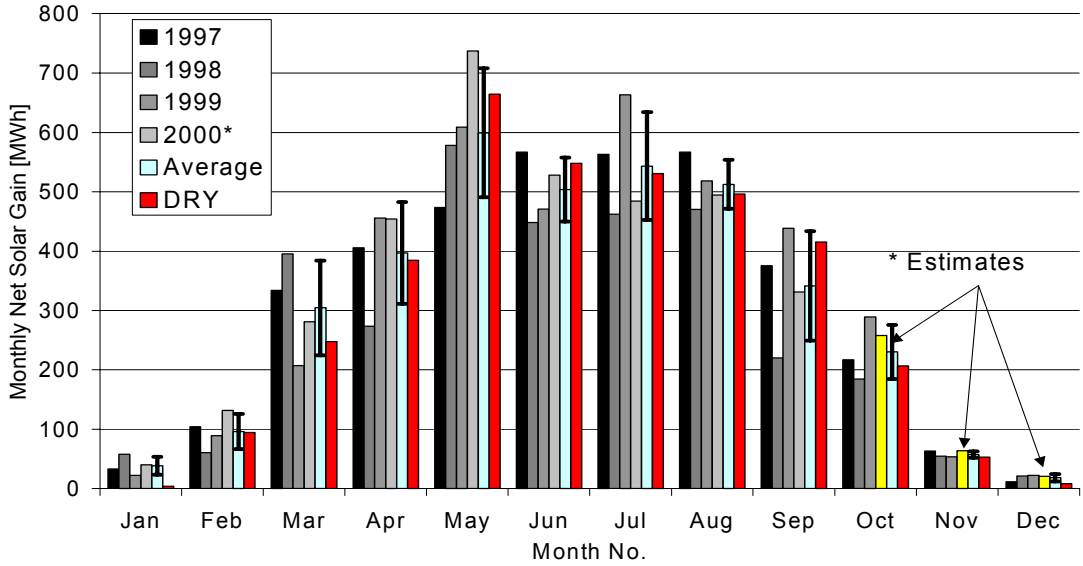

Figure 63 Monthly solar production computed for DRY meteorological data with a dynamic load model, compared with measured values of the Marstal plant for 1997-2000.

We find from Figure 63 that the computed net solar production (gain) is not estimated according to the measured which is not surprising, bearing in mind that the DRY data set has been applied. The values for May, June and September are computed too high, and from October to March too low. The annual production is estimated to 3654 MWh, while the average is measured to 3642 MWh.

The resulting monthly and annual values for the load and the net solar productions are:

Table 9. Monthly and annual computed values for heat demand, net solar gain in MWh and Solar Fraction (SF) for the DRY weather-data set.

[MWh]	Heat Demand	Net Solar Gain	SF
JAN	4628	4	0.1%
FEB	3409	95	2.8%
MAR	3103	248	8.0%
APR	2734	385	14.1%
MAY	1691	665	39.3%
JUN	829	548	66.1%
JUL	693	531	76.6%
AUG	579	496	85.7%
SEP	836	416	49.7%
OCT	1941	207	10.7%
NOV	3221	53	1.6%
DEC	3548	8	0.2%
Year	**27210**	**3654**	**13.4%**

6. PERFORMANCE OF CSHP

This chapter consists of a large amount of information that may be collected in a conclusion. However, this would make the conclusion rather fuzzy. Therefore, the experiences from central solar heating systems are gathered in this chapter, hoping that readers do not skip important facts. The facts are collected mainly from the Marstal plant and other Danish plants, but also from other publications.

An important scientific rule is to refer to the source of a given finding. In the current chapter, the author had to find a balance in collecting (in the sector) well-known findings, not to be cited, and findings which are relevant to be traced back to the source and hereby to be cited. However, many of the above findings can be traced back to the following sources:

- 🕮 The IEA-work of the 80s in (Dalenbäck, J-O., 1990), the European activities from the APAS-project in (Fisch, N., Guigas, M., and Kübler, R., 1996), (Dalenbäck, J-O., 1995) and (Zinko, H., Bjärklev, J., and Margen, P., 1996).
- 🕮 The guideline by (Leenaerts, C, 1997) relevant to be revised and enlarged to include CSHPxS and CSHPDS.
- 🕮 IEA-activity on Large Solar Systems in general by (Geus, de A. C., 1996).
- 🕮 Publications from the ELSSH-network.
- 🕮 Work presented at international conferences and workshops.
- 🕮 National published and unpublished work (in Danish).

In the current chapter, the thermal performance of CSHP will be in focus followed by a survey on the economical performance, closing the chapter with some short comments on the environmental performance of the technology.

6.1 THERMAL PERFORMANCE

Thermal performance is here defined as the ability to transform solar irradiation into heat and to deliver this heat to a final consumer. Before reporting on the performance of CSHPs, a proposal for a procedure is put forward, with which one is able to estimate the wide range of spread in solar production for solar energy systems. This procedure is proposed in section 6.1.1.

The short-term performance of the Marstal case is shown in section 6.1.2 followed by a comparison of the findings with other plants in section 6.1.3. In the final section 6.1.4, the long-term perspective is then applied on the Saltum plant where 10 years of operation can be used for the analysis of a possible "degradation" of the technology and consequently a decrease in solar production.

6.1.1 Proposal for an overall procedure for the assessment of the thermal performance of solar energy technologies

Solar irradiation is strongly fluctuating, and the thermal performance for solar systems reflects this. In the following sections, the terms "worst case" and "best case" are used repeatedly, to describe a monthly or yearly period with very "poor" or very "strong" solar irradiation. By the introduction of this concept, one is able to estimate the extremes in solar production and hereby the risks for the application of solar energies in general. This approach is similary proposed by (Adsten, M., Perers, B., and Wäckelgård, E., 2000) for small solar heating systems.

Based on years of monitoring the weather conditions in Denmark, EMD-Online at http://www.emd.dk, the worst and best case periods can be found. It turns out that both cases were observed during the last three years, best case in 1997 and worst case in 1998. It is also worth mentioning that the average is found in 1990 and that the solar irradiation is very close to the average in 1999.

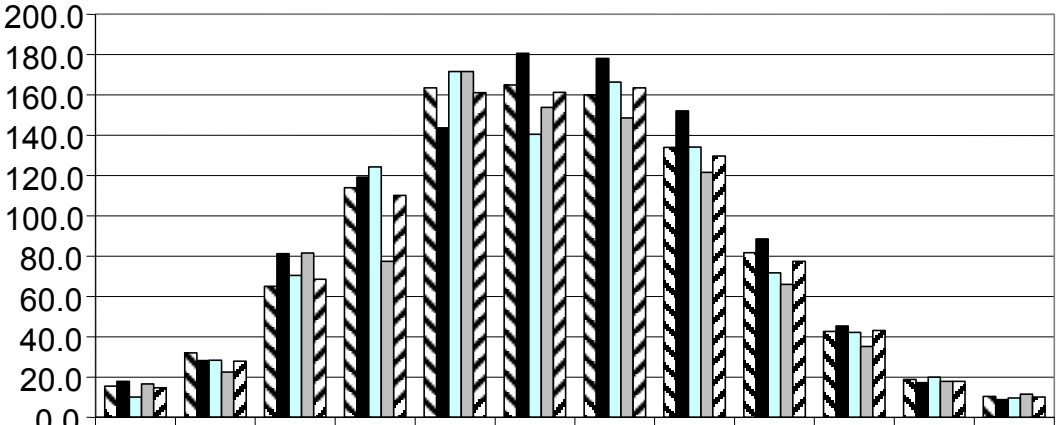

	JAN	FEB	MAR	APR	MAY	JUN	JUL	AUG	SEP	OCT	NOV	DEC
DRY	15.5	32.0	65.0	114.0	163.4	164.9	160.0	134.0	81.7	42.6	18.9	10.3
1997	17.8	28.1	81.3	119.2	143.6	180.7	178.2	152.1	88.6	45.4	17.3	8.7
1990	10.1	28.3	70.4	124.3	171.5	140.4	166.4	134.1	71.7	42.1	20.0	9.5
1998	16.6	22.5	81.6	77.4	171.6	153.8	148.6	121.5	66.0	35.2	17.8	11.5
EMD	14.7	27.9	68.6	110.2	161.1	161.2	163.5	129.7	77.5	43.1	17.8	10.2

Figure 64. Monthly solar irradiation on horizontal plane, for the DRY reference year, EMD-data for north Jutland for 1990, 1997, 1998 and the normal year defined by EMD. Source: EMD-Online at http://www.emd.dk.

Before analysing the data, it is worth mentioning that the DRY reference data and the EMD normal year are in reasonable agreement. In general, we also find for the data sets that the monthly deviations are very large, even for the "average" year of 1990.

What can these observations be used for?

The year, representing the average, e.g. 1990 or 1999, can be applied for the control of computations with reference year data, the TRY and DRY data sets.

The ambient data for the best and worst case can be applied to estimate the boundaries for the fluctuation of the solar production of the solar energy technology. This is seen as a very important tool for the documentation of a given technology and hereby an argument for the evaluation of such technologies.

Similar findings are reported by (Adsten, M., Perers, B., and Wäckelgård, E., 2000). The results from this study will be discussed in the relevant sections below. It is relevant to state that the method has shown applicable for simulated thermal performance analysis, but here it is proposed as a design tool.

Having observed that 1997 is the "best case" and 1998 the "worst case", we can conclude that the observations made in the solar plants since 1997 can be applied to document the variety of expected solar production for solar technologies with similar dependencies of solar irradiation and performance (possibly even more generally applicable for other solar energy technologies, space heating etc.). The author finds this observation very important, and it is stated here as a hypothesis:

The variety in thermal performance for solar (heating) technologies can be found by the upper limit found for 1997 and the lower limit in 1998. A value very close to the average performance can be found for 1990 and 1999.

See Table 11 and Figure 71 for a case study.

6.1.2 Detailed performance analysis – The Marstal case

The monitoring results from the Marstal plant can be found on the Internet on http://www.solarmarstal.dk. From these figures and a report on the plant performance, (Holm, L., Ulbjerg, F., Nielsen, J. E., Sørensen, P. A., and Tambjerg, L., 2000), we are able to extract the average yearly net solar gain to 3642 MWh or approximately 430 kWh/m^2 solar collector per year. The monthly heat demands and solar production for the last years are as shown in Figure 65 and Figure 66. The corresponding yearly heat loads are for 1997, 27100 MWh, for 1998 27700 MWh, for 1999 26600 MWh and in average 27100 MWh.

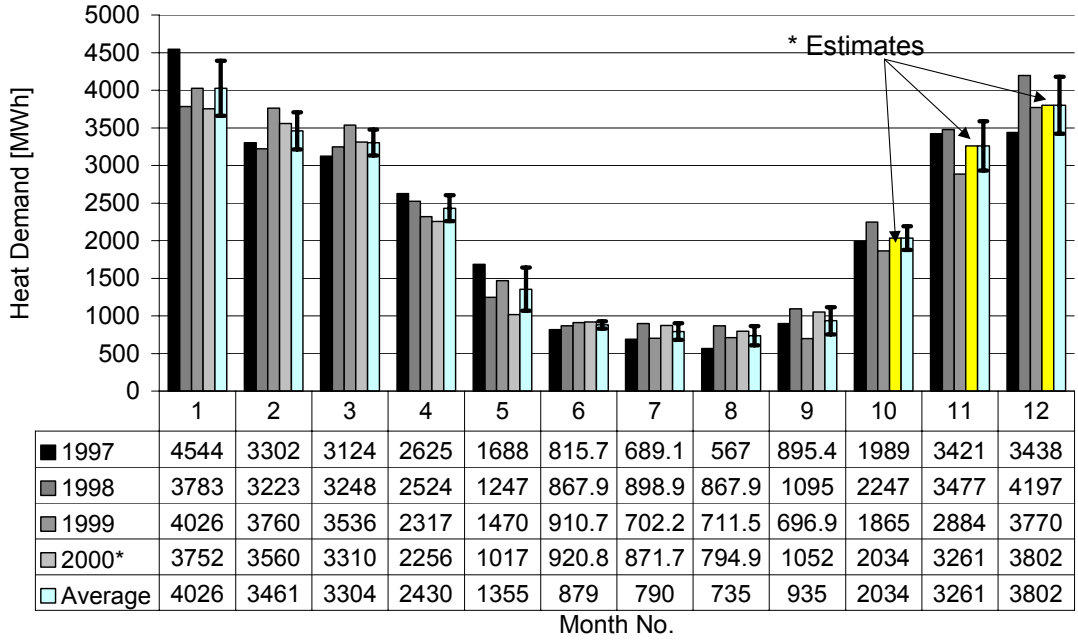

	1	2	3	4	5	6	7	8	9	10	11	12
1997	4544	3302	3124	2625	1688	815.7	689.1	567	895.4	1989	3421	3438
1998	3783	3223	3248	2524	1247	867.9	898.9	867.9	1095	2247	3477	4197
1999	4026	3760	3536	2317	1470	910.7	702.2	711.5	696.9	1865	2884	3770
2000*	3752	3560	3310	2256	1017	920.8	871.7	794.9	1052	2034	3261	3802
Average	4026	3461	3304	2430	1355	879	790	735	935	2034	3261	3802

Figure 65. Measured heat demand for the Marstal central solar heating plant from 1997 to 2000.

From the Marstal case, shown in Figure 65, we find the monthly load values for the last four years, and the corresponding averages and standard deviations for the plant. The absolute deviation in monthly values is in average 21% of the total heat demand in the Marstal district heating. The maximum variation for monthly data over the involved years is 40%. This variation is surprisingly high and seems to reverse the findings based on correlation analysis by other researchers, applying multi-regression analysis to find this correlation between solar irradiation and heat loads, discussed in (Heller, A., 2000c). In this work, the correlation is estimated to 1-2% (% is defined as the influence of the solar irradiation on the total load.).

Reflecting a little on the results, we find that the solar irradiation has a very strong correlation to the ambient temperature. The multi-regression analyses show a very strong correlation between ambient temperature and load, and a very weak correlation between solar irradiation and heat demands. In the results of Figure 65, the influences of the solar irradiation on the heat demand, direct and indirect through the ambient temperature is shown. Hence, no contradiction is found. However, the conclusion on the influence of solar irradiation on heat demands in district heating is very different when using the following two postulates:

1. Based on multi-regression analysis: Solar irradiation influences heat loads by 2% of the total value.
2. Based on the above figure: The monthly heat load varies in average 20% of the total monthly value with a maximum observed variation of 40%.

We see that the first formulation does not include the indirect influence of solar irradiation over the affected ambient temperature on the heat demands. Hence, the second description of the dependency of the total heat load on the solar irradiation will be applied in the following. The total yearly net solar gain is for 1997, 3700 MWh, for 1998 3200 MWh, for 1999 3800 MWh and in average 3650 MWh.

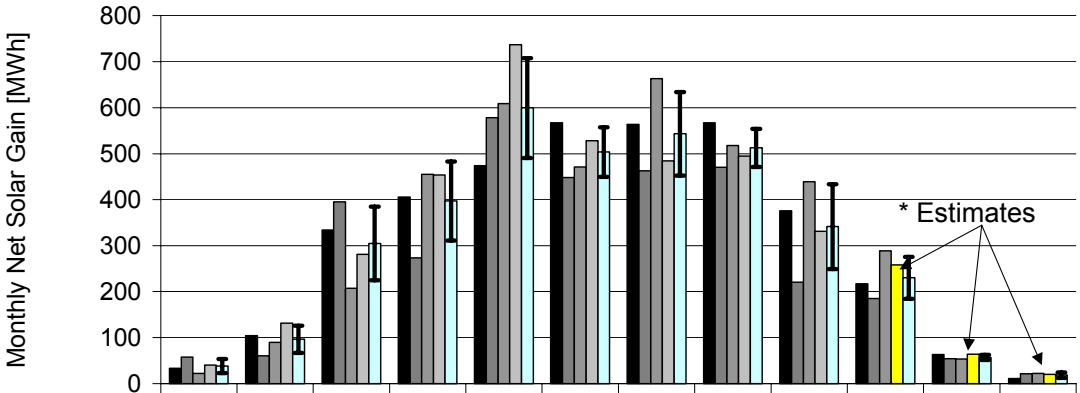

	Jan	Feb	Mar	Apr	May	Jun	Jul	Aug	Sep	Oct	Nov	Dec
1997	32.9	104.2	334.2	405.4	473.3	567	563.1	567	375.6	216.9	63.6	11.2
1998	58	60.5	395.3	273.2	578.3	448.4	462.3	470.3	220.1	184.8	54.3	21.4
1999	22.1	89.5	207.2	455.5	608.8	470.8	663.3	518.1	438.7	288.8	53.7	22.4
2000*	40.2	131.6	281	453.9	736.9	527.9	484.3	494.4	331.3	258	64	21
Average	38	96	304	397	599	504	543	512	341	230	57	18

Figure 66. Measured net solar production for the Marstal central solar heating plant from 1997 to 2000.

We find the total, monthly net solar production for the Marstal plant in Figure 66. Focussing on the summer months, where the main solar production lies, we find the following spread in observation between monthly values of the involved yeas: The average is at 40% with an extreme value by 50%.

Comparing the results with the load values, the solar sensitivity is much larger.

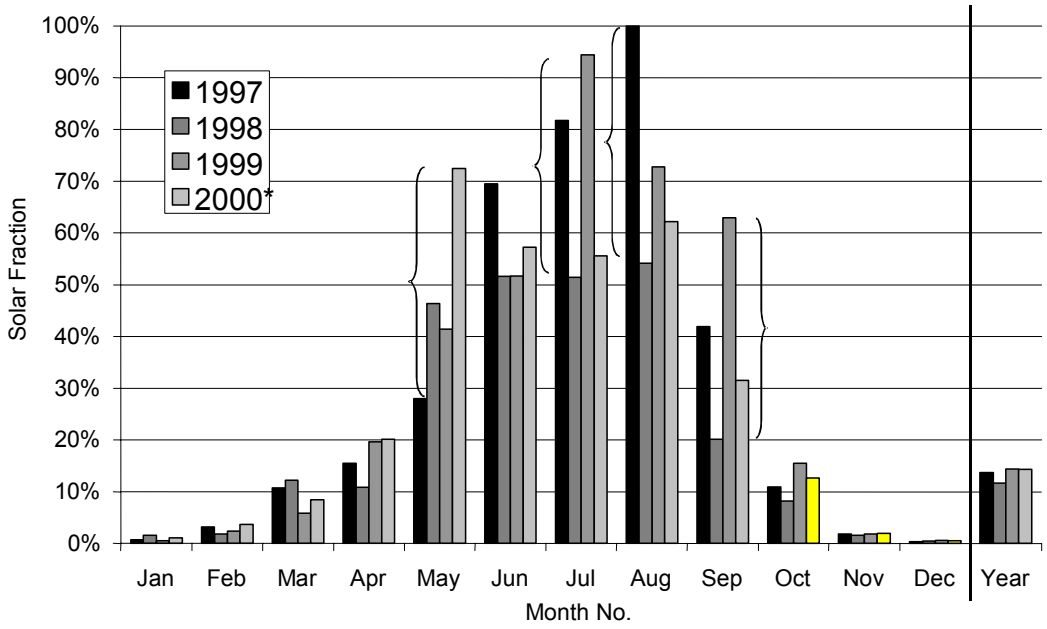

Figure 67. Measured solar fraction for the Marstal central solar heating plant from 1997 to 2000.

The solar fraction visualised in Figure 67 is defined by $SF = \frac{Q_s}{Q_{DH}}$, involving both the heat demand and the net solar gain, and we are able to conclude on the influence of deviation of solar irradiation on the solar fraction on this definition term. Since changes in solar irradiation influence the solar gain stronger than the heat load, the solar fraction is more significantly affected than the other quantities

Going one step further in the analysis of the monitored plant performance in Marstal, we find the following plot in Figure 68.

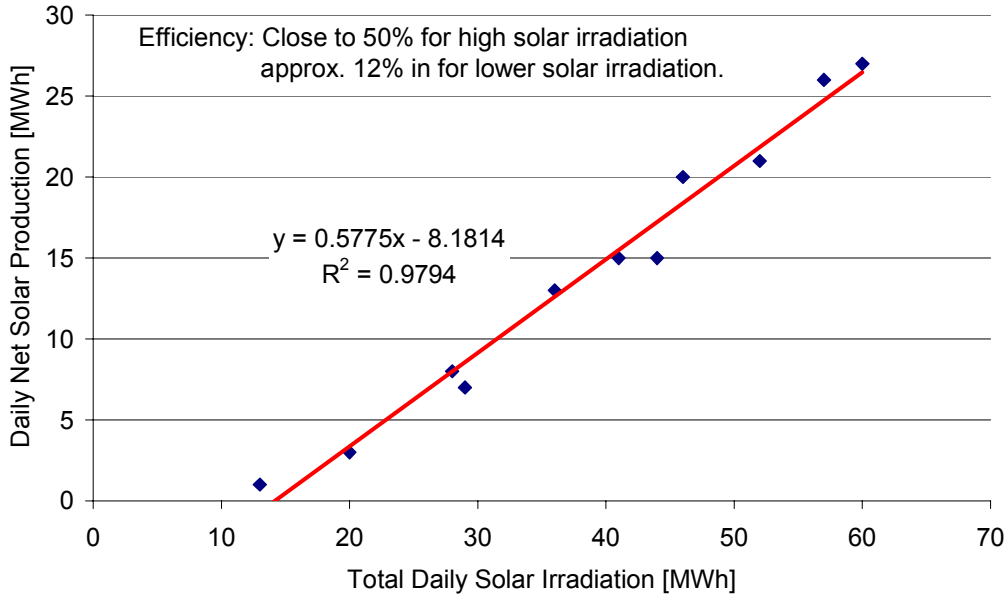

Figure 68. Net solar production versus net solar irradiation on the collector field.

It is clearly seen from Figure 68 that there is a strong linear correlation between the solar irradiation on the collector field and the resulting solar production. This subject will be followed up later in relation to comparison between plants and possible quality monitoring procedures in the final chapter.

By defining a solar efficiency as $SE = \frac{Q_s}{Q_t}$, where Q_s is the net solar gain and Q_t the total solar irradiation on the collector field for a given period, we are able to evaluate a given technology. From Figure 68, we find a top performance of 50% for high solar irradiation and approximately 12% for low solar irradiation. The corresponding monthly and annual values for the last three years are found in Table 10.

Table 10. Monthly and annual average solar efficiency, SE, for the years 1997-1999.

Jan	10.0%
Feb	24.0%
Mar	39.5%
Apr	40.5%
May	43.0%
Jun	38.6%
Jul	40.1%
Aug	39.1%
Sep	36.8%
Oct	34.2%
Nov	18.9%
Dec	8.7%
Year	**37.1%**

From the table we find that:

- The solar efficiency is higher in the first half year than in the second.
- The summer efficiency is higher than the winter efficiency. This is, among others, due to the fact that the solar irradiation in the winter time cannot be utilised due to the low incident angle and the strong shading between rows.

The yearly performance is computed to 37% in 1997, 38% in 1998 and 35% in 1999 which is a little surprising, bearing in mind that 1997 was the best case and 1998 the worst case.

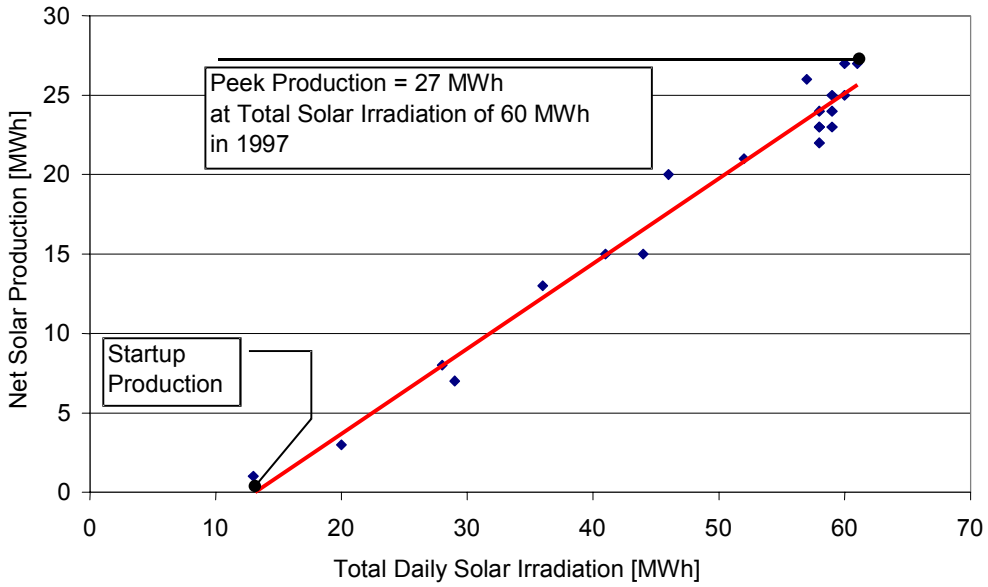

Figure 69. Net solar production versus net solar irradiation on the collector field – once more.

Focusing differently on Figure 68, as done in Figure 69, the top daily net production is close to 27 MWh for the Marstal plant configuration 1997, and more in 1999. This corresponds to a daily peak production of 1.12 MW for the whole field or 0.14 kW per m^2 solar collector.

Another important observation from Figure 69 is related to the "many" dots in the upper end of the graph. Here we find a situation which occurred between August 4 and August 12, where solar irradiation was very strong and the tank was filled up. We find from the dots that the overall performance was not very influenced by the energy content of the tank (drop from 27 to 23 MWh/day). This shows that the tank performance is very similar for cold and hot conditions, a sign interpreted as robustness of the system and proper tank design. The latter requires a closer analysis of the temperature stratification of the tank.

6.1.3 Plant comparison

The yearly productions are:

Table 11. Annual solar energy production per m^2 solar collector area in kWh for Danish CSHPs.

** estimates, October 2000*

Year	Ry	Saltum	Hoejslev	Ottrup-gaard	Anders-vaenge	Marstal	Ærøs-køb ing
Area	**3,025**	**1,000**	**375**	**560**	**233**	**8064/9040**	**2040/4900**
1990	377	-	-	-	-	-	-
1991	364	-	-	-	-	-	-
1992	373	-	-	-	-	-	-
1993	349	-	-	-	-	-	-
1994	372	-	-	-	-	-	-
1995	425	431	493	-	-	-	-
1996	380	248	373	466	390	-	-
1997	440	250	400	532	411	461	-
1998	334	-	-	387	-	400	-
1999	390	201	-	470	-	424	443
*** 2000**	347	-	-	380	-	423	375
Average	**377**	**283**	**422**	**447**	**401**	**427**	**409**

Table 11 shows the net solar gain in kWh/m^2 for a number of Danish central solar heating plants. Missing values are in the beginning due to the fact that the plants were not built, and later on due to the fact that the values were not yet collected.

The table is rather compressed and will therefore be discussed in detail in the following:

- The Ry plant is documented over 10 years of operation, and will be discussed in detail in section 6.1.4.
- The Ottrupgaard plant shows very high values. This is due to the fact that the plant is equipped with a large thermal storage.
- The Saltum plant produced in the same range as the other plants for 1995, then it showed very low values. This dramatic result is a consequence of the introduction of co-generation with highest priority for production of electricity, leading to a high amount of heat. Hence, solar production is very low. Except from the well-known fact that solar energy must be prioritised highest in an energy-mix for a plant, nothing can be deduced from this observation.
- All observed plants produce between 386 and 427 kWh/m^2/anno.
- A single peak performance of close to 500 kWh/anno is monitored.

To show the impact of the "best" and "worst" cases discussed in section 6.1.1, we find the following based on these considerations:

Table 12. Results from comparison of the solar production for different plants.

Annual Net Solar Gain in kWh/m^2	First Generation	Second Generation
Best case (1997)	440	461
Average (1990, 1999)	377	427
Worst case (1998)	334	400

We find clearly that the second-generation plants produce more heat than the first generation plants. This is indeed a surprising result and will be discussed later in relation to the control strategies of the different plant designs.

The Danish Solar Energy Centre has produced a plant performance statistic for the year 1999, (Nielsen, J. E. and Honoré, C., 2000). Here 9 large domestic hot water plants, 11 so-called "district-heating similar" solar heating plants and 6 district-heating plants are included. Main findings showing additional observations to the above presented are:

- CSHP produce in average 405 kWh/m^2. This is compared with the 402 kWh/m^2 found above. This is in very good agreement, even though the plants involved are not all similar.
- The cold inlet temperature to the collector field is for CSHP more "constant" and lower compared to other large systems, especially compared to the domestic hot-water systems. This is one reason for the better results.
- All observed solar heating systems show the above found liner correlation between solar irradiation and solar production. This is discussed in the following:

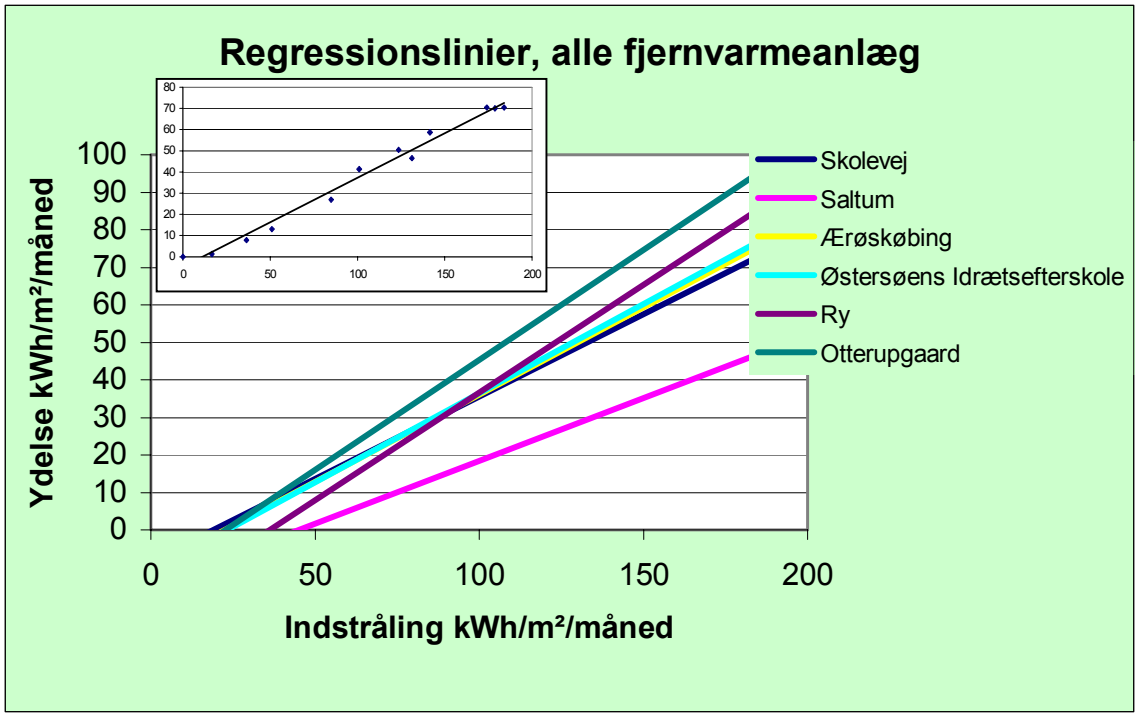

Figure 70. Regression between solar irradiation and solar gain for six CSHPs in Denmark for the year 1999. Source: (Nielsen, J. E. and Honoré, C., 2000) (Danish text).

The regression lines in Figure 70 can be compared with the regression line of Figure 68 by recalculating the values by the collector field area (small copy). We find that the Marstal plant starts up at very low solar irradiation values, but with a rather low slope compared with other

similar plants, such as the plant in Ærøskøbing. This method of comparing plants does not reflect on the "boundary conditions", the temperature level or load of the district heating. A more appropriate method for comparison must consider these conditions.

Moreover we find from the graph above that the Saltum plant starts up very slowly and does not improve with high solar irradiation. Here, the reason is a very high inlet temperature to the solar plant.

6.1.4 Long-term performance – The Ry case

Saltum is the oldest plant installed in Denmark, and one of the oldest in Europe. From the plant, we get an idea of the long-term performance during the last decade, from 1990 to 2000. The statistical key-values are presented in Table 13.

Table 13. Statistical key-values for the long-term case, the Ry CSHPxS.

	[MWh/a]	
Average	1141	
Minimum	1009	$\Delta_{max-min} = 323$
Maximum	1332	
Standard Deviation	97	

The corresponding results behind these statistics are found in Figure 71.

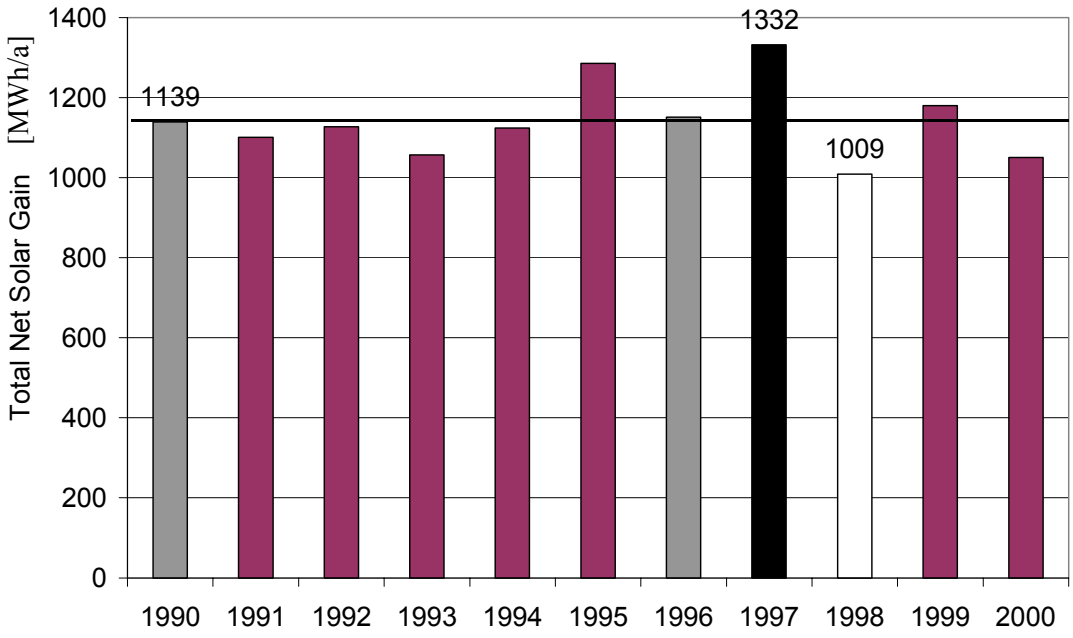

Figure 71. Annual performance for the Ry case. Note that from October, the 2000 value is estimated.

Based on the 10 years of operation in Ry, we find that the net solar production is rather constant, within 100 MWh (<10%), except for the seasons with extreme solar conditions. By analysing the values, we find a tendency of increased efficiency for the later years. The

tendency is, on the one hand, too weak to be interpreted. On the other hand, there is no evidence of a decreasing production of the applied solar collector modules.

Note: The values in the figure above support the idea of the proposal in section 6.1.1.

6.2 ECONOMIC PERFORMANCE

Prior to analysing the trends in the price development of central solar heating plants during the last decade, the Marstal example is examined in detail.

6.2.1 The Marstal case

The facts in this example are taken from the official revision report for the Marstal plant. No estimates are involved. The prices are given in 1996-values.

Table 14. Financial Key-values for the investment in the Marstal CSHP. 1996-values.

Description	**Investment**	
	DKK	**Euro**[8]
Ground work	1,358,431	182,585
Solar collector enterprise	9,576,050	1,287,103
Pluming	999,195	134,300
Diesel generator *	557,378	74,916
Steel tank storage	1,466,000	197,043
Control system *	488,441	65,651
Electrical installations (Control Sys. and Building) *	453,000	60,887
Transmission DH piping	1,582,901	212,756
Distribution piping of collector field in ground	437,524	58,807
Changes to existing heat plant	319,009	42,878
Craft work (mostly for Control Building) *	1,280,461	172,105
Gardening *	67,000	9,005
Technical Consultants	1,114,809	149,840
Ground Buy	477,940	64,239
Own work by the DH company	380,281	51,113
Diverse	528,575	71,045
In Total	**21,086,995**	**2,834,274**
Subsidies by the Danish Energy Agency	*5,000,000*	*672,043*
DH company investment in total	**16,086,995**	**2,162,231**

[8] 1 Euro equals 7.44 Danish crowns.

From the figures in Table 14, we can extract the following key-values to be compared with other plants, reported in literature: Building costs are marked in the table with asterisks, estimated to 3,845,475 DKK or 516,865 Euro including the control system.

Note: In the analysis below, the subsidies are not taken into consideration. Hence, the findings can be directly applied for other conditions.

Analysing the impact of the individual investments, we find the following percentile share:

Table 15. Share for the main structures for the Marstal CSHP.

Description	Share (%)
Ground buy	2.3
Ground work	6.4
Collector field in total	47.5
Steel tank storage	7.0
Connection to the existing plant incl. transmission pipe	9.0
Building	18.2
Designing etc. Consultants	5.3
Others	4.3

From these figures, we find a total cost per installed collector area of approximately 2614 DKK or 351 Euro.

Moreover, we find, from for the revision report that the variable expenses for maintenance and operation for the Marstal plant consists of the following shares:

Table 16. Yearly, variable expenses for maintenance and operation for the Marstal CSHP.

Description	DKK	Euro
Diesel generator operation	103,000	13,844
Electricity for pumping and building operation etc.	21,000	2,823
Maintenance	26,000	3,495
Insurance	25,000	3,360
In total	**175,000**	**23,522**

Hereby the yearly variable cost is estimated to 0.8% of the total investment. The manpower is set to zero due to the fact that the investment does not necessitate an increase of staff. In fact, one could even assign the plant an income for better conditions for the employees due to more spare time in the summer months.

There are a number of different economical methods for the evaluation of the economical profitability of investments.

According to the plant owner, the simple pay back time for the Marstal plant is estimated to 7-8 years, due to a special, local financing and an over-price for the non-solar heat of 0.02 DKK./kWh.

Assuming an annual production of 3500 MWh (above found to be 3642 MWh in average) to a heat price of 0.42 DKK/kWh, as is the case for Marstal, we find a simple payback time of 14 years. Assuming a more realistic energy price for Denmark in general of 0.50 DKK./kWh we get a payback time of 12 years. It is worthwhile pointing out that such long-term investments

are very common in the district heating branch which is used to large investments in the plant and network infrastructure.

The cost-benefit ratio or cost/performance ratio is estimated to 6.0 DKK./kWh/a or 0.81 Euro/MWh/a for the Marstal plant, including all the above investments.

Table 17. Results from a risk assessment for the Marstal case with an energy price of 0.5 DKK./kWh.

Simple Pay Back Time in Years	Marstal Case
Best case (1997)	11.4
Average (1990, 1999)	11.6
Worst case (1998)	13.1

The results in Table 12 show that the uncertainty for the investment in large-scale solar heating is in the range of 2 years which is about 11% of the best result.

6.2.2 Tendencies of price performance for CSHPs in the last decade

Comparing plants built in different years and in different countries involves a number of assumptions presented below:

For comparing the price trends of CSHP, the plant investments must somehow be normalised, made comparable. This is done by the individual authors referred to and cannot be controlled by this author. The currency exchange rates are applied as shown in Table 18.

Table 18. Currency exchange rates applied in the price calculations below.

Currency	Exchange rate to Euro
Danish Crowns	7.44
Swedish Crowns	7.90

An investment made in 1980 would (under similar conditions) be more expensive today, due to the fact that money has lost value. In the present work, this is corrected by a price index, as described in Table 19. The values are found by assuming the year 2000 to be the neutral year (Index = 100) and the inflation to be 1% each year computed from year to year[9]. This is certainly a simplification, but a reasonable one, bearing in mind that price indexes vary from one country to another.

Table 19. Price index applied in the price calculations below.

Year	Index
1988	88.6
1989	89.5
1990	90.4
1991	91.4
1992	92.3
1993	93.2
1994	94.1
1995	95.1
1996	96.1

[9] Alternatively one could apply a more official index from e.g. a governemental, statistical offices.

1997	97.0
1998	98.0
1999	99.0
2000	*100.0*

The details of the investments must be comparable. If one plant includes the ground and building investments, so must the other plant. This is not possible within the current work due to lack of information. Hence, the analysis is based on facts published by others, and the findings from Marstal are adjusted to be comparable with the others.

Comparing the results from the APAS-project, (Dalenbäck, J-O., 1995) with the findings from the Marstal plant, we find a price reduction as plotted in Figure 72.

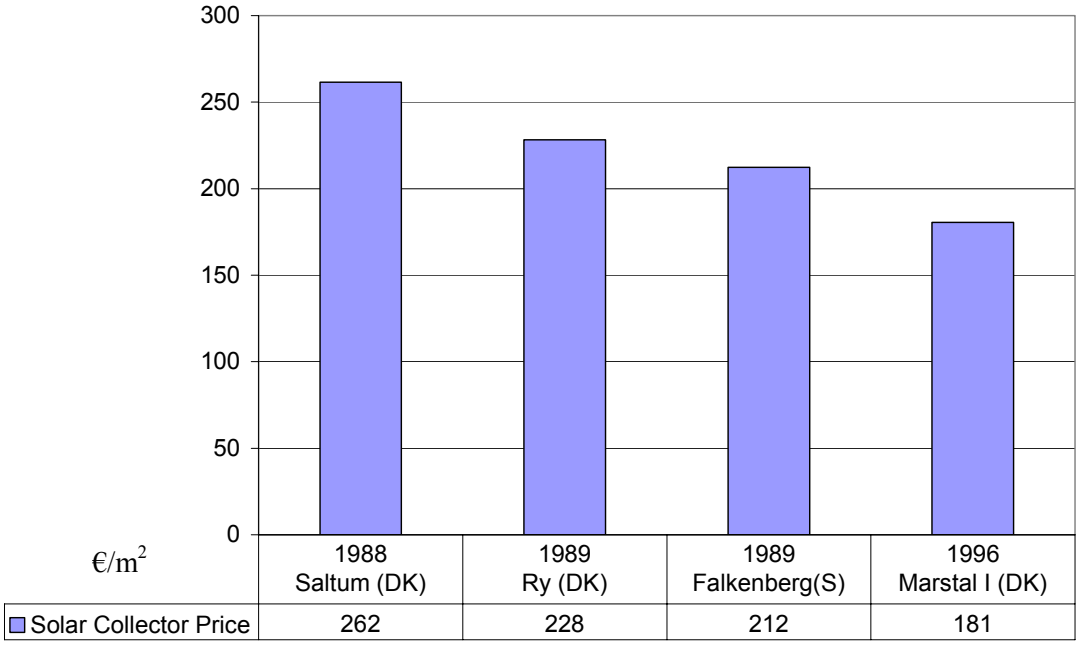

Figure 72. Price development for solar collectors in CSHPs for the last decade. Note: Price adjusted to year 2000 in €/m^2.

We find a price reduction for the main component of central solar heating systems, the solar collector, of 31% in relation to the first plant. This is mainly due to the semi-industrial production, but also to some minor savings in the collector field piping.

For the price development of the whole plant, the plant design must be taken into consideration. Comparing similar figures from the different authors, we find a reduction between similar plants of:

From the Falkenberg to the Kungälv plants, a reduction of 32-35% in relation to the older plants, including price indexing is found by (Dalenbäck, J-O., 2000). This is a reasonable comparison for two plants with small thermal storage involved.

From the Ry plant to the Marstal plants a reduction of 11% is found in relation to the older plants, by applying price indexing and price found as presented by (Sørensen, P. A., 2000). This certainly does not reflect on the involved storage capacity of the Marstal plant. Correlating the solar fraction, representing the storage capacity involved, we find a price development as sketched in Figure 73.

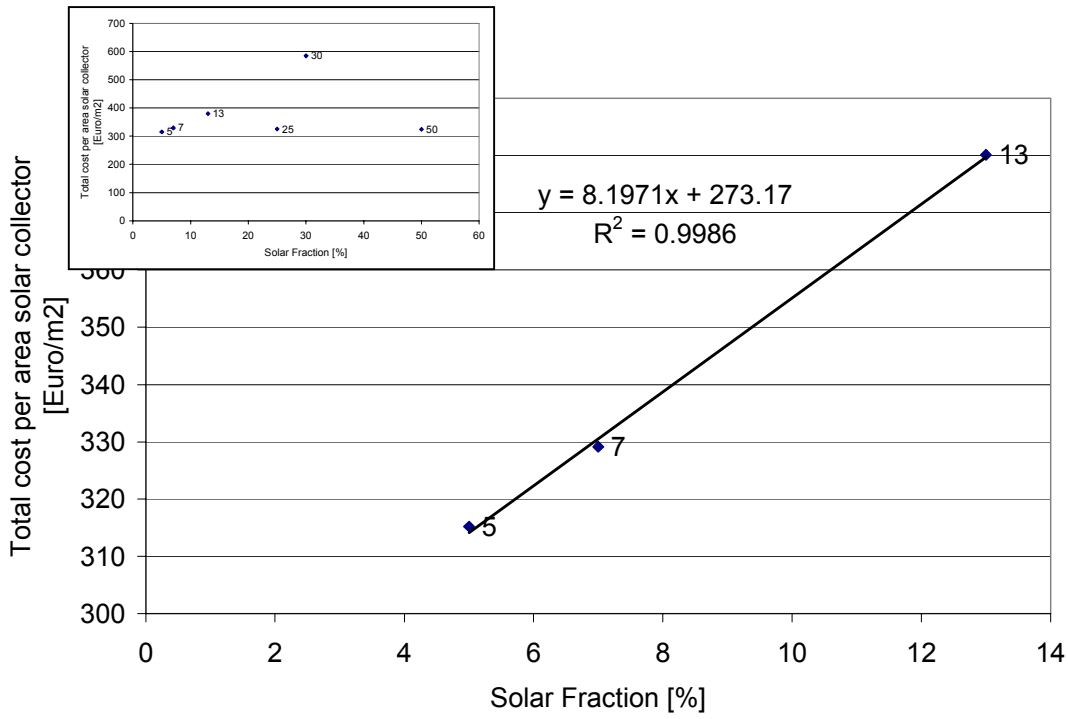

Figure 73. Solar Fraction (Storage capacity) versus price for CSHPs. Note: Price adjusted for year 2000.

As we find in the main plot of Figure 73, there is a linear relation between the solar fraction and the price. Unfortunately, applying estimates for future plants by (Sørensen, P. A., 2000) does not show this tendency. (See small plot in the figure.)

An alternative comparison of the different plant designs can be made as follows: By assuming a Marstal design with no seasonal storage (not possible in reality), we can estimate the cost for a Ry-design built today. The cost for such a plant can be estimated to between 65-75% of the costs for the Marstal plant which is approximately 230-260 Euro/m^2. The reduction from index-corrected plant price in Ry from 294 Euro/m^2 is therefore 11-22%, dependent on the assumptions.

6.3 ECOLOGICAL PERFORMANCE

Values behind the current environmental assessment are based on the same values applied by the Danish Energy Agency, (Energistyrelsen, 2000). Assuming an efficiency for the thermal plant of 80% and the application of fuel oil for heating, we find a replacement of 380 ton waste oil and a resulting reduction of pollutants as shown in Table 20, last column, for the Marstal plant.

Table 20. Evaluation of emission reduction due to application of central solar heating in district heating.

Emission	kg/GJ	kg/MWh			Reduction [t]
CO_2	78.000	280.800			107.0
NO_x	0.495	1.782	GJ/ton	MWh/ton	0.7
SO_x	0.150	0.540	40.4	11.2	0.2

Similar calculations by the plant owners show even better results.

An environmental assessment was carried out on large-scale solar heating already a few years after the first plant was erected, (Dalenbäck, J-O., 1995). The main reason for impact on the environment was shown to be based on electricity consumption mainly for pumping. The production of electricity has close to a double impact in terms of emissions per produced output unit, compared to heat production. This is a bit more confusing for areas with co-generation, but not relevant for the Danish plants which according to regulations must lie outside the co-generation areas.

Monitoring on the Marstal plant shows that the plant delivers 1 MWh for each 4.4 kWh consumed for pumping, (Holm, L., Ulbjerg, F., Nielsen, J. E., Sørensen, P. A., and Tambjerg, L., 2000). For the first DK-generation plants, the consumption is approximately 4 times higher, due to the different flow control.

An alternative way of evaluating the impact of an (energy) technology is to apply a Life Cycle Analysis (Assessment). The methodology behind this tool is rather complex and cannot be described in detail here. Some main points are that the production of the materials, system components and the system in total, the energy consumption in the lifetime of a technology and even the disposal is taken into consideration in the analysis. Such an analysis on 15 different solar collector designs is performed and published by (Jacobsen, D. T. and Nielsen, J. E., 1999). The main findings are:

- The simple, environmental payback time for collectors is in all cases around 0.8 years and for the system in total (small, domestic hot water system) around 1.5 years.
- A main source of environmental toxicity is the application of coated materials and metals. This impact must be reduced by disposing the used collectors in the end of the life cycle. This subject must be addressed in the future.

6.4 COMMON EXPERIENCES

In general, central solar heating works well, and in most cases, as expected. This is a very important finding due to the fact that the technology has no serious teething problems.

The CSHP technology is differentiated to a variety of designs and therefore applicable in a wide range of systems.

As expected, the technology does not cause additional need of manpower for existing district-heating companies due to its simplicity. In fact, the need for manpower is reduced, especially in summertime, where DH-operators may enjoy their well-earned vacations. Albeit simple, this is a very important argument for the marketing and hereby penetration of the technology.

An important finding from the Marstal plant influences the design rules applied in the past. It was recommended that the design must deal with the worst case with strong solar irradiation over a long period. This can be done be applying a small collector array, or a large storage volume. In Marstal, the production was exceptionally high in the first year of operation. Demand and tank volume could not buffer one more day of solar production. To avoid overheating with resulting damages, the collector loop was run in the night, cooling down a part of the tank volume. This incidence proves the fact that the design guidelines can be reconsidered by including nighttime cooling. The results are designs, optimised for higher solar fractions. Note: This recommendation can certainly not be sufficiently applied for plants without thermal storage (CSHPxS).

In the publications by among others (Dalenbäck, J-O., 1995), (Isakson, P. and Schroeder, K., 1996), (Dalenbäck, J-O., 2000) and the many publications from the European Large-Scale Solar Heating Network, the following subjects led to serious problems with CSHPs, relevant to mention here:

- Certainly some predictions regarding plant performance prior to the designing of solar plants turned out to be erroneous. The district-heating network conditions must be very well known and the operation of the DH-system according to low-temperature recommendations. This base lining is a general problem for the implementation of renewable energy technologies (and changes in general). It is very important for the success of projects that the data for the designing is realistic.
- Minor damage was reported in the past in relation to prefabricated collectors. Glasses were broken and rubber bands as convection barriers (Teflon) loosened. The manufacturers have problems such as these under control.
- Stratification in tanks is very important for the operation of solar heating in general. Lacks of perfect stratification are repeatedly reported, due to misplaced inlet arrangements or inexpedient design of the inlets, e.g. the Falkenberg plant.
- Corrosion in steel tanks (and also in piping) is a frequent subject. Regardless of the fact that the designing of steel tanks is a well-known technology, corrosion is reported for e.g. the Falkenberg and the Marstal plants.
- The design of collector fields is rather simple, but must be done with care. Problems are seen in the early plant designs. The pressure distribution must be distributed according to guidelines. By letting the producer design the field, as practised in Marstal, this balance is ensured.
- For the flow and pressure balancing of solar collector fields, design tools from e.g. district heating can be applied with success.
- Sensors involved in the plat control and monitoring must be chosen and placed carefully. Many instances of erroneous monitoring equipment are reported, among others the fast degradation of a solar sensor at the Marstal plant, reported above. This subject is certainly not special for the central solar heating systems; but due to the fact that solar heating always struggles with over-stretched "economical values", mistakes have a greater impact, compared to other energy systems, where the capacity is large enough to counterattack such "eventualities". This is not possible in solar heating.
- Solar collector loops must be purified from time to time to avoid flow imbalances. By monitoring the outlet temperatures at the rows, as implemented at the Marstal plant, imbalances would be observed before doing damage.
- Collectors must be cleaned in southern European regions due to lack of rain which also causes increased dust diffusion on the collector covering, thus decreasing the efficiency. Studies on this subject are presented in Solar Energy by Elsevier Science.
- Vegetation around the collector field must be kept low. In Marstal this is successfully achieved by letting sheep grass in the collector area and by two yearly grass cuttings. Hereby the necessary manpower is minimal.

Going into more detail with the Marstal plant we find:

- At the Marstal plant, due to economical reasons, two pumps were chosen to service the necessary range of flow rate. After the first experiences with this configuration, it is recommended to install a single pump able to service the whole range of flow rates.
- Solar heating involves a transport medium. This medium is exposed to very low temperatures in wintertime. Hence, anti-freezing additives are applied for the water in the collector loop. A propylene glycol water mixture is applied in Marstal. It turned out that this mixture in some way had a rather large impact on the efficiency of the plate heat exchangers. No explanation for or solution to this problem is found at the time of writing

these experiences. To solve the problem in Marstal immediately, the heat exchanger was equipped with additional plates.

- The open connection of the secondary side to the storage tank and the district-heating network as applied in Marstal, led to flow disturbance. The pressure in the district-heating loop is rather high. Contra-valves had to be replaced to avoid inexpedient flows in the wrong direction.
- The storage volume at the Marstal plant is designed with a ratio of storage volume to the collector area of 260 litres per m^2. The plant was designed to supply the whole demand in the summer months. This could not be achieved and will be discussed later in the analysis chapter.
- The control strategy leads to fluctuating return temperatures from the collector field. The designer of the plant expected better performance. This subject will be discussed later in this work.
- The one pyranometer applied in Marstal deteriorates very fast. Such instruments should not be applied. The experiences from different plants should be collected and made available to others.
- The pyranometers of type SOLDATA HDX, applied at the Marstal plant, showed sufficient accuracy for the given task. The SOLDATA type SP instrument generally showed values too high.
- The outlet temperature from each row is monitored at Marstal. After taking the plant into operation, the flow through the individual rows was balanced by an adjustment of valves at the entry of the rows. By comparing the monitored outlet temperatures, unbalances would be observed. This is a recommendable method for others to apply. Under the supplementary monitoring programme, the flow rate of the plant was not adjusted perfectly, leading to differences in outlet temperature up to 5 K between rows.
- Based on data analysis, an unwanted flow was observed during night-time - from the district-heating system back to the heat exchanger - leading to unnecessary heat losses. The error was only identified due to the advanced monitoring. Therefore, it is advisable and economically justifiable to install such advanced monitoring systems at solar heating plants of a certain size, (see economical sections). Nevertheless, in such a case, it would be wise to design an automatic control algorithm that could observe relevant conditions and eventually alert the operating staff. If such an automatic system is not applied, the data must be analysed by the operator which is a rather demanding task, even with online plotting.
- The control strategy in Marstal is able to control the temperature back from the collector field in a range of 1.5 K around the set point temperature, if solar irradiation does not fluctuate too much. For strongly changing conditions (in an time interval of e.g. ¼-hour), the strategy leads to corresponding temperature control in a range of up to 5 K.

7. ANALYSIS BY SIMULATION

7.1 METHOD AND TOOLS

In the previous chapter, a simulation model is prepared and described. In this chapter, the final tool is used for analysing and hereby exploring the characteristics of central solar heating systems. Hereby, the model is applied above the range of validity which is the objective of doing the modelling and simulation. To get an insight into the model parameter, variations are carried out for a wide range of parameters. The results are then applied in a sensitivity analysis.

The parameter variation method is applied to gain insight into the model by analysing the impact of changes on the final results. Here, well-defined steps change a single parameter. The objective is to examine the trends in changes on overall results, here the net solar gain which is the energy delivered to the district heating by the solar plant.

As the objective of the parameter variation method was to investigate the trends of changes in results, the objective of the sensitivity analysis is to make the impact of parameters on the results comparable. The parameters applied are chosen to represent the variety that can be expected in real life systems. Hereby, one gains insight into the sensitivity of changes in parameters on the total results. Especially sensitive parameters can then be handled with special care.

Note: The tools applied are very powerful for users of models with limited insight into a given model and system. By simple simulations, the basic features of a model can be found and necessary precautions taken to avoid erroneous results.

To be able to compare the many results produced by the methods, the base or reference case of the previous chapter is applied, representing the Marstal case. Hereby, as a side effect, we are able to evaluate the actual plant design in Marstal.

7.2 PARAMETER VARIATION ANALYSIS

7.2.1 Numerical Parameters

Before performing any changes to the solar system parameters, some preliminary analyses are applied on the parameters for the simulations and the numeric. Hereby, confidence in the simulation tool is gained.

7.2.1.1 Tolerance for convergence and solution finding

Two parameters are to be chosen for controlling the tolerance: 1) a parameter for tolerance control of numerical integration 2) a convergence criterion parameter. The two parameters are examined for settings between 1 and 0.0001. We find that the results, e.g. in net solar gain, converge from high to lower parameter values. For very small values, this convergence is disturbed by numerical and computational limits. Hence, the results jump in the range of the value that is seen as the most accurate. Below, two examples are shown for parameter value 0.01, for which the convergence result is not found, and for the parameter value 0.001, for which the results are converging to a stable level, here interpreted as the correct value.

Note: The value is valid for temperature computations, e.g. 0.01 equals 1% by 100^{o}C, boiling water. For derived values, as e.g. energy and power, the tolerances are larger.

For the two values of tolerance, we find the sensitivity as shown in Figure 74.

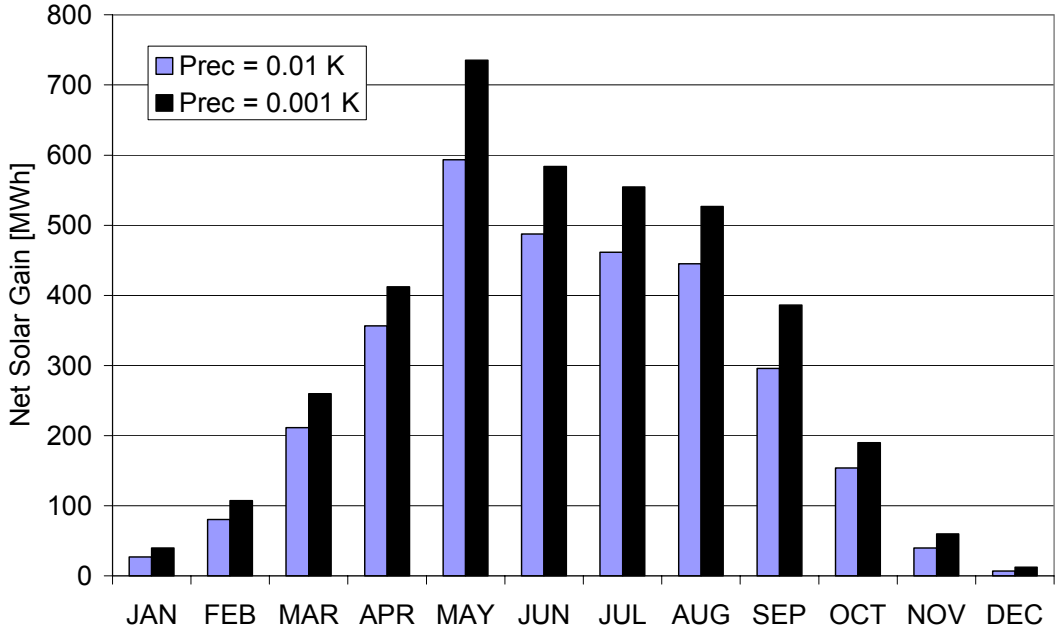

Figure 74. Monthly net solar gain for tolerance values of 0.01 and 0.001.

It is clear from the results in Figure 74 that the simulations are very sensitive to these parameters. The time for computation is very similar for the two tolerance settings. Therefore, it is chosen to apply the tolerance of 0.001 for all simulations in this work.

7.2.1.2 Time step of computations

Simulations involve two "independent" time steps: 1) time step for data input reading and data output, 2) time step for computations.

For the input-output time step, the value of one hour is chosen for all the following simulations.

The computational time step is examined by choosing hourly, half-hourly, quarter-hourly and five-minute numerical intervals. Assuming the latter most accurate, we find a deviation in the hourly computations of 22% and all the others within 1% of this result.

The time for simulations increases strongly due to decreasing computational time steps. For a whole year simulation, the time for computation is increased from 2 minutes up to $^1/_4$ hour on a computer with a clock frequency of 266MHz. Therefore, the time consumption for computations must be taken into account when choosing this parameter.

Unless no other values are presented explicitly, $^1/_4$-hour numerical time steps are chosen in this work. Note: Component models as the storage tank TYPE 140 and the MFC-solar collector module are using internal time steps, not analysed in this work.

7.2.2 Loads

The boundary condition for central solar heating plants is very strongly related to the demand in heat by consumers connected to the district heating. This subject is discussed in detail in (Heller, A., 2000c). Here, the sensitivity of the parameter is investigated by carrying out simple manipulations to the load profile. The base-case load is multiplied by a factor and hereby enlarged and decreased linearly. We find for a variation in load of 10% that the net solar gain

changes approximately 2% which is surprisingly low. This is due to the fact that the solar production is gathered in the summer month where the load is already very small. Computations involving long-term storage would be much more sensitive to this parameter.

7.2.3 Collector Field Design and Shading

The collector field model is defined by the type of collector, a tilt angle, distance between collector rows, the piping of the collector loop and a heat exchanger as a boundary.

There are three component models applicable for the TRNSYS program, as mentioned in the validation chapter. Here it was found that the standard component, TYPE 1, is not applicable due to lack of including the thermal mass into computations and hereby an unrealistic, dynamic representation. Therefore, the MFC-solar collector type is modelled to include the mass. We found very good agreements between measured and computed values in two cases: 1) when representing the whole collector field by a single model component 2) when representing the collector field by the maximum number of components (four). No major differences were observed, and consequently the computation is carried out by the single component model.

In the current analysis, the overall design for the collector field, e.g. number of modules in row and hydraulic schemes, is not changed. This limitation is partly chosen due to the fact that any change to the hydraulic conditions would demand exact flow and pressure modelling to avoid flow imbalances. Hence, detailed hydrodynamic simulation would be necessary in this case.

The simplest parameter to examine is the area for the collector field. The results on the net solar gain are shown in Figure 75.

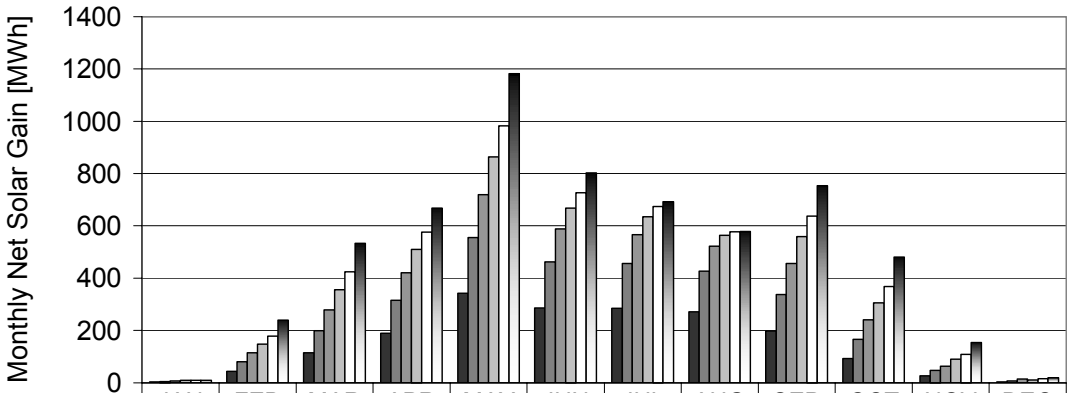

	JAN	FEB	MAR	APR	MAY	JUN	JUL	AUG	SEP	OCT	NOV	DEC
4000	3	43	115	190	342	286	285	271	198	93	26	3
7000	5	80	200	315	556	463	456	426	337	166	48	7
10000	8	114	279	420	720	589	566	523	457	241	64	14
13000	9	148	356	510	864	667	635	564	559	306	90	11
16000	10	178	424	576	982	726	674	577	637	368	109	16
22000	10	239	534	668	1181	802	692	579	754	481	154	20

Figure 75. Monthly net solar gain versus solar collector area for a parameter variation between 4000 and 22000 m^2 applied at the case plant.

From Figure 75 we find an increased net solar gain for all periods, except January, August, September and December. For the two winter months, the lack of solar irradiation explains the missing increase in net solar gain. For the summer months, August and September, we find a rather interesting observation - the increase in solar gain is flattening out as the area is increased. This can be explained by the fact that for these conditions the demand in the district heating is covered and the tank storage filled up. Hence, the produced heat cannot be utilised.

The annual values in net solar gain for the increase of area show an upward tendency for the whole range of parameter variation, but also show a tendency to flattening out for high values.

Note: It is worthwhile to compare the figure from the parameter analysis on the solar collector area with the observation for the tank volume below.

Due to the application of rows in the designing of solar collector fields, shading between rows must be taken into consideration. The rows in a field shade the rows behind. The TRNSYS program includes a component model for estimation of shading on fixed and tracking surfaces.

Shading is affected by a number of parameters, the dimensions of the solar collector modules, the length of the rows, number of rows and most relevant, the distance between rows and the horizontal tilt angle for the collectors. The parameters intercept each other and a presentation of the analysis is therefore built up, gradually.

To get a first insight into shading, a set of parameter variations on the number of collector rows and width of rows are carried out. These parameter variations showed very little impact on the net solar gain. The reason for this result can be found in the implementation of the shading model in TRNSYS. To exemplify the subject, it is assumed that the sun rises on a spring morning in the south east of the collector field. When the solar rays hit the collector field, the incident angle is very low and oriented from the side of the field (Northern European climate with collector field oriented to the south). Hereby, the solar irradiation reaches the outer part of each row. In the centre of the rows, the sun cannot reach the collector due to shading. According to own simulations, the TRNSYS-model does not seem to account for this side-incident. No details are presented in the manual of the program. This consideration must be kept in mind when proceeding in the examination of the field parameters.

The error made by this assumption is very low for plants as the one in Marstal, where the number of rows is high and the "length" of the rows very wide.

Figure 76 shows the impact of changes of the distance between rows on the net solar gain.

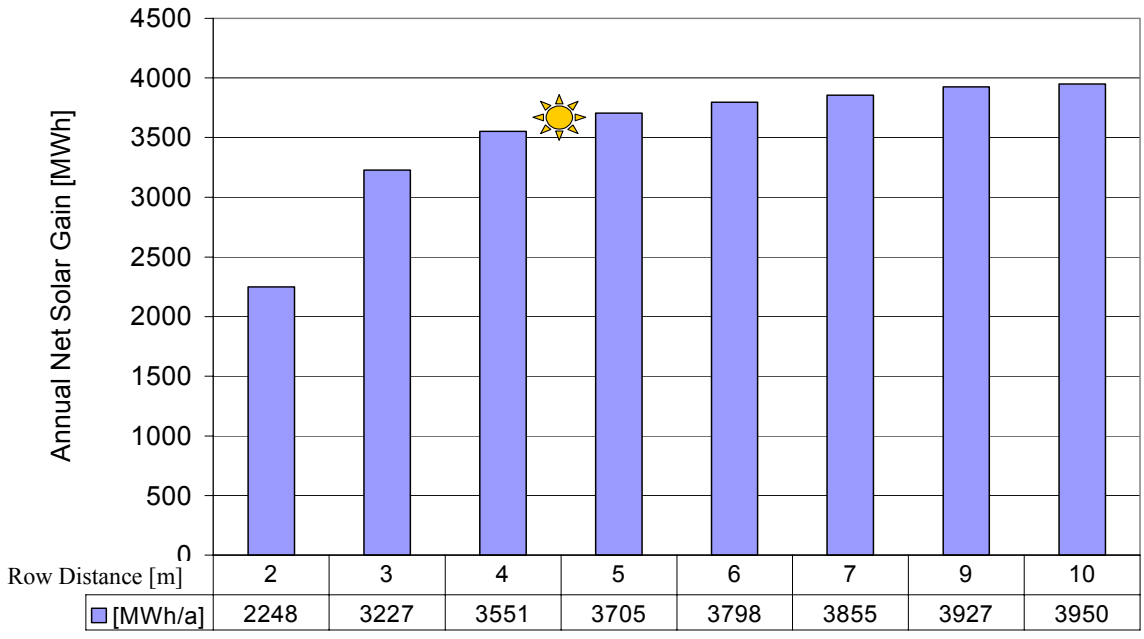

Row Distance [m]	2	3	4	5	6	7	9	10
[MWh/a]	2248	3227	3551	3705	3798	3855	3927	3950

Figure 76. Parameter analysis on the distance between rows for values from 2 to 10 metres with step size 1 metre.

In Figure 76, we find a clearly decreasing influence of the row distance on the annual net solar gain which was expected due to decreasing shading. The solar gain is increased drastically between 2 and approximately 4 metres, flattening out for larger distances. Hereafter, the net solar gain is not affected anymore by the distance between rows. Note: The distance applied in Marstal is 4.5 metres visualised by the "sun".

The tilt angle of the collector modules is another factor affecting the shading and hereby the solar gain. For a distance between the rows of 10 meters, we find the following impact of changing tilt angle of the collectors on the net solar production, shown in Figure 77.

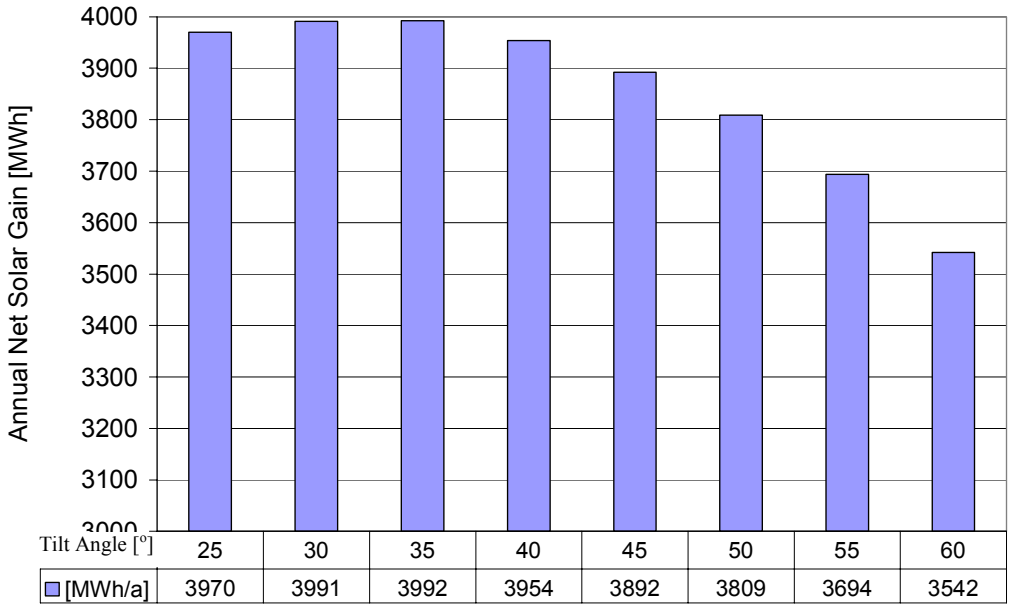

Tilt Angle [°]	25	30	35	40	45	50	55	60
[MWh/a]	3970	3991	3992	3954	3892	3809	3694	3542

Figure 77. Annual net solar gain versus collector tilt angle (measured from the horizontal/) for a distance between rows of 10 metres. (No shading on the rows for this distance.)

We find in Figure 77 that the arch-shape for the dependency of the solar production on the tilt angle is shown for a very wide distance between rows. This is similar to the case with small and large roof-mounted solar collectors. Before examining the case with smaller distance between rows, we take a close look at the monthly values for the current "10-meter case" in Figure 78.

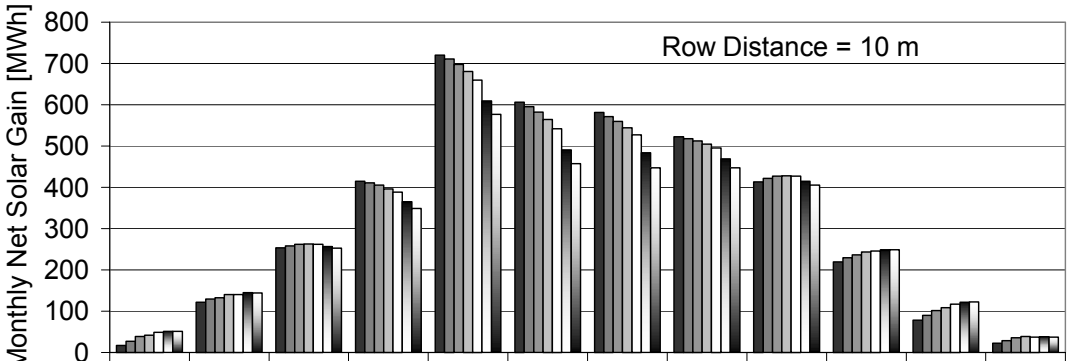

	JAN	FEB	MAR	APR	MAY	JUN	JUL	AUG	SEP	OCT	NOV	DEC
25	17	122	254	415	720	606	581	522	413	220	79	23
30	27	129	258	411	711	596	571	518	422	230	91	29
35	39	133	262	405	698	582	560	512	427	237	102	36
40	41	141	263	396	681	564	544	505	428	243	109	39
45	49	140	263	389	659	542	527	495	427	246	118	37
55	52	145	257	365	609	491	484	469	415	249	122	38
60	51	145	253	349	577	458	447	448	405	249	123	38

Figure 78. Monthly net solar gain versus collector tilt angle (measured from the horizontal) for a distance between rows of 10 metres. (No shading on the rows for this distance.)

The analysis of the results from Figure 78 is presented separately for each season.

We find for the winter months, e.g. January that the solar gain increases for a tilt angle increased from 25 to 45 degrees from the horizontal.

In the "shoulder months", spring and autumn, e.g. Martch and September, we find an arch-shaped affection of the tilt angle on the net solar gain.

In summer, the increase of tilt angle leads to decreasing solar production for the whole range of variation applied here.

Weighting the impact of the individual months on the yearly total, remembering the heat demand for the relevant periods, we find the results shown in Figure 77.

Reducing the distance between the collector rows to 4.5 metres, we can imagine the influence for the three periods introduced in the previous example (10 m). Please note that the range for the parameter variation is enlarged from a 0 to a 60 degree tilt angle for the finding of an optimum tilt angle.

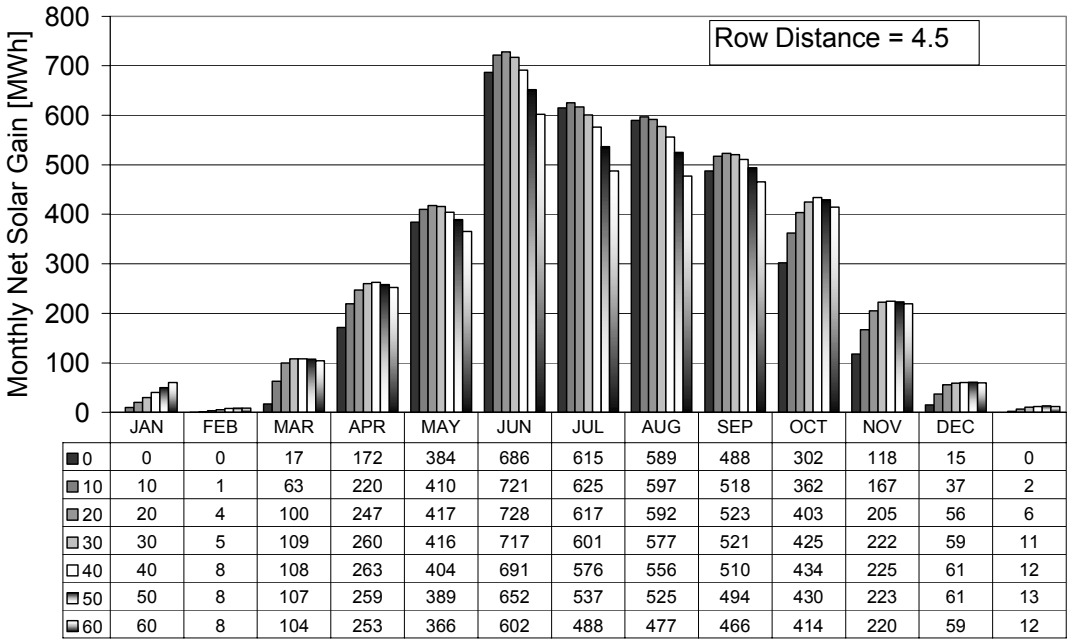

	JAN	FEB	MAR	APR	MAY	JUN	JUL	AUG	SEP	OCT	NOV	DEC	
0	0	0	17	172	384	686	615	589	488	302	118	15	0
10	10	1	63	220	410	721	625	597	518	362	167	37	2
20	20	4	100	247	417	728	617	592	523	403	205	56	6
30	30	5	109	260	416	717	601	577	521	425	222	59	11
40	40	8	108	263	404	691	576	556	510	434	225	61	12
50	50	8	107	259	389	652	537	525	494	430	223	61	13
60	60	8	104	253	366	602	488	477	466	414	220	59	12

Figure 79. Monthly net solar gain versus collector tilt angle (measured from the horizontal) for a distance between rows of 4.5 metres. (The Marstal case.)

We find the following results:

For the winter months, e.g. January, the tendency that increased collector tilt angle results in increased solar production is strengthened.

The arch-shape in the month with poor solar irradiance is showing already an arc-shape, but with different optimum than the summer month. As the optimal tilt angle in the cold month is around 40°, the optimal tilt angle in summer is between 10 and 20°. The final result on the total yearly production is visualised in Figure 80.

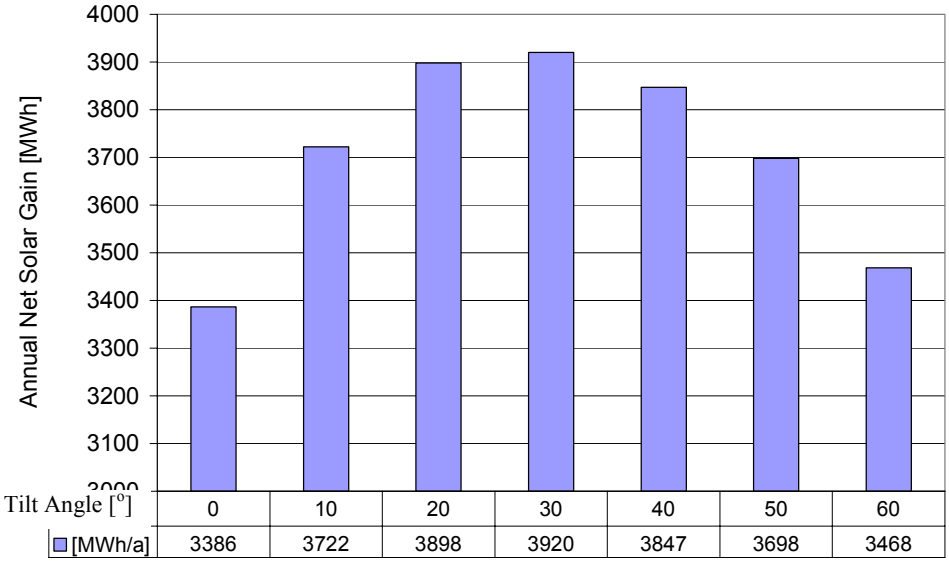

Tilt Angle [°]	0	10	20	30	40	50	60
[MWh/a]	3386	3722	3898	3920	3847	3698	3468

Figure 80. Annual net solar gain versus collector tilt angle (measured from the horizontal) for a distance between rows of 4.5 metres. (The Marstal case.)

By comparing Figure 80 with Figure 77, we find that the optimal tilt angle for the row distance of 4.5 metres is less accentuated and to be found around 30° from horizontal. This corresponds reasonable with the findings by others, e.g. an optimum at tilt angles in the range between 30 and 40 are expected by (Mikkelsen, S. E., 1988) and by simulations in the computer program SEASONSOL by (Olsen, O., 1993).

7.2.4 Storage Tank Design

The storage capacity of the CSHP certainly has a very strong impact on the solar fraction and hereby the solar production, if the plant design is aimed at supplying more than the summer supply. The dominating parameters are the volume of the storage, the stratification conditions for the tank and the heat loss to the ambient. Stratification is not investigated here due to its complexity which lies beyond the scope of this work. This does not mean that it is not an important subject. The remaining parameters to be analysed are therefore related to the geometrical dimensions and insulation conditions of the tank.

In Marstal, a volume of 2100 m^3 is applied which is 260 litres per square metre solar collector in the 1996-design. In the very sunny summer of 1997, the tank showed severe difficulties with storage of the solar production for a series of sunny days of 6-7 days. It is therefore important to find an optimal tank design from the designing stage.

In this first parameter analysis, the impact of the storage heat loss is examined. At the Marstal plant, the heat loss is measured to 478 kWh over a period of 27 hours which is in average 17 kW by high fluid temperatures. Assuming an ambient temperature of 20°C and a tank temperature of 80°C, we can estimate the heat loss to approximately 280 W/K.

Estimating the heat loss for the tank on the design guidelines for short-term, thermal storage by (Witt, de J., 1990), we find a heat loss for a corresponding storage of 11.5 kWh, for an ambient temperature of zero degrees. Hereby the estimate by de Witt is below the measured value.

In the TRNSYS-model, the heat loss is defined by a UA-value in W/K. By using an insulation thickness of 0.2 metres (used at the storage tank in Marstal) and a thermal conductivity for the insulation material of λ_i=0.04 W/(K m), we find a thermal transmittance of approximately 0.2 W/(m^2 K). Assuming that half of the tank has been heated up, the affected area of the tank is approximately 450 m^2. Hereby we find a UA-value of ca. 90 W/K, much lower than found above. However, the measurement involves a rather large uncertainty. Hence, the value based on the real thickness of the insulation is applied in the following computations.

The sensitivity of the result for the whole CSHP is as shown in Table 21.

Table 21. Parameter variation: Tank insulation thickness. Annual net solar gain versus insulation thickness, for values from 0.1 to 0.5 metres with step size of 0.1 metres.

Ins. Thickness [m]	**0.1**	**0.2**	**0.3**	**0.4**	**0.5**
Annual Net Solar Gain (NSG) [MWh]	3602	3639	3657	3660	3664
Change in NSG in %	98.98%	100.00%	100.49%	100.58%	100.69%

We find that the impact of the tank insulation is below 2%, when halving and doubling the insulation thickness. This rather small impact is mainly due to the rather limited storage time for the hot water in the tank. Hence, the simulation values are kept at the settings measured at the Marstal plant.

The impact of the storage volume on the net solar production is seen in Figure 81.

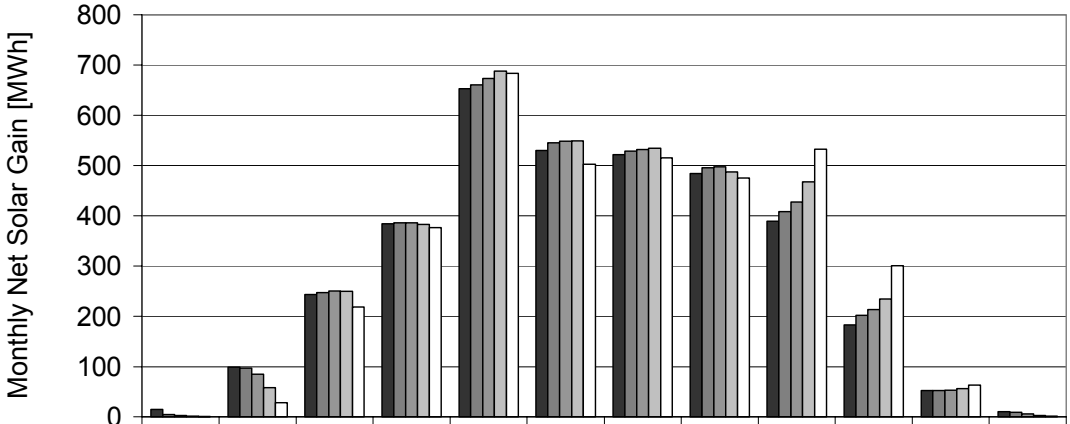

	JAN	FEB	MAR	APR	MAY	JUN	JUL	AUG	SEP	OCT	NOV	DEC
1000	15	99	243	384	653	530	522	484	389	183	52	10
2000	5	97	247	386	661	545	529	496	408	202	53	9
3000	3	85	251	386	673	548	532	497	428	214	53	6
5000	2	58	250	383	688	549	534	488	467	235	56	3
10000	1	28	219	377	683	502	515	475	533	301	63	2

Figure 81. Monthly net solar gain versus storage volume, for a parameter variation from 1000 to 10000 m^3.

We find from Figure 81 that the net solar gain for the months of January, February and December decreases due to increased heat loss to the ambient.

In the spring and summer months, we find an arch-shaped tendency for increased storage volume. This is due to the balance between increased heat stored and utilised by the district heating on the one hand, and the increased heat loss due to increased volume on the other hand. We find that the optimal volume for this period is close to 5000 m^2 storage volume.

The strong influence due to increased volume can be found in autumn, where the demand is high and the stored solar gain can be utilised efficiently. Here we find that an increase in storage volume will lead to increased net solar gain for the whole parameter variation.

From these monthly values, we expect the existence of an optimal storage volume for the base case. The result in annual performance is shown in Figure 82.

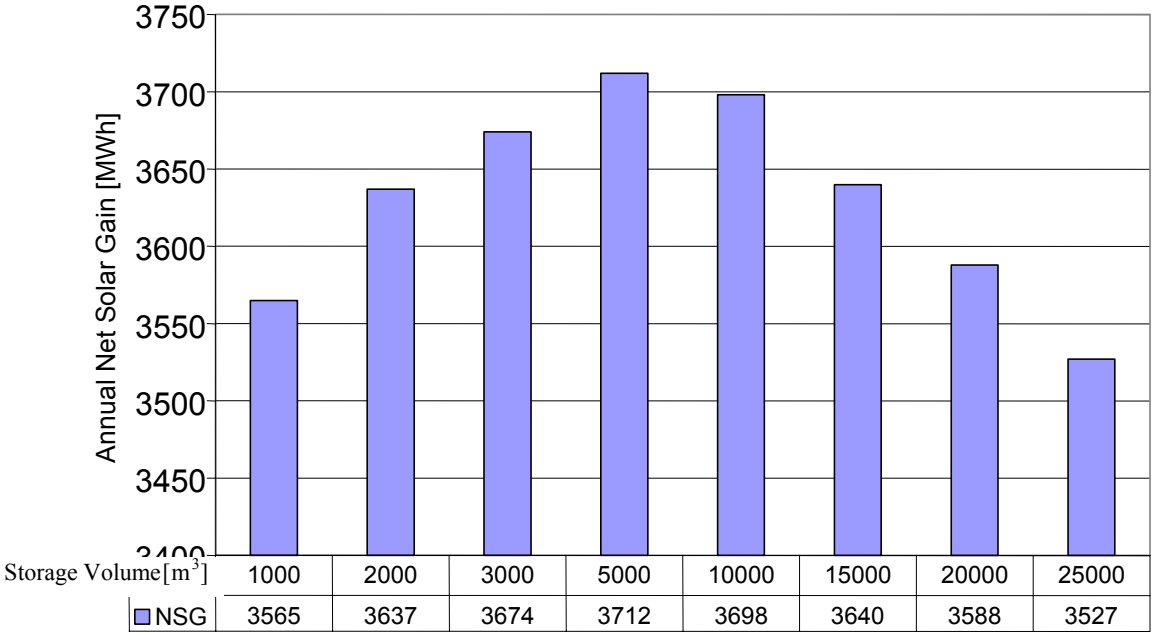

Figure 82. Annual net solar gain versus storage volume, for a parameter variation from 1000 to 25000 m^3 with different step sizes.

As expected, we find a thermally optimal storage volume for the Marstal plant at a volume of 5000 m^3 content. This can be seen as the maximal production for the plant with the given design, e.g. tilt angle, control strategy and so on. The Marstal case involves a storage volume of 2100 m^3 that is below the thermal optimum. The result from this variation will be reused in the design study chapter below.

7.2.5 Other parameters

Many other parameters could be investigated, e.g. the coefficients involved in the solar collector model etc. However, such analyses would give an insight into the models, but the values are known from testing and by applying the values as measured at the Marstal plant or other relevant plants. Consequently, it makes no sense to document such parameter variations.

7.3 SENSITIVITY ANALYSIS

In the sensitivity analysis method, the parameter changes are set to 25% of a given parameter value, symbolically seen, in the positive and the negative direction. Hereby, the impact of the parameters on given results is made comparable. In the current analysis, the following result quantities for the simulations are examined:

1. The annual solar collector field output.
2. The annual net solar gain which is the utilised solar gain delivered to the district heating net.
3. The annual solar fraction which is the net solar gain divided by the heat demand.
4. The annual solar efficiency which is the net solar gain divided by the solar irradiation on the collector field in the horizontal plane.

The sensitivity on the following parameters is examined for a change in 25% to the parameter values:

1. Solar collector field area.
2. Tank volume.
3. Collector tilt angle.
4. Collector row distance.

The heat loss due to tank insulation and the heat loss due to heat loss in the solar collector loop were also investigated, but showed too small sensitivity to be included. We get the following results from the analysis:

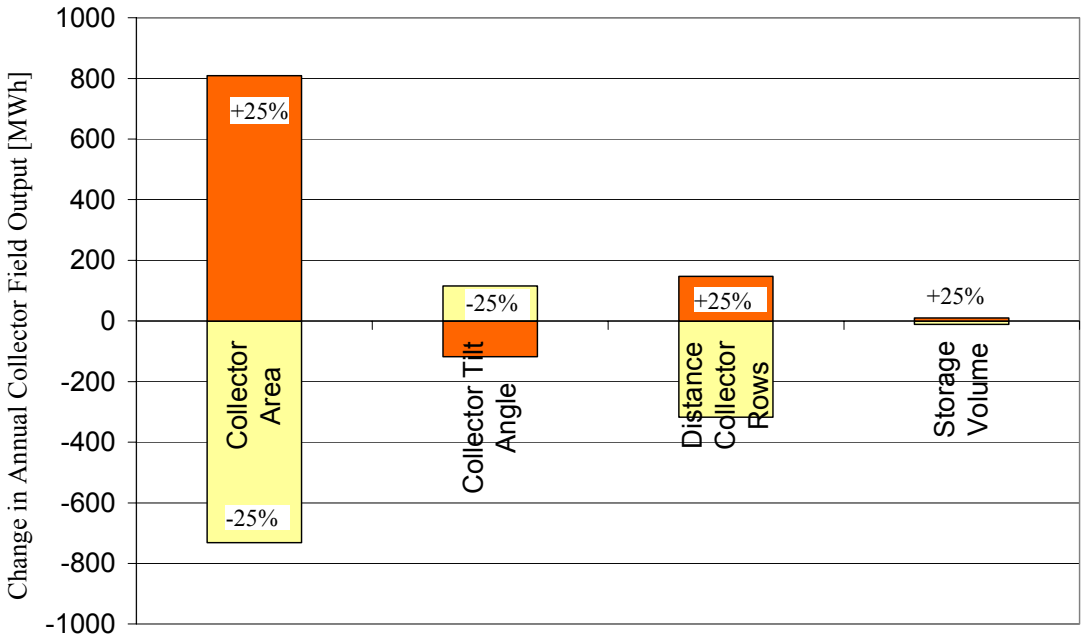

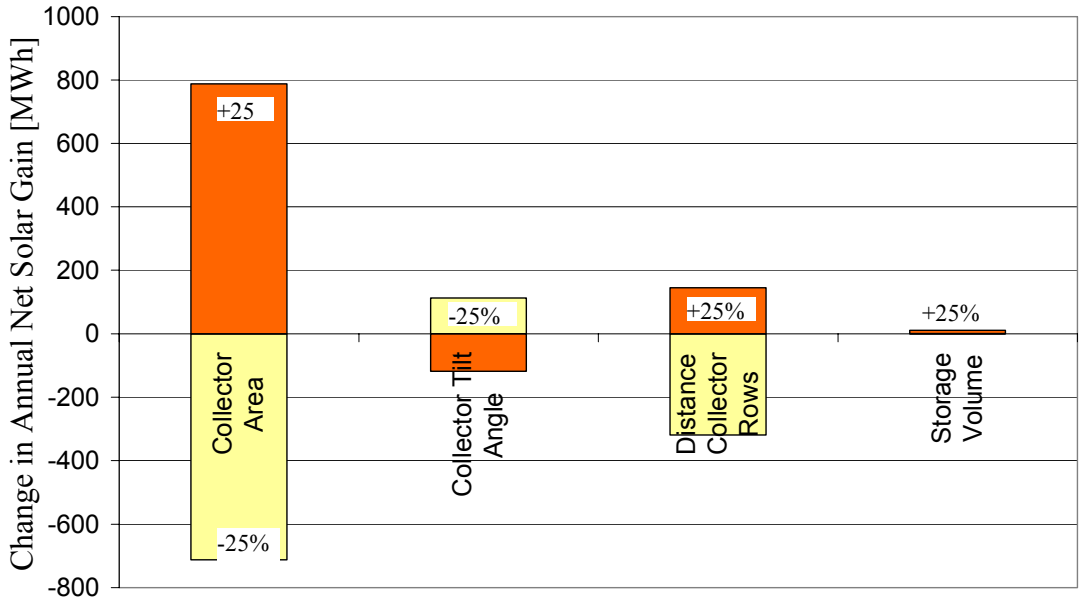

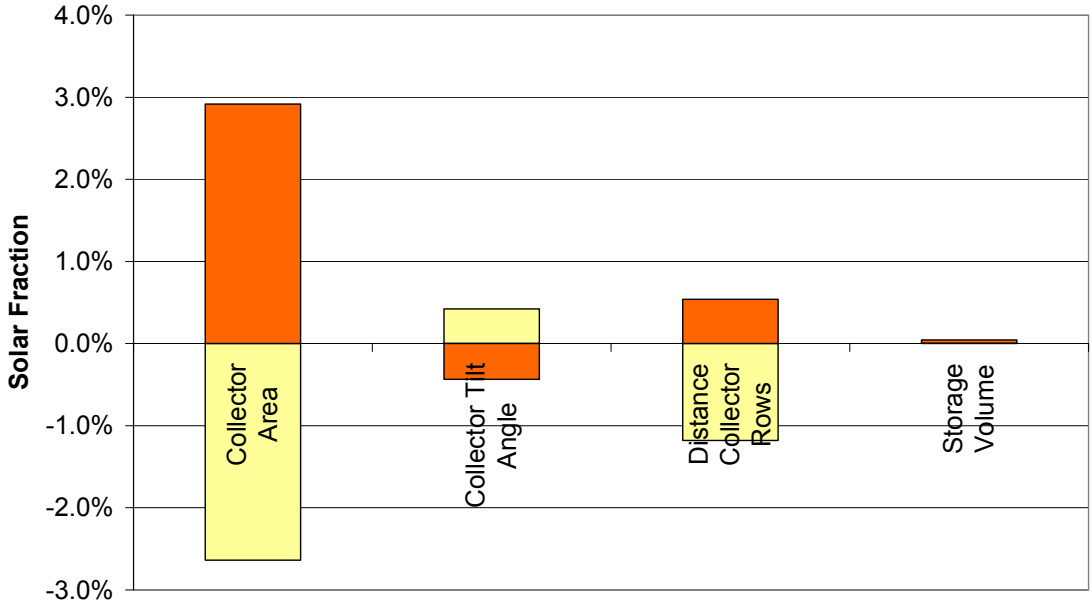

Figure 83. Results from a sensitivity analysis for a ±25% change in parameter settings for a selected set of parameters, Collector Area, Collector Tilt Angle, Distance between Collector Rows and Storage Volume. The sensitivity is analysed on four key-values: Annual Output from Solar Collector (top), Annual Net Solar Gain and Solar Fraction.

To summarise the results, we find that

- Found for all result quantities, the collector area has the largest impact on the results, followed by the distance between rows, the tilt angle and the tank volume with lowest impact.
- The impact on the collector output is slightly stronger than the impact on the net solar gain. Note that a model assumption of constant heat exchanger efficiency has been made and this must be taken into account.
- Opposite to the other parameters, the increase in tilt angle leads to decreasing solar production values.

8. DESIGN STUDIES

In this chapter mainly variable contra constant flow is examined. At the end of the chapter some main findings from studies previously published by the author are recalled and discussed, among others the designing of a low-energy settlement and the application of high-efficiency solar collectors.

8.1 VARIABLE FLOW CONTRA CONSTANT FLOW

The most innovative characteristic of the Marstal CSHP is the employment of variable flow. The plant owner, Marstal Fjernvarme A/S, and the designer, Flemming Ulbjerg, RAMBØLL list two reasons for this solution.

1) The demand for control of the fluid temperature back from the collector field with the objective that post-heating is not necessary for longer periods in summer.

2) The avoidance of parasitic energy usage for pumping.

Temperature control can be achieved by bypass pumping which is to let a part of the flow bypass the solar collector field. This will certainly not satisfy the second objective of the control design, and will therefore be excluded from the current considerations.

An alternative method of temperature control is to apply variable flow, more precisely to control the pumping rate. The main obstacle to such pumping control is the time delay in the system described in Chapter 2. The simplest control method would be to measure the return temperature and then to adjust the flow rate according to the obtained outlet temperature from the collector field. Due to the long-flow circulation time, this control strategy would lead to very slow control reactions. This is a much too inaccurate control and will result in pending temperatures. General solutions for close loop control can be found in books about basic control theory. Implementations of this theory can be found in e.g. (Meaburn, A. and Hughes, F. M., 1993), defining the objective for a control strategy, "to be able to produce a fast and well-damped closed loop response", and proposing a flow-control method for distributed solar collector fields. An alternative approach can be found in (Zunft, S., 1995) going one step further by including the influence of the solar irradiation in the control strategy applying a more physical and theoretical approach. The control strategy of the Marstal plant is comparable with the Zunft-approach due to the fact that the meteorological conditions are included in the control strategy, but with a more solar-theoretical approach.

Note: Others have presented the control strategy of Marstal and experiences hereof before, e.g. (Jensen, N. A., 2000). In the current work, a more theoretical approach is adopted to evaluate the control strategy. The method applied is to utilise simulation in the computer program TRNSYS with the model developed in the chapters above. By simulation, an ideal variable flow control strategy is examined which is very difficult to obtain in real-world experiments. Hereby we get an idea of the idealised performance with a temperature back from the collector field. Based on the findings from the ideal control we are able to evaluate the performance of the variable flow-control-implementation at Marstal plant. Most CSHP's before Marstal apply constant flow control. The two main control-strategies are examined and compared with regard to solar production and other key-findings. The section is then finalised by the discussion of some alternative flow-control-strategies for the solar collector loop.

8.1.1 Measured performance at the Marstal plant

Before making any analysis based on simulations and giving the reader an insight to the real response at the Marstal plant, some findings from (Heller, A. and Dahm, J., 1999) and (Heller, A., 1998) are repeated here and set into perspective from the viewpoint of the current work.

The temperature control is examined on a day with strong solar irradiation. In Figure 84, we find the meteorological conditions for the analysed day. Note that the solar irradiation is measured in the collector plane which is 40° tilt from horizontal.

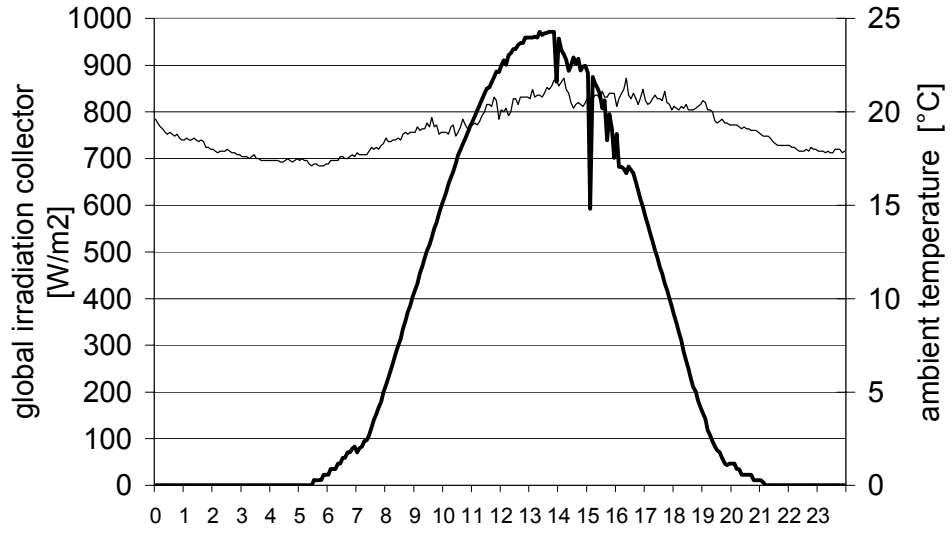

Figure 84. Measured ambient temperature, solar irradiance for the Marstal plant on 23 July 1997.

We find from Figure 84 that solar irradiation is observed on the collector plane from approx. 05:00 to 21:30. The irradiance is below 100 W/m^2 until approx. 08:00. There are two drops in solar irradiation around 14:00 and 15:00.

The resulting flow and utilised solar power in the secondary (tank side) loops (top plot), as well as the corresponding temperatures into and out of the collector row (bottom plot) are shown in Figure 85.

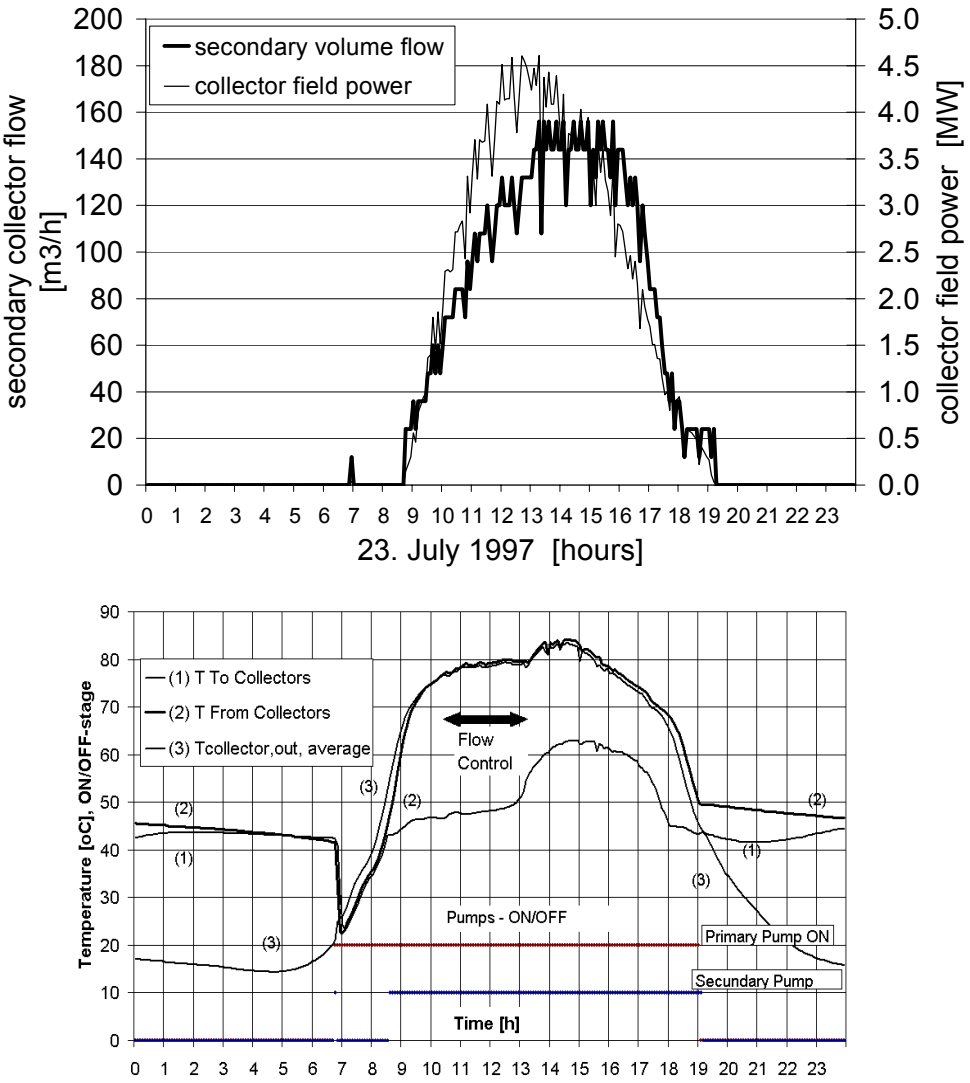

Figure 85. Measured flow rates and corresponding temperatures for the Marstal plant on 23 July 1997.

In the bottom plot (1) is the temperature in the fluid to the collector field, (2) the temperature back from the collector field and (3) the average temperature out of the collector rows. The pump activities can be seen at the bottom of the same figure. The primary (Primary Pump ON) and the secondary (Secondary Pump ON) are plotted by dots. If the values are 0 the pump is off, if the value is higher than 0 the pump is on.

Note: All time specifications are approximate.

From Figure 85 we observe:

- From the plots we find that the primary and the secondary pumps start at 06:50. The secondary pump stops right after again. This was an unnecessary start-up at the secondary pump which should be avoided.
- A start-up based on a threshold of 100 W/m^2 would start the primary pump at 08:00 and therefore delay the preheating period by approximately one hour.
- The secondary side starts up again around 08:30, approx. 1½ hours after the primary side.
- The flow rates are increased rapidly until 12:00, at which point the maximum flow rate is reached. Then the control is kept up for a while and lowered from approx. 14:00.

Focussing on the temperature development when the primary pump is running we find:

- From 07:00, the temperature out of the collectors rises rapidly.
- The temperature back from the collector field is increased till the set temperature is reached at approx. 11:00 and then kept constantly until 15:00.
- After this point, the pump runs at maximum speed. Hence, the temperature cannot be kept at the set point due to strong solar irradiation. Simultaneously, the cold side temperature is also increased. This is due to the fact that the lower part of the tank is heated up.
- In the late afternoon, the temperature decreases slowly. The control strategy tries to adjust the flow rate, but does not succeed perfectly.
- The minimum flow rate for the primary pump is reached at 18:00.
- At 19:00, the primary pump stops, followed by the secondary pump shortly after.

We can conclude from the above observations that the plant is starting and closing down efficiently, with a single irrelevant start-up in the morning. This could partly be avoided by placing the temperature sensors for the control strategy to and from the field, outside the control building.

The above temperature plot demonstrates that the control algorithm is able to keep the return temperature from the field within 2 K which is seen as very accurate. For days with stronger solar fluctuations the control and responses are more complicated than shown here. E.g. the startup and close down conditions are observed during the daytime, resulting in fluctuating outlet temperatures. For simplification reasons, these periods are excluded from the analysis.

8.1.2 The simulation analysis

For the current analysis, a TRNSYS-component, here called TYPE 210, is designed by the author. The component is able to compute the flow rate for the solar collector loop for a number of different control strategies. Although the component includes the flow control of the secondary side, the focus is here put on the primary side, the collector loop control. The strategy can be chosen by two parameters representing the modes of the control strategies:

1) The S-Mode controlling the start-up conditions.
2) The F-Mode, controlling the flow control algorithm.

The following modes are implemented:

Parameter Name	Mode	Description
S-Mode	1	A threshold start-up of the primary side. E.g. if the solar irradiation is above 100 W/m^2 then run (ON) else stop, no flow (OFF). This mode is applied in most existing CSHP's.
	2	The Marstal control start-up, as described below.
F-Mode	1	ON-OFF flow control, where the flow rate is always set to maximum flow rate when running.
	2	The Marstal flow control, as described below.
	3	An experimental variation of F-Mode 2. Applied for the below experiments with alternative control strategies.
	4	The ideal flow control strategy where the flow is adjusted until the outlet temperature is obtained. The algorithm is described below.

Another component was missing in the TRNSYS standard component library for the control model of the Marstal plant. Here the standard-component TYPE 11, a flow diverter and flow mixer mode, is extended by renaming it to TYPE 111 and adding a Mode 11. A very simple algorithm is applied to decide the split of the inlet flow into two outlet flows that are controlled by an input parameter defining the flow through outlet 1. If the inlet mass flow is above the desired outlet through port 1, then the rest is directed out of port 2. If the flow is less than the desired flow rate, the whole inlet flow is put through port 1.

Note: The source code for the two non-standard components are to be found in the Appendices.

For the following analysis we apply weather data from the DRY reference year. We find a solar irradiation on a horizontal plane for June in Figure 86.

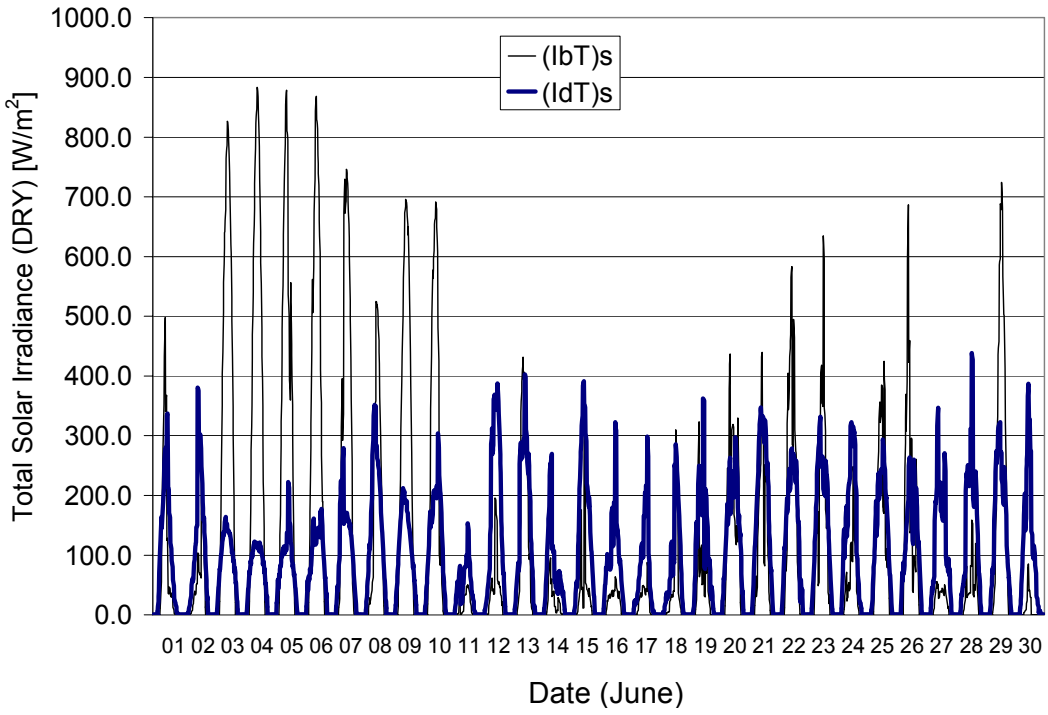

Figure 86. Beam, (IbT)s, and diffuse, (IdT)s, solar irradiation on tilt collector plane with regard to shading by applying the Danish meteorological data set DRY for June.

We find from Figure 86 that June consists of a first period with steady, strong solar irradiance and a second period with fluctuating solar irradiation. Hereby June includes most of the conditions that can be observed during the summer period for any solar installation.

Before going into detail with the simulation of different control strategy the assumptions of the below case must be specified. The case includes a minimum and maximum flow rate for the flow control with continuous control between. If start-up conditions are met, the pump is started up at a minimum flow rate. The flow rate is then controlled by the algorithm that is applied for the given examination. At the turndown of the solar loop, the flow is reduced to the minimum, kept there until the conditions for running the primary loop is not met anymore. Then the pump is stopped. For the current examinations, the maximum flow rate is at 180 m^3/h and the minimum at 22 m^3/h, a turndown ratio of approx. 8, similar to the Marstal case. The set point temperature for the examinations is 82 °C.

The secondary loop is controlled independently, based on the temperature difference between hot fluid temperature back from the collector field and the tank bottom temperature, plus the demand that the primary loop must be running. In the computer model, the control algorithm of

the secondary side (at the tank and DH-side) is more complex than demanded in the real-world plants. This is due to the fact that there is no pressure control of the system and therefore the model is to control situations that will be controlled by nature in real systems. E.g. the algorithm must differentiate for the case with tank bottom temperatures that are lower or higher than the net return temperature. If this is not taken into consideration, the control will result in negative values for the solar production.

8.1.3 Ideal variable flow control strategy

As we find above, one of the objectives for the application of variable flow is to obtain an outlet temperature from the collector field with constant set point temperature. In the simulation, it is possible to find the mass flow rate that is adjusted to obtain the exact set point temperature from the following equation:

$$\dot{M}_p = \frac{P_c}{c_p\left(T_{c,out} - T_{c,in}\right)} \tag{10}$$

where $M_{p,dot}$ is the mass flow rate in the primary collector loop in kg/s,
P_c actual collector field power in W,
c_p specific heat capacity of the fluid medium in kJ/(kg K),
$T_{c,in}$ cold inlet temperature to the collector loop in °C,
$T_{c,out}$ warmed outlet temperature from the collector loop in °C.

By assuming the outlet temperature to reach the set point temperature, we find from (10) the necessary mass-flow rate to obtain the goal. The TRNSYS-program itself controls the necessary iterative process of finding the outlet temperature and the corresponding flow rate.

Applying the resulting flow control in the simulations we find a temperature to and back from the collector field as shown in Figure 87.

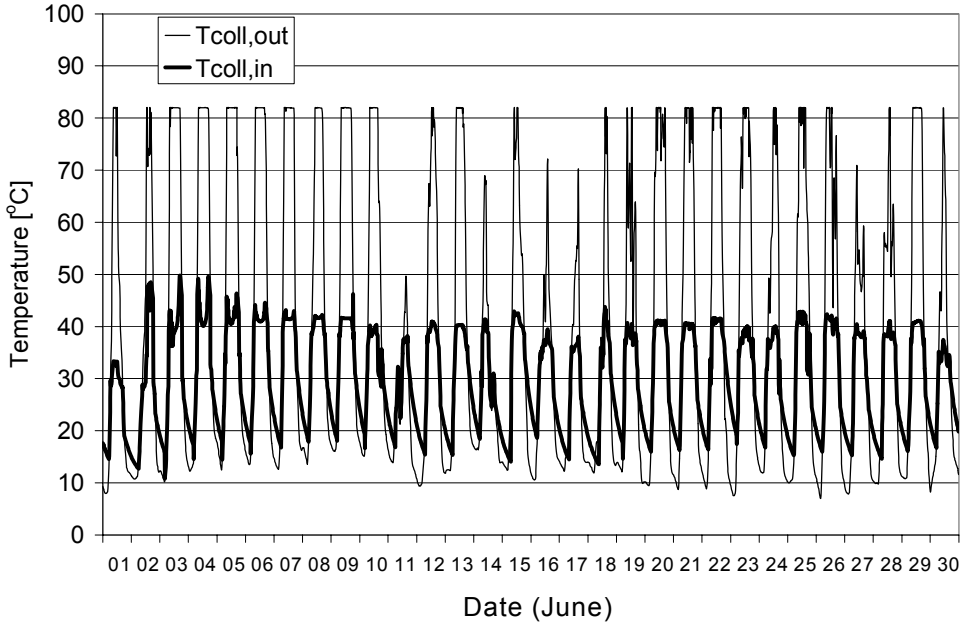

Figure 87. Cold fluid temperature to the collector field, Tcoll,in, and hot temperature back from the field, Tcoll,out, in degrees Celsius for June in the Danish meteorological data set DRY for the ideal, variable flow control strategy.

It gets clear from Figure 87 that the return temperature of the ideal flow control strategy is kept to the set point temperature of 82 degrees Celsius. Due to the cold tank temperature, there is no observation of temperatures above the set point.

Note that the span for the control is large enough to even meet the set point temperature for very low solar irradiance values, e.g. the 20 to the 25 June. For a few days, the control is not able to meet the set point temperature, e.g. the 11, 14, 16 and 17 June. As we find from Figure 88, the pump is reaching its minimum flow rate for these cases.

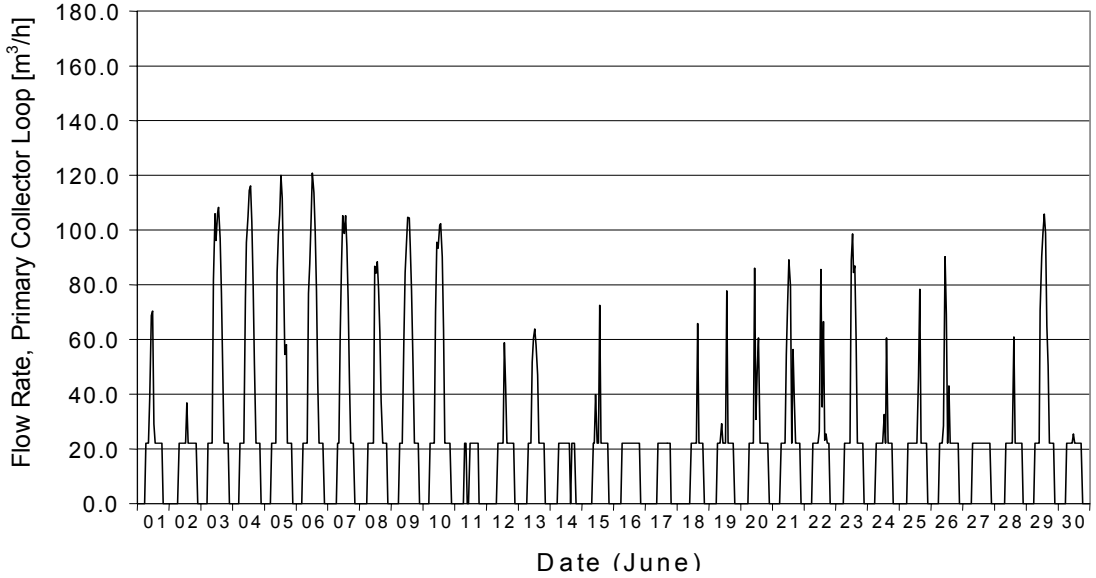

Figure 88. Volume flow rates in the primary loop in m^3/h, leading to the temperatures in Figure 87 for June in the Danish meteorological data set DRY.

Furthermore, we find from Figure 88 that the flow rate in general is rather low in relation to the maximum flow rate of 180 m^3/h. This should be kept in mind for later discussions.

The solar production, given in net solar gain, is presented in Figure 89.

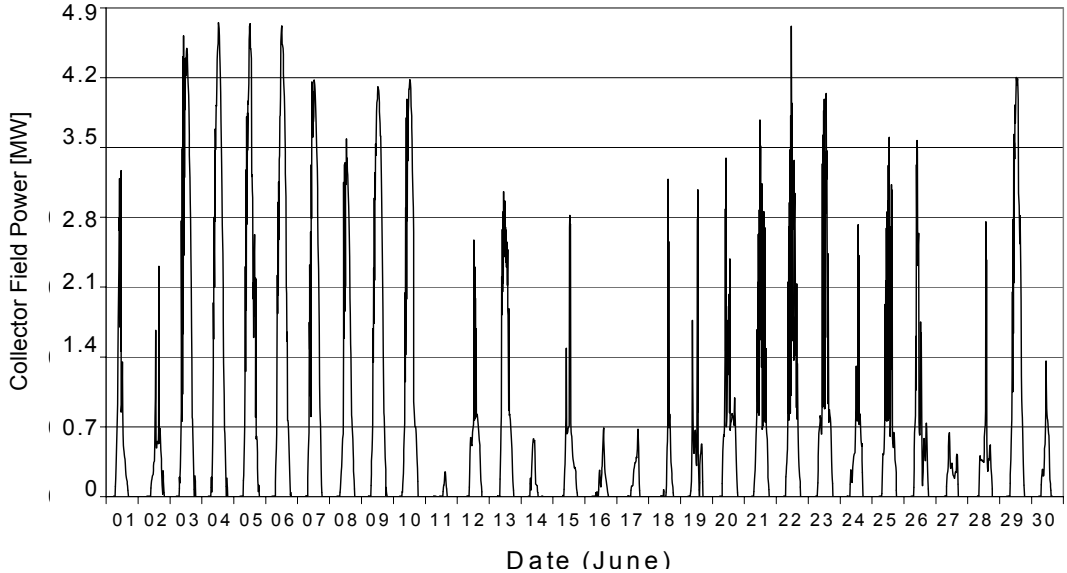

Figure 89. Outlet power for the collector field in MW for the corresponding period and conditions as in Figure 87 for June in the Danish meteorological data set DRY.

We find from Figure 89 that the power is fluctuating strongly. We find that for e.g. on the 11 and 16 June the production is close to zero, even though the pump runs during the whole day. Here an intelligent control would be able to see that this day will be very poor in solar irradiance and stop the pumping completely. This is on the other hand very difficult to be implemented in automatic algorithms and possibly needs weather forecasting methods.

The top, bottom and average storage temperatures during the year for the idealised, variable flow-control strategy are plotted in Figure 90.

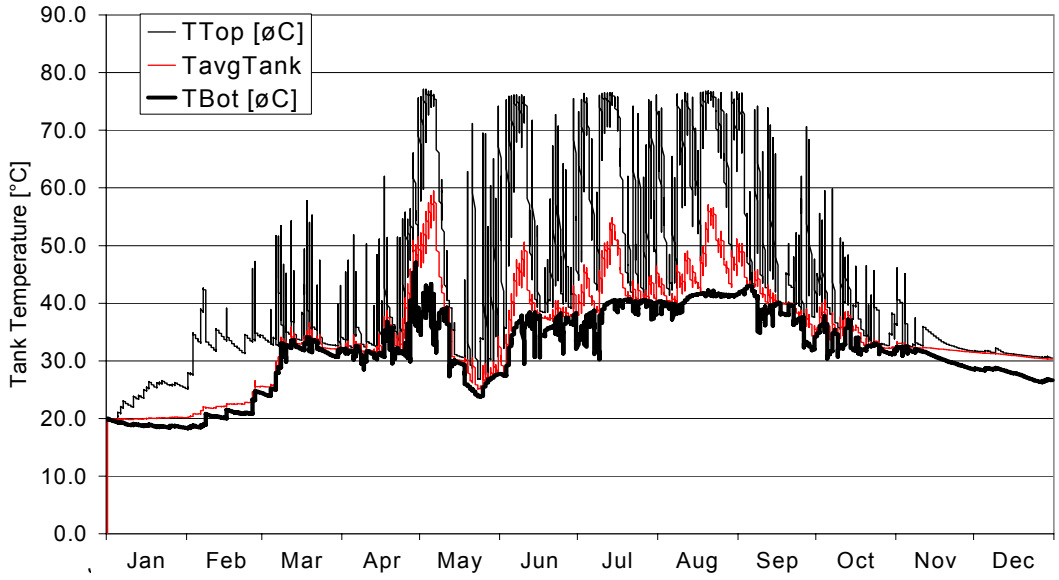

Figure 90. Tank top, bottom and average storage temperatures during the year with an ideal, variable control strategy in degrees Celsius for June in the Danish meteorological data set DRY.

We see from Figure 90 that the tank is loaded at the top of the storage, leading to very high temperatures at the top of the tank. Hereby the tank is strongly stratified which is good for the efficiency of the storage. We find that the tank temperature is kept above the necessary supply temperature in the district heating of 72°C.

We find from the at times strongly decreasing temperatures at the top of the tank that the tank is emptied within a very short period. This is the case for diurnal storage capacities. From the figure, we find no overheating of the tank by the given conditions. The bottom tank temperatures are around 25 degrees Celsius in winter and close to 40 in summer. This is very similar to the findings in Marstal. A rather high temperature rise of the tank bottom is found in end April and start May, showing that the tank is close to be filled up.

8.1.4 Variable flow control strategy – Marstal versus ideal

In this section the findings from the ideal variable control-strategy is compared to the findings with the computer-implemented control strategy of the Marstal version. This implementation is a little different from the real implementation found in Marstal. The secondary start-up condition on the primary side - that the highest measured outlet temperature from the collector field must be 8-10 degrees above the tank bottom temperature – is not implemented due to lack of knowledge of the heat transport from the collector to the temperature sensors at the outlet of the collector modules, when the plant is not running. This is not seen as a severe error due to the low impact of the start-up on the overall results. The secondary side is, as mentioned in the introduction to the current section, represented by a more complex control model which may introduce minor deviations from the real plant behaviour.

For a repetition, the estimated efficiency, η_e, for the collector field under operation is given by the expression

$$\eta_e = \eta_0 - k_1 \frac{\Delta T}{G} - k_2 \frac{\Delta T^2}{G} \tag{11}$$

where G global irradiance, W/m^2
η_0 start efficiency
k_1 heat loss coefficient, linear part of efficiency expression, W/(m² K)
k_2 heat loss coefficient, quadratic part of efficiency expression, W/(m² K^2).

The temperature difference is found by $\Delta T = \frac{T_{set} + T_{coll,in}}{2} - T_a$ involving the demanded set point temperature, T_{set}, the measured temperature to the collector, $T_{coll,in}$, and the ambient temperature, T_a. The resulting estimated efficiency, η_e, is then inserted into the expression for the estimation of the flow rate, $\dot{M}$, in m^3/s.

$$\dot{M} = \frac{\eta_e \cdot G \cdot A}{c_p \left(T_{set'} - T_{coll,i}\right)} \tag{12}$$

where η_e is the estimated efficiency for the collector field,
G global irradiance, W/m^2,
c_p the specific heat capacity of the fluid in the collector loop, kJ/(kg K)
$T_{set'}$ real applied set point temperature described in the text below, °C,
$T_{coll,in}$ inlet temperature to the collector loop, °C.

The set point temperature, T_{set}, from the documented expression is according to the description of the interface[10] in Marstal found by the expression $T_{set'} = G \cdot X + SP_{\min}$, where X is an adjustable value, in Marstal set to X=0.05. SP_{min}, given in °C, is the minimum temperature that should be obtained by the control strategy. Not stated in this expression is the fact that the algorithm includes an upper limit for the set point temperature which in most cases is similar to the desired outlet temperature. Hereby the expression for the real set point temperature, $T_{set'}$, is now

$$T_{set'} = \min(G \cdot X + SP_{\min}, SP_{\max}) \tag{13}$$

where SP_{max} is the upper limit temperature for the control strategy in °C.

Applying the resulting flow control in the simulations we find a temperature to and back from the collector field as shown in Figure 91.

[10] $T_{set'}$ is therefore wrongly stated in the previous work by the author.

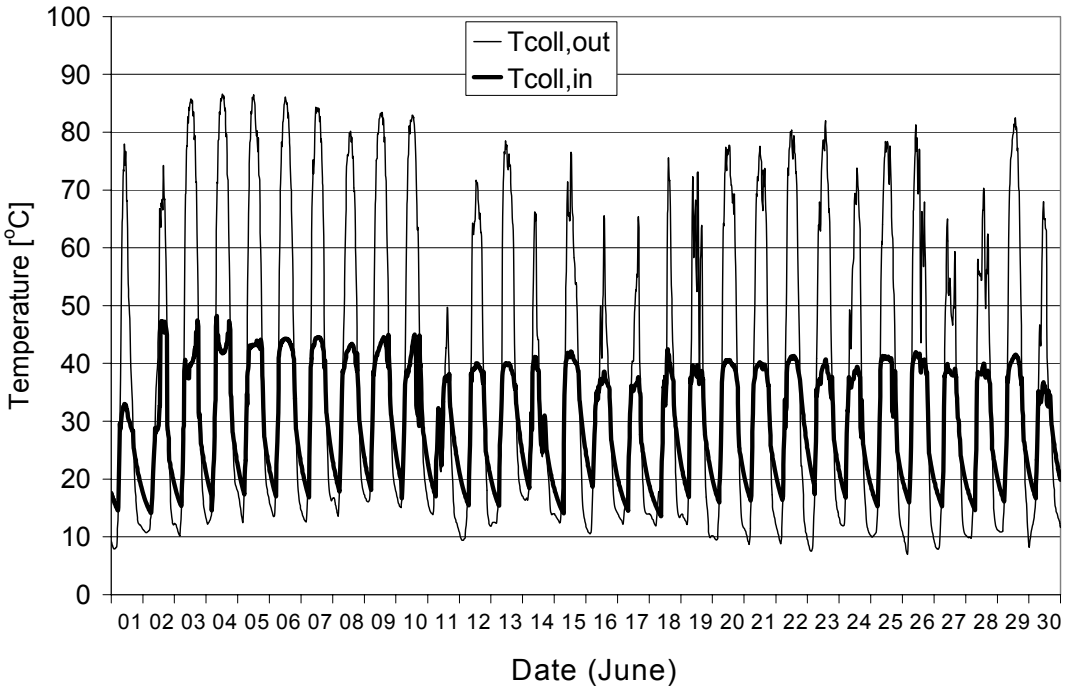

Figure 91. Cold fluid temperature to the collector field, Tcoll,in, and hot temperature back from the field, Tcoll,out, in degrees Celsius for June in the Danish meteorological data set DRY for the Marstal variant of a variable flow control strategy.

We find from the outlet temperature in Figure 91 that the set point temperature is not obtained perfectly, but the control-strategy is able to keep the outlet temperature close to the set point of 82 °C in the given case. The temperature seems, from the plotted results, to be controlled within a range of approx. 3K, whereas measurements show a range of 2K. Hence, the real plant is doing slightly better than the simulation model. However, the correspondence between the model and reality is reasonable for further analysis.

For periods with rather fluctuating and low solar irradiation, e.g. 20 to 25 June, the outlet temperature of the solar field is rather high by controlling the flow rate to a low value as shown in Figure 92.

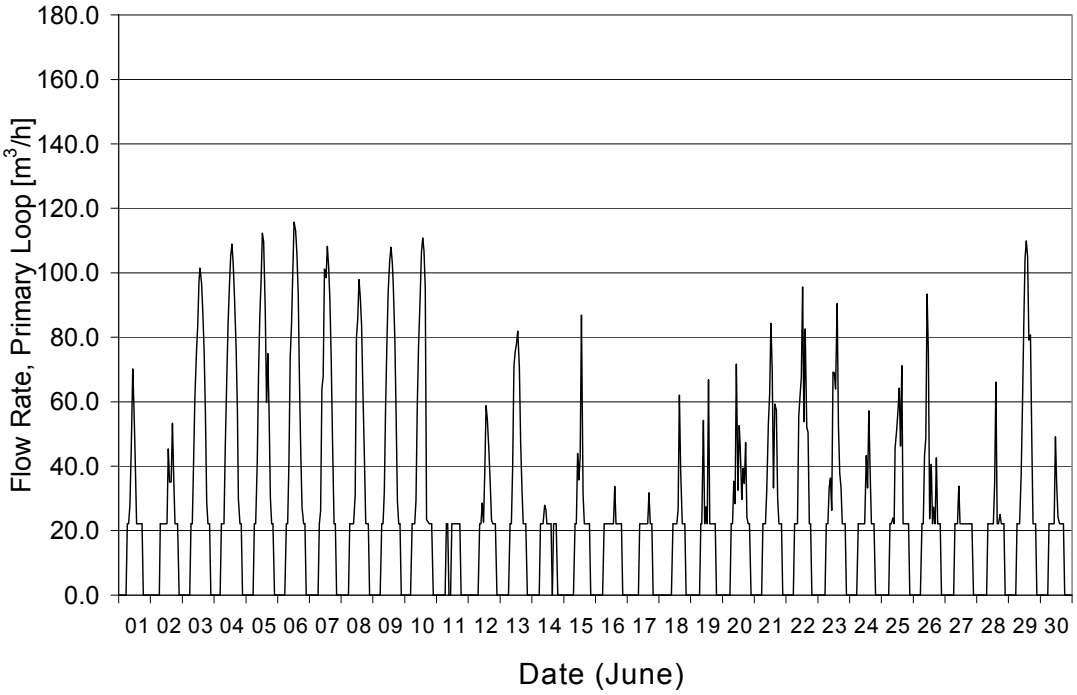

Figure 92. Volume flow rates in the primary loop in m^3/h, leading to the temperatures in Figure 91 for June in the Danish meteorological data set DRY.

Comparing Figure 92 with the ideal counterpart in Figure 88 we find small differences only. The speed of flow adjustments is slightly slower and the maximum obtained flow rate is consequently lower.

We also find from Figure 92 that the flow rate in general are kept rather low to obtain the necessary outlet temperature of 82 degrees Celsius. Measurements from the real plant show flow rates that are typically between 100 and 120 m^3/h for summer conditions. Comparing with the findings in the first part of the figure (3 to 10 June), there is an acceptable good agreement between measured and computed flow rates.

Finding a flow rate of typically 100-120 m^3/h, the question is raised, if the dimensioning of the pumps should be reconsidered. The minimum flow rate determines how fast the algorithm is able to rise the temperature to the set point. The maximum flow rate sets the limit for keeping the temperature down to the set point. As we find, in this case, the control is able to keep the set point temperature with even very low flow rates. Hence, the pump control and pump size can be optimised from case to case on such considerations.

The corresponding net solar production for June is given is presented in Figure 93.

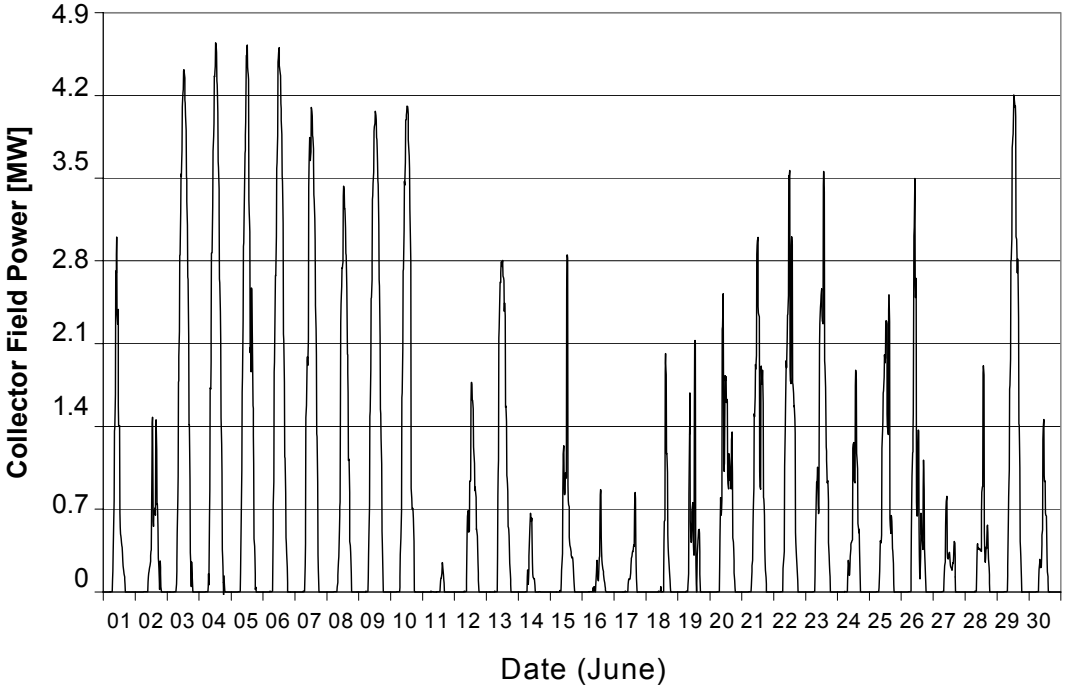

Figure 93. Outlet power for the collector field in MW for the corresponding period and conditions as in Figure 86 for June in the Danish meteorological data set DRY.

Comparing Figure 93 with Figure 89, we find that the production in Marstal is very similar to the one with the ideal control strategy. The main deviations especially occur for the days with strongly fluctuating solar irradiation, e.g. in the latter half of June. However, generally, the findings from the ideal control are also valid for the Marstal implementation.

In the tables below, we will find some major key-values for the Marstal variable flow control compared to the values from the ideal case. Positive values show that the ideal, variable flow control strategy leads to higher values than the implementation in Marstal.

Table 22. Key values for the heat output of the collector field with the Marstal control strategy during June, Danish DRY, compared to the findings for the ideal variable flow-strategy above.

Note label "Diff. to Ideal" is applied for the difference between Marstal compared to the ideal, variable flow control strategy.

Description	Observation	Diff. to Ideal	Unit
Hourly peak solar production of the collector field with no losses in piping and heat exchanger.	4.2	0	MW
Output from solar collector field during the period in total.	470	-5	MWh

For the whole year we find the key values as presented in Table 23.

Table 23. Annual key values for the solar production and the necessary auxiliary heat source for the Marstal control strategy, compared to the findings for the ideal variable flow control strategy.

Note label "Diff. to Ideal" is applied for the difference between Marstal and to the ideal strategy.

Description	Observation	Diff. to Ideal	Unit
Number of hours during the year with no auxiliary demand.	244	+7	-
.. with auxiliary heating demand under 0.5 MW.	2082	-79	-
.. with auxiliary heating demand under 1 MW.	3086	-12	-
Sum of auxiliary demand.	24120	-270	MWh
Auxiliary share on total heat demand of 27000 MWh (AF).	88.6	-1	%
Solar Collector Production.	3176	+273	MWh
Solar direct to district heating with no storage (storage-bypass).	1662	+89	MWh
Tank-bypass in % of total load.	6.1	+0.3	%
Net solar gain.	3093	+271	MWh
Annual net solar gain per collector area.	344	+31	kWh/m^2
Solar Fraction (SF).	11.4	+1	%

From Table 23 we find that the solar production for the Marstal implementation is 9% higher from the ideal control strategy. This is seen as a rather good result. From Table 24 and Table 25 we find the details for this deviation showing no surprising results. In short, the result is that the imperfection of the strategy leads to increased solar gain and to a decreasing auxiliary demand for low power.

Analysing the utilisation of the storage tank, we find from the simulation for the Marstal variable flow strategy the key values as shown in Table 24.

Table 24. Annual key values for the storage tank utilisation for the Marstal control strategy, compared to the findings for the ideal variable flow-control-strategy.

Note label "Diff. to Ideal" is applied for the difference between Marstal and to the ideal strategy.

Description	Observation	Diff. to Udeal	Unit
Number of hours with temperatures above the set point temperature.	118	+118	-
Number of hours with injection through top inlet arrangement.	805	-45	-
Total upload to the top of the tank.	1220	-231	MWh
Number of hours with injection through the middle inlet of the tank.	402	327	-

Total upload to the "middle" of the tank.	292	+177	MWh
Total output from tank to district heating.	1431	-53	MWh
Heat loss from tank.	50	0	MWh
Heat loss from tank.	3.1	0	%
Tank to district heating in % of total load.	5.3	-0.2	%

As to be expected the number of observed hours with temperature above the set point value, compared to the ideal case, is increased due to imperfection. The load to the top of the tank is decreased, leading to more flow in the lower part of the tank further accentuated due to the fact that the total stored energy is increased. This is due to more observations with low temperatures back from the collector field. In total the tank volume is used for more storing but with less stratified content as shown in Figure 94.

The top, bottom and average storage temperatures during the year are plotted in Figure 94.

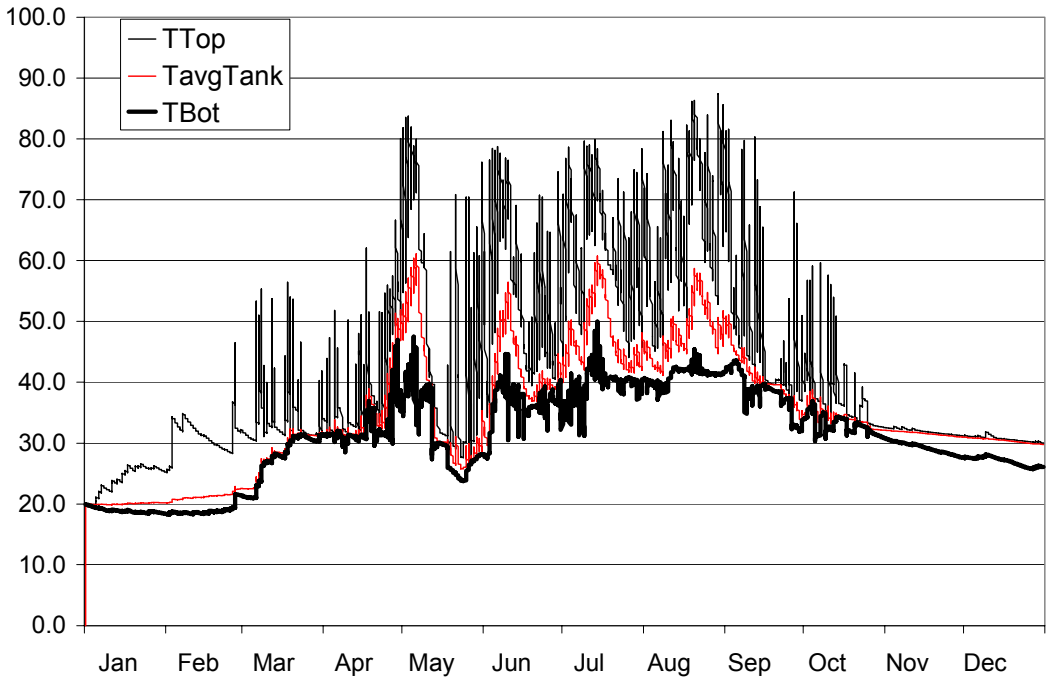

Figure 94. Tank top, bottom and average storage temperatures during the year with an Marstal variable flow control strategy in degrees Celsius for June in the Danish meteorological data set DRY.

We find that by comparing the temperature curves for the top, bottom and average tank temperature in Figure 94 with the plots from Figure 90, the top temperature of the tank is lowered for some periods. This is due to the less perfect temperature control. However, the result is still a very well stratified storage content.

All in all, we can conclude from the above comparison of the Marstal and the ideal, variable flow control strategies that the Marstal implementation is reaching close to a theoretically, ideal solution. As the range for fluctuation in the Marstal plant is measured to around ±2 K, the model controls the temperature in a range of ±3 K. With this, the model is in good agreement with the measured values, and from this point of view, it can be accepted for further analysis.

8.1.5 Constant versus variable flow control strategy

Most existing CSHPs and other solar thermal plants are controlled by very simple means. The pump on the primary side is controlled by a threshold value for the start-up and full-power operation for the pumps. Hereby the flow is constant in the primary and secondary loops. For this control strategy and the boundary conditions as described in Figure 86 we find the following results by simulation. The results are compared with the findings from the variable flow-control- strategy in combined plots.

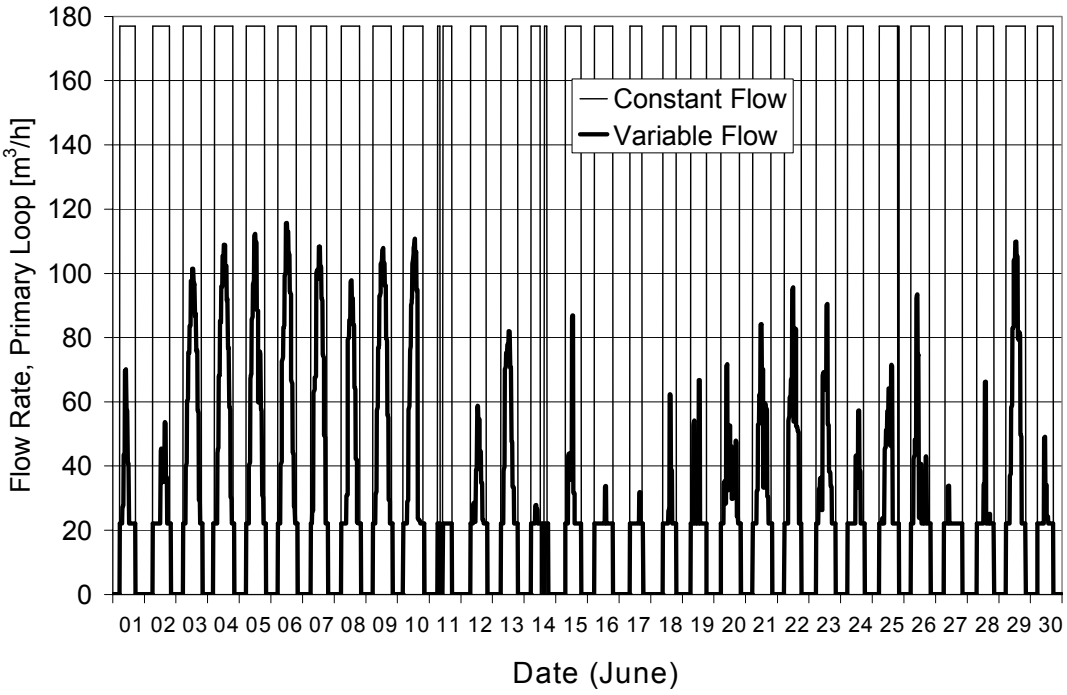

Figure 95. Comparison of the flow rate for the variable contra the constant flow control in the solar collector loop for June in the Danish DRY meteorological data set.

Comparing the resulting temperatures from the two control strategies, we find the cold flow temperature to the collector field as shown in Figure 96 and the resulting hot fluid temperature back from the field as compared in Figure 97.

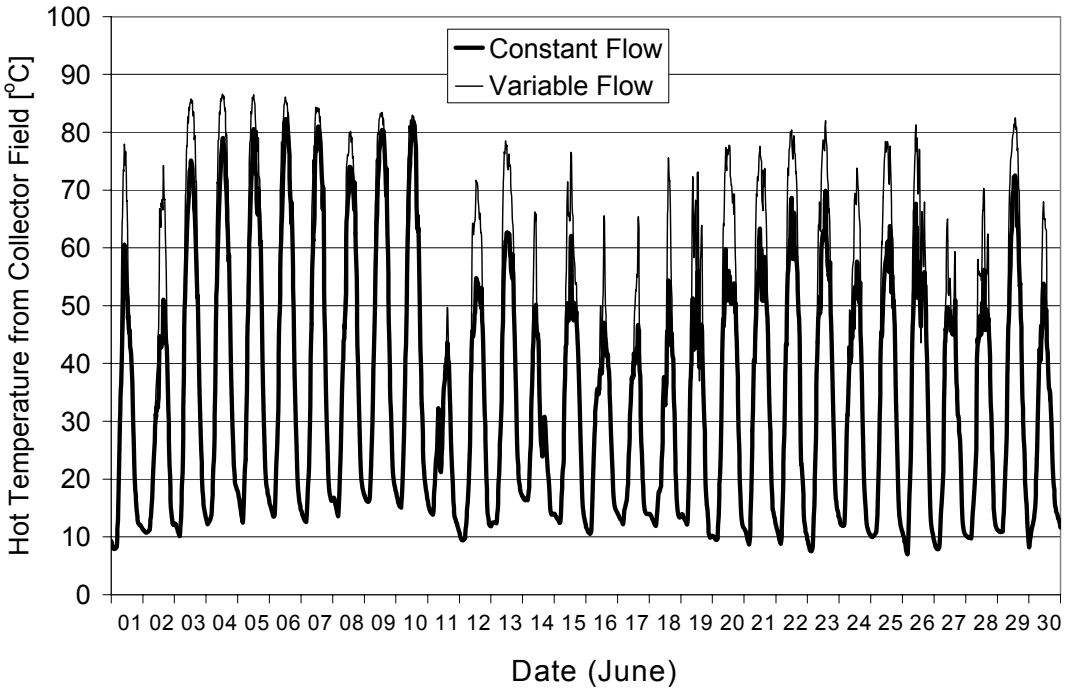

Figure 96. Comparison of the outlet temperature for the variable contra the constant flow control in the solar collector loop for June in the Danish DRY meteorological data set.

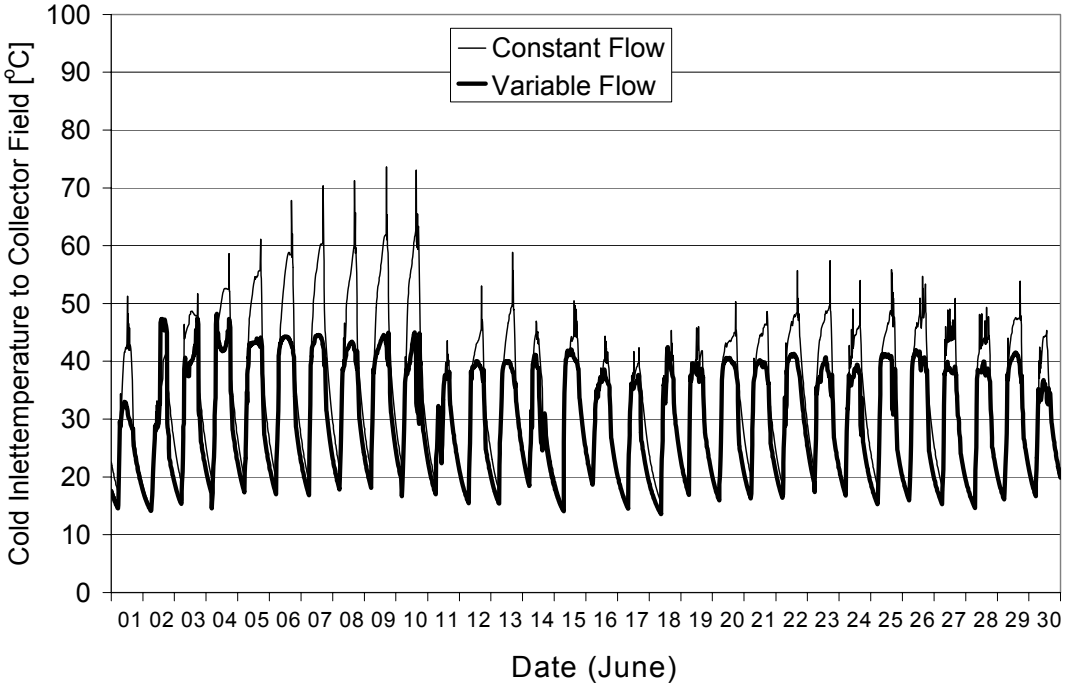

Figure 97. Comparison of the inlet temperature for the variable contra the constant flow control in the solar collector loop for June in the Danish DRY meteorological data set.

As expected the hot back temperature for the variable flow-control-strategy is higher than for the constant flow control, except for the 11 June. More relevant to be mentioned is the fact that

the cold temperature to the collector field is strongly influenced by the flow control. Here we find that for the variable flow the cold temperature is kept low, around 40 degrees. For the constant flow-control, the temperature increases during the whole period much above this value. This is due to a number of reasons, mainly the influence of the tank bottom temperature. Due to higher flow rates for the constant flow control, the tank volume is changed faster, leading to increased mixing and hereby higher tank temperature at the bottom. Hence, the temperature to the collector field is increased. This is certainly a drawback for the constant flow variant. The finding is substantiated in the key-values below, after having a look at the results in energy terms.

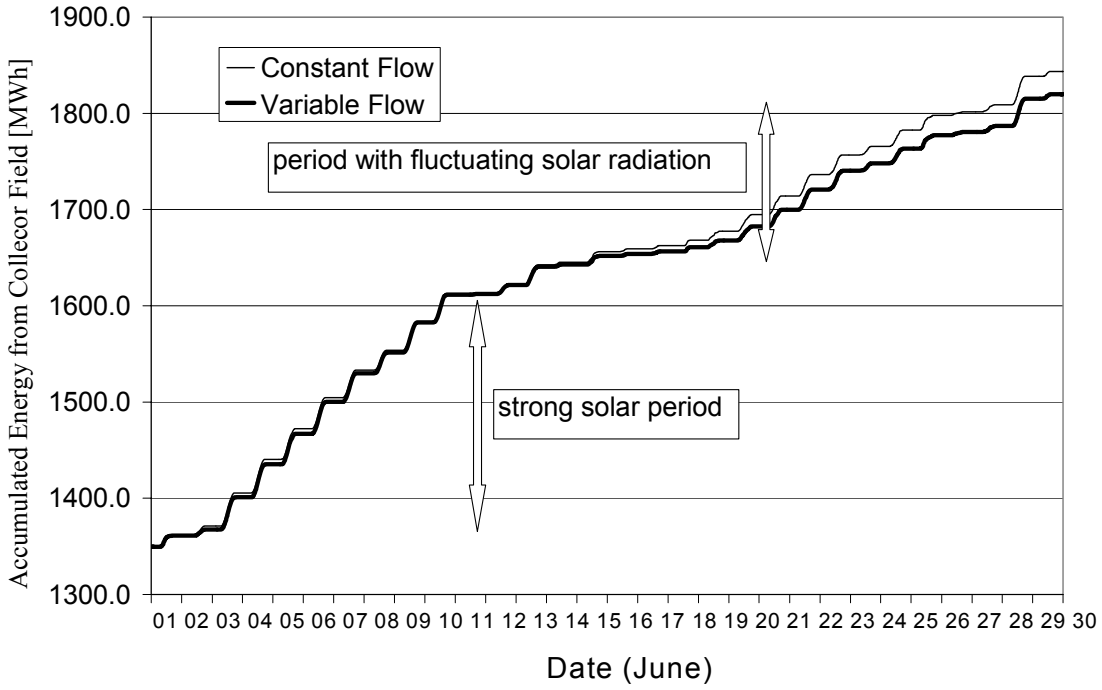

Figure 98. Comparisons of the accumulated solar-effect from the collector field for the variable contra the constant flow-control in the solar collector loop for June in the Danish DRY meteorological data set. In order to get the two curves to start at the same level, the constant flow graph is adjusted to the starting value of the variable flow, namely approx. 1350 MWh.

We find from Figure 98 that the solar gain for the constant flow control is higher. The difference comes mainly from the period with strong fluctuating solar irradiance. Note that the solar gain is double for the first half of June.

We found above that the tank volume is utilised less efficiently. However, the total solar gain for the constant flow is increased due to better efficiency in the collector loop. Hence, the increased solar gain is stronger than the drawbacks in tank utilisation.

Key-values for the constant flow-control-strategy are shown in the tables below and compared to the values from the variable flow control.

Table 25. Key values for the heat output of the collector field for the constant compared with the variable flow-control-strategy during June.

Note label "Diff. to var." is applied for the difference between the constant and the variable flow control strategies.

Description	Observation	Diff. to var.	Unit
Hourly peak solar production of the collector field with no losses in piping and heat exchanger.	4.2	0	MW
Output from solar collector field during the period in total.	494	+24	MWh

For the whole year we find the key values as presented in Table 26.

Table 26. Annual key-values for the solar production and the necessary auxiliary heat-source for the constant flow-control-strategy.

Note label "Diff. to var." is applied for the difference between the constant and the variable flow control strategies.

Description	Observation	Diff. to var.	Unit
Number of hours during the year with no auxiliary demand.	119	-125	-
.. with auxiliary heating demand under 0.5 MW.	2227	+145	-
.. with auxiliary heating demand under 1 MW.	3206	+120	-
Sum of auxiliary demand.	23810	-310	MWh
Auxiliary share on total heat demand of 27000 MWh (AF).	87.5	-1.1	%
Solar collector field output.	3507	+331	MWh
		+9	%
Solar heat directly to district heating with no storage (storage-bypass).	1130	-532	MWh
Tank-bypass in % of total load.	4.2	-1.9	%
Net solar gain.	3398	+305	MWh
Annual net solar gain per collector area.	377	+33	kWh/m^2
(Solar Fraction (SF).	12.5	+1.1	%

We find that the constant flow strategy is increasing the total annual production from the collector field by 9% of the constant production of the collector field. In spite of the increased number of hours with demands for auxiliary heating, and the less efficient utilisation of the tank-storage, the result in solar fraction is increased by 1.1% only.

Going into more detail with the utilisation of the storage-tank, we find from the simulation for the Marstal variable flow strategy the key values as shown in Table 27.

Table 27. Annual key values for the storage tank utilisation for the constant flow-control-strategy.

Note label "Diff. to var." is applied for the difference between the constant and the variable flow control strategies.

Description	Observation	Diff. to var.	Unit
Number of hours with temperatures above the set point temperature.	208	+90	-
Number of hours with injection through top inlet arrangement.	625	-180	-
Total upload to the top of the tank.	1142	-78	MWh
Number of hours with injection through the middle inlet of the tank.	1110	+708	-
Total upload to the "middle" of the tank.	1226	+934	MWh
Total output from tank to district heating.	2265	+166	MWh
Heat loss from tank.	61	+11	MWh
Heat loss from tank in relation to the stored energy.	2.6	+0.5	%
Tank to district heating in % of total load.	8.3	+3.3	%

The number of hours where the control strategy leads to solar production at temperatures that are higher then the set point is increased. However, we find clear evidences for the postulate above that the tank storage is utilised in a less efficient manner by the constant flow control. Lower temperatures are stored for the main part of the time and therefore the inlet in the middle of the tank is used more than for the variable flow case. The stored energy is increased in total but at a lower average temperature as shown in Figure 99.

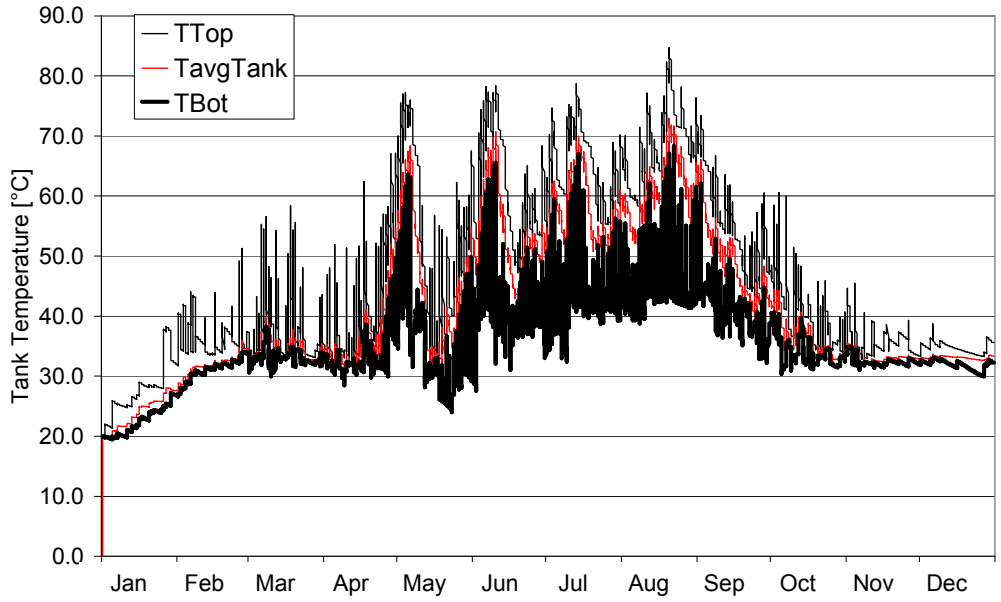

Figure 99. Tank top, bottom and average storage temperatures during the year with an ideal control strategy in degrees Celsius for June in the Danish meteorological data set DRY.

The tank stratification found in Figure 94 is mixed strongly by the constant flow rate in Figure 99, where the difference in top and bottom temperatures are lower. On the one hand, the total energy stored in the tank is increased for the constant flow variant, compared to the variable flow control. On the other hand, the "quality" of the energy is decreased due to mixing and lower temperatures back from the collector field. This is a very important finding from this comparison.

The findings can simply be visualised by the following plots with no repeated comments:

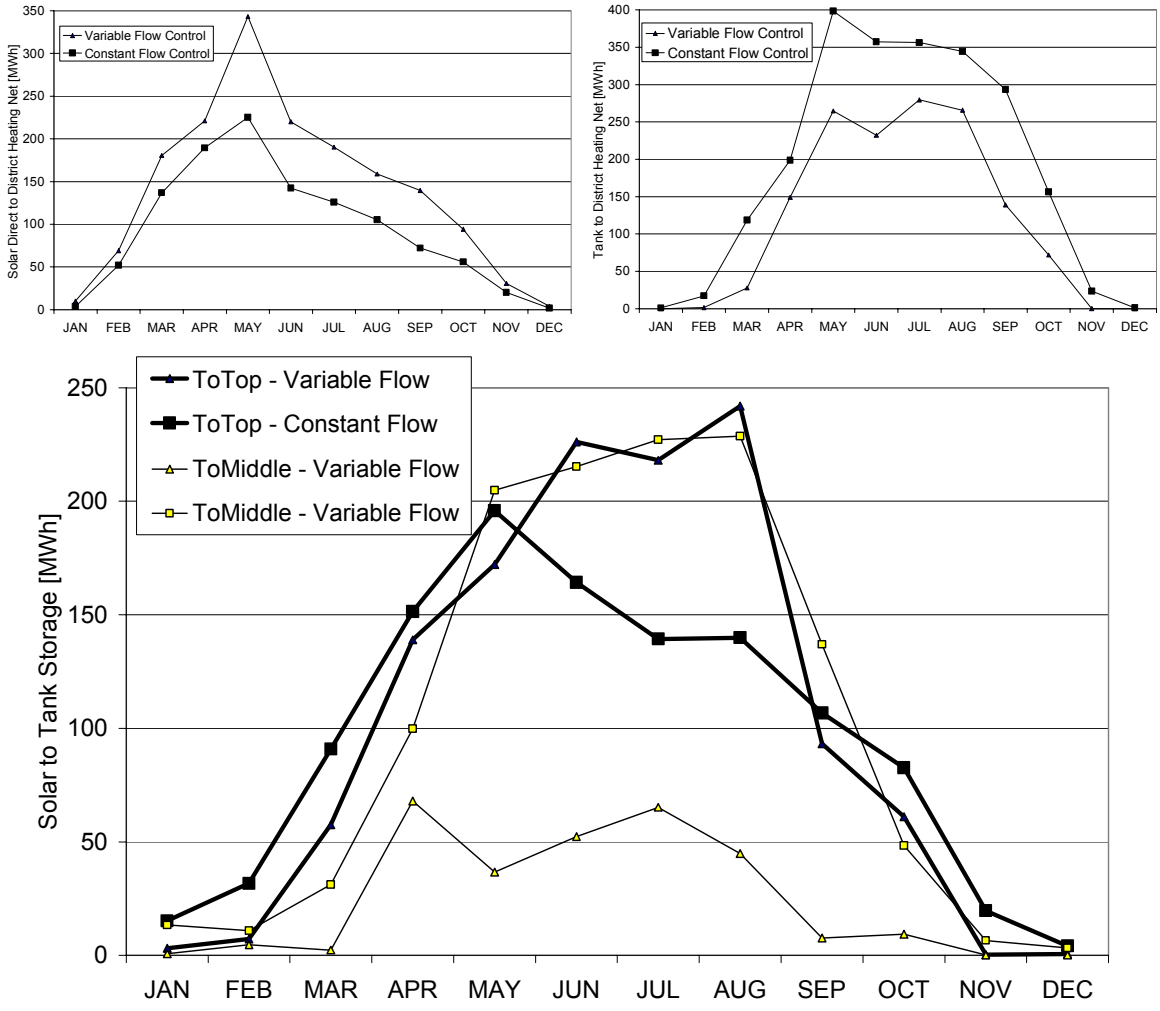

Figure 100. Monthly solar share direct to the district heating (top, left) and indirect through the storage tank (top, right). Solar to storage tank – inlet arrangement use at the top of the tank and the middle of the tank.

By simulation, Jochen Dahm, Chalmers University of Technology, Sweden, and the current author (Heller, A. and Dahm, J., 1999) found the following two figures describing the influence of the above control strategies on monthly solar fraction.

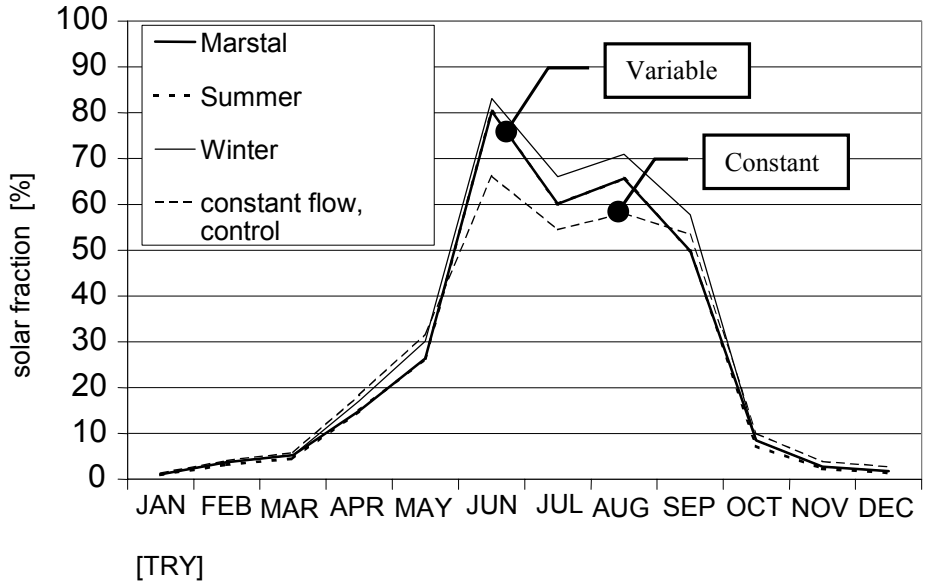

Figure 101. Monthly solar fraction for different control strategies. Note: TRY reference data set is applied. Source: (Heller, A. and Dahm, J., 1999).

The important graphs here are the "Variable" and the "Constant". We find clearly from Figure 101 that the solar-fraction for the Marstal plant is higher than for the constant flow operation. This was seen as prove of the fact that the total efficiency for the variable flow is better than for the constant flow operation, although the solar gain shows opposite tendencies. The main reasons for this finding is similar to the findings in this work, but needs further reflections on the assumptions the findings are based on as done below.

Repeating this considerations by the current simulation model, we find the corresponding plot as shown in Figure 102.

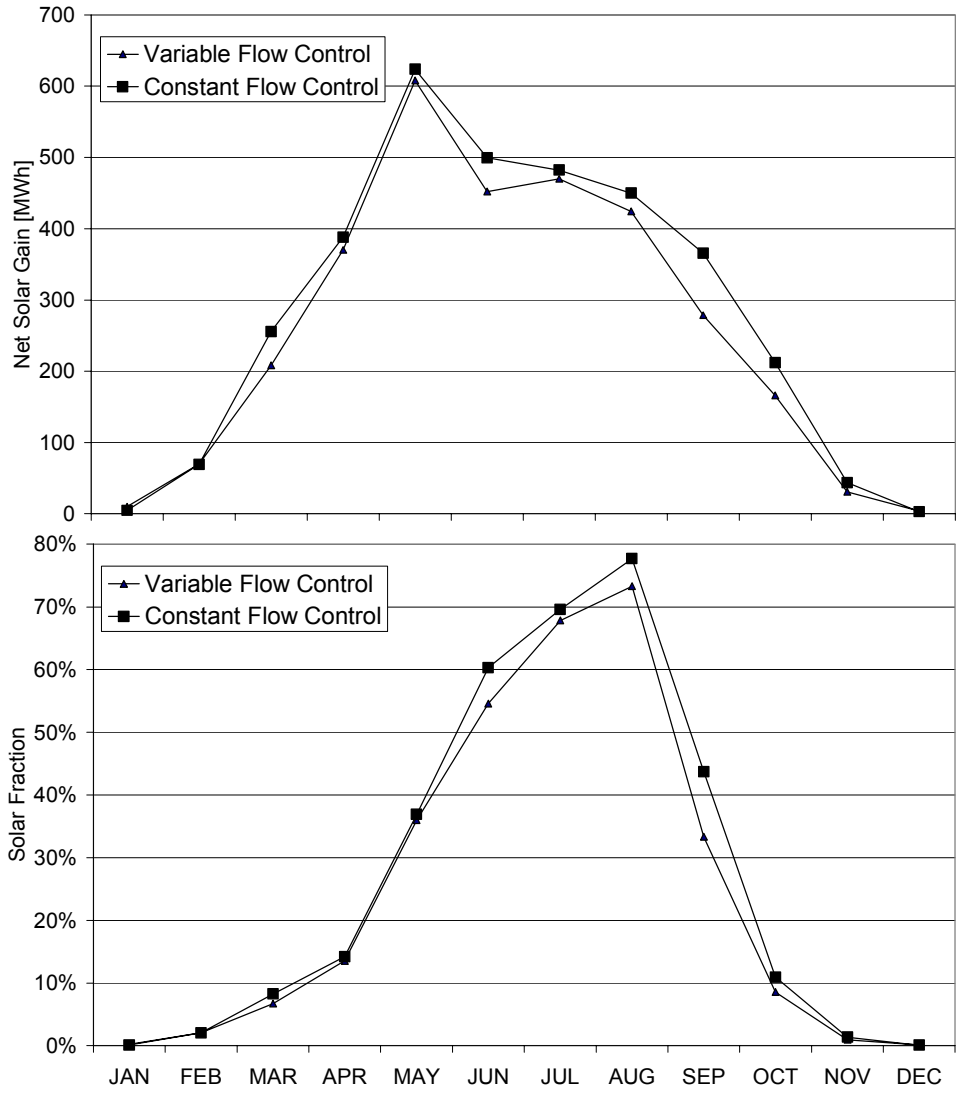

Figure 102. Monthly net solar gain (top) and solar fraction (bottom) for different control strategies. Note: TRY reference data set is applied.

As opposed to the observation in the previous work, we find from Figure 102 that both the net solar gain and the solar fraction are lower for the variable flow compared to the constant flow. The reason for the deviation between the results is mainly the assumptions on the auxiliary heater efficiency. If the efficiency is very high, the result in the current work is directly applicable. If the efficiency is low or the conditions for running the auxiliary heating is high, the findings from the first study are valid. As an example, it can be mentioned that biomass burners must run at a certain high power level and for a certain period to obtain high efficiencies. For such an auxiliary heating, the solar fraction from the variable flow-control would be superior to the results from a constant flow control. Conversely, for a very efficient gas boiler with a large range of output, the constant flow control would often be a preferable solution. However, the choice of strategy also depends on other aspects that will be discussed in the final statements in this section.

8.1.6 Alternative control strategies

Two alternative control methods, based on control theory, have already been mentioned in the introduction to this section, (Meaburn, A. and Hughes, F. M., 1993) and (Zunft, S., 1995).

At the Kungälv plant, a similar approach as for the Marstal plant is applied, (Dalenbäck, J-O., 2000). Here, instead of controlling the speed on the secondary side, a temperature-controlled valve is applied which is the same as the bypass mentioned in the introduction to the current chapter.

The control strategies with variable and constant flow controls are not excluding each other. Combinations of variable and constant flow control may in many cases be the most optimal solution. The criterion for whether one or the other strategy is applied could be to set a threshold set point for the efficiency for which the set temperature claim to the control strategy is lifted. E.g. if the solar collector field efficiency is below 0.2 the set temperature is set to a low value. Such a threshold would lead to an improvement of the annual net solar gain of a few percentages, at the expense of an increased demand for electricity. Alternatively, the pump is run at a constant speed but low rate, to save electricity for pumping.

A more complex and "exotic" alternative would be to apply a repeated on-off control strategy, where the flow in the collector field is stopped for low efficiencies, resulting in heating up half of the medium in the collector loop. Having reached a certain temperature, the collector loop could be started and the flow shifted by half the volume, then stopping again.

The Marstal control strategy can be adjusted by the following means:

The Marstal algorithm includes the quadratic term of the efficiency equation. Due to the fact that this term has a minimal impact of 0.2% on the efficiency, this term can be eliminated.

The control algorithm in Marstal compensates for the lack of knowledge of the solar gain by applying a collector efficiency expression instead. This introduces a number of uncertainties, especially in relation to the temperatures involved in leading to the objected temperature responses, but also due to the fact that the efficiency is valid for a limited range of boundary conditions. These conditions are not met for large periods of real plant operations. Hence, if an algorithm involves the efficiency for the collector field, a number of improvements can be adopted to find a more realistic efficiency estimate, to be found in basic theories for solar technology:

1. Taking the thermal capacities for the mass outside the collector field into consideration.
2. Involve a correction for the tilt angle.
3. Involve a correction factor for the incident angle.
4. Involve a correction factor for the flow rate.

For adjustment 1, different approaches can be adopted. Instead of using the temperatures at the outlet of the collector field, the temperatures at the collector rows could be used. Hereby the mass in the connecting piping being of the same range as the collector mass can be eliminated from the efficiency. Doing so, the heat loss in the piping must be taken into consideration by other means. Alternatively, simulation methods can be utilised, e.g. by finding thermal mass corrections for the heat loss coefficients of the efficiency expression. This can be done by parameter fitting methods.

For adjustments 2 - 4, the following sets of expression can be adopted:

The basic efficiency expression can be extended to include the correction for flow, incident angle and tilt angle of the collector field as follows according to the collector data sheets or e.g. (Svendsen, S., 1981):

$$\eta = c_f \left[\eta_0 \cdot c_i - k_1 \cdot c_t \frac{T_m - T_a}{G} - k_2 \cdot c_t \frac{(T_m - T_a)^2}{G} \right] \quad (14)$$

where
- η the solar collector efficiency,
- η_0 start efficiency for mean absorber temperature equal to amb. temperature,
- k_1 first order heat loss coefficient, W/(K m^2),
- k_2 second order heat loss coefficient, W/(K^2 m^2),
- G solar irradiance, W/m^2.
- T_m mean fluid temperature, °C,
- T_a ambient temperature, °C,
- c_f correction factor for flow rate,
- c_i correction factor for incident angle,
- c_t correction factor for collector tilt angle.

The factor for flow correction shows an influence on the efficiency in general. The factor for incident angle correction has an influence on the start efficiency only and the factor for collector- tilt-angle influences the heat loss terms, but not the start efficiency.

The individual correction factors can be found by linear expressions described below.

Correction for flow rate: The expression for de actual mass flow rate, M in kg/s, is:

$$c_f = m_0 + m_1 M \quad (15)$$

where m_0 and m_2 are coefficients to be found by test sequencing or simulation. Results from laboratory experiments are visualised in Figure 103.

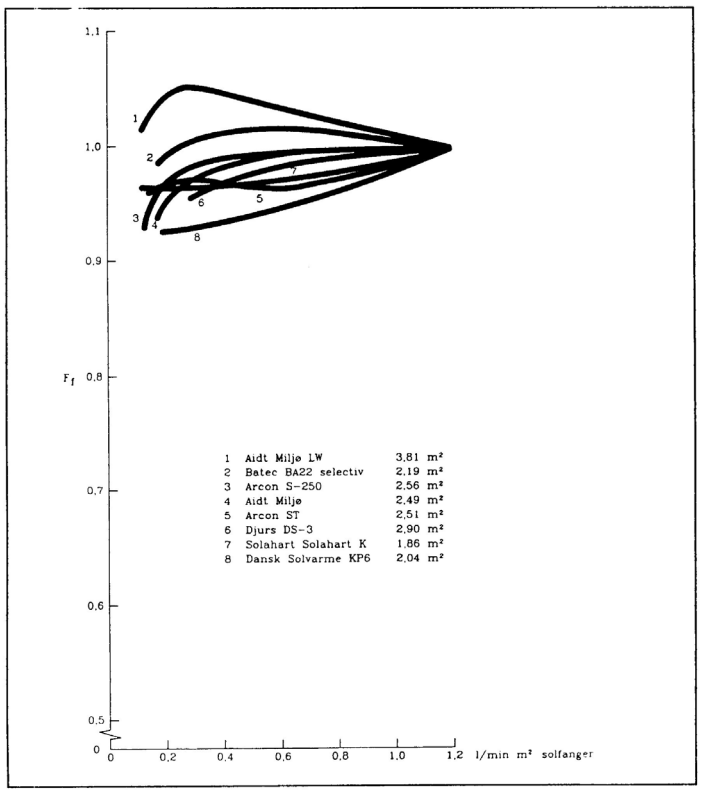

Figure 103. Correlation between mass flow rate trough solar collector and the correction factor, c_f, for the efficiency expression (14). Source: (Furbo, S., 1993).

Figure 103 shows the correlation between mass flow rate and correction factor for this influence on the collector efficiency. For test conditions with flow rates of 1.2 l/min/m^2, the correction factor is 1. We find that the correlation is not linear. However, a linear correction assumption is applied in literature. The coefficient of the correction factor expression in (15) is not known to the author for the ARCON-HT plane collector, but is known for the smaller ARCON-ST solar collector, where m_0 = 0,95 and m_1 = 0,042. These values can be applied until better values are found for the correction for the mass flow rate by testing or theoretical means.

Correction for collector tilt angle: Tests sequences are carried out with tilt angles of 45 degrees. The solar collectors in the known CSHP's are placed with tilt angles between 35 and 40 degrees. In the parameter study the optimum is found to be between 30 and 35 degrees for a row distance of 4.5 metres. Hence the findings for the test conditions must be corrected to these set up conditions by the linear correlation for the correction factor, c_t, as an expression of the tilt angle, S, in degrees from horizontal by:

$$c_t = s_0 + s_1 S \tag{16}$$

where the coefficients s_0 and s_2 are found by testing or by theoretical means. By testing, the coefficients for the ARCON SCAN-CON-ST collector are found to s_0 = 1,127 and s_2 = -0,0028. Certainly, the application of the ST-values for the HT-collector introduces a large uncertainty. However doing so we find, by inserting the findings from the data sheet that for a tilt angle of 40° we find $c_t = 1{,}127 + (-0{,}0028) * 40 = 1{,}015$ and c_t = 1.001 for the test tilt angle of 45°. This means that the efficiency is increased by 1.4% due to the lower tilt angle.

Correction for incident angle: The expression for the correction for incident angles, c_i, for a given angle of incident for the actual solar irradiation, V, is:

$$c_i = \frac{i_v(V) \cdot G_b + i_v(60°) \cdot G_d}{G} \tag{17}$$

where the coefficient i_v is found by the incident angle modifier expression $i_v(V) = 1 - \tan^a\left(\frac{V}{2}\right)$ with the exponent a found by testing. Other incident angle modifiers are known from literature, e.g. in (Duffie, J. A. and Beckman, W. A., 1991). The value is for the ARCON SCAN-CON ST-collector a=3.6. The value for the HT-collector is not found on the data sheet, but due to the similar cover and absorber designs of the two collectors, it is expected that the value is similar.

Theoretical method for finding the coefficients involved in the correction factors: The coefficients for different collector designs can also be found by theoretical methods also to be found in e.g. (Duffie, J. A. and Beckman, W. A., 1991). Here computer simulation is one powerful technique. Detailed models for the thermal, hydro-dynamical and optical performance of the collectors are modelled for different collector designs. By simulation with reference data, the coefficients for non-testing conditions can be found.

The application of the efficiency expression in the control strategy of the Marstal plant is done for the estimation of the power output from the collector field. This can be done by measurements and has been tested at a small plant for the heating of a public swimming pool in Marstal. The strategy showed severe oscillation in the outlet temperature that was not satisfactory. Hence, the actual control strategy was designed. However, the approach is seen as a realistic alternative. The reason for the oscillation is the fact that the power is measured on the temperature at the outlet of the collector field. This temperature is the result of the conditions for a few minutes before and is not representative for the collector row. Assuming that the outlet temperature is mostly dependent on the heat production in the last few modules in the row, we are able to design a revised and more stable control by applying the temperatures at these last modules for the estimation of the power. Hereby the outlet temperature would be

more damped than found in the test plant in Marstal. Detailed designing can be done by utilising simulation programs as the above.

8.1.7 Partial conclusions on the control strategy design study

In the above analysis we found that the Marstal variable control strategy is very well designed and leads to similar results as a perfect, ideal control strategy where the outlet temperature is exactly the set point outlet temperature. From this point of view, the strategy is well designed.

Measurements show, however, an oscillating temperature of ±2K, whereas the implementation in the computer program shows a variation of ±3K. Here from we find that the real control is doing better than the computer counterpart. However, the correspondence is seen as a documentation of the realistic computations by the computer model.

From the comparison of the variable contra constant flow control we find that both variations can be valuable for given conditions:

Simulations show that the solar plant performance for the variable flow is reduced in collector output by 7.6% and in net solar gain by 7.4%, compared to the constant flow control. As a comparison, (Dalenbäck, J-O., 2000) computes a reduction of 10-15% due to the application of variable flow control, based on the assumption that the inlet temperature to the collector is not affected by the control strategy.

The variable flow increases the stratification in storage tanks, whereas the constant flow tends to mix up the content of the store. Combinations are possible and recommendable which is exemplified in this work by proposing alternative control strategies. Here an efficiency threshold value is introduced with the purpose of determining whether the variable or the constant flow control should be applied. Another improvement of the accuracy of the Marstal control strategy could be to include correction factors for tilt angle, incident angle and mass flow rates.

The constant flow control is very simple and leads to high efficiencies for systems with flexible auxiliary heating, e.g. gas and oil boilers. For auxiliary heating that demands high outputs for keeping up the efficiency, the variable flow control is a better alternative, due to the increased number of hours with full solar share. The current study shows that the number of hours where the auxiliary heating is not needed increased by 125 hours for the application of variable flow compared to the constant flow. The demand for low effects is also reduced by a similar number of hours. According to (Sørensen, P. A., Tambjerg, L., Holm, L., and Ulbjerg, F., 2000), the higher temperature of the variable flow control leads to reduction in post-heating of between 130 and 150 hours a year. This corresponds reasonably with the current work. Moreover, for biomass plants the number of start-ups must be kept low because such plants must run for a rather long period to be effective. This is supported by the constant flow control.

On the one side, the application of flow control involves an increased demand for investments in control computers, sensors and more importantly, the pump frequency controller. On the other hand, one has to estimate and subtract the improved efficiency of the system, including a reduction in electrical energy due to the application of variable flow. The designer of the Marstal plant, Flemming Ulbjerg, RAMBØLL estimates the cost of the control strategy at 6700 Euro and the payback time at 2 years (not published).

8.2 PLANT DESIGN

In the following sections, the tools developed above will be utilised to design the next generation of CSHP. Most of the proposals are already introduced in ongoing projects, among others the next extension of the Marstal plant by an additional collector field.

What are the demands on the coming plants?

One traditional objective is the increase in solar fraction and demonstration of the fact that there are no limits in the application of central solar heating systems. This can simply be achieved by increasing the collector area and storage volume by simple optimisation and subsequently solving the problem of building a heat- and watertight long-term storage. Hence, no attempt is made in the current work to support this challenge.

The integration of CSHP in biomass heating plants is seen as one of the most relevant activities in the dissemination of CSHPs. The work involves knowledge of the plant operation of biomass. Here the author lacks insight and prefers to co-operate on projects with experts from other fields. No findings will be presented on this subject.

The development in collector designs is a continuous activity carried out by the researchers and developers and brings along new possibilities for plant design. As already described in Chapter 2, CSHP, high performance solar collectors are already on the market, others are under development. The possibility of reducing heat loss from plane solar collectors by applying vacuum or air-gel technologies gives the technology a potential for further development. Concentrating solar collectors are also seen as a potential competitor on the market, especially when the optimal performance is increased and cost reduced, as demonstrated in the MaReCo-design. In the following, a trough solar collector design will be examined for the application in large-scale solar heating.

8.2.1 A future settlement

The design of a future settlement is a more open question and has been examined by (Laustesen, J. B., Svendsen, S., and Heller, A., 2000) in the first instance. The author has contributed in relation to method definition, the price estimates, programming and the detailed modelling, to be found in the appendices.

In this work, a methodology was developed which may have relevant potential for future work. In short, the method is as follows: Two models are applied in the designing of a new settlement. (1) A fast and simple model for the optimisation and encircling of a given area with an optimum, and (2) a "slow" and detailed model for the precise definition of the optimum design. Loads are generated by detailed modelling as presented in (Heller, A., 2000c), or according to standards. A model for space heating can be made according to (Dansk Standard, 1986) with the relevant addenda. The domestic hot water model can be designed according to standardised methods, (Dansk Standard, 2000). The heat loss for district heating can be simplified by (Dansk Standard, 1994). Hereby a load profile is prepared. A simple spreadsheet-simulation-program is applied for fast optimisation. Here, the computer program MINSUN would be a possible alternative, (Mazzarella, L., 1989). The results in thermal performance are then checked by a few simulations in a more detailed simulation. Hereby an accurate solution is found by a fast method.

The results of these investigations indicate that it is possible to design a future settlement involving low-energy housings and a central low-energy distribution system supplying the settlement with solar heating and waste heat from a local incineration plant. The economy is found similar to a system consisting of semi-low energy buildings and a hereby increased central solar heating plant. This result was not expected, and it emphasises the relevance of the investigation of these alternatives.

8.2.2 Trough collectors

The trough collector technology has been known for many decades and multi-megawatt arrays were mounted in the United States of America for production of electricity. Characteristic for trough solar collectors is the high efficiency at high temperatures. While the plane collector is also able to utilise energy from the diffuse part of the solar irradiation, the trough is only able to utilise the direct beam. The utilisation of the direct radiation is enhanced by one-axial "tracking" of sun.

The application of such troughs is coming into focus in Europe in relation to solar thermal electricity and solar chemistry. A commercially available parabolic trough from Industrial Solar Technology (IST) was tested at the European Solar Research Centre in Almaria, Spain and at a test facility erected at the Deutsches Zentrum für Luft- und Raumfahrt (DLR) in Cologne, Germany. The test facility is described in (Krüger, D., Heller, A., Hennecke, K., and Duer, K., 2000) and can be found in the Appendix. The co-operation was initialised by the presentations by (Fend, T., Binner, P., Kemme, R., Riffelmann, K-J., and Pitz-Paal, R., 1999), showing reasonable results for such systems under German conditions. Especially due to the application of variable flow to reach high temperatures back from the solar collector field, as found in Marstal, the application of high efficiency seemed to be a relevant alternative.

First introductory results on the Danish TRY climatic data set are found in Figure 104.

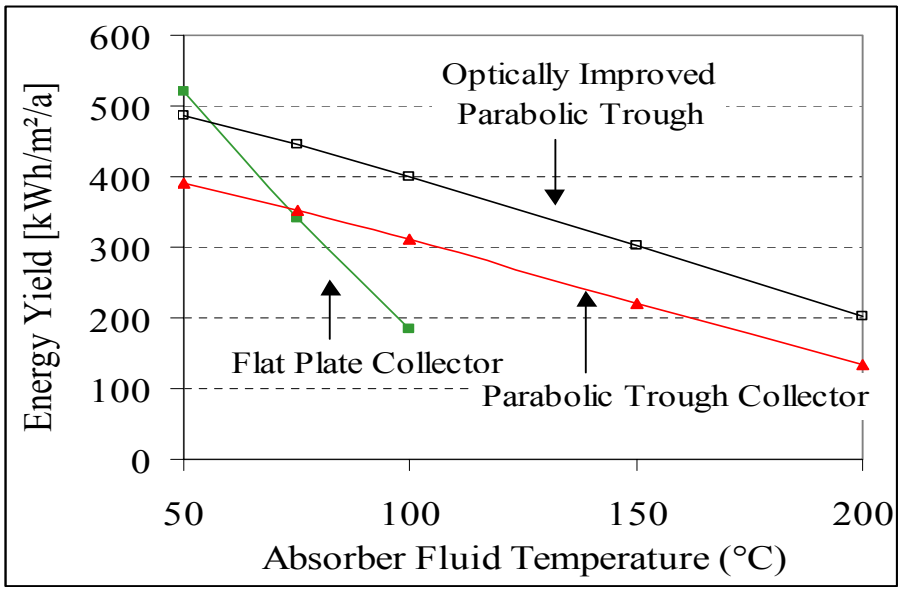

Figure 104. Estimated energy gain for a plane solar collector versus a parabolic trough by IST and an improved trough collector with the Danish TRY weather data set.

It is rather clear from the results in Figure 104 that the application of the high performance collector is obvious for high temperatures. More surprising is the fact that this seems to be the case already from temperatures around 60°C for the IST-type collector. However, the plottet result depends on the collector area applied for the study.

Motivated by these findings the CSHP-model applied by (Heller, A. and Dahm, J., 1999) was redesigned for system computations of the Marstal case. The simplified finding is presented in Figure 105.

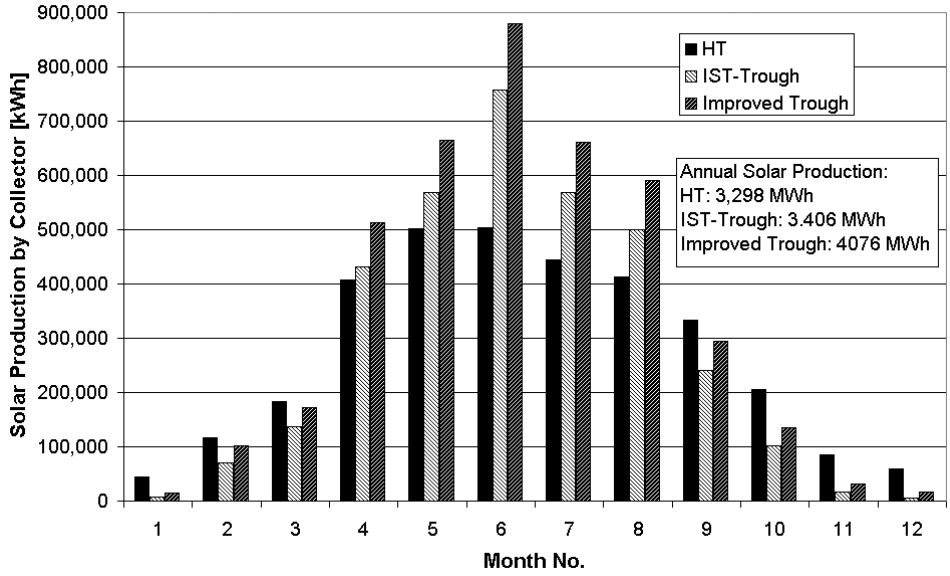

Figure 105. Comparison of collector field output for the plane solar collector applied in Marstal, the IST-trough collector and an improved trough type collector.

From Figure 105, we clearly find evidence of an improvement of the CSHP-technology by applying high performance solar collector technologies as the troughs for a Marstal-like case with approx. 8000 m^2. The plane model results in a solar production (with TRY reference data) of 3298 MWh/a, the IST-model of 3406 MWh/a and the improved IST-model of 4076 MWh/a.

The simulation model applied in this study was hampered by problems with the integration of the trough module into the CSHP-model. The non-standard in the TRNSYS module developed by (Schwarzboezl, 1999) was applied to avoid conflicts between the control strategy of the trough and the one implemented for the Marstal plant. Because of problems with numerical convergence due to the involved flows, the inlet temperature to the collector field was to be set at a fixed value. Hence, the results presented here should be subject to reservations.

Based on the experiences with the subject from the publication above, a second attempt is presented here. This time, the TRNSYS non-standard type developed by (Jones, S. A., 1997) is applied instead of the previous implementation of the trough collector field. This second module includes an algorithm for the control of the outlet temperature from the collector field by variable flow control. Another difference between the two attempts is the application of two sets of weather data. In the first attempt, the data from the TRNSYS software was applied, and in the second attempt, the Danish TRY data set. Similar to the results shown in Figure 105 for the 9000 m^2 base case of the previous analysis section, results from the second attempt are presented in Figure 106.

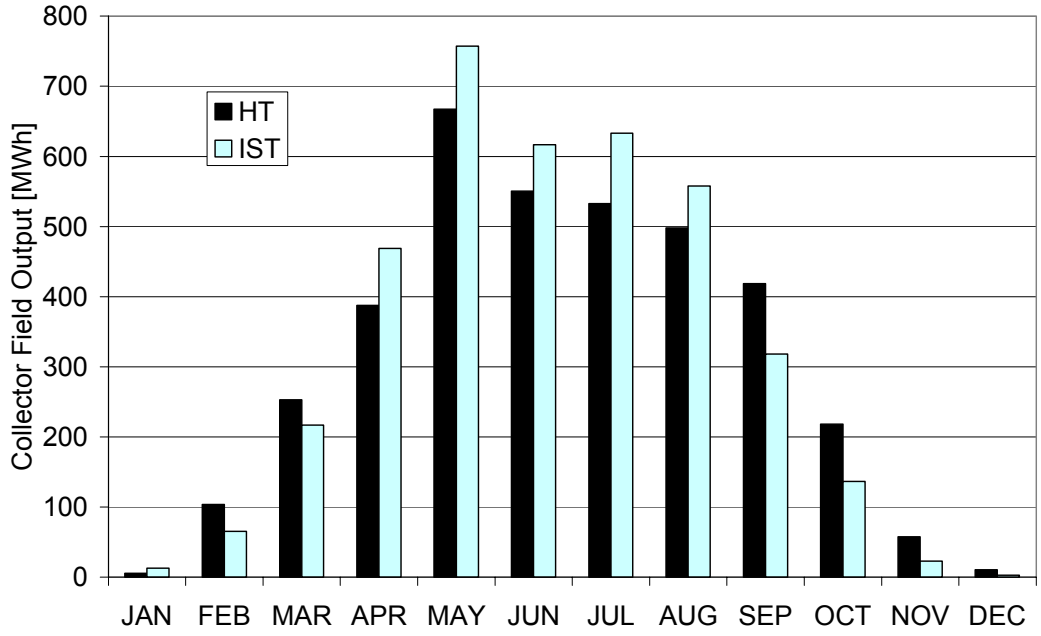

Figure 106. Comparison of collector field output for the plane solar collector applied in Marstal and the IST-trough collector.

By comparing Figure 106 with the results from Figure 105, we find that the different applied reference data has an impact on the results due to systematically different results especially for May. The annual solar gain from the plant is computed at 3654 MWh/a for the plane and 5724 MWh/a for the IST-trough collector field. Hereby the difference is estimated to 70 MWh/a, which is less than the finding of the previous work at 108 MWh/a. In addition, the solar fraction is similar for the two technologies according to the later computations.

Comparing two set point temperatures for the trough technology makes it clear that the control strategy for this technology is even more important than for the plane collectors.

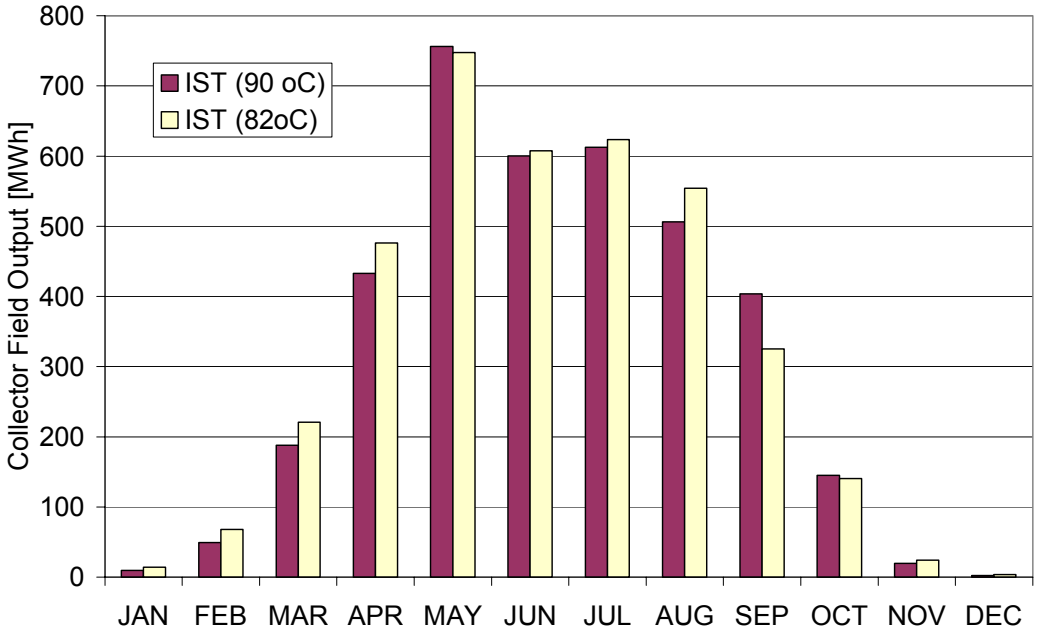

Figure 107. Comparison of the IST collector field for two different set point temperatures of the back temperature from the field.

We find clearly from Figure 107 that the result from the trough collector field can be adjusted, similar to the control strategy from Marstal, namely winter and summer mode. In this way, the production in wintertime and summertime can be kept high, and the annual production can be increased by approximately 1% compared to the plane collector.

In the first computation attempt, an improved trough solar collector was proposed. This collector is not commercially available today, but should be realistic in the next order to the producer of the troughs. European producers could play a mayor role in this respect. If such an improved trough collector was to be applied, the production would certainly be more accentuated than is the case with the existing IST collector. The uncertainties for the computations and the technology as such are still rather large and testing under North European climatic conditions would be relevant.

However, the above computations do not reflect the main advantage of applying high-efficient solar collectors! This is due to the fact that collectors were applied separately, instead of a combination of both in a single plant. The main point is the combination of the two concepts in a combined collector field configuration. The individual fields are utilised in range with high performance. Based on the results in Figure 104, the plane HT-collector is more efficient for temperatures below approximately 60 degrees. Above this temperature, it is more appropriate to apply the trough collectors. In this way, the total efficiency for the collector field is kept high for a wider temperature range.

The objective of future work must therefore be to optimise the combination of different technologies to the best price-performance. To be able to do this the model tool from above must be enhanced by a control algorithm for both collector fields.

9. CLOSING

The closing consists of three parts. The first part puts the central solar heating technology in perspective by comparing the technology with other possible alternatives. The potential for the CSDHP and some comments on barriers for the penetration of the technology are subsequently discussed. In this way, we get an idea of the relevance for the technology.

In the second part, a summary of the most relevant findings from the current work will be collected and discussed and a conclusion will be presented.

The thesis is then finalised by an outlook for the technology, the developments and the research in the field.

9.1 PUTTING THE TECHNOLOGY INTO PERSPECTIVE

9.1.1 CSHP versus other solar heating technologies

Central solar heating is one possible solar heating technology. The purpose is typically to service a large area with hot water for space heating, domestic hot water consumption and other purposes. Hereby CSHP, large-scale solar and combined solar heating technologies are different from small solar heating designed for the preparation of domestic hot water only. The potential in application is therefore larger.

The installation in a large central system involves less components which makes optimisation and maintenance more efficient, but the heat loss due to distribution can be relatively high. A comparison of some main key-values is given in Table 28.

Table 28. Comparison of key-values for solar heating technologies.

**NF: Source: (Mahler, B. and Fisch, N., 2000), project Neckarsulm.*

**SF: Source: (Furbo, S., 1999).*

** Seasonal Pit Water Storage, 65 €/m^3 storage volume. Price for installation incl. collector field based on the Marstal case = 330 €/m^2. Estimate by (Wesenberg, C., 1996) is approx. 550 €/m^2 solar collector incl. tank storage.*

*** Domestic Hot Water Only.*

	Unit	DHW	Medium	CSHPDS	CSBHP (SS) *NF	CSDHP (SS) (estimates)
Typical Collector Area	m^2	2-6	10-100	> 500	> 500	> 500
Collector Cost	€/m^2	310	265	160	151	160
System Cost	€/m^2	665	400	350	460	* 400-550
Annual Net Solar Gain	kWh/m^2	* SF > 360	400	> 425	255	> 300
Typical Storage Capacity	m^3/m^2	0.02-0.05	0.1	0.3	0.3	0.3
Typical Solar Fraction	%	** 5%	** 8-10%	>13	50	>30

We see clearly from Table 28 that the cost-benefit ratio decreases for large solar heating systems, due to price reduction for both collector and system costs. The solar fraction is

certainly increased due to size. By introducing seasonal storage, the investment increases significantly, by approximately 40%. The solar fraction is increased, but at the cost of the price-performance. For a comparison with the above findings, (Mahler, B. and Fisch, N., 2000) found a price-performance of 4.0 [Euro/m^2/a] for small solar heating systems, 1.4 for CSHP with short-term storage and 2.3 for CSHP with long-term storage.

The main drawback for the ground mounted CSHP systems is the fact that land is "wasted"; land which could be used for agriculture or growing of energy crops instead. The roof-mounted solutions are superior in this respect.

9.1.2 Potential for application of CSHP

The potential for central solar heating plants is estimated in different studies and will be discussed in this section.

Specifications of heat demand for district heating are in general performed in two terms, net and gross heat demands. Net heat demand is the demand at the consumer, while gross heat demand is the demand including the heat loss in the system (in some cases in primary energy). In spite of the net figures presented below, solar heating must meet the gross demands. In the previous energy master plan for Denmark, (Energiministeriet, 1990) and (Energiministeriet, 1990), the net heat demand is estimated as shown in Table 29.

Table 29. Net heat demands for domestic hot water and space heating.

Net heat demand [PJ]	1988	2000	2005	2015	2030
	166	176		184	188

The current energy master plan for Denmark does not focus on this aspect, but aims at a reduction of 1% in net heat demand compared to the previous plan, (Miljø- og Energiministeriet, 1996). This does not change the values in any significant way.

Approximately 50% of the above heat demand is met by central and decentralised district heating systems, (Energistyrelsen, 1998a). Seen from this point of view, the potential is enormous. The fact that district heating is introduced, mainly to increase the system efficiency for the production of electricity by co-generation, means that the potential in areas with co-generation is simply not there due to the "waste-heat" from electricity production. Hence, the potential must be found in the remaining areas.

The increased application of natural gas, strongly promoted by the government, further reduces the potential. But this situation can be amended after all, contrary to co-generation where it does not make any sense to replace the heat.

The Danish potential for CSHP in the short term is in the rather old APAS-project estimated at 4.0 PJ/a for block systems and 2.2 PJ/a for district heating systems and an additional potential of 0.7 and 6.9 PJ/a until the year 2015, (Zinko, H., Bjärklev, J., and Margen, P., 1996).

A more diffuse proposal is defined by the Danish Solar Energy Council, where the potential for CSHP in connection with decentralised district heating is estimated at 30%. This value is according to (Energistyrelsen, 1998b) 82 PJ/a which leads to a potential of approx. 20 PJ/a.

A final estimate of the potential for CSHP in Denmark is presented by (PlanEnergi, 2000). The potential for CSBHP is in the short term estimated at 0.4 PJ/a and in the longer run to 0.7 PJ/a. The potential for CSDHP is estimated to be 59,000 m^2 installed solar collector the next 2-3 years, corresponding to 0.2 PJ/a, plus an additional potential of 0.3 PJ/a in the longer perspective.

On a European scale, the potential is estimated at 0.6 PJ/a for block systems and 1.8 PJ/a for district heating systems, with a potential of an increase of 2.2 PJ/a. This potential would demand an installation of approximately 60 mill. square metre solar collectors for large systems in total, (Fisch, N., Guigas, M., and Kübler, R., 1996), pp 6.

The European Commission's "Campaign for Take-Off", (EU, 1999), states the objectives of installing 15 mill. m^2 solar collectors until 2003, specifying 2 mill. of the 15 mill. in district heating systems to be placed in Sweden, Denmark and Germany. This would mean a yearly installation of 760,000 m^2/a, whereas the number of plants under design consist of approximately 50,000 m^2 in Sweden and Denmark. Germany is certainly doing well, but the objectives will not be met.

9.1.3 Barriers

The term "barrier" is to define the obstacles for the penetration of central solar heating technology. Here the subject is presented in a descriptive manner with no scientific method behind. A more developed method would of course be more appropriate.

As shown above, the success of the technology has been demonstrated in the last decade. Hence, no uncertainties of the abilities can be pointed to as obstacles for the penetration. Therefore, the technological level is no barrier for the penetration of large-scale solar heating.

Economical barriers are an important factor. The Marstal plant shows energy prices of down to 0.06 Euro per kWh leading to payback periods between 8-12 years, depending on the situation. Such investments are very typical for district heating companies and cannot be seen as a barrier. However, the heat price in district heating is in general approx. 5 Cents per kWh, hence solar heating is more expensive in the short run.

Another subject in relation to the investment is the economical uncertainties that the decentralised heating plants face, (Plan & Project, 1998). The Danish government has set an objective for plants above a certain size to convert into co-generation plants. This involves a rather large investment that excludes additional investments in the utilisation of solar heating. However, the Danish Energy Agency seems to address the problem in the last few months by a help package to the involved plants, including heating plants (from the Internet site http://www.ens.dk). Thus, it may be possible to solve these critical conditions for the plants and to reduce the barrier for solar heating. This must be judged in the years to come. This is similar to the case regarding impacts of the liberalisation of the market for electricity on the dissemination of renewable energy technologies, as pointed out by, among others, (Meyer, N. I., 2000).

A newly introduced criterion for the support of a given energy technology is called "CO_2-reduction cost" (Danish: skyggepriser). The background for this method is the fact that reduction of CO_2 is the key to reduction of the impact of human activities on the global environment. Here the cost of the reduction of one ton of CO_2– emission into the atmosphere is estimated on the basis of a well-defined set of computations, (Energistyrelsen, 1995). The latest result from such estimates by (PlanEnergi, 2000) shows CO_2-shading prices in the range of 130-600 €/ton. This is a very high price compared to other alternatives, e.g. biomass (wood pills: 30 €/ton) and geothermal heat. Based on such considerations, central solar heating is given a low priority by the authorities and politicians. Therefore it is not highly prioritised to support the penetration of solar heating technologies by subsidies, a subject frequently discussed by politicians, administrators and planners.

9.2 SUMMARY, DISCUSSION AND CONCLUSION

The main task of the current study is to collect facts on the performance of central solar heating plants connected to district heating systems. The objective is to improve the knowledge of the technology and to overcome the obstacle of "aversion to take risks". By documenting the successful demonstration of the technology, the risk is diminished, and a more efficient deployment of this renewable solution is strengthened.

In the current work, the basic concepts are described, a historical view is presented of the development of CSHP's and experiences are collected from the plants in Denmark as well as some findings from literature. In Chapter 6, findings are presented for the thermal, economical and environmental performance and the development that has been seen during the last decade. The main findings are that the technology has been working well for more than 10 years already, with no sign of degradation in solar production. The average net solar gain is above 400 kWh/m^2 for all well-run plants. The price is reduced by 11% even though the solar share is increased by 7-10% and the control strategy is more advanced. The main reason for this price reduction is the cost reduction in solar collector modules (by 30%) and the more efficient piping work.

The potential for the application of the technology is very large, but market barriers still seem too strong for an investment in CSHP in a broader sense. It is a hope that the current work can be applied for documentation of the stability of the technology. Among other aspects, the work proposes a method for the risk assessment for the investment that is strongly dependent on the solar irradiation and hereby on the fluctuating climatic conditions. This is done by designing and simulating the plants with data from the "worst" and the "best" cases measured. The best case is measured in 1997 and the worst case in 1998. As average 1990 or 1999 can be applied. By simulating the plant designs with a reference year and analysing the variation by applying the data from the two years, the variation for the production can be estimated and the design adjusted accordingly. By such analysis the pay-back time for the Marstal plant is estimated to approx. ±1 year from the pay-back time based on average production data.

The author is privileged to be able to examine the newly built central solar heating plant in Marstal in great detail. This is in the first run based on the plant monitoring system and was subsequently extended by own measurements on the plant. From these measurements, positive and negative experiences are gained and recommendations stated in Section 4, for example recommendations concerning adjustment of the control strategy and the involved sensors. The findings are not central for the current work but are still relevant for designers to be taken into considerations.

A computer simulation model is designed in the computer program TRNSYS® and the model validated on the data from the Marstal plant. The computations show very good agreement with the measurements for the short-term comparison, especially for the MFC solar collector module. This is especially important due to the fact that the validation case involves variable flow control. Hereby the current work showed that the MFC solar collector model of the TRNSYS environment is applicable for such conditions.

The validated central solar district-heating model is generalised by a number of means: 1) The application of reference weather data (Danish Design Reference Year). 2) General load profiles. 3) A variety of control strategies known today. Two heat load models, representing the district heating heat load, are implemented: a) A data input model that relies on data from other sources. Here a model is built in the current work to support such simulations. b) A simplified degree-hour model, where the only necessary inputs are the total district heating demand and the ambient temperature part in %. The final model involves the solar collector loop, the secondary loop with storage tank and the control strategies applied at this time. Hereby simulations of different control strategies can be compared by the same basic model.

When applying the generalised model on the Marstal case, the results are less comparable with the measurements from the three years collected in Marstal. Hereby we find the important conclusion that the boundary conditions for the simulation of large-scale solar heating are very strongly fluctuating and especially the heat demands in district heating systems rather difficult to estimate. From this point of view we find that the degree-hour method is sufficient for heat load simulations of existing district heating plants. For better-defined new district heating systems the simulation approach is recommended. Details on this subject can be found at the end of Section 5.2.

The final simulation model is then examined by a parameter variation analysis and a sensitivity analysis. From these analyses, the knowledge within the CSHP-research community is supported in general. However the analysis is an important method for practicians utilising such complex tools as the TRNSYS-model developed in the current work. The two methods give a good understanding of the model and its limitations. Basic errors can also be found by such simple procedures. Hence the methods are recommended for eduction reasons and for the control of models that are prepared by others.

Two main control strategies are applied in large-scale solar heating in general: 1) Constant flow control. 2) Variable flow control. For the constant flow control, the fluid of the solar collector field is pumped with maximum pump speed, by simple on-off control of the pump. Alternatively, the flow rate in the collector loop is controlled to obtain high outlet temperatures and savings of electricity for pumping. The control aims to keep the outlet temperature at a given set point temperature that is chosen to satisfy the supply temperature in the district heating. By this strategy, no post-heating is necessary in large periods in summer.

The generalised simulation model is applied for the comparison of the two main control strategies and hereby to evaluate the strategies and to find more optimal solutions. See Section 8.1.2. From this study we find that the annual net solar gain decreases due to the high outlet temperature of the variable flow control. In other words, the efficiency of the collector field is reduced due to higher outlet temperatures. If the auxiliary heating involves high efficiencies also for very low heat demands, e.g. gas heating, the application of variable flow is therefore not recommendable. If the efficiency and the environmental impact of an auxiliary heating are more dependent on the “load”, things must be reconsidered. We find the following characteristics for the two control strategies that can be applied for such considerations:

The high outlet temperature from the solar collector field leads to less periods with auxiliary demands. The utilisation of a possible storage volume is better for the variable flow strategy due to more stable and higher inlet temperature at the top of the tank and due to less flow through the tank volume, both leading to better thermal stratification of the tank contents. This better stratification of the storage volume leads to lower inlet temperatures to the solar collector field and hereby improved efficiency. (However, as mentioned above this improvement cannot counterbalance the decreased efficiency due to high outlet temperatures for the variable control case.) The total stored energy for the variable flow control is less compared to the constant flow control.

The current study shows that the two control strategies can be combined, leading to a compromise with lower electricity consumptions, high outlet temperatures and collector efficiencies in Section 8.1. Some improvements can be done to get a more accurate temperature control by different means. In the Marstal control design, the efficiency of the collector field is estimated to get an idea of the power and hereby to find the flow necessary to obtain a certain outlet temperature. In the study two improvements are described: 1) If the efficiency expressions are applied, the estimation of the efficiency can be improved by including correction factors for incident angle, tilt angle and flow rates. 2) Alternatively, instead of basing the power estimation on the collector field efficiency, the power can be measured. However a control on this measurement would lead to unwanted oscillations. To avoid such

fluctuating outlet temperatures some correction can be based on temperature measurements along the collector row.

The thesis includes two design studies for the design of future large-scale solar heating plants: 1) For a new settlement of low energy buildings and its heat supply structure. 2) The application of high-efficiency solar collectors in combination with the today dominating flat-plate solar collectors.

The design study for a new low-energy settlement is carried out by the author in co-operation with colleagues from the Department. In the study the assumption is made that 1000 low-energy buildings are supplied with district heating with the main share (70%) of heat from large-scale solar heating with seasonal storage and the rest from an incineration plant. The study involves three insulation levels for the buildings and different insulation levels for the district heating. The question was to find if it seems a reasonable solution to combine low-energy settlements with a common distribtution system and central solar heating. The main answer is that the different system designs show similary economical results and hereby that the analysis is relevant for further work. These results are, however, preliminary due to the assumptions and the tools applied in the study. Hence it is relevant to reproduce the findings by more accurate studies.

Another main finding from these activities is a fast and practicable method for optimisation of solar heating plants by applying a fast and simple simulation tool in combination with a detailed simulation model. The simple tool is applied for the encirclement of a possible optimum. The advanced tool is then applied to analyse the surroundings of the optimum by detailed analysis and hereby to ensure that the optimum is realistic and accurate.

The second design study on the application of high performance (HP) solar collectors in combination with flat-plate solar collectors is based on the fact that the former shows high efficiencies for high temperatures and the latter high efficiencies for low temperature ranges. Hence the combination is expected to give an improved total solar production. As examples for such high-performance solar collectors there are tubular vacuum pipe collectors, concentrating collectors (CPC) and trough collectors.

The case study for a trough collector design shows that the HP collectors can lead to a large increase of solar production in summertime. Due to the poor performance for low radiation compared to the flat-plate HT collector, the increased performance during summertime is lost during the low-radiation periods. Due to the high cost for the HP collectors, such an application is not recommended. Alternatively a combination is proposed where the plane collectors are applied for low temperatures and the high performance collector for high temperature ranges. Hereby, the combination increases the annual efficiency for the HT collector while still gaining high efficiencies for the HP collectors. It was not possible for the author to build a model within the time frame of the current work. It was therefore not possible to prove this hypothesis in the current work. Hence the main point of the study is still open and to be examined by later work.

The current study exposes subjects which are not central for the work, but nonetheless relevant to summarise:

The design study of the future settlement and experiences with results found by designers, applying simple simulation tools mainly show that such simple tools can give surprisingly realistic results. Contrary to the detailed, dynamic simulation tools which involve a large number of parameters and choices, thus enlarging the risk of errors. From this point of view, it is recommended to apply simple models, unless the advanced models have been examined and validated in detail. This is a built-in feature of the TRNSYS environment, where the advanced models are hidden in an interface-program with a selected number of parameters to be adjusted by less experienced users. Hereby, the advanced tool is made very simple. Unfortunately, this does not solve the problem with time-consuming simulations.

9.3 OUTLOOK

9.3.1 The barrier issue

Generally speaking, there are two main barriers for the penetration of solar heating : 1) the installation cost, leading to relatively high energy prices which is not the case with other renewable energy technologies, 2) the high cost of CO_2-emission reduction for solar heating, even for the very efficient central solar heating variant. Both hurdles are defined by economic costs. The most important subject in the future is to examine these methods in relation to a long-term optimal development towards sustainability. It seems that the two methods are too short-sighted to meet the extensive reorganisation we are facing today. It is a postulate by the author that the methods promote investments in technologies which merely adjust, but do not solve the problem in a sustainable manner. To exemplify this postulate it is found that almost all countries in the developed world reduce the CO_2-emissions by replacing oil and coal by natural gas. Hereby investments are placed and fixed to non-sustainable solutions and the exploitation of natural resources is still supported, leading to an even faster exhaust of natural gas. In a time frame similar to the investments, the resources of natural gas are exhausted and the investments wasted, necessitating new investments. Choosing an apparently more expensive solution today, the total cost is smaller in the long run.

In relation to the price-performance and hereby the installation costs, the author expects an increase of the potential for CSHP due to:

- Increased efficiency in co-generation with less heat for district heating as a result.
- Stronger impact of electricity production sources not coupled with heat production, e.g. from wind mills.

Hereby, the district heating system must be reconsidered. The questions are then if district heating, especially the large-scale systems, is optimal. The answer is neither "yes" nor "no", but rather that there are metropolises with demand for supply to be met by central systems. Here CSHP can play a major role. Large-scale district heating can be split up into smaller systems. Hereby, the heat loss (inefficiency) of large connection pipelines is avoided. The application of CSHP is also relevant in this respect. In relation to newly established areas, central systems lead to higher total efficiencies. These subjects must be addressed in future research studies.

A continuous production of 5000 m^2 per year per production line would lead to a decrease in the costs of solar collectors by 30% or more. Hereby, the technology would be competitive to other non-renewable technologies.

The barrier of "risk-avoidance" will hopefully be overcome through work such as this thesis and the huge effort by among others the Marstal district heating company, the consultants, entrepreneurs involved and the contributions by the members of European Large-Scale Solar Heating Network.

A final step in this direction would be the development of a quality monitoring procedure for large-scale solar heating. First, basic stones in an attempt to improve an optimal operation of large-scale solar heating is presented by the statistics for large scale solar systems in (Nielsen, J. E. and Honoré, C., 2000) and a more advanced method by (Ellehauge, K., 1994). By the latter method, a plant operator is able to predict the performance from a few measurements. Hereby, the operation can be examined and optimised. The method is developed for medium size block solar heating plants and must first be evaluated on central solar heating before it can be applied. However, online simulation with measured data would be a more powerful method, but implies a number of unsolved challenges. A short-term monitoring method – for in-situ use - is proposed by (Uecker, M., Krause, M., Vajen, K., and Ackermann, H., 2000). A more permanent monitoring implies subjects addressed by (Beikircher, T., Benz, N., Gut, M.,

Kronthaler, P., Oberdorf, C., and Schölkopf, W., 1999). Such work must be focused on in the coming years to bring an online operation optimisation to a mature level.

The CSHP is one of the technologies applicable in a sustainable future. There are still many details to be examined and barriers to be removed before the goal is within sight.

9.3.2 Simulation and modelling

The simulation model of the current work lacks a control module for the examination of different control strategies. Therefore a module ought to be built before doing any further design on e.g. a combination of different collector types. This is important due to the fact that the Marstal plant and others are planning extensions in 2001 and 2002.

Validation of the storage tank module is still missing for large, long-term storage. Prior to solving this task successfully, the design of large-scale solar heating with high solar fraction is rather inaccurate and should therefore be subject to certain reservations.

The current work suffers from poor parameter estimation methods. In future work the author will include stochastic methods for parameter estimations of e.g. heat capacities in the system, heat loss coefficients for the storage tank. It turns out that parameter estimation is a sub-class or an optimisation. Hence, in the future the author will apply a numerical technique solving the two subjects simultaneously. By these improvements the "toolbox" is seen as complete for solving problems of the above categories.

It is necessary to combine simulation models from different sources. Two basic trends are visible at this time. One is implemented in the newer TRNSYS Version 15, (Klein, S. A. and many others, 2000), where the program is able to interact with other computer programs. The other tendency is to "translate" the modules into a general simulation language such as Modelica to be found on the Internet http://www.modelica.org. To make this method work, a "translation tool" between TRNSYS and Modelica must be developed. The strength of this path is the ability to utilise the most advanced numerical techniques with minimal effort. In this way, the rather limited solver of the TRNSYS-program can be eliminated.

A basically different approach for the improvement of the simulation models is to re-model them in a general simulation platform such as MATLAB® by Mathworks. Such tools are presented by (Wemhöner, C., Hafner, B., and Schwarzer, K., 2000) and (Buzás, J. and Farkas, I., 2000). The main strength of this approach is the generality and flexibility. The drawback is the lack of validated component models. However, this path seems the most promising solution for the future development.

The application of simulation models typically results in a huge mass of plots and numbers. It is very difficult to interpret such results. Methods must be found to help the users keep track of the questions asked and to focus on finding the answers. If this is possible, the simulation method is one of the most important methods for designing a sustainable world. With this method, the over-sizing of technical solutions can be avoided by detailed analysis and designing which is not possible by simple assumptions on steady-state conditions and so on. The thesis points out that such an effort is very important, if the path to sustainability is to be successful.

NOMENCLATURE

Greek:

A	helping value
A	solar collector area in m^2
B	helping value
C	helping value
D	helping value
G	global irradiance in W/m
G_b	beam part of global irradiance in W/m^2
G_d	diffuse part of global irradiance in W/m^2
G_T	total irradiance (on tilt plane) in W/m^2
GD	degree-day value
GD_p	normal degree-day value
GD_p	degree-day value for a given period
GH	degree-hour value
H	depth of the pipe centre in m
I_b	beam solar irradiance in W/m^2
I_d	diffuse solar irradiance in W/m^2
L	length in m
$\dot{M}_p$	mass flow rate in primary loop in kg/h or kg/s
$\dot{M}_{sh,ist}$	objective mass flow rate in kg/h or kg/s
$\dot{M}_{sh,soll}$	demanded mass flow rate in kg/h or kg/s
N	total number of time-steps for the simulation interval
N_{year}	number of seconds in a year
P	probability
P_Row_c	computed power from solar collector row or field in W
P_Row_m	measured power from solar collector row or field in W
Q	heat load in W
Q_{DH}	heat demand in district heating network in total in kWh
Q_n	normalised heat load in W
Q_p	heat load for a given period in W
Q_{sh}	ambient temperature dependent heat load in W
Q_s	net solar gain in kWh
Q_t	total solar energy on the solar collector field in kWh
R_c	thermal insulance for a polymer cover in m K / W
R_{cp}	thermal insulance for the couple pipe in m K / W
R_g	thermal insulance for the ground in m K / W
R_h	thermal insulance between the two pipes in m K / W
R_i	thermal insulance for the insulation material in m K / W
R_s	thermal insulance for steel pipe in m K / W
S	measured potential in mV
T_a	ambient temperature in ^oC
$T_{coll,out}$	measured outlet temperature back from the collector field in ^oC
$T_{coll,in}$	measured inlet temperature to the collector field in ^oC
T_{cw}	cold water supply temperature in ^oC
T_d	helping temperature measured reference temperature in the conversion between voltage and temperature in ^oC
T_g	(undisturbed) ground temperature in K which under code conditions is 8.8^oC
$T_{h,ist}$	obtained hot supply temperature in ^oC

$T_{h,soll}$	demanded hot supply temperature in ^oC
T_i	inlet temperature in ^oC
$T_{l,soll}$,	demanded hot supply temperature in ^oC
$T_{l,ist}$,	obtained hot supply temperature in ^oC
T_m	mean fluid temperature in ^oC
T_m	helping temperature measured reference temperature in the conversion between voltage and temperature in ^oC
Tout_c	computed outlet temperature from solar collector row or field in ^oC
Tout_m	measured outlet temperature from solar collector row or field in ^oC
T_{ref}	measured reference temperature in the conversion between voltage and temperature in ^oC
T_s	supply temperature from district heating plant in ^oC
T_{set}	set point temperature for the temperature back from the collector field in ^oC
T_{set1}	set point temperature for the efficiency expression in the control strategy in ^oC
T_o	outlet temperature in ^oC
T_1-T_{10}	measured temperatures between collector modules in ^oC
ΔT	temperature difference in K
UA	heat transfer capacity rate in W/K
U	heat loss coefficient in W/(m^2 K)
V	volume flow rate in m^3/s
V	angle of incident from horizontal for solar radiation on collector °
Y	dependent model variable
X	independent model variable element

a	coefficients in power polynomium for conversion between voltage and temperatures
a	exponent in solar angle modifier computations
c	coefficients in efficiency correction expressions
c_f	correction coefficient for flow rate condition
c_i	correction coefficient for solar radiation incident angle condition
c_p	specific heat capacity in kJ/(kg K)
$c_{p,g}$	specific heat capacity of the ground material in kJ/(kg K)
c_t	correction coefficient for tilt angle condition
d_o	outer diameter of pipe polymer cover in m
d_i	inner diameter of steel pipe in m
d_y	diameter of the steel pipe in m
dT_i	temperature difference between collector outlets in K where the index *i* is a counter
e	error
i	step counter in the time domain
i_v	incident angle of solar irradiation on collector, °
k	advection parameter describing the flow characteristics
k_1	heat loss coefficient, linear part of efficiency expression, W/(m² K)
k_2	heat loss coefficient, quadratic part of efficiency expression, W/(m² K^2)
l	length in m
m_0	bias coefficient in linear regression of flow correction factor computation
m_1	slope coefficient in linear regression of flow correction factor computation
$\dot{m}$	mass flow rate on kg/s
n	counter
s	mass flow ratio between the mass flow through the house installation and the total flow in the DH
s_0	bias coefficient in linear regression of solar incident angle correction factor
s_1	slope coefficient in linear regression of solar incident angle correction factor

t	time in s
x	position in space in m
x	position along the pipe in m

Roman:

Δ	difference
Σ	sum
α	thermal diffusivity for the pipe material in m^2/s
α_g	thermal diffusivity of ground material in m^2/s
β	model coefficients
β	helping value in m^{-1}
λ_i	thermal conductivity or the insulation material in W/(m K)
λ_{iso}	thermal conductivity or the insulation material in W/(m K)
λ_g	thermal conductivity or the ground in W/(m K)
τ	time in a given unit
η	efficiency for solar collector field
η_e	estimated efficiency for solar collector field when running
η_0	start efficiency for solar collector (here also for collector field) for mean absorber temperature equal to ambient temperature
ρ	density in kg/m^3
ρ_g	density of the ground in kg/m^3

Indices:

c	cover
cp	coupled pipe
g	ground
h	high
i	number of the actual element (1,2,..,n)
i	insulation
i	inner
ist	actual
l	low
n	total number of independent elements that shape the dependent variable
n	normal period for the degree day method
o	outer
p	actual period for the degree day method
s	steel pipe
soll	demanded
sh	degree day dependent part

Symbols:

$\rightarrow$	Finding start.
$\leftarrow$	Finding end.

REFERENCES

Adsten, M., Perez, B. & Wäckelgård, E. (2000) *The Influence of Climate and Location on Collector Performance*, In Print, Solar Energy.

Aggerholm, S., Zachariassen, H., Christensen, G., Olufsen, P., Clausen, V. & Pedersen, P.E. (1995) *Bygningers energibehov (Energy consumption of buildings)*, SBI Anvisning148, Statens byggeforskningsinstitut, ISBN 87-563-0945-7, ISSN 0106-6757.

Ambrosetti, P., Andersson, H.E.B., Liedquist, L., Fröhlich, C., Wehrli, Ch. & Talarek, H.D. (1984) *Results of an Outdoor and Indoor Pyranometer Comparison Document No. III.A.3*, Kernforschungsanlage Jülich GmbH, Postfach 1913, D-5170 Jülich, Germany.

Andersen, P. (1998) *Vandudsivning fra Ottrupgård Sæsonvarmelager (Water losses at the Ottrupgaard thermal, seasonal storage)*, Rapport 1, Geotechnical Institute, Denmark.

Arkar, C., Medved, S., Novak, P., Frankovic, B. & Lenic, K. (1998) *Long-term Operation Experiences with Large-Scale Solar Systems on Slovenian and Croatian Costal Region*, Eurosun'98, Slovenia, Volume III, pp. 2.2-1-2.2-6.

Aronsson, S. (1996) *Fjärrvärmekunders värme- och effektbehov - Analys baserad på mätresultat från femtio byggnader (Heat load of buildings supplied by District Heating - An analysis based on measurements in 50 buildings)*, Ph.D.-Thesis, Department of Building Services Engineering, Chalmers University of Technology, ISBN 91-7197-383-4, ISSN 0346-718x, Gothenburg, Sweden.

Beikircher, T., Benz, N., Gut, M., Kronthaler, P., Oberdorf, C. & Schölkopf, W. (1999) *In situ short-term test for large solar thermal systems*, ISES Solar World Congress, Jerusalem, Israel, pp. 20-20.

Berger, R. (1997) *Dynamic Simulation Model for Analyzing Combined Solar-Biomass District Heating Plants* Project No. XVII/4.1030/AL/67/95/AUS, Technisches Büro, Energietechnik - Systemanalyse, Arnethgasse 39/11, 1160 Vienna, Austria.

Boye-Hansen, L. & Furbo, S. (1995) *Solvarmeanlæg med tømning (Solar Heating System with Drain Back)*, Meddelelse Nr. 275, Thermal Insulation Laboratory, Technical University of Denmark, Building 118, DTU, 2800 Lyngby, Denmark, ISSN 1395-0266.

Buzás, J. & Farkas, I. (2000) *Solar Domestic Hot Water System Simulation using Block-Oriented Software*. Eurosun 2000, Copenhagen.

Bøhm, B. (1994) *Optimum operation of district heating systems Laboratory of Heating and Air Conditioning*, Technical University of Denmark, ISBN 87-88038-29-7.

Bøhm, B. (1998) *Simpel fjernvarmemodel (Simple district heating system model)*. Educational publication.

Bøhm, B. (1999a) *Heat losses from buried district heating pipes with specific interest in the transient behaviour.* Polyteknisk Press.

Bøhm, B. (1999b) Communication.

DANVAK. (1999) *DANVAK Grundbog Varme- og Klimateknik,* ISBN: 87-982652-1-0. Teknisk Forlag A/S, Copenhagen.

Dahm, J. (1998) *TRNSYS TYPE 80 Description*, Unpublished.

Dahm, J. (1999) *Small District Heating Systems*, Ph.D.-Thesis, Department of Building Services Engineering, Chalmers University of Technology, ISSN 0346-718X, Gothenburg, Sweden.

Dalenbäck, J.-O. (1990) *Central Solar Heating Plants with Seasonal Storage: Status Report D14:1990*, Swedish Council for Building Research, Stockholm, Sweden.

Dalenbäck, J.-O. (1993) *Solar heating with seasonal storage - Some aspect of the design and evaluation of systems with water storage*, Ph.D.-Thesis, Dept. of Buildings Service Engineering, Chalmers University of Technology, ISBN 91-7032-855-2, ISSN 0346-718X, Gothenburg, Sweden.

Dalenbäck, J.-O. (1995) *Large-Scale Solar Heating Systems - Evaluation of Existing Plants*, CIT Energiteknisk Analyse AB, Gothenburg, Sweden.

Dalenbäck, J.-O. (2000) *Solar District Heating Plant Kungälv*, Eurosun 2000, Copenhagen.

Dalenbäck, J.-O. (2000) *Hot water consumption and circulation losses.* Communication.

Dansk Standard. (1986) *Beregning af bygningers varmetab*, 5. Udg. Dansk Standard DS 418, Teknisk Forlag.

Dansk Standard. (1994) *Code of practice for distribution networks for district heating.* DS 439.

Dansk Standard. (2000a) *Tillæg 4 til DS 418, Beregning af bygningers varmetab - Tillæg om kuldebroer, fundamenter, terrændæk, kældergulve og -vægge samt samlinger omkring vinduer og døre.*

Dansk Standard. (2000b) *Tillæg 3 til DS 418, Beregning af bygningers varmetab. Tillæg omhandlende betonsandwichelementer samt kileformet isolering.*

Dansk Standard. (2000c) *Tillæg 2 til DS 418, Beregning af bygningers varmetab. Tillæg omhandlende løsfyldsprodukter.*

Dansk Standard. (2000d) *Tillæg 1 til DS 418, Beregning af bygningers varmetab. Tillæg omhandlende vinduer og yderdøre.*

Dansk Standard. (2000e) *Code of practice for domestic hot water supply installations, DS 439.*

Dansk Standard. (1994) *Code of practice for distribution networks for district heating. DS 448.*

Duer, K. & Svendsen, S. (1993) *Construction of a Seasonal Heat Storage based on a Pit with Clay Membrane*, ISES Solar World Congress, Budapest, Hungary.

Duffie, J.A. & Beckman, W.A. (1991) *Solar Engineering of Thermal Processes*, Second Edition, ISBN: 0-471-51056-4, Wiley.

EC. (1991) *Growth, Competitiveness and Employment White Paper. EC Publications, Luxenbourg.*

Ellehauge, K. (1993) *Små markedsførte solvarmeanlæg brugsvandsopvarmning - funktionsafprøvning og ydelsesmålinger. Opbygning af prøvestand (Small solar heating systems for DHW, operation and performance monitoring. Test stand designing)*. R-93-37, Thermal Insulation Laboratory, Technical University of Denmark.

Ellehauge, K. (1994) *Kontrol af ydelsen af store solvarmeanlæg*, Nr 94-28, Thermal Insulation Laboratory, Technical University of Denmark.

Energiministeriet. (1990a) *Energy 2000 - A Plan of Action for Sustainable Development - Bilag.* Ministry of Energy.

Energiministeriet. (1990b) *Energy 2000 - A Plan of Action for Sustainable Development.* Ministry of Energy.

Energistyrelsen. (1995) *Generelle forudsætninger for samfundsøkomiske beregninger.* Danish Energy Agency.

Energistyrelsen. (1998b) *Energistatistik 1997.* Danish Energy Agency.

Energistyrelsen. (1998a) *Energy in Denmark 1998 - Development, Policies and Results.* Danish Energy Agency.

Energistyrelsen. (2000) *Beregningsforudsætninger for Danmarks Energifremtider- Background Data for the "Danish Energy Future".* Danish Energy Agency, Ministery of Environment and Energy, Landemærket 11, Copenhagen, Denmark.

Elsayed, M.M. (1991) *Monthly-average Daily Shading Factor for A Collector Field*, Solar Energy 47, (4):287-297, ISBN 0038-092X/91.

Eriksson, L., Zinko, H. & Dahm, J. (1998) *District Heating with low system temperatures*, ZW, Energiteknik AB, Sweden.

Esbensen Consultants. (1991) *Måling og evaluering af 44 m^2 low flow solvarmeanlæg på Sønderborg Søfartsskole (Measurement and Evaluation of Solar Heating System at Maritime School in Soenderborg).*

EU. (1999) *Campaign for Take-Off.* European Communities, DGXVII.

Fend, T., Binner, P., Kemme, R., Riffelmann, K.-J. & Pitz-Paal, R. (1999) *Efficiency Improvement of Parabolic Trough Collectors by Means of Additional End Reflectors*, ISES Solar World Congress, Jerusalem, Israel.

Fisch, N., Guigas, M. & Kübler, R. (1996) *Large-Scale Solar Heating (Executive Summary Report)*, Steinbeis Transferzentrum, Rationelle Energienutzung und Solartechnik - Stuttgart, Hessbrühlstr. 21 c, D-70565 Stuttgart.

FN. (1988) *Vores Fælles Fremtid. Brundtland-kommissionens Rapport om Miljø og Udvikling.* Mellemfolkeligt Samvirke, FN, ISBN: 87-7028-515-2.

Furbo, S. (1983a) *Optimal udformning af low-flow solvarmeanlæg, (Optimal designing of low flow solar heating systems)*, Meddelelse Nr. 238, Thermal Insulation Laboratory, Danish Technical High School.

Furbo, S. (1983b) *Test Procedures of Thermal Energy Storage Systems for Solar Thermal Applications (Final Report).* Thermal Insulation Laboratory, Danish Technical High School.

Furbo, S. (1999) *Små solvarmeanlæg til brugsvandsopvarmning - Status og fremtid (Status and future for small DHW solar systems)*, SR-9925, Department of Buildings and Energy, Technical University of Denmark, ISSN 1396-402X.

Geus, de.A.C. (1996) *Large Solar Energy Systems, Final Report of the Task 14*, Large System Working Group, IEA Advanced Solar Energy Systems, T.14.LS.1, TNO Building and Construction Research, P.O.Box 49, 2600 AA Delft, the Netherlands.

Handelsministerium. (1976) *Dansk Energipolitik*, Danish Ministry of Trade.

Heller, A. (1997a) *Floating Lid Constructions for Pit Water Storage - A Survey*, R-011, Department of Buildings and Energy, Technical University of Denmark, ISSN 1396-4011, ISBN 87-7877-01-6.

Heller, A. (1997b) *Floating Lid Constructions for Large Pit Water Heat Storage*. Megastock '97, Sapporo, Japan, Volume 1, pp. 503-508.

Heller, A. (1998) *Optimering af styringsstrategien for solvarmecentralen i Marstal (Optimisation of Control Strategy at the Marstal Central Solar Heating Plant).* Sagsrapport, SR 9910, Department of Buildings and Energy, Technical University of Denmark.

Heller, A. (2000a) *15 Years of R&D in Central Solar Heating in Denmark*, Solar Energy, 69, (6), 0038-092X.

Heller, A. (2000b) *Advances in Large-Scale Solar Heating and Long Term Storage in Denmark*. Eurosun 2000, Copenhagen.

Heller, A. (2000c) *Development of Seasonal Storage in Denmark*, Terrastock 2000, 8th International Conference on Thermal Energy Storage, Volume 1, pp. 47-52. **See Appendix for this paper.**

Heller, A. (2000d) *Pit Water Storage Ottrupgaard, Denmark*, Terrastock 2000, 8th International Conference on Thermal Energy Storage, Volume 1, pp. 267-274.

Heller, A. (2000e) *Demand Modelling for Central Heating Systems*, R-040, Department of Buildings and Energy, Technical University of Denmark, Denmark, ISSN 1396-4011, ISBN 87-7877-042-4.

Heller, A. & Dahm, J. (1999) *The Marstal Central Solar Heating Plant: Design and Evaluation*, ISES Solar World Congress, Jerusalem, Israel.

Heller, A. & Furbo, S. (1997) *First Experience from the World Largest Fully Commercial Solar Heating Plant.* ISES Solar World Congress, Taejon, Korea.

Hewlett Packard. (19 A.D.) *Practical Temperature Measurements 290*, Hewlett Packard.

Hilmer, F. (1996) Modellierung des Betriebsverhaltens nicht abgedeckter Sonnenkollektoren bei zeitlich veränderlichem Fluidstrom (Modelling of operation for uncovered solar

collector with transient flow), Dr.rer.nat.-Thesis, Physics, Philipps-Universität Marburg.

Holm, L. (2000) *Variable Flow in Large Scale Thermal Solar Plants.* Eurosun 2000, Copenhagen.

Holm, L., Ulbjerg, F., Nielsen, J.E., Sørensen, P.A. & Tambjerg, L. (2000) *Måleprogram for solvarmeanlæg hos Marstal Fjernvarme (Monitoring Programme for the Central Solar Heating Plant at the Marstal District Heating).* Marstal District Heating, Marstal, Denmark.

Illum, K. (1996) *Fremtidens Sollandskab (Future Solar Landscape)*, Aalborg Universitetsforlag, Badehusvej 16, DK-9000 Aalborg, Denmark.

Isakson, P. (1995) *Solar Collector Model for Testing and Simulation*, Ph.D.-Thesis, Department of Building Services Engineering, Royal Institute of Technology, ISSN 0284-141X ISRN KTH/IT/M--36--Solar Energy, Stockholm, Sweden.

Isakson, P. & Eriksson, L.O. (1993) *Matched Flow Collector Model for simulation and testing. MFC 1.0 beta.* Manual.

Isakson, P. & Schroeder, K. (1996) *CSHPDS, Central Solar Heating Plant with Diurnal Storage at Falkenberg - Final Report* (Chapter from: Large Solar Energy Systems), T.14.LS.1, IEA, SHC, Task 14, Large System Working Group, TNO Building and Construction Research, Delft, the Nederlands.

ISO. (1999) *Thermal performance tests for solar collectors.* Part 1, ISO-Standard.

Jacobsen, D.T. & Nielsen, J.E. (1999) *Life Cycle Assessment of Solar Collectors in Denmark*, ISES Solar World Congress, Jerusalem, Israel.

Jensen, M.J. & Lund, H. (1995) *Design Reference Year, DRY - Et nyt dansk referenceår*, Meddelelse , Nr. 281, Thermal Insulation Laboratory, Technical University of Denmark, ISSN 1395-0266.

Jensen, N.A. (2000) *Variable Flow in Large Scale Thermal Solar Plants*. Eurosun'98, Slovenia, Volume III, pp. 2.23.1-2.23.6.

Johnsen, K., Grau, K. & Christensen, J.E. (1993) *tsbi3 - EDB-program til termisk simulering af bygninger og installationer*, Statens Byggeforskningsinstitut, Hørsholm, Denmark.

Jones, S.A. (1997) *Parabolic Trough field Model, TRNSYS TYPE 96.* Unpublished work,

Jordan, U. & Vajen, K. (2000a) *Influence of the DHW-load on the Fractional Energy Savings: A Case Study of a Solar Combi-System with TRNSYS simulations.* Eurosun 2000, Copenhagen.

Jordan, U. & Vajen, K. (2000b) *Stochastic Hot Water Consumption Profile*, Unpublished work.

Julio, D.S. & Ruberti, A. (1984) *General Methodologies in Systems Science and Mathematical Modelling*, UNESCO (1):1-13 . ISBN 90-277-1661-7.

Kübler, R., Fisch, N. & Hahne, E.W.P. (1997) *High temperature pit storage projects for the seasonal storage of solar heating*, Solar Energy 61, (2):97-105.

Karlsson, B. & Wilson, G. (2000) *MaReCo design for horizontal, vertical and tilted installation*, Eurosun 2000, Copenhagen.

Kielsgaard, H.K., Nordgaard, H.P. & Ussing, V. (1983) *Seasonal Heat Storage in Underground Warm Water Stores (Construction and testing of a 500 m^3 store)*, 134, Thermal Insulation Laboratory, Technical University of Denmark.

Klein, S.A. & many others. (1996) *TRNSYS - A Transient System Simulation Program. 14.2*, Solar Energy Laboratory, University of Wisconsin—Madison, USA.

Klein, S.A. & many others. (2000) *TRNSYS Version 15 - A Transient System Simulation Program*, Solar Energy Laboratory, University of Wisconsin—Madison, USA.

Kristensen, F. (1995) *Måling på et større solvarmeanlæg BO-90 med tagrumssolfanger og luft-til-vand varmeveksler (Measurement on a large solar heating system with roof-solar collector and air to water heat exchanger).* 279, Thermal Insulation Laboratory, Technical University of Denmark, Building 118, DTU, 2800 Lyngby, Denmark, 1395-0266.

Krüger, D., Heller, A., Hennecke, K. & Duer, K. (2000) *Parabolic Trough Collectors for District Heating Systems at High Latitudes?* Eurosun 2000, Copenhagen. **See Appendix F for this paper.**

Larsson, G. (1999) *Dynamik i fjärrvärmesystem (On Dynamics in District Heating Systems)*, Thesis, Department of Thermo and Fluid Dynamics, Chalmers University of Technology, Teknologtryck, Chalmers, Göteborg, ISBN 91-7197-814-3, ISSN 0346-718X, Gothenburg, Sweden.

Laustesen, J.B. (1999) *Solvarmecentraler (Central Solar Heating Plants)*, Department of Buildings and Energy, Technical University of Denmark, Brovej, Building 118, DTU, DK-2800 Lyngby. **See Appendix F for this paper.**

Laustesen, J.B., Svendsen, S. & Heller, A. (2000) *A Central Solar Heating Plant for New Settlements*, Eurosun 2000, Copenhagen.

Lawaetz, H. (1984) *Beregning af rumvarmebehov*, Notat , 3/84, DTI, Varme- og installationsteknik.

Lawaetz, H. (1987) *Sol- og vindkorrekton af graddage (Solar and wind correction of degree days)*, Notat , DTI, Varme- og installationsteknik, ISBN 87-7511-733-9.

Lawaetz, H. (1993) *Sæsonvarmelagring i store ståltanke*, Solar Test Centre, Technological Institute of Denmark, Taastrup, Denmark.

Leenaerts, C. (1997) *Project Development Guide for Central Solar Heating Plants with Seasonal Storage*, A Report of CSHPSS Working Group, A10:1997, Energie-Buro, Nederland, Swedish Council for Building Research, Stockholm, Sweden, ISBN 91-540-5797-3.

Ljung, L. (1987) *System Identification*, ISBN 0-13-881640-9 025. Prentice-Hall International.

Mack, M., Schenk, C. & Köhler, S. (1998) *Kollektoranlagen im Geschosswohnungsbau - eine Zwischenbilanz*, 11. Internationales Sonnenforum '98, pp. 45-52.

Madsen, H., Pálsson, H., Sejling, K. & Søgaard, H.T. (1990) *Models and methods for optimization of district heating systems, Part I: Models and indentification methods*, 1323/98-14, Institute for Mathematical Modelling, Technical University of Denmark.

Mahler, B. & Fisch, N. (2000) *Large Scale Solar Heating Systems for Housing Developments*, Eurosun 2000, Copenhagen.

Mazin, M. & Maleki, M. (1995) *Optimering af varmt brugsvandssystem (Optimisation of a domestic hot water system)*, M.Sc.Eng.-Thesis, Thermal Insulation Laboratory, Technical University of Denmark.

Mazzarella, L. (1989) *The MINSUN simulation program application and user's guide*, International Energy Agency, Solar Heating and Cooling Programme, Task VII.

Meaburn, A. & Hughes, F.M. (1993) *Resonance characteristics of distributed solar collector fields.* Solar Energy 51, (3).

Meyer, N.I. (2000) *Renewable Energy in Liberalised Energy Markets*, Eurosun 2000, Copenhagen.

Mikkelsen, S.E. (1988) *Projektering af større solfangeranlæg - Systemudformninger og diagrammer til beregning af ydelse og tab. (Design and dimensioning of large solar heating systems - System design and diagrams for the calculation of gain and losses).* 48, Thermal Insulation Laboratory, Technical Highschool of Denmark.

Miljø- og Energiministeriet. (1995) *Danmarks energifremtider- Energy Future in Denmark*. Danish Ministry of Energy and Environment.

Miljø- og Energiministeriet. (1996) *Energy 21,* Danish Ministry of Energy.

Mills, A.F. (1992) *Heat Transfer*. International School Edition, IRWIN, ISBN: 0–256–12817–0.

Nielsen, J.E. & Honoré, C. (2000) *Ydelsesstatistik - store anlæg, 1999 (Plant Performance Statistics for Large Solar Heating Systems, 1999).* SolEnergiCentret, Technological Institute of Denmark.

Olsen, O. (1993) *SAESONSOL - Manual til Version 3.0 (SEASONSOL - Manual for the version 3.0)*, Thermal Insulation Laboratory, Technical High School of Denmark.

Overgaard, L.L. (1998) *Målemetoder i forbindelse med solvarme*, Education publication.

Pálsson, O.P. (1993) *Stochastic Modelling, Control and Optimization of District Heating Systems*, Ph.D.-Thesis, Dept. for Mathematical Statistics and Operation Analysis, Technical University of Denmark.

Pálsson, H. (1997) *Analysis of Numerical Methods for Simulating Temperature Dynamic in Distric Heating Pipes,* 6th International Symposium on District Heating and Cooling Simulation.

Pálsson, H., Larsen, H.V., Bøhm, B., Ravn, H.F. & Zhou, J. (1999) *Equivalent models of district heating systems - for on-line minimization of operational costs of the complete district heating system.* Department of Energy Engineering, Technical University of Denmark. RISØ National Laboratory, Systems Analysis Department.

Pedersen, V.P. (1992) *Målinger og evaluering af varmeakkumuleringstank i Hørby (Measurements and evaluation of thermal storage tank in Hoerby)*, Nr. 92-10, Cenergia Energy Consultants, Thermal Insulation Laboratory, Technical High School of Denmark and Folkecentret for VE, Ballerup, Denmark.

Perers, B. (20 A.D.) *Optical modelling of solar collectors and booster reflectors under non stationary conditions. Application for collector testing system simulation and evaluation*. Ph.D.-Thesis, Uppsala University, Sweden, ISBN 91-554-3496-7.

Plan & Project. (1998) *Situationen på landets barmarks kraftvarmeværker.* Plan & Projekt A/S for the Danish Energy Agency.

PlanEnergi. (2000) *Udredning vedrørende tilrettellæggelse af en målrettet indsats for etablering af store solvarmeanlæg i Denmark.* PlanEnergy S/I, Rambøll A/S.

Porsvig, M. (1999) *Note from Meeting in the Seasonal Storage Expert Group.* Unpublished work.

Qin, L. (1998) *Analysis, Modelling and Optimum Design of Solar Domestic Hot Water Systems*, Ph.D.-Thesis, Department of Buildings and Energy, Technical University of Denmark.

SBI. (1982) *Vejrdata for VVS og energi - Dansk reference år TRY- Meteorological data for HVAC and energy - Danish Test Reference Year TRY.* SBI-Rapport 135, Statens Byggeforskningsintitut.

Schwarzboezl. (1999) *Process Heat Parabolic Collector Model, TRNSYS TYPE 97.* Unpublished work.

Sejling, K. (1993) *Modelling and Prediction of Load in District Heating Systems*, Ph.D.-Thesis, Technical University of Denmark.

Streicher, W. (2000) *Documentation of Reference Buildings for IEA SHC Task 26.* Unpublished work.

Svendsen, S. (1981) *Solfangers effektivitet- Målt og beregnet*. (Solar Collector Efficiency – Measured and Computed) Meddelelse Nr. 109, Thermal Insulation Laboratory, Technichal Highschool of Denmark.

Svendsen, S. & Carlsson, P.F. (1995) *Solvarmeanlæg til brugsvands- og rumopvarmning (Solar Heating for DHW and space heating)*, Thermal Insulation Laboratory, Technical University of Denmark, Brovej, Building 118, DTU, 2800 Lyngby, Denmark, ISSN 1395-0266.

Sørensen, B., Kuemmel, B. & Maibom, P. (1999) *Long-Term Scenarios for Global Energy Demand and Supply (Four Global Greenhouse Mitigation Scenarios)*, Tekst Nr. 359, IMFUFA, Roskilde University, Roskilde, Denmark.

Sørensen, P.A. (2000) *Key Note on Solar Heating Plants and Long Term Storage.* Eurosun 2000, Copenhagen.

Sørensen, P.A., Tambjerg, L., Holm, L. & Ulbjerg, F. (2000) *Solar Production for the Marstal Plant 1997-1999*, Eurosun 2000, Copenhagen.

Uecker, M., Krause, M., Vajen, K. & Ackermann, H. (2000) *Monitoring of Solar Systems - Theoretical and Experimental Investigation on Measurements of Solar Radiation.* Eurosun 2000, Copenhagen.

Urbaneck, T. (2000) *Central Solar Heating Plant with Gravel Water Storage in Chemnitz (Germany).* Eurosun 2000, Copenhagen.

Ussing, V. (1991) *Forsøgsborehulslager og ombygning af damvarmelager til gruslager (Bore Hole Storage and reconstruction of Pit Water Storage to Gravel Storage).* nr. 219, Thermal Insulation Laboratory, Technical High School of Denmark, Building 118, DTU, 2800 Lyngby.

Vajen, K. (2000) *Hot water consumption and circulation losses.* Communication.

Vajen, K., Krämer, M., Orths, R., Boronbaev, E.K., Paizuldaeva, A. & Vasilyeva, E.A. (2000) *Concept of a Solar Absorber System for Preheating Feeding Water for District Heating*, Eurosun 2000, Copenhagen.

von Weizäcker, E., Lovins, A.B. & Lovins, H.L. (1998) *Factor Four: Doubling Wealth - Halving Resource Use*, ISBN: 1853834068. Earthscan.

Wemhöner, C., Hafner, B. & Schwarzer, K. (2000) *Simulation of Solar Thermal Systems with CARNOT Blockset in the Environment MATLAB® SIMULINK®.* Eurosun 2000, Copenhagen.

Werner, S.E. (1984) *The Heat Load in District Heating Systems*, Chalmers University of Technology, Sweden.

Wesenberg, C. (1990) *Skitseprojekt, Sol til sommerstop i eksisterende halmvarmeværk - Forsøgsanlæg (Sketch, Solar for existing straw heating plants - Pilot plant).* Nellemann Consultants, Denmark.

Wesenberg, C. (1991) *Slutrapport fra projekt lertætnet damvarmelager til solvarmecentral (Final Report for project: Clay Liner tightened Pit Water Storage for Central Solar Heating Plant). Store Lagre* 2, Nellemann Consultants, Denmark.

Wesenberg, C. (1994a) *Development of Pit Stores in Denmark, Part 2: Details and Experiences from the Ottrupgåad Pilot Plant. Reconstruction of the Tubberupvaenge Storage Pit.* Workshop on Large-Scale Solar Heating pp. 107-113.

Wesenberg, C. (1994b) *Ottrupgaard, Denmark*, Workshop on Large-Scale Solar Heating pp. Appendix D.

Wesenberg, C. (1996) *Sol/sæsonvarmelagre, Statusrapport, Lertætnet damvarmelager med flydende lågkonstruktion, Status for udvikling (Seasonal storage, Clay tightened pit water storage with floating lid, Status and development). Store Lagre* 4, NNR Consultants, Denmark.

Wesenberg, C. (1998) *Rekonstruktion af Tubberupvaengetanken, Del 2: Bygning og driftssættelse (Reconstruction of Tubberupvaenge Storage: Part 2: Building and Operation Start)*. NNR Consultants, Odense, Denmark.

Witt, de .J. (1990) *Korttids-varmelagre (Short-term storage - Technical Note)*, 2/1990, Danish Gas-Technological Institute.

Wittrup, S. (2000) *Energiforbruget skal ned*, *Ingeniøren* (Nr. 41):5.

WMO. (1983) *Guide to Meteorological Instruments and Methods of observation,* Fifth Edition, No. 8, Secretariat of the World Meteorological Organization, Geneva, Switzerland.

World Commission on Environment and Development. (1987) *Our Common Future*, ISBN: 019282080X, Oxford University Press, UK.

Yang, L. (1994) *District Heating House Stations with Hot Water Storage (Simulation and Evaluation of Dynamic Performance)*, Laboratory of Heating and Air Conditioning, Technical University of Denmark, ISBN 87-88038-31-9.

Zinko, H., Bjärklev, J. & Margen, P. (1996) *The market potential for solar heating plants in some European countries (Large-Scale Solar Heating Systems).* ZW Energiteknik, Nyköping, Sweden.

Zunft, S. (1995) *Temperature Control of A Distributed Collector Field,* Solar Energy 55, (4):321-325, ISBN 0038-092X/95.

Ørsted, H. & Majland, O. (1987) *Demonstrationsprojekt Vester Nebel, Slutrapport (Demonstration Project, Vester Nebel - Final Report).* Esbjerg Kommune, Forsyningsvirksomhederne, Esbjerg, Denmark.